THE UNIVERSITY
of EDINBURGH

MICRORNA REGULATION OF DRUG METABOLISM IN STEM CELL – DERIVED HEPATOCYTES

DAGMARA SZKOLNICKA

MSc

University of Edinburgh 2015

College of Medicine and Veterinary Medicine

The dissertation is submitted for the degree of Doctor of Philosophy

TABLE OF CONTENTS

ABSTRACT

The liver is a multi-functional and highly regenerative organ. While resilient, the liver is susceptible to organ damage and failure. In both the acute and chronic settings liver disease has dire consequences for health. A common cause of liver damage is adverse reactions to drugs which can lead to drug induced liver injury (DILI). This creates major problems for patients, clinicians, the pharmaceutical industry and regulatory authorities. In the context of drug overdose or serious adverse reactions, liver failure can be acute and life threatening, and in some cases require orthotopic liver transplantation. While transplantation is highly successful, such an approach has limitations and justifies basic science attempts to develop better human models to study liver injury and to develop scalable intervention strategies. With this in mind, we have studied the importance of microRNAs (miRs) in regulating human drug metabolism in pluripotent stem cell – derived hepatocytes and their potential to reduce liver toxicity in response to toxic levels of paracetamol. miRs are small non-coding RNAs that are approximately 20 - 24 nucleotides long and their major function is to fine tune gene expression of their target genes. Recently, it has been demonstrated that microRNAs play a role in regulating the first phase of drug metabolism however the second phase of drug metabolism, drug conjugation, has not been studied in detail. Drug conjugation is a crucial stage in human drug metabolism, and any alterations in this process can lead to changes in compound pharmacology, including therapeutic dose and clearance from the body. To test the importance of miRs in regulating phase II drug metabolism we opted to study the metabolism of a common used analgesic, paracetamol. When taken in the appropriate amounts paracetamol is modified by sulfotransferases (SULTs) and UDP - glucuronosyltransferases (UGTs) and removed from the body without organ damage. However, when paracetamol is taken above the recommended dose it is metabolised by phase I enzymes to generate a toxic intermediate N-acetyl-p-benzoquinone imine (NAPQI), which if untreated can lead to massive hepatocyte cell death and liver failure, placing the patient in a life threatening situation.

In order to promote non-toxic drug metabolism, in the context of drug overdose, we employed candidate miRs to regulate different parts of the paracetamol metabolism pathway. In summary, we have focused on studying human drug metabolism in the major metabolic cell type of the liver, the hepatocyte.

We have identified a novel microRNA (called miR-324-5p) which regulates phase II drug metabolism and reduces cell cytotoxicity. Additionally, a supportive role of anti-microRNA-324 in response to fulminant plasma collected from paracetamol overdose patients is also observed. The findings of this project are novel, provide proof of concept and exemplify the power of stem cell based models to identify new approaches to treating human liver damage.

DECLARATION

The thesis is the result of my own work and includes nothing which is the outcome of work done in collaboration, except where indicated in the text. The portions of the thesis that were done in collaboration have been explicitly designated within the Acknowledgments or figure legends. The names of the collaborators and the nature of their contribution have been stated.

Dagmara Szkolnicka

LIST OF FIGURES AND TABLES

ABBREVIATIONS

AA	Activin A
ABC	ATP-Biding Cassette
ADH	Alcohol Dehydrogenase
AFP	Alpha - Fetoprotein
ALB	Albumin
ALDH	Aldehyde Dehydrogenase
ALT	Alanine Aminotransferase / Alanine Transaminase
Ant	Antagomir
ARNT	Aryl Hydrocarbon Receptor Nuclear Translocator
AST	Aspartate Transaminase
ATP	Adenosine Triphosphate
A1AT	Alpha -1 - Antitrypsin
BAL	Bio-artificial Liver
BCA	Bicinchoninic Acid
BCRP	Breast Cancer Resistance Protein
BMP	Bone Morphogenetic Protein
BSA	Bovine Serum Albumin
B2M	B2 Micoglobulin
CAR	Constitutive Androstane Receptor
CDH	Cadherin
CDX	Caudal – Related Homebox
CEBP	CCAAT/Enhancer Binding Protein
CES	Carboxylesterase

CK	Cytokeratin
Ctrl	Control
CTNND	Delta Catenin
CYP	Cytochrome P450
DE	Definitive Endoderm
DGCR	DiGeorge Syndrome Critical Region
DILI	Drug-Induced Liver Injury
DMEs	Drug-Metabolising Enzymes
DMSO	Dimethylsulfoxide
DTT	Dithiothreitol
Ecad	Ecadherin
ECL	Enhanced Chemiluminescence
ECM	Extracellular Matrix
EDTA	Ethylenediaminetetraacetic acid
EPHX	Epoxide Hydrolase
ER	Endoplasmic Reticulum
EtOH	Ethanol
E8	Essential 8 Medium
FACS	Fluorescence Activated Cell Sorting
FGF	Fibroblast Growth Factor
FOXA	Forkhead Box Protein
GAPDH	Glyceraldehyde 3-Phosphate Dehydrogenase
GLDH	Glutamate Dehydrogenase

GMP	Good Manufacturing Practice
GST	Glutathione S - Transferase
GSH	Glutathione
GSSG	Oxidised Glutathione
HBL	Hepatoblast
HCC	Hepatocellular Carcinoma
HCM	Hepatocyte Culture Medium
HCV	Hepatitis C Virus
hESCs	Human Embryonic Stem Cells
HGF	Hepatocyte Growth Factor
hiPSCs	Human Induced Pluripotent Stem Cells
HLA	Human Leukocyte Antigen
HLC	Hepatic-Like Cells
HMGB	High-Mobility Group Box
HNF	Hepatic Nuclear Factor
HSD	Hydroxysteroid Dehydrogenase
HZ	HepatoZYME Medium
ICC	Immunocytochemistry
IMDs	Inherited Metabolic Disorders
KO-SR	Knockout Serum Replacement
KLF	Kruppel Like - Factors
L15	Leibovitz's L-15 Medium

MAPK	Mitogen-Activated Protein Kinase
MEFs	Mouse Embryonic Fibroblasts
MEFS-CM	MEFS Conditioned Medium
MMPs	Matrix Metalloproteinases
um	micrometer
miR	MicroRNA
mg	milligram
ml	millilitre
mM	millimolar
MRP	Multidrug Resistance Associated Protein
MT	mTeSR-1®
NAC	N-acetylcysteine
NADPH	Nicotinamide Adenine Dinucleotide Phosphate
NAPQI	N-acetyl-p-benzoquinone imine
ng	nanogram
NNMT	Nicotinamide N-Methyltransferase
OATP	Organic Anion – Transporting Polypeptide
OCT	Octamer
OSM	Oncostatin M
PB	Phenobarbital
PBS	Phosphate Buffered Saline
PCR	Polymerase Chain Reaction
P-gp	P-glycoprotein
PHH	Primary Human Hepatocytes

PI3K	Phosphoinositide 3-Kinase
pmol	Picomol
Pre	Precursor
PROX	Prospero homebox
PSCs	Pluripotent Stem Cells
PXR	Pregnane X Receptor
RISC	RNA-Induced Silencing Complex
RLU	Relative Light Units
ROCK	Rho-Associated Protein Kinase
RPMI	Roswell Park Memorial Institute (Medium)
RT	Reverse Transcriptase
SD	Standard Deviation
SE	Standard Error
SOP	Standard Of Procedures
SOX	Sex Determining Region Y Box
SNP	Single Nucleotide Polymorphism
SSEA	Stage Specific Embryonic Antigens
SULT	Sulfotransferase
TGF	Transforming Growth Factor
THBS2	Thrombospondin 2
TPMT	Thiopurine S-Methyltransferase
TRBP	TAR RNA Binding Protein
TWIST	Twist – Related Protein

UGT	UDP – glucuronosyl transferase
UTR	Untranslated Region
VEGFR	Vascular Endothelial Growth Factor Receptor
WB	Western Blot
WT	Wild Type

ACKNOWLEDGMENTS

I would like to thank my supervisors Dr. David Hay and Prof. Stuart Forbes for the opportunity to carry out my PhD and their continual guidance and support throughout the project. Especially, I would like to thank Dr. David Hay for giving me a lot of opportunities to develop my scientific skills and career.

I would like to thank my colleagues, especially Balta Lucendo –Villarin and Claire Medine for teaching me different laboratory techniques and helping me with flow cytometry. I would like to thank Joanna Moore and Kenneth Simpson for providing plasma samples.

Finally, I would like to thank my fantastic parents and friends for all their support and belief in me.

PUBLICATIONS

1. **Szkolnicka, D**., Lucendo –Villarin, B., Moore, J., Simpson, K., Forbes, S., and Hay, D (2015) Reducing hepatocyte injury and necrosis in response to paracetamol using non-coding RNAs. *Stem Cells Translational Medicine*. Manuscript under revision. Impact Factor: 5.7

2. Lucendo-Villarin, B., Cameron, K., **Szkolnicka, D**., Rashidi, H., Bates, N., Kimber, SJ., Flint, O., Forbesm SJ., and Hay, DC (2015) Polymer supported directed differentiation reveals a unique gene signature predicting stable hepatocyte performance. *Advanced Healthcare Materials*. DOI: 10.1002/adhm.20500391. Impact Factor: 5.7

3. Godoy, P., Schmidt-Heck, W., Natarajan, K., Lucendo-Villarin, B., **Szkolnicka, D**., Asplund, A., Bjorquist, P., Widera, A., *et al* (2015) Gene networks and transcription factor motifs defining the differentiation of stem cells into hepatocyte-like cells. *Journal of Hepatology*. DOI: http://dx.doi.org/10.1016./j.hep.2015.05.013. Impact Factor: 11.3

4. Cameron, K., Lucendo-Villarin, B., **Szkolnicka, D**., and Hay, DC (2015) Book Chapter: Serum-free directed differentiation of human embryonic stem cells to hepatocytes. *Methods in Molecular Biology: Protocols in In Vitro Hepatocyte Research*. http://www.springer.com/in/book/9781493920730

5. Zhou,X., Sun, P., Lucendo-Villarin,B., Angus, AGN., **Szkolnicka, D**., Cameron, K., Farnworth, SL., Patel, AH., and Hay, DC (2014) Modulating innate immunity improves hepatitis C virus infection and replication in stem cell – derived hepatocytes. *Stem Cell Reports*. **3**(1): 204-214. Impact Factor: 5.3

6. Lucendo–Villarin, B., Cameron, K., **Szkolnicka, D**., Travers, P., Khan, F., Walton, J., Iredale, J., Bradley,M., and Hay, DC. (2014) Stabilising hepatocellular phenotype using optimised synthetic surfaces. *Journal of Visualized Experiments*. 91; e51723. Impact Factor: 1.3

7. **Szkolnicka, D**., Farnworth, SL., Lucendo-Villarin, B., and Hay, DC. (2014a) Deriving functional hepatocytes from pluripotent stem cells. *Current Protocols in Stem Cell Biology*. Unit 1G.5. DOI: 10.1002/9780470151808.sc01g05s30.

8. **Szkolnicka, D**., Farnworth, SL., Lucendo-Villarin, B., Storck,C., Zhou,W., Ireadale, JP., and Hay, DC. (2014b) Accurate prediction of drug – induced liver injury using stem cell-derived populations. *Stem Cells Translational Medicine*. **3**(2):141-148. Impact Factor: 5.7

9. Medine, C., Lucendo-VIllarin, B., Storck, C., Wang, F., **Szkolnicka, D**., Khan, F., Pernagallo, S., Black, J., Marriage,H., Ross,J., Bradley,M., Iredale,J., Flint,O., and Hay, DC. (2013) Developing high-fidelity hepatotoxicity models from pluripotent stem cells. *Stem Cells Translational Medicine*. **2**(7): 505-509. Impact Factor: 5.7

10. **Szkolnicka, D**; Zhou, W., Lucendo-Villarin, B; and Hay, DC. (2013) Pluripotent stem cell - derived hepatocytes: Potential and challenges in pharmacology. *Annual Reviews in Pharmacology and Toxicology*. **53**: 147-59. Impact Factor: 18

CHAPTER ONE

INTRODUCTION

1. INTRODUCTION

1.1 LIVER AS AN ORGAN

The liver is the largest internal organ in the human body providing different metabolic, endocrine and exocrine functions. The major endocrine functions include secretion of variety of hormones such as angiotensinogen, thrombopoietin, and insulin-like factors, whereas exocrine functions include formation of the bile. The liver is also an essential organ for reconditioning blood, drug detoxification, glycogen storage, regulation of cholesterol and fatty acid transport, urea metabolism and secretion of major serum (plasma) proteins such as albumin and apolipoproteins (Si-Tayeb *et al*, 2010a). The specific structure of the liver is essential to maintain multifunctional nature of the organ.

The liver lobule is the basic architectural unit of the liver. The lobule consists of plates of hepatocytes separated by sinusoidal spaces that are connected to a network of blood vessels capillaries. The liver lobules are in the shape of hexagon with each of the six corners demarcated by the presence of a 'portal triad' of vessels consisting of a portal vein, bile duct, and hepatic artery (Figure 1.1). The blood supplied from both the hepatic artery and the portal vein enters the sinusoidal space, and through endothelial fenestrae comes into direct contact with the basal surface of hepatocytes – the major metabolic cells of the liver. Once these cells absorb metabolites and toxins, the blood leaves the lobule through the central vein. The apical surface of the adjoining hepatocytes secretes bile into the bile canaliculi that then flows through intrahepatic bile ducts to the extrahepatic bile ducts, where it is finally stored in gall bladder before release into the duodenum (Zorn, 2008).

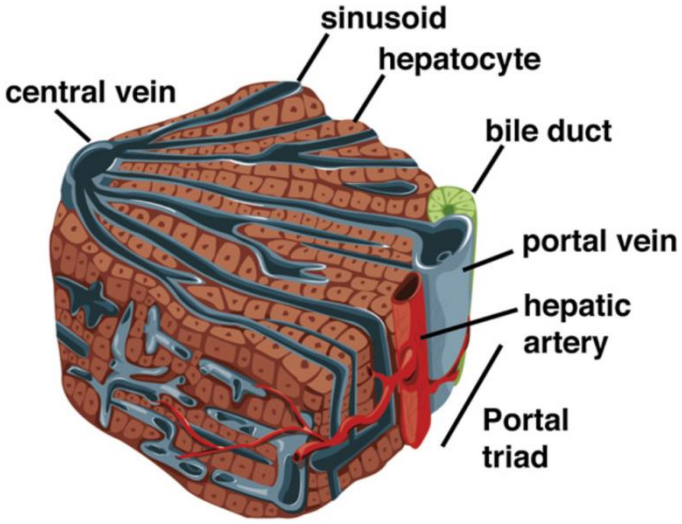

Figure 1.1: Liver lobule. Illustration showing overall structure of a portion of a liver lobule. The 'portal triad' consisting of portal vein, bile duct and hepatic artery is surrounded by hepatocytes lined by sinusoidal endothelium that radiate toward a central efferent vein. Picture adapted from Si-Tayeb *et al*, 2010a.

Hepatocytes (parenchymal cells) make up approximately 70-80% of the liver mass (Blouin *et al*, 1977). Their function is supported by the non-parenchymal cells; cholangiocytes (biliary epithelial cells), sinusoidal endothelial cells, endothelial cells, natural killer cells, Kupffer cells (resident liver macrophages), infiltrate and hepatic stellate cells (Kmiec, 2001).

The polarized nature of hepatocytes is essential to proper function (Figure 1.2). The basolateral surface of hepatocytes is directly connected with sinusoidal endothelial cells what facilitates the transport of endocrine secretions to the blood stream, whereas tight junctions between hepatocytes allow for the canaliculus formation. The canaliculus collects bile salts and bile acids that are transported across the apical side of the hepatocyte (Wang and Boyer, 2004).

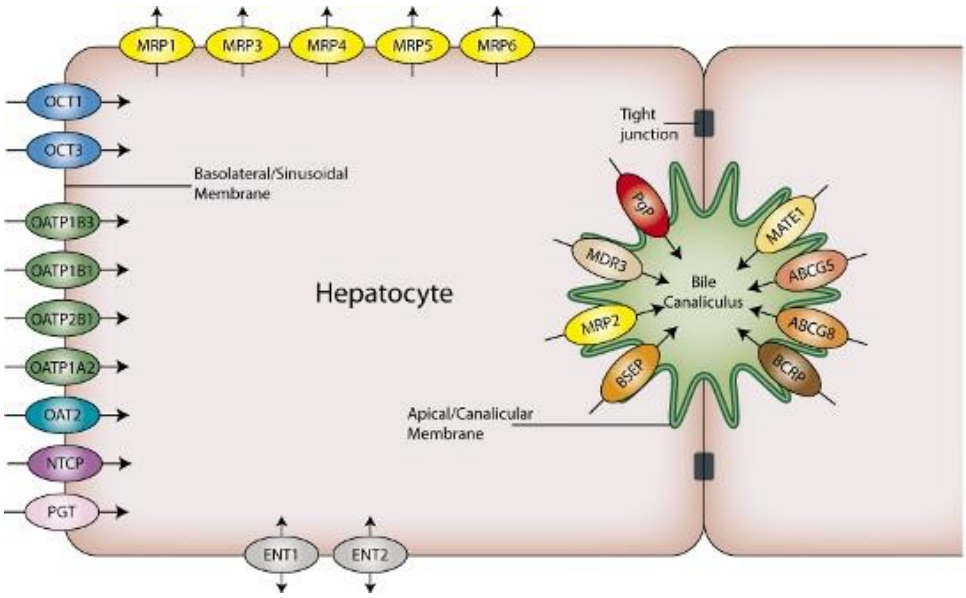

Figure 1.2: Hepatocyte polarity. Polarization of hepatocytes is essential for endocrine and exocrine secretions. Picture adapted from Solvo Biotechnology (www.solvobiotech.com). Abbreviations: MRP1/MRP2/MRP3/MRP4/MRP5/MRP6, Multidrug resistance-associated protein 1/2/3/4/5/6; MDR3, Multi-drug resistant ABC transporter 3; BSEP, Bile Salt Export Pump; BSRP, Breast Cancer Resistance Protein; PgP, P-glycoprotein; MATE1, Multidrug And Toxin Extrusion 1; ABCG5/ABCG8, ATP- binding cassette subfamily G member 5/8; OCT1/3, Organic Cation Transporter 1/3; OATP1B3/1B1/2B1/1A2, Organic Anion-Transporting polypeptide 1B3/1B1/2B1/1A2; OAT2, Organic Anion Transporter 2; NTCP, Sodium-Taurocholate Cotransporting Polypeptide; PGT, Prostaglandin Transporter; ENT1/2, Equilibrative Nucleoside Transporter 1/2.

The delivery of hepatocytes which are fully polarized and functional for long periods of time is currently a major challenge to the field. As a consequence, *ex vivo* hepatocytes rapidly dedifferentiate and die. Therefore it is important that we learn from human liver development and homeostasis, in the adult, to improve our cell based models.

1.2 OVERVIEW OF THE LIVER DEVELOPMENT

Studies on different animal models such as the mouse, rat, chicken, zebrafish have identified many genes and molecular pathways regulating embryonic liver development and proven that hepatogenesis is evolutionary conserved (Zaret, 2008)

There are three primary germ layers in the early embryo: ectoderm, mesoderm, and endoderm (Figure 1.3). During gastrulation, the endoderm germ layer is established and forms a primitive gut tube that is further subdivided into foregut, midgut, and hindgut regions. Tremblay and Zaret (2005) fate mapping studies in the mouse embryo at embryonic day 8.0 identified that embryonic liver originates from the ventral foregut endoderm. At day 9.0 of embryonic development, the hepatic diverticulum, an out-pocket of thickened ventral foregut epithelium is formed next to the developing heart. The anterior portion of the diverticulum gives rise to the liver and intrahepatic biliary tree, whereas the posterior portion forms the gall bladder and extrahepatic bile ducts. Subsequently, the hepatoblasts delaminate from the epithelium and invade the septum transversum mesenchyme (STM) (Le Douarin, 1975). At later stages of embryonic development (e9.5-e.15), STM contributes fibroblasts and stellate cells. The bi-potential hepatoblasts residing next to the portal veins become cholangiocytes (biliary epithelial cells), while the ones located in the parenchyma differentiate to hepatocytes (Lemaigre, 2003). The maturation of hepatocytes and biliary network continues until birth to generate liver specific tissue architecture. Later the liver bud is vascularized to become major fetal haematopoietic organ.

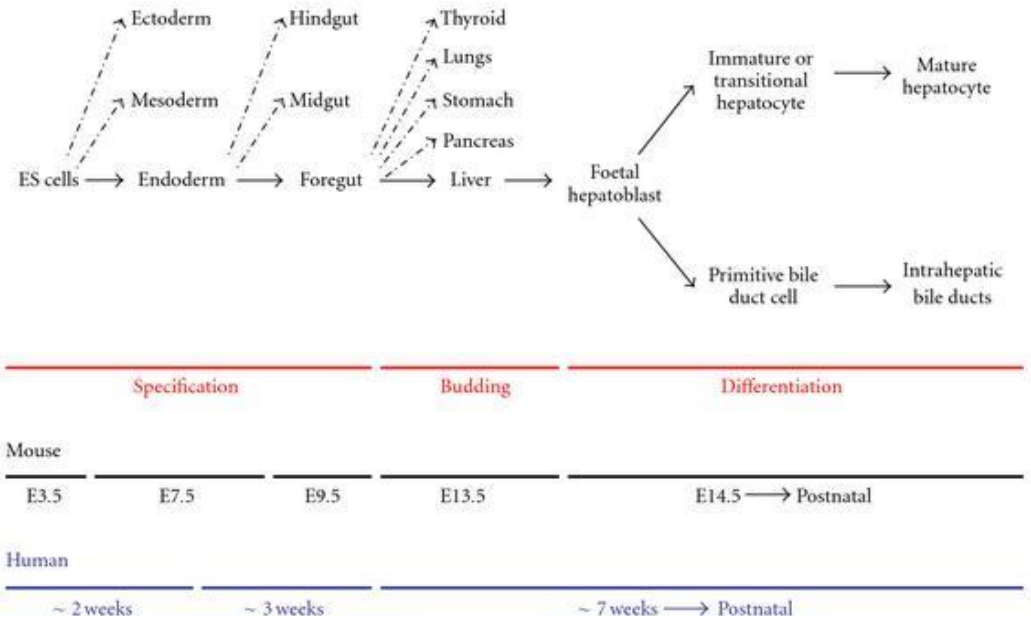

Figure 1.3: Stages of mouse and human liver development. Embryonic stem cells derived from the inner mass of the blastocyst give rise to three principal germ layers: ectoderm, mesoderm, and endoderm. The anterior region of the endoderm forms the foregut. Following hepatic specification of foregut endoderm, hepatic cells (hepatoblasts) will bud into the septum transversum mesenchyme and continue to proliferate and differentiate. Hepatic and bile epithelial cells maturation continues until several weeks after birth. The red bars highlight the key stages of liver development. The black and blue bars indicate mouse and human liver development respectively. Picture adapted from Kung *et al*, 2010.

1.2.1 ENDODERM FORMATION

In Amniotes the definitive endoderm (DE) is formed during the gastrulation process where it emerges as a sheet of cells from anterior end of the primitive streak (Grapin-Botton, 2008). A wide number of studies have demonstrated that the DE formation involves epithelial – mesenchymal transition (EMT) and requires Snail/Slug gene to repress E-cadherin expression (Nakaya *et al*, 2008; Blanco *et al*, 2007). The movement of the endoderm is strictly controlled by the mesoderm-derived Sdf1/Cxcl12b acting on C-X-C chemokine receptor type 4 (CXCR4) -expressing endoderm in zebrafish and *Xenopus* (Fukui *et al*, 2007; Mizoguchi *et al*, 2008).

Transforming growth factor β (TGFβ) signalling has been demonstrated to be essential in endoderm formation. One of the major TGFβ growth factors, Nodal, has been shown to initiate both endoderm and mesoderm formation in a concentration – dependent manner, where high levels of this protein induce endoderm and low levels lead to mesoderm formation (Zorn and Wells, 2007; Shen, 2007; Dougan *et al*, 2003). The other TGFβ growth factors such as growth/ differentiation factor 1 (Gdf1) and 2 (Gdf2) are expressed in the node like Nodal and enhance its activity by forming heterodimers (Tanaka *et al*, 2007). Although Nodal is essential for *in vivo* endoderm development, Yasanuga *et al* (2005) and D'Amour *et al* (2005) have demonstrated that endoderm can be efficiently generated *in vitro* from mouse and human embryonic stem cells using only Activin A as a surrogate of Nodal.

To generate endoderm, Nodal directly stimulates SRY-box 17 (Sox 17) expression which in turn activates hepatic nuclear factor 1β (HNF1β) and Forkhead A family (FoxA1-3) in part through synergistic interactions with β-catenin (Sinner *et al*, 2004). In vertebrates, GATA family (Gata 1-6) that is partially regulated by Nodal signalling has been shown to control the expression of different factors involved in activation of endoderm such as hepatic nuclear factor 4 (HNF4) (Morrisey, 1998).

Nodal is a downstream target of Wnt pathway. Conlon *et al* (1994) and Huelsken *et al* (2000) have proven that lack of Nodal or β-catenin signalling in mouse embryos resulted in failure of primitive streak formation, suggesting that interaction between Nodal and Wnt is essential to form definitive endoderm. Further studies on Wnt pathway revealed that specifically Wnt3 acts in synergy with Nodal, as the mouse germ layer formation and expression of mesendoderm markers are dependent on that gene (Liu, 1999).

1.2.2 FOREGUT SPECIFICATION

High Nodal signalling is required to make anterior definitive endoderm that at later stages of gastrulation is developed to epithelial gut tube surrounded by mesoderm (Zorn and Wells, 2007). The mesodermal signals (such as Wnt and Fibroblast Growth Factor (FGF)) pattern the gut tube to three particular domains: foregut (expressing Hhex), midgut (expressing Pdx1), and hindgut (expressing Cdx), where foregut is the major precursor for liver, pancreas, gall bladder and lungs. (Moore –Scott *et al*, 2007; Tremblay and Zaret, 2005). Several studies have demonstrated that temporal and spatial gradients of Wnt (McLin *et al*, 2007) and FGF (Dessimoz *et al*, 2006) along with mesenchyme-derived bone morphogenetic protein (BMP) (Roberts *et al*, 1995) and retinoic acid (Stafford *et al*, 2004) direct the patterning along the anterior-posterior axis necessary for hepatic competence in the ventral foregut region. Wnt and FGF secreted from the posterior mesoderm have been demonstrated to promote dose-dependent expression of Pdx1 and CdxB, which specify midgut and hindgut respectively (Kumar *et al*, 2003; and Wells and Melton, 2000) and suppress the expression of Hhex important in the formation of foregut (Dessimoz *et al*, 2006). The anterior (endoderm) region inhibits the signalling of Wnt and FGF, which results in the establishment of foregut identity. In addition, Wnt-antagonists such as secreted frizzled – related protein 5 (Sfrp5) expressed in the foregut endoderm are expressed to weaken/inhibit Wnt activity in the foregut region (Dessimoz *et al*, 2006; McLin *et al*, 2007).

Transcription factors such as Foxa2, Gata 4-6 and Hhex play an important role in foregut organogenesis, therefore hepatic competence is strictly dependant on the activity of these genes. Studies using DNA footprinting to identify potential elements that control albumin expression revealed that Foxa2 and Gata 4 were capable to bind the albumin enhancer before the onset of albumin expression, suggesting that these factors were enhancing the chromatin accessibility to allow hepatic genes to be transcribed in response to external stimuli (Bossard and Zaret, 1998; Gualdi *et al*, 1996).

1.2.3 HEPATIC SPECIFICATION

Specification of the hepatocytic lineage from the foregut endoderm requires two major signals: FGF signal (FGF1, FGF2, and FGF8) from cardiac mesoderm and bone morphogenetic protein (BMP2 and BMP 4) signal from septum-transversum-mesenchyme (STM) (Jung *et al*, 1999; Chung *et al*, 2008, Deutsch *et al*, 2001; Rossi *et al*, 2001; Chung *et al*, 2008; Shifley *et al*, 2012).

Several studies have demonstrated that removal of cardiac mesoderm as well as inhibition of either FGF signalling or FGF receptors (FGFR-1 and FGFR-4) located on the endodermal cells led to liver induction failure due to lack of albumin mRNA expression. The downstream pathways of FGF signalling are still unclear, however a few studies suggest that FGF controls MAP kinase pathway and PI3K pathway that regulate hepatic gene expression and hepatic growth respectively (Jung *et al*, 1999; Kinoshita and Miyajima, 2002; Calmont *et al*, 2006).

A number of studies demonstrated that BMP family plays an essential role in hepatic induction (Duncan and Watt, 2001; Shin *et al*, 2007). Zimmermann *et al* (1996) studies identified that BMP4-deficient embryos or suppression of the BMP signalling by a natural antagonist, Xnoggin, resulted in liver bud failure and inhibition of albumin production. Moreover, Xnoggin signalling was also capable of suppressing the albumin in FGF- induced endodermal cells, suggesting that BMP signalling is required to enhance the FGF –mediated induction of liver development. The other studies also suggested that knockdown of BMP gene in mice resulted in reduced expression of GATA4 – one of the major liver –enriched transcription factors that regulates the hepatic factor signalling network (Rossi *et al*, 2001; Darlington, 1999).

1.2.4 LIVER BUD FORMATION

Once hepatic specification is established, hepatic endoderm breaks down and allows newly-formed hepatoblasts to invade the STM. This results in the formation of the liver bud. The process of delamination strictly depends on the activity of certain transcriptional factors such as Hhex, GATA4, GATA6, as wells as on Prox 1,

and Onecut. Studies have demonstrated that in Hhex -/- embryos, the epithelium arrests in a simple columnar state, therefore preventing hepatoblasts to invade STM (Bort *et al*, 2006; Keng *et al*, 2000). In addition, GATA 4 -/- embryos lack STM (Watt *et al*, 2007), and along with GATA6-/- embryos have been demonstrated to have early defects in foregut morphogenesis (Zhao *et al*, 2005, Zhao *et al*, 2008). Prox 1 and Onecut were shown to control the expression of extracellular proteins (ECM) and matrix metalloproteinases (MMPs) that are important in hepatoblast migration and liver bud colonization (Margagliotti *et al*, 2007; Margagliotti *et al*, 2008).

In addition, endothelial signals such as vascular endothelial growth factor receptor gene (Vegfr-2) and hepatoblast chemoattractant Neurturin are required for proper migration of the early bi-potential progenitors into the stroma of the STM (Matsumoto *et al*, 2001; Tatsumi *et al*, 2007).

Once the cells have migrated, the STM secretes a variety of factors such as FGF, BMP, Wnt, TGFβ, HGF and retinoic acid that promote liver bud growth and hepatoblast survival (Berg *et al*, 2007; Shin *et al*, 2007; McLin *et al*, 2007; Ishikawa *et al*, 2001; Negishi *et al*, 2010).

1.2.5 HEPATOCYTE DIFFERENTIATION AND MATURATION

Once specified, the bi-potential hepatoblasts express markers of fetal (α-fetoprotein; AFP) or adult (hepatic nuclear factors 4a (HNF4a) and 6 (HNF6), albumin (ALB)) hepatocytes and biliary epithelium (cytokeratin 17 (CK17) and 19 (CK19)). Hematopoietic cells colonize the nascent liver bud and express certain signals to induce hepatocyte specification.

Notch signalling is one of the first signals to induce the differentiation of bipotential hepatoblasts by either promoting or inhibiting the differentiation either to cholangiocytes (bile ducts) or hepatocytes respectively (Tanimizu and Miyajima, 2004). The other hematopoietic signal, oncostatin M (OSM) in combination with glucocorticoids induces hepatocyte maturation by activating gp130 receptor and JAG/Stat3 signalling pathway and promoting polarization of the epithelium via

E-cadherin expression (Kinoshita *et al*, 1999; Kamiya *et al*, 1999). Hepatocyte growth factor (HGF) secreted from STM and non-parenchymal cells as well as Wnt signalling are important in hepatocyte proliferation, survival, maturation and liver zonation (Kamiya *et al*, 2001; Monga *et al*, 2002; Nejak-Bowen and Monga, 2008).

1.2.6 FETAL, NEONATAL AND ADULT LIVER

As liver plays a major role in synthesis of proteins and biotransformation of xenobiotics, it is important to take into consideration development changes of this organ and different metabolic capacity at fetal, neonate and adult stage. During gestation, the fetus is able to rely on metabolic activity of maternal liver in order to allow fetal liver to develop these functions. In the neonate, the liver still remains immature and undergoes several changes in its functional capacity during the early postnatal period; however the immaturity of the organ has little consequences on the healthy term neonate. Contrary to term neonates, preterm neonates are susceptible to the effects of immature liver, placing them at risk of hypoglycaemia, cholestasis, hyperbilirubinemia, bleeding and impaired drug metabolism (Grijalva and Vakili, 2013).

There are several postnatal changes in liver development before it gains the full synthetic and metabolic capacity of the adult organ. At birth, hepatocytes are arranged in plates at least three cells thick between the portal triads and central veins and by five months after birth, the sheets have thinned to two cells thick. Until five years of age, these extra layers of cells defend the neonate from entrance of potentially toxic substances from the sinusoids before obtaining the one sheet of cells as established in adult liver (Macsween, 1994; Gow *et al*, 2000).

What is more, during neonatal stage hepatocytes increase in size as well as in diameter of hepatic lobules and quantity of endoplasmic reticulum (ER). In addition, in the early postnatal period, sinusoidal fenestrae increase in density along with establishment of metabolic zones within the acinus (Barbera-Guillem *et al*, 1986; Gow *et al*, 2000).

Contrary to hepatic architecture, bile duct and bile canaliculi structure are immature in mammalian liver, and development of these biliary cells continue 1-2 weeks after birth as indicated in mouse and rat liver models (Shiojiri, 1997).

In the case of liver circulation, the fetal organ receives highly oxygenated blood and nutrients via the umbilical vein that supplies approximately 75% of the total blood to the liver (Haugen *et al*, 2005). In man after birth, with the loss of the umbilical vein input, a larger proportion of the portal vein blood flow is shunted away from the liver through the *ductus venosus* (Rudolph, 1983; Nagano *et al*, 1999). In general, the closure of the *ductus venosus* occurs within 2 weeks of life in the majority of neonates, however in preterm neonates this process might be significantly delayed causing portacaval shunt (Kondo *et al*, 2001; Loberant *et al*, 1999). This liver shunt may result in direct pass of metabolic and pharmacologic substances from the portal into the systemic circulation and may interfere with child's growth and development (Fugelseth *et al*, 1998).

As adult liver performs various metabolic functions (i.e lipogenesis and drug detoxification), the embryonic liver has much less metabolic activity and rather, functions as a hematopoietic microenvironment (Kinoshita *et al*, 1999). Increasing evidence indicate that hematopoietic stem cells (HSCs) originating from the aorta – gonad-mesonephrons (AGM) region migrate to the fetal liver to generate numerous definitive HSCs. The hematopoietic microenvironment in the fetal liver is created by a complex of cell types, including epitehliocytes, resident macrophages, and several stromal cell populations of mesenchymal origin such as hepatic stellate cells, fibroblasts, myofibroblasts, vascular smooth muscle and endothelial cells, and mesenchymal stromal cells (Payushina *et al*, 2012). These cell types secrete different adhesive factors (e.g E-selectin, VCAM-1), chemoattractants (eg. stromal cell-derived factor -1) or extracellular matices (e.g fibronectin and collagen) that support proliferation and survival of hematopoietic stem cells in the fetal liver. Although the majority of liver metabolic functions appear peri- or postnatally, haematopoiesis – supporting activity of the liver is lost during late-fetal development. Subsequently, HSCs migrate to the bone marrow or around spleen around the perinatal stage to constitute the adult type of hematopoietic system.

Plasma protein synthesis and level of biotransformation significantly differ among fetus, neonates, and adult. The main serum protein produced by the fetal liver is alpha-fetoprotein (AFP) which reaches its final concentration by the end of the first trimester. The albumin (ALB) synthesis begins at 16th week of gestation and reaches the adult levels by the end of gestation (37 weeks). The coagulation proteins (e.g fibrinogen) are usually low in newborn infants and reach adult levels within first days after birth.

Generally, the hepatic drug metabolism pathways in the fetal and neonate livers are immature which results in prolonged drug elimination and increased plasma half-lives.

The phase I metabolic enzymes such as cytochromes P450 families demonstrate significant differences in expression and activity in the fetus and neonate compared to adults. At birth, the cytochrome proteins are expressed at 30% of adult concentration, and they reach adult levels by 1 year of age.

It is important to mention that CYP3A7 is the major cytochrome in human embryonic, fetal and newborn liver (Kitada and Kamataki, 1994). Once it reaches its peak point at early neonatal period, the enzymes activity transitions to CYP3A4, one of the major adult cytochromes. CYP3A4 expression and activity then reaches 30 - 50% of adult levels from 3 to 12 months of age (Lacroix *et al*, 1997).

Phase II enzymes that are responsible for detoxification of certain substrates, demonstrate different level of expression throughout liver development. It has been proven that neonates have limited enzymatic glucuronidation capacity as indicated by their limited ability to conjugate bilirubin during early postnatal life resulting in unconjugated hyperbilirubinemia (Krauer and Dayer, 1991). Bilirubin is biotransformed by UDP-glucuronosyltransferase 1A1 (UGT1A1, UGTs) and its expression is low during fetal and early postnatal development, and reaches 25% of adult levels by 3 months of age (Coughtrie *et al*, 1988). Contrary to UGTs, hepatic sulfotransferases (SULT) that are responsible for sulfate conjugation of xenobiotics are much highly expressed in fetus and neonate, potentially suggesting their essential role in detoxification in early liver development (Alcorn and McNamara, 2002).

Mooij *et al* (2014) study has demonstrated that hepatic expression of human influx and efflux transporters depends on the age. Hepatic Phase III transporters such as MRP2, OATP1B1 and OATP1B3 were significantly decreased in all paediatric age when compared with adults. What is more, MDR1 (P-gp) gene expression in fetuses, neonates and infants was notably lower than in adult livers.

1.3 LIVER DISEASES

Some of the most common causes of liver injury include adverse drug reactions, alcohol and drug abuse, nonalcoholic steatohepatitis, and viral infection (Musana *et al*, 2004; Adams and Angulo, 2006). These factors lead to liver fibrosis, which results in the accumulation of extracellular matrix proteins (EMPs). Fibrogenic cytokines such as TGF-β, angiotensin II, and leptin play an important role in this process, regulating the production of collagen during liver injury (Duffield *et al*, 2005; Battaler and Brenner, 2005). Accumulation of EMPs leads to scar formation and upon chronic exposure may result in liver cirrhosis (Iredale, 2007). This has dire consequences for liver function and increases the risk of developing hepatocellular carcinoma (HCC) (Gines *et al*, 2004; Schrader *et al*, 2011). HCC is the third most common cause of cancer-related death worldwide (Vara *et al*, 2011), and advances in research are required to better understand HCC progression and treatment.

Recent studies (Schrader *et al*, 2011) have demonstrated that the biochemical composition of the extracellular matrix (ECM) is an important factor in HCC biology. In these studies, matrix stiffness consistent with chronic liver disease promoted HCC proliferation, whereas the less-stiff physiological environment fostered cellular dormancy.

Because the liver plays a major role in metabolism, mutations or polymorphisms that affect metabolic or synthetic activity can have profound effects on liver function and therefore susceptibility to injury. For instance, the gene mutation in Wilson's disease occurs on chromosome 13, and in homozygous form leads to the diminished function of the hepatic protein ATP7B. This subsequently results in a decreased excretion of

the biliary copper and accumulation of this element in hepatocytes, potentially leading to serious hepatocellular damage (Ala *et al*, 2007).

What is more, a genetic mutation in SERPINA1 gene that encodes alpha-1-antirypsin (A1AT) protein, leads to the A1AT deficiency in the blood and lungs, and deposition of excessive abnormal protein in liver cells (Stoller and Aboussouan, 2005).

To study this issue in greater depth, researchers are developing human models that more accurately predict the relationship between genotype and phenotype. These models are essential to establishing a better understanding of human disease. For most patients, genetic factors will result in different responses that may affect drug absorption, distribution, efficacy, and excretion. This is extremely interesting in the context of race and ethnicity (Xie *et al*, 2001). In most populations, phase I (CYP450) and phase II (UGTs, SULTs, NATs, GSTs, and TPMT) drug metabolizing activities are polymodal, resulting in either extensive, intermediate or poor drug metabolism (Wilkinson, 2005; Jancova *et al*, 2010). For example, single nucleotide polymorphisms in N - acetyltransferases may cause slow or rapid acetylation. Thus, they become a predisposing factor affecting the sensitivity of individuals to drugs. Different variations of alleles in drug-metabolizing enzymes may also play an important role in the development of various types of cancers. For instance, genetic polymorphism of glutathione S transferases (GSPT1 and GSTA1) may increase the risk of developing HCC (Chen *et al*, 2010).

Therefore, the level of interindividual sensitivity to different drugs is an important predictive measurement that will lead to a better understanding of drug toxicity and "tipping points" and likely reduce the instances of drug-induced liver injury (DILI) and/or the predisposition to HCC (Kaplowitz, 2004).

1.4 MODELLING LIVER BIOLOGY AND DISEASE *IN VITRO*

There are significant morbidity, mortality, and economic burden associated with human liver disease. Therefore, developing new systems that improve the study and prediction of liver disease is likely to lead to more effective interventions in the future.

Current approaches use human and animal cell cultures, with primary human hepatocytes viewed as the most physiologically relevant model for examining hepatocyte biology *in vitro*. However, the predictive nature of these models is severely limited because of the scarcity and poor quality of these cells. To bypass issues of scarcity, several groups used different techniques to immortalize human hepatocytes. Unfortunately, the derived cell lines exhibited poor function and karyotypic instability, limiting large-scale application (Allain *et al*, 2002; Cai *et al*, 2000; Delgado *et al*, 2005; Wege *et al*, 2003). More recently, the HepaRG and Fa2N-4 cell lines were established and possess CYP450 activity (Guillouzo *et al*, 2007; Mills *et al*, 2004; Hariparsad *et al*, 2008). Although the HepaRG and Fa2N-4 cell lines may be attractive sources of cells for modelling human drug metabolism, their usefulness in predicting drug toxicity is not optimal because they remain more resilient than primary human hepatocytes to toxicological insult.

1.5 PLURIPOTENT STEM CELLS (PSCs) AS RENEWABLE SOMATIC CELL-BASED MODELS

In recent years, somatic and stem cell populations have been studied for their ability to differentiate or transdifferentiate into hepatocyte-like cells (HLCs). Additionally, many studies have confirmed that fetal and adult liver stem cells have biopotential properties and are able to differentiate into hepatocytes and cholangiocytes (Dalgetty *et al*, 2009; Medine *et al*, 2010; Schmelzer *et al*, 2006).

The approach taken in this project as well as widely used by others employs PSCs; human embryonic stem cells (hESCs) and induced PSCs (iPSCs). Both populations may provide new opportunities for improving cell-based models owing to their renewable nature, plasticity, and isolation from a known genetic background. hESCs are derived from the inner mass of blastocysts unsuitable for human implantation and demonstrate self-renewal and pluripotency (Reubinoff *et al*, 2000, Thomson *et al*, 1998). hESCs were first derived from the inner cell mass (ICM) of the blastocyst stage (100-200 cells) of emryos generated by *in vitro* fertalization. hESCs are characterised by two unique properties: self-renewal, capable of dividing

indefinitely in culture, and pluripotency, the ability to differentiate to variety of cell types from all germ layers; the endoderm, mesoderm, and ectoderm (Cai *et al*, 2006; Hoffman and Carpenter, 2005; Vazin and Freed, 2010). These pluripotent stem cells are defined by the expression of pluripotent transcription factors; Oct 3 / 4, Nanog, and Sox2 in addition to their cell surface antigen pattern; defined by the presence of stage specific embryonic antigens (SSEA 3 and 4) and tumour rejection antigens (Tra 1-60 and Tra-1-81). Pluripotency is measured using a combination of spontaneous (Fletcher *et al*, 2008) and directed differentiation to cell types including muscle (Xiao *et al*, 2008) , cardiomyocytes (Melkoumian *et al*, 2010), hepatocytes (Hay *et al*, 2008ab) and neuronal derivatives (Lee *et al*, 2007).

In recent years, significant progress has been made in differentiating PSCs into HLCs. The use of defined factors and serum-free media has facilitated the development of efficient procedures for HLC specification, which is likely to have significant impact in the short term and improve our understanding of human liver biology. Moreover, the development of defined procedures may have clinical applications in the future.

Current methods used for HLC generation are spontaneous and directed differentiation. The spontaneous technique involves formation of three-dimensional multicellular aggregates, termed embryoid bodies. In the presence of particular factors these three-dimensional structures differentiate into HLCs (Asahina *et al*, 2004; Lavon *et al*, 2004; Duan *et al*, 2007; Basma *et al*, 2009). Although this method is reproducible, its spontaneous nature has several drawbacks, including low efficiency during HLC production and mixed cell type generation.

Directed differentiation is based on the application of extracellular signals in two dimensions to mimic the physiological pathways required during human liver development and has proved to be more efficient (D'Amour *et al*, 2005; Agarwal *et al*, 2008; Cai *et al*, 2007; Hay *et al*, 2007; Hay *et al*, 2008; Duan *et al*, 2010). While both of these approaches to hepatocyte differentiation have been optimized, they still require further refinement if stem cell–derived technologies are to be widely adopted.

In addition to hESCs, iPSCs are used within the field. These cells can be derived from litmitless genetic background, offering significant advantages over hESCs.

Derivation of human iPSCs (hiPSCs) from somatic cells by the introduction of four transcription factors (Oct 3/4, Sox2, c-Myc, Klf4) has created new opportunities in regenerative medicine (Takahashi and Yamanaka, 2006). iPSCs were initially generated from murine fibroblasts and resembled ESCs in various ways including morphology, proliferation, gene expression, and teratoma formation. In 2007, Takahashi *et al* successfully reprogrammed human dermal fibroblasts into a pluripotent state. Similar to murine iPSCs, hiPSCs were able to differentiate into cell types of three germ layers *in vitro* and form teratomas *in vivo*. These studies were ground-breaking and have provided enormous potential to further our understanding of human biology and the influence of genetics. For example, recent studies have also focused on inherited metabolic disorders (IMDs) of the liver. IMDs are usually caused by genetic mutations that affect key enzymes within hepatocytes. Rashid *et al* (2010) made a breakthrough in determining the potential of iPSCs by studying phenotype-genotype interactions. The authors generated functional hepatocytes from iPSCs derived from patients with familial hypercholesterolemia, glycogen storage disease type I, and alpha-1 antitrypsin deficiency.

The results from these studies demonstrated that iPSC-derived hepatocytes recapitulate some of the pathophysiological features of the disease state. Such findings demonstrate the importance of iPSC models in better understanding human disease and may, in the future, lead to the development of platform technologies that could be used to identify novel medicines to better treat human disease.

1.5.1 USING DEFINED CELL NICHES TO STABILIZE CELL PHENOTYPE

Through co-culture of HLCs with other specific cell types and/or supplementation with growth factors, and ECMs, hepatocellular function will likely be improved and more closely align with human physiology (Ishii *et al*, 2008; Ishii *et al*, 2010; Tuleuova *et al*, 2010). Although co-cultures provide a supportive role, the undefined nature and the scarcity of primary material complicates culture definition and cost-effective scale-up

(Bhatia *et al*, 1997). Therefore, many laboratories have focused on other approaches to improve cell biology.

Recent studies by Miki *et al* (2011a; 2011b) demonstrated that oxygenation as well as continuous supply of cells with fresh medium using hollow fibre technology promoted hepatic gene expression. Additionally, studies demonstrated that defined medium, a synthetic tissue culture substratum, and posttranslational modifications play important roles in improving and maintaining hepatic function, phenotype, and life span (Hay *et al* 2011; Zhou *et al*, 2012; Hannoun *et al*, 2010; Lucendo-Villarin *et al*, 2012; Takayama *et al*, 2012; Takayama *et al*, 2013; Vuoristo *et al*, 2013; Medine *et al*, 2013). What is more, these improvements in combination with scale up abilities (Vosough *et al*, 2013), and serum-free differentiation approaches (Szkolnicka *et al*, 2013 and 2014a/b) provide potential GMP ready options for large scale manufacture.

1.5.2 RECENT ADVANCES IN GENERATION OF HEPATOCYTES

Recently, other approaches that bypass pluripotency have been developed to generate HLCs. For example, Huang *et al* (2011) and Sekiya & Suzuki (2011) have generated induced hepatocytes (iHEPs) from mouse fibroblasts.

The transdifferentiated iHEPs were produced from murine fibroblasts using viral transduction and expression of GATA4, HNF1a, and FOXA3 and inactivation of $p19^{Arf}$ or HNF4a expression in combination with FOXA1, FOXA2, or FOXA3. Three years later Huang *et al* (2014) and Du *et al* (2014) have generated metabolically functional hiHEPs from human somatic cells using viral transduction and expression of either FOXA3, HNF1A, and HNF4a or overexpression of hepatic nuclear factors (HNF1a, HNF4a, HNF6) in combination with the maturation factors such as ATF5, PROX1, and CEBPA. Although promising, the transdifferentiated cells depend on primary material and its availability. What is more, the transdifferentiation techniques still require further strategies to address the lack of proliferation of these cells and generation of mixed populations.

Scale-up of cell-based technologies is essential for their *in vitro* and *in vivo* application. Recent studies have improved the expansion of undifferentiated hESCs and hiPSCs as three-dimensional aggregates without the need for feeders or microcarriers (Amit *et al*, 2010; Larijani *et al*, 2011).

The resulting systems exhibited stable karyotype, sustained pluripotency, and self-renewal. These prototype systems hold great promise and may lead to a decrease in production costs and provide controllable systems for scaling up PSCs and their derivatives. MicroRNAs are additional key regulators in many cellular processes, including hepatocyte differentiation of hESCs. Kim *et al* (2011) demonstrated that microRNAs are modulated during hESC differentiation to hepatocytes. In particular, mir-122 played a significant role in regulating hepatic maturity; therefore, microRNAs appear important in delivering high-fidelity HLCs for *in vitro* and *in vivo* approaches.

In addition to pluripotent stem cell derived hepatocytes, liver stem cells can now be isolated and expanded *in vitro* in a three –dimensional structure (3D) offering a new promise for large-scale production. Huch *et al* (2013) have demonstrated that single mouse Lgr5+ liver stem cells can be expanded as epithelial organoids in Rspo1 (Wnt agonist)-based culture medium *in vitro* and subsequently can be differentiated into functional hepatocytes *in vitro* and *in vivo*. Two years later, the same group has reported a successful expansion of primary human bile duct cells as bipotent stem cells into 3D organoids (Huch *et al*, 2015). These cells are able to differentiate into functional hepatocytes *in vitro* and generate bona fide hepatic cells upon transplantation.

1.5.3 'OFF THE SHELF' CELL - BASED THERAPIES

Currently, orthotopic liver transplantation is the only effective treatment for fulminant or end-stage liver disease. Although successful, liver transplantation is significantly limited owing to a shortage of donor organs. The lack of sufficient donor livers led scientists and physicians to search for alternative transplantation strategies.

Two interesting areas of development are hepatocyte transplantation and the bioartificial liver device. Hepatocyte transplantation has been considered as a viable treatment for patients suffering from liver disorders (Azuma *et al*, 2007; Zern, 2009; Hay, 2010). Most recently, a peritoneal transplantation procedure carried out at Kings College Hospital (United Kingdom) had a positive outcome and removed the need for orthotopic liver transplantation.

Extracorporeal support is another option that uses the bioartificial liver devices fuelled with viable hepatocytes capable of performing essential liver functions. Although these devices have been successful in supporting patients until transplantation, the cell types used in these systems need to be improved. In particular, hepatocyte function, long-term stability, and cost-effective scale-up are key. In addition to the current clinical methodologies, a recent study with iPSC technology has provided hope that in the future, disease-causing mutations may be corrected using DNA editing tools. Yusa *et al*. (2011) achieved biallelic correction of a point mutation (Glu342Lys) in the alpha-1-antitrypsin gene (A1AT) by using a combination of zinc finger and piggyBAC technology. Importantly, genetic correction of hiPSCs restored function of A1AT in derived liver cells *in vitro* and *in vivo*. Although this approach is very promising, a number of important safety issues (Payne *et al*, 2010) must be addressed before this technology can be routinely deployed within the clinic.

1.6 DRUG METABOLISM

Drug metabolizing enzymes (DMEs) play central roles in the metabolism, elimination, and/or detoxification of xenobiotics or exogenous compounds introduced into the body (Meyer, 1996). These enzymes protect the body against the potential harmful exposure to certain endobiotics and xenobiotics from the environment. Most of the xenobiotic sources include environmental pollution, cosmetic products, food additives, and drugs. These compounds usually are lipophilic, leading to accumulation of these products in the body, resulting in toxicity.

In order to efficiently eliminate them and minimize the potential injury, they are subjected to one or multiple pathways that constitute the phase I, phase II metabolising enzymes and phase III transporters (Gonzalez and Tukey, Chapter 3; Xu et al, 2005) (Figure 1.4; Table 1.1).

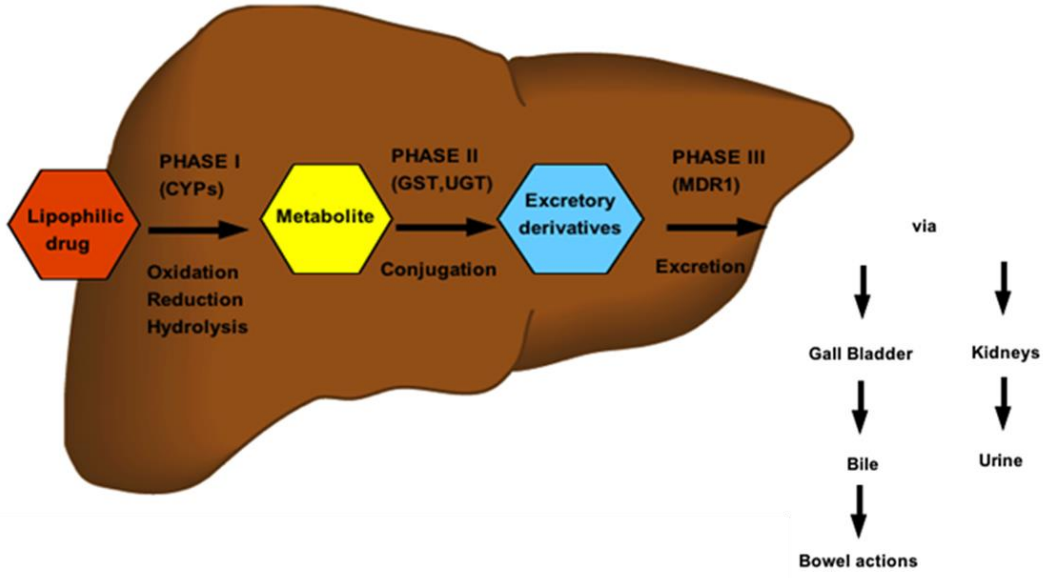

Figure 1.4: Phases of drug metabolism. Most of the drugs are lipophilic and therefore have to be processed by Phase I reactions that involve oxidation, reduction and hydrolysis. This leads to the formation of a highly reactive metabolite that has to be detoxified by Phase II conjugations reactions that involve enzymes such as GSTs and UGTs. Once metabolized, the waste product is excreted from the cell by Phase III transporters either to urine or bile. Abbreviations: CYPs, Cytochromes P450; GST, glutathione S-transferases; UGT, UDP-glucuronosyltransferases; MDR1, Multi-drug resistant ABC transporter 1. Picture based on the figure from www.diversehealthservices.wordpress.com.

ENZYMES/ TRANSPORTERS	REACTIONS
PHASE 1	
Cytochrome P450s (CYPs)	*C and O oxidation, dealkylation, others*
Flavin – containing monooxygenases (FMO)	*N, S, and P oxidation*
Epoxide hydrolases (mEH, sEH)	*Hydrolysis of epoxides*
PHASE 2	
UDP – glucuronosyltransferases (UGTs)	*Addition of glucoronic acid*
Glutathione S – transferases (GSTs)	*Addition of glutathione*
Sulfotransferases (SULTs)	*Addition of sulfate*
N- acetyltransferases (NAT)	*Addition of acetyl group*
Methyltransferases (MT)	*Addition of methyl group*
PHASE 3	
ATP –binding cassette transporters (ABC)	*Transport of ions, amino acids, peptides, sugars, drugs (drug efflux)*
Solute carriers transporters (SLC)	*Transport of peptidomimetics, translocation of cationic drugs (drug influx); antiporters*

Table 1.1: Phase I, Phase II enzymes and Phase III transporters involved in drug metabolism. Adapted from Gonzalez and Tukey, 2005. Abbreviations: C; carbon, O, oxygen; N; nitrogen; S; sulphur; P; phosphorus.

1.6.1 PHASE I

Phase I of drug metabolism involves oxidation, reduction, or hydrolytic reactions. In this phase, enzymes (Table 1.1) introduce a functional group leading to the modification of the drug. The modified drug usually carries hydroxyl (-OH), carboxyl (-COOH), sulfhydryl (-SH), or amine (NH_2) group. The role of functional group is to increase the water solubility of the drug and alter its biological properties. Reactions carried out by these enzymes usually lead to the inactivation of an active drug. Currently, cytochromes P450 enzymes are considered to play the major role in Phase I drug metabolism (Gonzalez and Tukey, 2005).

Cytochromes P450

Forms of CYPs and their distribution

Cytochromes P450 (CYPs) are microsomal enzymes found abundantly in the liver, gastrointestinal tract, lungs and kidney. Twelve families exist in all mammals, whereas only five of them can be found in human: CYP1, CYP2, CYP3, CYP4, and CYP7. Particularly, enzymes such as CYP1A2, CYP2C9, CYP2C19, CYP2D6, CYP3A4 and CYP3A5 play an important role in hepatic / extra-hepatic metabolism as well as reduce or alter the pharmacologic activity of many drugs and facilitate their elimination (Wilkinson, 2005; Lewis, 2003; Pascussi *et al*, 2003).

Function

Cytochromes (CYP) are a superfamily of enzymes that contain a molecule of heme that is non - covalently bound to the polypeptide chain. Heme, the oxygen-binding moiety that also is found in the haemoglobin, contains one atom of iron in a hydrocarbon cage that binds oxygen in the CYP active site as a part of the catalytic cycle of these enzymes.

These enzymes use O_2 and H^+ derived from the cofactor- reduced nicotinamide adenine dinucleotide phosphate (NADPH) to carry out the oxidation of different substrates. Metabolism of a substrate by a CYP results in the production of an oxidized substrate and a molecule of water as a by-product. However, for most of these enzymes the reaction is 'uncoupled', consuming more O_2 than the substrate metabolized and producing activated oxygen (O_2^-). This highly active molecule is usually converted to water by the enzyme superoxide dismutase (Lewis, 2003).

Substrates, inhibitors and inductors of CYPs

The major substrates, inducers and inhibitors are in the Table 1.2.

Table 1. Medications That Are Substrates, Inhibitors, or Inducers of CYP450 Isoenzymes[2,16-18]

	CYP1A2	CYP2C9	CYP2C19	CYP2D6	CYP3A4
Significant Substrates	Caffeine Clozapine Olanzapine Theophylline	Glipizide Nateglinide S-warfarin	Clopidogrel Phenytoin	Amitriptyline Atomoxetine Carvedilol Codeine Haloperidol Hydrocodone Metoprolol Tamoxifen Tramadol Tricyclic antidepressants	Alprazolam Amiodarone Calcium channel blockers Cyclosporine Fentanyl Methadone Midazolam Oxycodone Quetiapine Protease inhibitors Repaglinide Simvastatin Tacrolimus
Strong Inhibitors[a]	Fluvoxamine	Fluconazole	Fluvoxamine Isoniazid Lansoprazole Omeprazole	Bupropion Fluoxetine Paroxetine Quinidine Terbinafine	Clarithromycin Compounds in grapefruit juice Isoniazid Itraconazole Ketoconazole Nefazodone Protease inhibitors
Moderate Inhibitors[b]	Cimetidine Ciprofloxacin Fluoxetine	Amiodarone Fluoxetine Metronidazole Sulfamethoxazole	Cimetidine	Amiodarone Diphenhydramine Duloxetine Sertraline	Amiodarone Cimetidine Diltiazem Erythromycin Fluconazole Fluoxetine Verapamil
Major Inducers	Carbamazepine Phenytoin Phenobarbital Rifampin Compounds from cigarette smoking Compounds in St. John's wort	Carbamazepine Phenytoin Phenobarbital Rifampin Compounds in St. John's wort	Carbamazepine Phenytoin Phenobarbital Rifampin Compounds in St. John's wort		Carbamazepine Oxycarbamazepine Phenytoin Phenobarbital Rifampin Compounds in St. John's wort

AUC indicates area under the curve; CYP, cytochrome P450.
[a]Increases substrate plasma AUC values more than 5-fold.
[b]Increases substrate plasma AUC values 2- to 5-fold.

Table 1.2: **Substrates, inducers and inhibitors of major Cytochromes (P450) involved in drug metabolism**. The picture is adapted from Lynch, 2011.

Gene polymorphisms

Gene polymorphisms are a source of genetic variability. This is commonly found in CYP 450 enzymes and influences a patient's response to a particular drug. Persons that inherited two wild –type alleles of particular cytochrome enzyme are considered as 'extensive' (normal) metabolizers. However, inheritance of one or two variant alleles results in decreased enzymes activity or 'poor' metabolizer respectively (Lynch *et al*, 2007). Finally, people with multiple copies of wild-type alleles are considered as 'ultra-rapid' metabolizers (Phillips *et al*, 2001).

In the superfamily of cytochrome P450 enzymes, CYP2D6 was the first one to be identified with genetic polymorphism. The CYP2D6 enzyme is responsible for metabolizing more than 65 drugs on the market and to date around 78 variants of this protein have been identified (Kimura *et al*, 1989). The gene duplication of this enzyme occurs often in people with northeastern African background, whereas it is rarely seen in northern Europeans (Wilkinson, 2005). Contrary to 'ultra-rapid' genotype, the reduced activity of this protein is predominantly seen in blacks (variant CYP2D6*17) and in Southeast Asians (variant CYP2D6*10). As CYP2D6 is particularly involved in biotransformation of codeine to morphine, the pain relief effect is much more difficult to achieve in people with low enzyme activity (poor metabolism) (Sindrup and Brøsen, 1995).

CYP2C19 enzymes has two major variants CYP2C19*2 and CYP2C19*3 that account for more than 95% of cases of poor metabolism. As CYP2C19 is responsible for transforming proton – pump inhibitors (omeprazole, rebeprazole, lansoprazole) these variants are specifically important to Southeast Asia where poor metabolism accounts for approximately 10-25% (Wedlund, 2000). The enzyme CYP2C9 is considered to be the most predominantly expressed CYP enzyme in the human liver (Kirchheiner *et al*, 2004). It metabolizes approximately 10% of the drugs and the two inherited amino acid substitutions Arg144Cys(*2) and Ile359Leu (*3) are known to affect catalytic functions of this protein (Ieiri *et al*, 2000; Sullivan-Klose *et al*, 1996; and Stubbins *et al*, 1996). Patients with these specific CYP2C9 variations have lower mean daily warfarin doses and a greater risk of bleeding (Redman *et al*, 2008).

In case of CYP3A4, more than 20 mutations have been discovered, however the variations do not translate into significant interindividual variability *in vivo* (Ingelman-Sundberg *et al*, 2007). Different CYP3A4 polymorphisms have been described, with decreased (*8,*11, *13, *17), none (*20), and increased activity (*18A) allele *in vitro* (Bożina *et al*, 2009). However, their low frequency cannot explain common interindividual differences in CYP3A4 activity.

It potentially suggests that the enzyme is well preserved, and any possible CYP3A4 variations could be connected with genes that regulate this particular enzyme such as PXR, CAR, or GR transcriptional factors (Urquhart *et al*, 2007; Lamba *et al*, 2005; Hustert *et al*, 2001).

1.6.2 PHASE II

Phase II enzymes (Table 1.1) facilitate the elimination of drugs and lead to the inactivation of electrophilic and potentially toxic metabolites produced by oxidation in Phase I. Most of the phase I enzymes biologically inactivate the drug, whereas the phase II reactions produce a metabolite with improved water solubility and increased molecular weight (conjugation reactions), which serves to facilitate the elimination of the drug from the tissue. Currently, the three major families, UDP-glucuronosyltransferases, sulfotransferases and glutathione S -transferases, play a major role in metabolism of the different drugs.

UDP – glucuronosyltransferases (UGTs)

UGTs and their distribution

The mammalian UGT gene superfamily is known to consist of 117 members, where only four families have been identified in humans: UGT1, UGT2 (divided to 2A and 2B), UGT3 and UGT8.

The enzymes of each family share approximately 40% homology in their DNA sequences, whereas enzymes of each subfamily are approximately 60% similar (Burchell *et al*, 1995).

Currently, there are twenty – two human UGT proteins identified: UGT1A1, 1A3, 1A4, 1A5, 1A6, 1A7, 1A8, 1A9, 1A10; 2A1, 2A2, 2A3, 2B4, 2B7, 2B10, 2B11, 2B15, 2B17, 2B28; 3A1, 3A2 and 8A1 (Mackenzie *et al*, 2008; Miners *et al*, 2006; Sneitz *et al*, 2009). Although, UGTs can be distributed in different tissues, liver is the major location of expression of these proteins. Seven UGT enzymes such as UGT1A1, 1A3, 1A4, 1A6, 1A9, 2B7, and 2B15 have been considered to play a major role in human liver drug metabolism. It has also been described that several UGTs such as UGT1A7, UGT1A8, and UGT1A10 are expressed only in gastrointestinal (GI) tract, and they play an important role during first-pass metabolism of dietary supplements and drugs (Gregory *et al*, 2004; Tukey and Strassburg, 2000; and Cheng *et al*, 1999).

Function

UDP –glucuronosyltransferases (UGTs) play a major role in the process of glucuronidation. These enzymes are the most important enzymes of Phase II in human metabolism. They are responsible for metabolizing many different endobiotics (bilirubin, steroid hormones, bile –acids) as well as are considered to biotransform 40-70% of all clinical drugs (Wells *et al*, 2004). UGTs are a superfamily of a membrane-bound enzymes and catalyse the transfer of glucuronic acid from the cofactor UDP-glucuronic acid (UDPGA) to a substrate to form B-D-glucopyranosiduronic acids (glucuronides), metabolites that are sensitive to cleavage by B-glucuronidase. The enzymes are able to generate O-linked glucuronides that can be formed through the conjugation of UDPGA with aliphatic alcohols, phenols, carboxylic acids, or primary, secondary and tertiary amine linkages (Gonzalez and Tukey, 2005; Jancova *et al*, 2010).

Substrates, inhibitors and inductors of UGTs

The UGT enzymes have been shown to exhibit overlap in substrate specificities, and to date only a few substrate – selective forms of the enzymes have been identified. Glucuronidation of bilirubin, the major product of heme metabolism, is catalysed only by UGT1A1 (Wang *et al*, 2006). The enzyme has also been shown to moderately conjugate simple phenols, anthraquinones, and C_{18} steroids (Tukey and Strassburg, 2000). Isoforms such as UGT1A3, UGT1A9, and UGT2A1 are responsible for conjugation of carboxylic acids (Wen *et al*, 2007), UGT2B7 has been shown to metabolise opioids (Coffman *et al*, 1998), UGT1A6 shows high affinity for conjugating complex phenols and primary amines (Miners *et al*, 2006; King *et al*, 2000), whereas UGT1A10 preferentially conjugates bioflavonoids (Lewinsky *et al*, 2005). In general, a variety of nonsteroidal anti-inflammatory, analgesic, anticonvulsant and antiviral drugs have been described as putative (potential) inhibitors of glucuronidation reactions in humans. Currently, only hecogenin (steroidal saponin) and fluconazole have been shown as selective inhibitors of UGT1A4 and UGT2B7 respectively (Uchaipichat *et al*, 2006a; Uchaipichat *et al*, 2006b), whereas rifampicin has been demonstrated to be a putative UGT inducer in humans (Caraco *et al*, 1997).

Gene polymorphisms

Crigler-Najjar syndrome is a rare disorder that affects the metabolism of bilirubin, resulting in the production of high levels of unconjugated bilirubin that often leads to brain damage in infants (Bosma, 2003) It has been described that there are at least 50 mutations in UGT1A1 enzyme that cause the disease (Kadakol *et al*, 2000). The syndrome is an autosomal recessive disorder, where type I patients have complete absence of UGT1A1, whereas type II patients have partial activity of this particular phase II enzyme. In addition, Gilbert's syndrome, a disease with a similar pathology to Crigler-Najjar, is usually caused by mutation in UGT1 gene and is found in approximately 10% of the population (Ehmer *et al*, 2008).

Sulfotransferases (SULTs)

SULTs and their distribution

Currently, four families of SULTs have been identified in humans: SULT1, SULT2, SULT4, and SULT6. The SULT1 family has 9 members that are divided into four subfamilies: SULT1A1, 1A2, 1A3, 1A4; 1B1, 1C1, 1C2, 1C3; 1E1. The SULT2 family can be divided into two subfamilies: SULT2 (SULT2A1) and SULT2B, where SULT2B is comprised of two isoforms: SULT2B1a and SULT2B1b. SULT4 and SULT6 family have only one member: SULT4A1 and SULT6B1 respectively (Lindsay *et al*, 2008).

It has been reported that members of the same SULT family share approximately 45% amino-acid sequence identity while members of the same subfamilies share approximately 60% homology (Weinshilbourn *et al*, 1997).

SULT enzymes are divided into two major classes: cytosolic and membrane-bound ones. The membrane-bound SULTs are localised in the Golgi apparatus and are responsible for sulfonation of peptides and proteins, whereas the conjugation of xenobiotics such as drugs, steroids, bile acids and neurotransmitters occurs only in the cytosol (Gamage *et al*, 2006).

This group of enzymes is widely distributed. The SULT1A subfamily has been identified in liver, brain, intestine, breast, lung, adrenal gland, kidney, placenta, and blood platelets. SULT1A1 enzymes exhibit the highest expression in the liver, whereas SULT1A3/SULT1A4 is expressed in most of the tissues except of adult liver and SULT1B1 showed very low expression in liver, small intestine, colon and leukocytes. SULT1C subfamily is highly produced in human fetus, and SULT1E1 member shows predominant expression both in fetal and adult liver (Hempel *et al*, 2004). SULT2A1 shows the highest level of expression in liver, adrenal, duodenum and fetal adrenal gland (Duanmu *et al*, 2006).

SULT2B is majorly localised in human prostate (Shimizu *et al*, 2003), placenta (Dongning *et al*, 2004), lung (He *et al*, 2005), kidney (Kohjitani *et al*, 2006) and colon (Geese and Raftogianis, 2001), with no expression in the liver (Dongning *et al*, 2004). Human SULT4A1 has been identified in the brain (Liyou *et al*, 2003), and SULT6B1 is produced in testis and kidney (Lindsay *et al*, 2008).

Function

Sulfotransferases (SULTs) are the second most important group of Phase II enzymes. Sulfonation (sometimes referred as sulfation) reactions are important in metabolism of endogenous low – molecular compounds such as steroids, serotonin, and exogenous compounds (drugs, chemicals). This superfamily of enzymes is located in the cytosol or membrane of the cell, and conjugate sulfate (sulfonate) derived from 3'-phosphoadenosine-5'-phosphosulfate (PAPS) to the hydroxyl groups of aromatic and aliphatic compounds. It has been assumed (hypothesized) that SULTs are the major detoxification enzymes in the developing fetus, as no UGT transcripts were detected in fetal liver at 20 weeks of gestation (Strassburg *et al*, 2002). Additionally, it has been demonstrated that human fetal liver cytosolic fractions showed significant SULT activity towards a large number of substrates such as cortisol, paracetamol, testosterone (Ring *et al*, 1999).

Substrates, inhibitors and inductors of SULTs

SULT enzymes usually have different substrate preferences, however some overlap may be observed. SULT1A1 member usually is responsible for sulfonation of phenolic compounds (e.g phenols, benzylic alcohols, aromatic amines) and 4-nitrophenol has been used to selectively detect the activity of this particular enzyme (Dajani *et al*, 1998). SULT1A2 takes part in detoxifying substrates such as 2-naphtol or 4-nitrophenol, however it has been demonstrated that the enzyme may also generate chemically reactive and mutagenic hydroxylamine metabolites (Meinl *et al*, 2002).

SULT1A3 usually shows high affinity for catecholamines, whereas SULT1B1 is usually restricted to thyroid hormones (Fujita *et al*, 1997). SULT1C1 conjugates iodothyronines (Li *et al*, 2000) and SULT1E1 exclusively regulates metabolism of estrogen (Falany *et al*, 1995). SULT2A1 form is responsible for the sulfoconjugation of hydroxysteroids such as DHEA, bile acids, and androgens (Comer *et al*, 1993). Currently, no particular substrates have been identified for SULT4A1 and SULT6B1.

The inhibitors of this superfamily have been only identified for SULT1A subfamily. Compounds such as curcumin and quercetin have been proven to inhibit the activity of SULT1A1 in fetal and adult liver (Vietri *et al*, 2003; De Santi *et al*, 2002). In addition, King *et al* (2006) have demonstrated that ibuprofen may lead to SULT1E1 inhibition.

Conversely, retinoic acid has been potentially shown to induce the activity of SULT1A1, 2A1 and 1E1 in hepatic carcinoma cell line HepG2 as well as in intestinal carcinoma cell line Caco-2 (Maiti *et al*, 2005).

Gene polymorphisms

Several genetic polymorphisms have been identified for SULT1A1, 1A2, 1A3, 1C2, 2A1, 2A3, and 2B1, where the genetic differences of SULT1A1 have been the most well described (Lindsay *et al*, 2008). The substitution of arginine 213 (Arg213) to histidine amino acid results in variation of activity and thermal stability of SULT1A1. This mutation has been found in approximately 25-36% of Caucasians (Glatt *et al*, 2004). It has also been reported that mutations in this particular enzyme may lead to the development of lung cancer (Arslan *et al*, 2009) or urothelial carcinoma (Huang *et al*, 2009).

Glutathione S – Transferases (GSTs)

GSTs and their distribution

Two superfamilies of GSTs have been described: soluble GSTs and MAPEG (membrane- associated proteins in eicosanoid and glutathione metabolism). The first superfamily of enzymes is usually involved in the metabolism of toxic xenobiotics and endobiotics, whereas the other ones biotransform arachidonic acid (Jancova *et al*, 2010).

The soluble GSTs are subdivided into eight separate classes designated Alpha, Kappa, Mu, Pi, Sigma, Theta, Zeta and Omega. Most of them reside in cytoplasm, however it has been shown that they may be present in nucleus, mitochondria and peroxisomes (Soboll *et al*, 1995; Morel *et al*, 2004) There are seven classes of enzymes that are found in human: Alpha (A1-A4), Mu (M1-M5), Omega (O1-O2), Pi (P1), Kappa (K1), Theta (T1,T2) and Zeta (Z1). These enzymes share approximately 60% homology within a class but less than 30% identity with separate classes (Jancova *et al*, 2010). Both of the superfamilies are found in the liver, kidney, pancreas, heart, lung, brain and intestine (Hayes *et al*, 2000).

Function

The superfamily of glutathione S – transferases (GSTs) apart of detoxifying a variety of xenobiotics play an essential role in cellular protection against oxidative stress. GSTs are responsible for catalysing the conjugation of hydrophobic and hydrophilic compounds with reduced glutathione as well as play major role in detoxification of epoxides and metabolism of steroids or prostaglandins (van Bladeren *et al*, 2000). Contrary to UGTs and SULTs, GSTs defend against reactive oxygen species (ROS) that usually arise through metabolic processes caused by cytochromes P450 – mediated chemical reactions (Sheehan *et al*, 2001).

GSTs protect the cell by transferring glutathione to reactive electrophiles. The tripeptide glutathione that serves a substrate is synthesized from γ –glutamic acid, cysteine and glycine. In cells, the glutathione exists in reduced (GSH) and oxidised (GSSG) state, where the GSH: GSSG ratio is critical for maintaining a cellular environment in the reduced state. During metabolism of different xenobiotics, the GSSG content may arise which leads to potential oxidative damage (Gonzalez and Tukey, 2005).

Substrates, inhibitors and inductors of GSTs

The electrophilic compounds such as epoxides, quinones, sulfoxides and esters are potential substrates for GSTs as they are able to react with the thiol moiety of glutathione. Only a number of substrates have been identified for specific subfamilies of enzymes e.g ethacrynic acid (diuretic drug) for GSTP1, *trans*-stilbene oxide for GSTM1, and relatively small molecules such as methylene chloride react with GSTT1 (Ahokas *et al*, 1985; van Iersel *et al*, 1998; Bernardini *et al*, 2001; Thier *et al*, 1998). In case of inhibitors, retinoic acid has been identified to lower the activity of human placental and liver glutathione transferases (Kulkarni *et al*, 1995), whereas extracts from cruciferous vegetables (e.g broccoli, cabbage) or grapefruit extract may induce the activity of variety of human GSTs (Williamson *et al*, 1997).

Gene polymorphisms

Allelic variations have been identified for Alpha, Mu, Pi, and Theta GST enzymes. Lack of GSTM1, GSTT1, and GSTP1 genes have been associated with development of bladder, breast, lung or colorectal cancer as well as with higher susceptibility to asthma and allergies **(**Ritchie *et al*, 2009; Piirilä, *et al* 2001**).** Currently, polymorphism in MAPEG class of GST enzymes is unknown.

1.6.3 PHASE III

Phase III transporters (Table 1.1) are important in drug absorption and distribution, however their major role is to excrete conjugation products from Phase II. Preceding their excretion, the biotransformed metabolites require transmembrane movement from the internal to the external compartment of the cell. Transport of conjugates involves different transport proteins (export pumps) as the products of Phase II cannot be carried out by free diffusion due to the high lipid content of the cell membrane which acts as a natural cell barrier (Chen, 2012). The two major superfamily of transport proteins that are important in Phase III metabolism are ATP-binding cassette transporters (ABC transporters) and Solute Carrier Transporters (SLC Transporters), where ABC transporters are considered to be the most important in the drug efflux process (Russel, 2010).

ATP – Binding Cassette Transporters (ABC transporters)

ABC transporters and their distribution

Human ATP – binding cassette transporters (ABC transporters) are grouped into seven subfamilies (ABCA, ABCB, ABCC, ABCD, ABCE, ABCF and ABCG) encoding 49 different proteins (Sheps and Ling, 2007).

Only three major subfamilies out of seven: ABCB (ABCB1/MDR1), ABCC (ABCC1/MRP1, ABCC2/MRP2, ABCC3/MRP3, ABCC4/MRP4), and ABCG (ABCG2/BCRP) are specifically involved in drug transport (Szakacs *et al*, 2008). All of these subfamilies are widely distributed, especially in transporting epithelia such as liver, intestine and kidney as well as in tissues such as placenta and brain where the barrier function is crucial.

Function

In general, transporters can be categorized as the influx or efflux proteins, depending on the direction in which the carriers translocate the compounds. ABC transporters proteins are considered as the efflux transporters because they use energy derived from ATP hydrolysis to mediate the primary active export of drugs from the intracellular to the extracellular milieu, often against a steep diffusion gradient.

The major protein of ABCB family is MDR-1, also called P-glycoprotein (P-gp). This protein is usually located on the apical (canalicular) side of intestine, liver and kidneys and plays major role in reducing systemic drug exposure by limiting oral absorption and facilitating urinary and bile excretion (Brinkmann and Eichelbaum, 2001).

The multidrug resistance – associated proteins (MRP) belong to ABCC subfamily and mediate transport of organic compounds of Phase II such as glutathione, glucoronide, and sulfate conjugates but also are able to facilitate the efflux of cationic substrates in the presence of reduced glutathione. The MRPs have variety of functions depending on the hepatic localisation. MRP2 is located at the apical membrane, emphasizing its crucial role in excreting anionic drugs and conjugates at the last stages of metabolism (Nies and Keppler, 2007). MRP1 and MRP3 are located at the basolateral (sinusoidal) side of hepatocytes, therefore they efflux UGT-processed drugs from the intestine to the blood (Borst *et al*, 2007). Contrary to the other MRPs, MRP4 is located at the both sides of the membrane. In hepatocytes, the transporter is localized at the basolateral side but is expressed at the apical side of renal and proximal tubule cells, indicating renal drug elimination (Rius *et al*, 2003).

Breast Cancer Resistance Protein (BCRP/ ABCG2) is the only transporter from the ABCG subfamily that is involved in drug metabolism. These proteins require homo – or heterodimerisation to create an active transporter.

Substrates, inhibitors and inductors of ABC transporters

ABCB1/MDR1 (P-gp) can interact with a wide variety of substrates such as anticancer drugs, steroids, linear and cyclic peptides (Sharom, 2011). Some drugs such as cyclosporines are substrates and inhibitors, other drug like nifedipine are inhibitors, whereas digoxin is only a substrate (Schinkel *et al*, 1995; Anglicheau *et al*, 2006; Liow *et al*, 2007; Choi *et al*, 2013). It has been demonstrated that particular substrates for P-gp are also potential substrates for CYP3A4, confirming that the substrate overlap is connected with the coordinated regulation and tissue expression in the liver as well as with common role in protecting the host from the environmental toxins (Marzolini *et al*, 2004). The major substrates of subfamily ABCC1/MRP1 protein include conjugates of lipophilic compounds with glutathione, glucuronate, or sulfate, including cysteinyl leukotriens, 17β – glucoronosyl estradiol where the glutathione S-conjugate leukotriene C_4 has the highest affinity for this transporter (König *et al*, 1999). Leier *et al* (1996) identified that glutathione disulphide has low affinity for MRP1 potentially indicating that the export pump plays a role in oxidative stress where the levels of glutathione disulphide increase. The anticancer drug methotrexate is effluxed by MRP1 in its native form (Hooijberg *et al*, 1999). Contrary to MRP1, MRP2 transporter plays a major role in eliminating bilirubin glucuronosides. MRP3 preferentially transports glucuronosides and has 10-fold higher affinity for 17β - glucoronosyl estradiol than MRP2 suggesting that MRP3 eliminates these compounds when MRP2 protein function is impaired (Jedlitschky *et al*, 1997 and Loe *et al*, 1997). The first endogenous substrate identified for ABCG/BCRP protein was porphyrin/heme therefore the protein plays an important role in heme homeostasis regulation under hypoxic conditions (Krishnamurthy *et al*, 2004). The transporter mainly transports drugs such as cimetidine, antibiotics as well as effluxes irinotecan and SN-38, the major anticancer compounds (Doyle and Ross, 2003; Sarkadi *et al*, 2006; Nakatomi *et al*, 2001; Noguchi *et al*, 2014).

Gene polymorphisms

To date, around 29 short nucleotide polymorphisms (SNPs) have been reported in MDR1 gene. SNPs in exons 26 and 21 have been widely characterised in different ethnic populations. One of the major mutation in exon 26 (3435 C>T) does not affect the amino acid composition, however the P-gp function may be reduced in the intestine which results in differences in pharmacokinetic parameters for substrates such as digoxin (cardiac glycoside) (Brinkmann and Eichelbaum, 2001)

A couple of studies have demonstrated genetic variants in ABCC family transporters *in vitro*. In one study, the genetic variant Arg433Ser in MRP1 (ABCC1) protein decreased transport of leukotriene C4, where in the other study the same SNP conferred a 2.1 – fold resistance to doxorubicin anticancer drug compared to cells expressing the wild type MRP1 protein (Conrad *et al*, 2002). The genetic analysis of other proteins of this family have revealed that heterozygous SNP Arg412Gly in MRP2 that occurs in protein-substrate binding region results in loss of transporter activity (Hulot *et al*, 2005), whereas SNPs such as 211 C>T found at the promoter region of MRP3 leads to significantly lower mRNA levels of this particular gene (Lang *et al*, 2004). Krishnamurthy *et al* (2008) have demonstrated that SNPs in MRP4 protein such as r23765534 that often occurs in the Japanese population (>18%) reduce transporters function through impairment of membrane localization usually leading to high sensitivity to some drugs (e.g thiopurines).

Different genetic variants have been demonstrated to occur in ABCG2 (BCRP) transporter. Polymorphisms in this particular protein have been shown to be associated with adverse reactions in patients treated with anticancer drug gefitinib as well as have been found to be highly predictive of plasma uric acid levels in patients potentially suffering from hyperuricemia (Lemos *et al*, 2011).

Fukuda *et al* (2010) have identified that some SNP of the ABC transporter genes such as ABCB1 (MDR1), ABCB11(BSEP), and ABCC1 (MRP1) are associated with susceptibility of developing hepatocellular carcinoma (HCC), implying that aberrant hepatic clearance of toxic substances may increase the risk of hepatocarcinogenesis.

1.6.4 DRUG-INDUCED LIVER INJURY AND CURRENT BIOMARKERS

Genetic polymorphism of the major drug metabolic enzymes (Chapter 1; Paragraph 1.6) has been demonstrated not only to play a key role in pathogenesis of inherited metabolic disorders or liver cancers but also in drug-induced liver injury (DILI).

DILI represents a major human health concern as it accounts for approximately 50% of acute liver failure cases and is one of the leading causes of transplantation in Western countries (Lee, 2003). Currently, liver injury caused by either intrinsic or idiosyncratic drug reactions is a major challenge for industry and regulatory authorities as it terminates the further development of the substance both at the pre-clinical and clinical stages. What is more, in most cases the drug hepatotoxicity is recognized post-marketing therefore DILI is the significant reason for withdrawing drugs from the market (Williams *et al*, 2013).

Paracetamol (APAP; acetaminophen) accounts for approximately 50-80% of drug-associated cases of liver failure (Lee, 2003). Although paracetamol – induced hepatotoxicity is predictable (intrinsic) and well understood, it has been proven that half of the cases are believed to be the result of unintentional therapeutic misadventures (idiosyncratic) (Ostapowicz *et al*, 2002; Larson *et al*, 2005). Regardless of the drug or type of hepatotoxicity, DILI is difficult to assess due to lack of appropriate predictive models and specific biomarkers and therefore is a process of exclusion (Williams *et al*, 2013; Antoine *et al*, 2014).

Currently, different genetic risk factors (e.g polymorphism of metabolising and mitochondrial enzymes, MHC/HLA genotype) and environmental factors (e.g drug interaction; alcohol consumption) have helped researchers to understand the complexity of drug induced hepatotoxicity and improve 'personalized medicine'. Although these factors are promising, identification of all possible factors causing DILI and establishment of appropriate *in vitro*/*in vivo* models still remain a challenge in DILI prediction (Russmann *et al*, 2009; Tujios and Fontana, 2011).

To overcome these problems, serum biomarkers such as keratin 18 (K18), high mobility group box – 1 (HMGB1), and glutamate dehydrogenase (GLDH) in addition to current alanine/ aspartate transaminases (ALT/AST) and alkaline phosphatase (ALP) have been discovered (O'Brien *et al*, 2002; Antoine *et al*, 2012; Schutte *et al*, 2004; Wieckowska *et al*, 2006; Cummings *et al*, 2008) . Although very promising, the specificity of these markers to hepatic injury is still not well evaluated (Fontana, 2014, Antoine *et al*, 2014).

Recently, microRNAs have been demonstrated not only to be potential and sensitive biomarkers for DILI (e.g miR-122 and miR-192) (Wang *et al*, 2009; Starkey Lewis, 2011) but also they have been shown to regulate internal metabolic processes that may be useful determining the underlying biology and in the future assessment and treatment of serious drug-induced liver injuries (Yokoi and Nakajima, 2012; Yu and Pan, 2012).

1.7 MICRORNAS

MicroRNAs as gene regulators

MicroRNAs (miRs; miRNAs) are an important class of non-coding small RNAs that possess a large range of biological activities in a variety of organisms (Breving and Esquela – Kerscher, 2010). In the human genome approximately 1000 miRs have been encoded and they have been shown to play an important role in embryonic development, cell proliferation, tissue differentiation and metabolism (Liu and Olson, 2010; Darnell *et al*, 2006; Suh *et al*, 2004; Hwang and Mendell, 2006; Rottiers and Näär, 2012).

Nomenclature

According to miRBase (the microRNA database; www.mirbase.org) and Ambros e*t al* (2003) each microRNA has a specific name and identifier. The first three letters of the microRNA signifies the organism that the molecule comes from (e.g 'hsa' in hsa-miR-121 stands for 'human'). The mature microRNA is designated as 'miR', whilst 'mir' refers to microRNA gene and the predicted stem loop of the primary transcript. If two microRNA precursors are at different genomic loci but give rise to the same mature microRNA then they are designated as 'hsa-mir-121-1' and 'hsa-mir-121-2'. Letter suffixes usually denote closely related mature microRNA sequences such as 'hsa-miR-121a' and 'hsa-miR-121b'. If precursor gives rise to two mature microRNA strands then the molecule that is predominantly expressed (usually a guide strand) is designated 'hsa-miR-121', whereas the less abundant sequence (passenger strand, from the opposite arm) is denoted as 'hsa-miR-121*'. When the data is insufficient to determine which of the molecules is more predominant, then names like 'hsa-miR-121-5p' (from 5' arm) and 'hsa-miR-121-3p' (from opposite 3' arm) are given.

Genomic location

In regards to genomic location, miRs can be intergenic, intronic or exonic (Olena and Patton, 2010). The intergenic miRs are usually found in genomic regions distinct from their own transcripts and can be divided to monocistronic (with their own promoters) or polycistronic (where several miRs are transcribed as cluster of primary transcripts). The most studied group are intronic miRs that are found in the introns of protein – coding and non-coding genes and can be present as a single miR or a cluster of several miRs. The exonic miRs are the novel family of miRs where they overlap exon and intron of the non-coding gene (Bartel, 2004).

Regulation of microRNAs

The regulation of miRs is poorly understood, however several studies have proven that these molecules can be controlled by DNA-binding (c-Myc, HNF4a and p53) and epigenetic factors (DNA-methyltransferases; DNMT1 and DNMT3b) (Breving and Esquela – Kerscher, 2010; Chang *et al*, 2008; Chang *et al*, 2007; Han *et al*, 2007; Bender, 2008). MiR processing and maturation might also be under nuclear and cytoplasmic regulation. Factors such as ribonucleoprotein A1 (hnRNP A1) binds to primary microRNA stem loop regions (UAGGGA/U elements) and induces conformational changes to allow Drosha processing, whereas KH-type splicing regulatory protein (KSRP) recognizes the terminal loop of pre-miRs, therefore promoting Dicer- mediated processing in the cytoplasm (Michlewski *et al*, 2008; Trabucchi *et al*, 2009).

MiR biogenesis may also be negatively regulated by RNA binding protein LIN-28 (inhibition of Drosha/Dicer binding to pre-miR) and RNA editing (replacement of adenosine to inosine within the hairpin region of pre-miR) (Moss *et al*, 1997; Newman et al, 2008; Yang *et al*, 2006). Under certain conditions miR have been shown to be regulated by Hu-antigen R (HuR) (Bhattacharyya *et al*, 2006), Dead and Homolog 1 (Dnd1) (Kedde *et al*, 2007), and Importin 8 (Weinmann *et al*, 2009).

1.7.1 MICRORNA BIOGENESIS AND FUNCTION

MicroRNAs are usually transcribed by RNA polymerase to form long (>100 nt) hairpin primary structures called primary microRNAs (pri-miRs) (Lee *et al*, 2004). These molecules are then further cleaved by the endonuclease Drosha and its cofactor DGCR8 (DiGeorge Syndrome Critical Region 8) to form approximately 70 nt long precursor microRNA (pre-miR) (Denli *et al*, 2004). The pre-miR is then exported to the cytoplasm by exportin 5 (Yi *et al*, 2003) through the nuclear pore complex where it is further processed by the Dicer enzyme to yield ~ 22 nt long miR-miR* duplexes (Chendrimada *et al*, 2005).

The passenger strand (miR*) is usually degraded and the guide strand is incorporated to the RNA induced silencing (RISC/Argonaute) complex, although ocassionally both strands can give rise to mature and functional microRNAs (Khvorova *et al*, 2003). The complex then induces the gene silencing/activation at the post-transcriptional level with several mechanisms. The perfect match between miR and the coding region of the particular mRNA leads to the transcript cleavage processed by the Argonaute 2 (Ago 2) enzyme that out of four Argonautes present in mammals has a 'slicer' activity. If the match is perfect or imperfect between miR and 3'utranslated region (3'UTR) of the mRNA it usually leads to translational repression (inihibition of initiation factors and 40S/60S ribosomal subunits; ribosomal drop off) or stimulation (binding to 5'UTR elements of mRNA) as well as mRNA degradation / storage (deadenylation, decapping followed by 5'-3' degradation, storage in P- bodies) (Djuranovic *et al*, 2012; Henke *et al*, 2008; Vasudevan *et al*, 2007; Filipowicz *et al*, 2008). Recently, microRNAs have been found in exosomes (circulating plasma microvesicles), indicating their potential role in intercellular communication (Gibbings *et al*, 2009) (Figure 1.5)

It has been proven that microRNAs may also act at the transcriptional level by inducing the repressive chromatin state by recruting different epigenetic factors, may block the binding of polymerase II or basic trancriptional factors (Zardo *et al*, 2012; O'Connell, 2012; Pastori *et al*, 2010). In addition, it has also been reported that microRNAs may activate gene transcription by a process known as RNA activation (RNAa) (Place et al, 2007) (Figure 1.5)

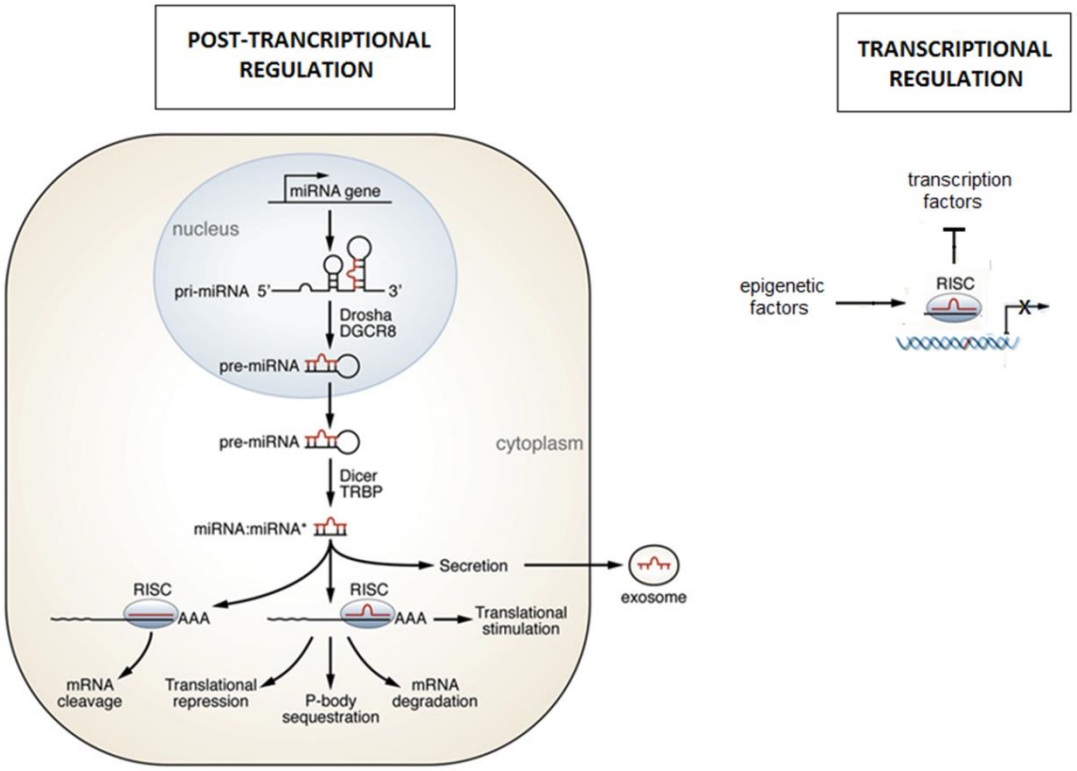

Figure 1.5: MicroRNA biogenesis. MicroRNAs are transcribed to form long pri-miRNA that is further cleaved by Drosha enzyme and DGCR8 to form ~ 70-100 nt long pre-miR. The pre-miR is further processed by the Dicer and the guide strand is incorporated to RISC/Argonaute complex that acts at post-transcriptional level (translational repression, P-body sequestration, mRNA degradation) or at trancriptional level (recruitment of epigenetic factors or basic transcriptional factors binding inhibition). Abbreviations: RISC, RNA-Induced Silencing Complex; TRBP, TAR RNA Binidng Protein; DGCR8, DiGeorge Syndrome Critical Region 8. Picture adapted from Liu and Olson (2010).

1.7.2 THE ROLE OF MICRORNAS IN LIVER DISEASES AND DRUG-INDUCED LIVER INJURY

MicroRNAs are estimated to control approximately 20-30% of mRNA targets, therefore it is not surprising that they regulate different biological process and may be involved in the pathogenesis of many human diseases. Currently, microRNAs have been demonstrated to play an essential role in the pathogenesis of lung (Oglegsby *et al*, 2010; Tomankowa *et al*, 2010), liver (Gramantieri *et al*, 2008), kidney (Wu *et al*, 2014), sickle cell disease (Chen *et al*, 2008), endometrium disease (Ohlsson Teague *et al*, 2009), and infectious disease (Gupta *et al*, 2009).

In the case of the liver, microRNAs have been involved in the pathogenesis of different liver cancers (Kota *et al*, 2009; Gramantieri *et al*, 2008), liver diseases (Zheng *et al*, 2010; Tang *et al*, 2009), HCV infection (Jopling *et al*, 2005; Hou *et al*, 2010) as well as in the important processes connected with lipid (Rayner *et al*, 2010; Esau *et al*, 2006) and drug metabolism (Pan *et al*, 2009; Takagi *et al*, 2010; Yokoi and Nakajima, 2013; Wang *et al*, 2014).

MicroRNAs have been shown to regulate the expression of drug metabolizing enzymes and transporters by direct targeting the 3' UTR of the gene transcripts or 'indirect' targeting the transcription factors (e.g nuclear receptors) that regulate these molecules. Therefore, modulation of the microRNA pathways may lead to an altered capacity of drug metabolism and disposition, and a different response to cell metabolism (Yu, 2009).

The microRNA regulation of drug metabolism in connection with new improved *in vitro* stem cell models may provide a better understanding of drug-associated injury and identify new targets which could lead to clinical translation in the future.

1.7.3 COMPUTER PROGRAMMES TO PREDICT MICRORNA BINDING

As deregulation of genes controlled by microRNAs is linked with many different disorders, including cancer and metabolic diseases, it is essential to reliably predict potential microRNA targets which might be involved in the pathogenesis of these diseases. In order to examine microRNA-mRNA binding efficiency, a variety of microRNA target prediction algorithms have been available online. The most commonly computational tools used are: TargetScan, PicTar, DIANA-microT, miRanda, rna22 and PITA. These algorithms take into consideration different parameters that contribute to the final score such as seed match type, 3' complementarity, free energy binding and conservation. In order to evaluate the authenticity of the target prediction programmes, there are two statistical parameters used to characterise their performance, namely: sensitivity (a percentage of correctly predicted targets out of total correct ones) and specificity (a percentage of correctly predicted among overall predicted ones).

It has been suggested that the emphasis should be put more on sensitivity in the search of all potential targets for specific microRNA and on specificity in the examination of microRNAs regulating a single gene (Witkos *et al*, 2011).

According to Alexiou *et al* (2009) research, TargetScan, DIANA-microT, and PicTar have a highest precision and sensitivity, and therefore are very useful to consider site conservation (Witkos *et al*, 2011). Contrary to these softwares, miRanda has been considered as a tool with low precision and too many false positives (John *et al*, 2004).

What is more, Baek *et al* (2008) studies on the influence of miR-223 on the protein output in mouse neutrophils demonstrated that TargetScan and PicTar where the best in predicting microRNA-mRNA binding sites that where validated in *in vivo* results. Moreover, only TargetScan total context score that is assigned to each result, correlated with protein downregulation in this study. Contrary to TargetScan, DIANA-microT tool examines each target site independently, and therefore it is not a useful programme to analyse microRNAs with multiple target sites (Kiriakidou *et al*, 2004; and Witkos *et al*, 2011). In addition, PITA and rna22 algorithms focus on novel features of microRNA-mRNA interactions; target site accessibility and pattern recognition, respectively. Although the latter ones might be useful, their microRNA target sites prediction is very low (Kertesz *et al*, 2007; Miranda *et al*, 2006).

1.8 THE OBJECTIVES OF THE THESIS

The study centres on the major metabolic cell type of the liver, the hepatocyte. The major interest was in the hepatocyte damage after drug overdose. While a number of models exist, their drawbacks outweigh their advantages, resulting in poor performance. To circumvent those issues, a reliable biological model is required. The project begins with the characterisation of the pluripotent stem cell – derived hepatocytes under defined and serum-free conditions. These hepatocytes may serve as a scalable, genetically stable, and renewable model to more appropriately study drug overdose. In addition to this, microRNAs have been demonstrated to play an essential role in drug metabolism and toxicity. This thesis therefore examines the hypothesis that the optimized hepatic model can serve as a platform to study paracetamol

(acetaminophen, APAP) toxicity *in vitro* and allow to understand the regulatory role of particular microRNAs in metabolism of a drug. The experiments focused on human APAP toxicity following overdose, with a view to identifying non-coding microRNAs which could reduce or attenutate this process.

The findings in the thesis may provide better understanding of the biological processes underlying drug-induced liver injury and potentially have application in managing DILI in the future.

CHAPTER TWO

MATERIALS AND METHODS

2.1 MATERIALS AND SOLUTIONS

2.1.1 REAGENT SOLUTIONS/CHEMICALS/SDS GELS

Table 2.1: Reagent solutions/ chemicals/SDS gels

NAME	CONTENT	SUPPLIER
SUMO SDS Lysis Buffer	2% SDS 50 mM Tris pH8 1 mM EDTA 10 mM Iodoacetamide	Sigma - Aldrich
		Sigma - Aldrich
		Sigma - Aldrich
		Sigma - Aldrich
RIPA Buffer	25 mM Tris HCl pH 7.6 150 mM NaCl 1% NP-40 1% Sodium deoxycholate 0.1% SDS	Thermo Scientific (Life Technologies)
Western Running Buffer	NuPAGE® MES SDS Running Buffer (x 20)	Life Technologies
Western Transfer Buffer	NuPage® Transfer Buffer (x 20)	Life Technologies
1 x PBS	0.01 M phosphate buffer 0.0027M potassium chloride 0.137 M sodium chloride	Sigma – Aldrich
Tween - 20		Sigma - Aldrich
DDT		Sigma - Aldrich
SeeBlue®	10 pre-stained protein bands (4-250 kDa)	Life Technologies
Protease Inhibitor Cocktails		Sigma - Aldrich
Protein Loading Dye	NuPAGE® LDS Sample Buffer (x4)	Life Technologies
Antioxidant	NuPAGE®	Life Technologies
SDS Gel	NuPAGE® 4-12% Bis Tris	Life Technologies

2.1.2 PLURIPOTENT STEM CELL LINES

Table 2.2: List of stem cell lines

CELL LINE	DESCRIPTION
H9	Female embryonic stem cell line (WT)
33D6	Induced pluripotent stem cell line (WT)
MAN 11	Female embryonic stem cell line (WT)
MAN 12	Male embryonic stem cell line (WT)

2.1.3 CELL CULTURE MEDIA, FACTORS, REAGENTS AND CULTURE PLATES

Table 2.3: List of cell culture media, growth factors, and reagents used.

REAGENTS/ FACTORS / MEDIA	SUPPLIER
L – GlutaMAX	Life Technologies
50 x B27 supplement	Life Technologies
Knockout Serum Replacement (KO-SR)	Life Technologies
Non-Essential Amino Acids (NEAA)	Life Technologies
2 – mercaptoethanol	Life Technologies
Foetal Bovine Serum	Life Technologies
Essential 8 (E8)	Life Technologies
Dulbecco's Modified Eagle Medium (DMEM)	Life Technologies
Knockout DMEM (KO-DMEM)	Life Technologies
RPMI 1640	Life Technologies
HepatoZyme ™ (HZ/HZM)	Life Technologies
Leibovitz's Medium (L-15)	Life Technologies
Lipofectamine RNAiMax	Life Technologies
EDTA	Life Technologies
Collagenase IV	Life Technologies
1 x Penicillin/Streptomycin (Pen/Strep)	Life Technologies
TrypLE	Life Technologies
Pierce™ BCA Protein Assay Kit	Life Technologies
mTeSR1	Stem Cell Technologies
Gentle Cell Dissociation Reagent	Stem Cell Technologies
Wnt3a	Peprotech
Activin A (AA)	Peprotech
Hepatocyte Growth Factor (HGF)	Peprotech
Oncostatin M (OSM)	Peprotech
Insuline (bovine pancreas)	Sigma – Aldrich
Tryptose phosphate broth	Sigma - Aldrich
Ascorbic Acid	Sigma - Aldrich
Hydrocortisone 21- hemisuccinate sodium	Sigma - Aldrich
P450 – Glo (TM) CYP Assay	Promega
CellTitre-Glo® Luminescent Cell Viability Assay	Promega
GSSG/GSH Assay	Promega
Caspase 3/7 activity Assay	Promega
MEF- Conditioned Medium (MEF-CM)	R&D Systems
Matrigel® (10 x)	BD Bioscience/Corning
Multiwell culture plates	Corning (Costar)/ Iwaki
Albumin ELISA Assay Kit	Alpha Diagnostics
Hepatocyte Culture Medium (HCM)	Lonza
ROCK Inhibitor (Y-27632)	Millipore/Calbiochem

2.1.4 MEDIA AND SUPPLEMENT PREPARATION FOR EACH CELL LINE MAINTENANCE AND DIFFERENTIATION STAGE

Table 2.4: Media and supplements used for culturing and differentiating PSCs.

Cell Line	Medium	Supplements	Re-seed dilution
Human Embryonic Stem Cells	mTeSR1 (MT)	N/A	1:3 / 1:4
	Essential 8 (E8)	N/A	1:4
Human Induced Pluripotent Stem Cells	MEF- Conditioned Medium (MEF –CM)	1% L-GlutaMAX per 100 ml of medium 10ng/ml basic fibroblast growth factor (bFGF)	1:2
	Essential 8 (E8)	N/A	1:3 / 1:4
Embryoid Bodies	Dulbecco's Modified Eagle Medium (DMEM)	20% FCS/FBS 1% L-GlutaMAX	N/A
hESC/hiPSC Derived Definitive Endoderm	Advanced RPMI 1640 medium	50 x B27 50ng/ml Wnt3a 100ng/ml AA 1% Pen/Strep	N/A
hESC/hiPSC Derived Hepatic Progenitors	Knockout DMEM (KO-DMEM)	20% KO-SR 0.5% L-GlutaMAX 1% NEAA 0.2% B-mercaptoethanol 1% DMSO 1% Pen/Strep	N/A
hESC/hiPSC Derived Hepatocytes	HepatoZyme™	10ng/ml HGF 20 ng/ ml OSM 1% hydrocortisone 21-hemisuccinate (10uM) 1% L-GlutaMAX 1% Pen/Strep	N/A
	Hepatocyte Culture Medium (HCM)		N/A
	Leibovitz's Medium (L-15)	10ng/ml HGF 20 ng/ ml OSM 1% hydrocortisone 21-hemisuccinate (10uM) 1% L-GlutaMAX 8.3% Tryptose phosphate broth 8.3 % FBS 1uM Insuline 0.2% Ascorbic acid 1% Pen/Strep	N/A

2.1.5 ANTIBODIES

Table 2.5: List of primary / secondary and flow antibodies

Primary Antibodies			
Antigen	*Type*	*Company*	*Dilution*
Oct 4	Rabbit Poly	Abcam	1:200 (WB) 1:250 (ICC)
Sox 17	Goat Poly	R&D Systems	1:500 (ICC)
Foxa 1	Mouse Mono	Abcam	1:200 (ICC)
HNF4a	Rabbit Poly	Santa Cruz	1:200 (WB) 1:100 (ICC)
AFP	Mouse Mono	Sigma - Aldrich	1:500 (ICC)
AFP	Mouse Mono	Abcam	1:200 (WB)
CYP3A	Sheep Poly	University of Dundee	1:100 (WB)
A1AT	Mouse Mono	Abcam	1:200 (WB)
Albumin (ALB)	Mouse Mono	Sigma - Aldrich	1:2000 (WB) 1:500 (ICC)
E-cadherin	Mouse Mono	Abcam	1:200(WB) 1:100(ICC)
GSTP1	Rabbit Poly	Abcam	1:50 (ICC)
GSTT1	Rabbit Poly	Abcam	1:500 (ICC)
SULT1A1	Mouse Mono	Abcam	1:100 (ICC)
SULT2A1	Rabbit Poly	Abcam	1:250 (ICC)
UGT1A1	Mouse Mono	R&D Systems	1:100 (ICC)
ABCC1	Mouse Mono	Abcam	1:50 (ICC)
ABCG2	Mouse Mono	Abcam	1:100 (ICC)

B-actin	Mouse Mono	Sigma	1:10000 (WB)
DAPI (Hoechst3342)		Life Technologies	2 drops per ml
Secondary Antibodies			
Antigen	*Host*	*Company*	*Dilution*
Anti-Goat 488	Donkey	Molecular Probes	1:400
Anti-Mouse 488	Rabbit	Molecular Probes	1:400
Anti-Rabbit 568	Goat	Molecular Probes	1:400
Anti – Rabbit 488	Goat	Molecular Probes	1:400
Anti-mouse IgG HRP	Goat	DAKO	1:1000 (ALB 1:2000)
Anti-rabbit IgG HRP	Swine	DAKO	1:1000
Anti- goat IgG HRP	Rabbit	DAKO	1:1000
Anti- sheep IgG HRP	Rabbit	DAKO	1:1000
Flow Cytometry Antibodies			
Antigen	*Type*	*Company*	*Dilution*
Anti –human Tra – 1-60	PE	eBioscience	1:50
Anti-human Tra – 1-81	APC	eBioscience	1:50
Anti-human CD15(SSEA1)	FITC	eBioscience	1:50
Anti-human SSEA4	PE	eBioscience	1:50
Mouse IgG1 κ Iso Control	APC	eBioscience	1:50
Mouse IgG1 κ Iso Control	FITC	eBioscience	1:50
Mouse IgG1 κ Iso Control	PE	eBioscience	1:50

2.1.6 PRIMERS (Taqman)

Table 2.6: List of primers and LightCycler 480 cycle conditions

GENE	SUPPLIER	PRIMER ID
OCT 3/4	Applied Biosystem	Hs00742896_ s1
NANOG	Applied Biosystem	Hs02387400_g1
SOX17	Applied Biosystem	Hs00751752_s1
CXCR4	Applied Biosystem	Hs00237052_s1
NODAL	Applied Biosystem	Hs01086749_m1
HNF4a	Applied Biosystem	Hs01023298_ m1
HNF1B	Applied Biosystem	Hs01001604_m1
AFP	Applied Biosystem	Hs01040601_m1
ALB	Applied Biosystem	Hs00910225_m1
ECAD	Applied Biosystem	Hs01023895_m1
GSTT1	Applied Biosystem	Hs00184475_m1
SULT2A1	Applied Biosystem	Hs00234219_m1
UGT1A1	Applied Biosystem	Hs02511055_m1
B2M	Applied Biosystem	Hs00984230_ m1
GAPDH	Applied Biosystem	Hs02758991_g1
	Cycle Conditions (LightCycler 480 system; Roche)	
Step	***Temperature / Time /Ramp Rate***	
Pre-Incubation (1 cycle)	95°C / 10 min / 4.8°C/s	
Amplification (40 cycles)	95°C / 10 sec / 4.8°C/s 60°C / 30 sec / 2.5 °C/s	
Melting (1 cycle)	95°C/ 1s/ 4.8°C/s 60°C/ 1 min/ 2.5 °C/s 99°/ Continuous/ 0.11°C/s	
Cooling (1 cycle)	40°C / 30s/ 2.5°C/s	

2.1.7 MICRORNA PRECURSORS AND ANTAGOMIRS

All precursors (Pre-miR™) and antagomirs (Ant-miR™) were purchased from Ambion (Life Technologies). The oligonucleotides are listed in Table 2.7 below:

Table 2.7: List of precursors and antagomirs

microRNA	Type	Company	miRBase (miR) Accession Number
hsa-miR-122-5p	Precursor	Ambion (PM11012)	MI0000442/MIMAT0000421
hsa-miR-122-5p	Antagomir	Ambion (AM11012)	MI0000442/MIMAT0000421
hsa-miR-483-3p	Precursor	Ambion (PM12478)	MI0002467/MIMAT0002173
hsa-miR-483-3p	Antagomir	Ambion (AM12478))	MI0002467/MIMAT0002173
hsa-miR-24-3p	Precursor	Ambion (PM10737)	MI0000080/MIMAT0000080
hsa-miR-24-3p	Antagomir	Ambion (AM10737)	MI0000080/MIMAT0000080
hsa-miR-148a-3p	Precursor	Ambion (PM10263)	MI0000243/MIMAT0000243
hsa-miR-148a-3p	Antagomir	Ambion (AM10263)	MI0000243/MIMAT0000243
hsa-miR-324-5p	Precursor	Ambion (PM10253)	MI0000813/MIMAT0000761
hsa-miR-324-5p	Antagomir	Ambion (AM10253)	MI0000813/MIMAT0000761
Negative Control	Precursor	Ambion (AM17110)	
Negative Control	Antagomir	Ambion (AM17010)	
Cy3- Negative Control	Precursor	Ambion (AM17120)	
Cy3-Negative Control	Antagomir	Ambion (AM17011)	

2.2 MAMMALIAN CELL CULTURE AND DIFFERENTIATION

2.2.1 MAINTENANCE OF PLURIPOTENT STEM CELL CULTURES

Coating of culture dishes with Matrigel®

A 10 ml stock bottle of Matrigel® (MG; BD Biosciences, UK) was thawed overnight at 4°C on ice. 10 ml of KO-DMEM (Life Technologies, UK) was added to the stock bottle and mixed using a pipette. Matrigel® was aliquoted to 1ml aliquots and stored at -20°C. When required, the aliquot of Matrigel® was thawed at 4°C overnight before being coated to avoid the formation of a gel. Approximately 17 ml of cold KO-DMEM was added to 1 ml aliquot, mixed and added to the wells, depending on the plate format.

Table 2.8: The amount of Matrigel® per well of the specific plate format.

Plate Format	Volume / Well
6 well plate	1 ml
12 well plate	0.5 ml
24 well plate	0.3 ml

The MG-coated plates were either stored overnight at 4°C or left for an hour at room temperature before adding a cell suspension.

Culturing hESC and hiPSC populations

a) hESC and hiPSC cultured in MEFs-free conditions (CM, MT, E8)

hESCs were cultured for over 30 passages on Matrigel® coated 6 well plates and were fed either with 3 ml of mTeSR-1® (MT, Life Technologies) or Essential 8 ® (E8, Life Technologies). After 24 hours, the medium in the plates was aspirated and 3 ml of fresh MT or E8 was added. The cells were incubated at 37°C in 5% CO_2 for optimal growth.

hiPSC were cultured on Matrigel® coated 6 well plates and fed either with 3 ml Mouse Embryonic Fibroblast Conditioned Medium (MEF-CM, R&D) supplemented with 10ng/ml basic Fibroblast Growth Factor (bFGF) or Essential 8 ®

(E8, Life Technologies). After 24 hours, the medium was aspirated and 3ml of fresh medium (MEF-CM or E8) was added. The cells were incubated at 37°C in 5% (v/v) CO_2 for optimal growth.

b) hiPSC cultured on Mouse Embryonic Fibroblasts (for EB formation)

A vial of irradiated MEFs (GlobalStem® MEF CF-1) of concentration 5 x 10^5 cells per ml was resuspended in 10 ml of MEFs medium. The fibroblasts were spun down at 1000 rpm for 5 min. Once the supernatant was aspirated, MEFs were resuspended in 12 ml of MEFs medium and plated in Matrigel® coated plates (2ml/well). The MEFs/Matrigel® coated plated were incubated at 37°C and 5% CO_2 for optimal attachment. Once MEFs attached, induced pluripotent stem cell line (33D6) was passaged onto MEFs and cultured in 3ml Mouse Embryonic Fibroblasts Conditioned Medium (MEF-CM, R&D) supplemented with 10ng/ml basic Fibroblast Growth Factor (bFGF). After 24 hours, the medium was aspirated and 3ml of fresh medium was added. The cells were incubated at 37°C in 5% (v/v) CO_2 for optimal growth. Once the cells reached confluency of ~ 80 - 90%, they were split for embryoid body (EB) formation.

Gradual Transition of hESCs/hiPSC from CM to MT or E8

Human embryonic and induced pluripotent stem cells were cultured on Matrigel® (BD Biosciences, UK) coated plasticware in Mouse Embryonic Fibroblast Conditioned Medium (MEF-CM; R&D Systems) before being transferred into mTeSR-1® (MT, Life Technologies, UK) or Essential 8 (E8, Life Technologies). The cells were split at 1:3 (hESCs) or 1:2 (hiPSCs) ratio and left overnight to settle down at 37°C. They were then transferred into 75:25 ratio of CM to MT (or E8) followed by 50:50, 25:75 and finally 100% MT or E8. Each stage was maintained for 48 hours.

Transition of hESCs from MT to E8 medium

Human embryonic stem cell lines were cultured on Matrigel® coated plasticware in mTeSR1 (MT) medium before transfer into Essential 8 (E8). hESCs were then transferred either to a 50 / 50 ratio of MT to E8 or directly in to 100% E8.

Passaging hESC and hiPSC populations

hESCs (MEFs-free conditions) were split at ratio 1:3 (hiPSC at ratio 1:2) using a collagenase type IV (200 U/ml) (Life Technologies) for CM and MT conditions or EDTA (1:1000 dilution of 0.5M solution; Invitrogen) for E8 conditions to passage them. The medium was aspirated, and the cells were washed once with 3-4 ml of PBS. 1 ml of collagenase or EDTA was added and the cells were incubated at 37°C (5% CO_2) for approximately 3-10 min (collagenase IV) or 4 min (EDTA). At the point the cell colonies begin to lift off at the edge, the collagenase was aspirated and cells were washed once with PBS. 3 ml (2ml for hiPSC) of fresh medium was added and the cells were scraped off. Subsequently, 1 ml of cell culture was added to the fresh plate containing 2 ml of fresh medium. When placing the cells in the incubator, the culture container was agitated to ensure even distribution of colonies.

Freezing and thawing hESC and hiPSC populations

hESC and hiPSC at the 90% confluency were removed from their substrate (~ 3 ml medium suspension) to the 15 ml falcon tube and centrifuged at 1000 rpm for 5 min. The supernatant was aspirated and cells were resuspended in the 0.5 ml of freezing medium [mixture of 10% dimethyl sulfoxide (DMSO; Sigma-Aldrich] and 90% knockout serum replacement (KO-SR; Life Technologies)) and subsequently placed in cryotube. The cells were stored in -80°C for 24-48 hours and later transferred to liquid nitrogen for long term storage.

The cells were thawed by placing the cryotube in water bath at 37°C. Once thawed, the colonies were gently placed in 4 ml of MEF-CM + 10ng/ml bFGF in the 15 ml falcon tube. The cells were then centrifuged at 1000 rpm for 5 min. The supernatant was aspirated and the colonies were resuspend in 3 ml of fresh MEF-CM (+ bFGF) and placed on MEFs/ Matrigel ® - coated plate. Once cells reached ~ 90% confluency, transition to serum-free media could be performed (see paragraph 2.2.1).

Mycoplasma Testing

hESCs or hiPSCs were routinely tested for Mycoplasma presence. To determine any contamination MycoAlert™ kit (Lonza) was used. Fresh medium was added to 40-80% confluent stem cells. After 24 hours, the supernatant was collected to Eppendorf tube. The sample was spinned down at 1500 rpm (2000 x g) for 5 min. A volume of 100 ul of the clear supernatant was added to a well of 96 - well microplate. A volume of 100 ul of assay control and 100 ul of assay buffer (negative control) were transferred to two separate wells of the microplate. A volume of 100 ul of MycoAlert™ reagent was added to each sample and control and incubated for 5 min at room temperature. Following the incubation, the microplate was placed in the luminometer (Promega) and the reading was taken (Reading A). A volume of 100 ul of MycoAlert™ substrate to each sample was added and incubated for 10 min. Following the second incubation, the microplate was placed in the luminometer and the reading was taken (Reading B).

The ratio (Reading B / Reading A) was calculated. The ratio of Reading B to Reading A was used to determine whether a culture was contaminated by Mycoplasma as follows:

Table 2.9: Interpretation of the Mycoplasma test results.

Ratio	Interpretation
< 0.9	Negative for Mycoplasma
0.9 - 1.2	Borderline: quarantine cells and retest in 24 h
>1.2	Mycoplasma contamination

2.2.2 EMBRYOID BODY (EB) FORMATION

Human embryonic stem cells (hESCs) generate embryoid bodies (EBs) at 90-100% of confluency. hESCs were cultured in MEFs-free conditions, whereas human induced pluripotent stem cells (hiPSCs) were cultured on MEFs to generate EBs. The medium was aspirated and cells were washed once with PBS. 4ml of EB medium was added (80% DMEM, 20% FCS/FBS, and 1% L-GlutaMAX) and cells were scraped to a low cluster plate and incubated at 37°C for 48 hours to promote cell aggregation. The EBs were fed with fresh EB medium every two days for 7 days until the aggregates were well defined and vacuolated. Subsequently, the EBs were transferred to 0.5% gelatin-coated chamber slides (BD Biosciences, UK) in 1 ml of EB medium and incubated at 37°C. The EBs on chamber slides were fed every other day for 14 days to allow them to spontaneously differentiate. After 14 days, the EBs were fixed with methanol (alternatively PFA), and stained for specific markers of three germ layers. Protocol based on Hannoun (2011).

2.2.3 HEPATIC DIFFERENTIATION OF PLURIPOTENT STEM CELLS

hESC were routinely cultured in feeder – free conditions using mTeSR1 or E8 medium and maintained in a humidified 37°C, 5% CO_2 incubator. hiPSCs were routinely cultured either in CM or E8 medium. Prior to differentiation, cells were split to a specific plate format either using ‘colony plating’ or ‘single - cell plating’ method.

a) Colony plating (both hESCs and hiPSCs) – used for PSCs characterisation

Pluripotent stem cells were split and passaged using the same method as indicated in paragraph 2.2.1 (section: passaging hESC and hiPSC populations).

b) Single - cell plating (only hESC H9 cell line) – used for paracetamol toxicity studies/transfection experiments (see Szkolnicka *et al*, 2014a for details)

hESCs (H9) (at ~ 80-90% confluency) were dissociated into single – cell suspension using StemCell Technologies Dissociation Reagent. Once dissociated, cells were transferred to DMEM medium and centrifuged at 300 g (alternatively 1000 rpm) for 5 min at room temperature. The supernatant was aspirated and the cell pellet was resuspended in MT medium containing ROCK inhibitor (Y-27632) to a final concentration of 10 uM. Cells were seeded on a specific plate format at ~ 2 x 10^5 viable cells per cm^2 (Table 2.10)

Table 2.10: The surface area of a well of a specific plate format.

Plate format	**Surface area per well**
6 – well	9.5 cm^2
12 – well	3.8 cm^2
24 – well	1.9 cm^2
48- well	0.95 cm^2 (Corning / Costar)
48 – well	0.76 cm^2 (Iwaki)
96 - well	0.32 cm^2

The differentiation of hESCs was initiated at 20-40% confluence (hiPSC in CM conditions ~50% and in E8 conditions ~ 20-40%), by replacing medium pluripotent stem cell medium with endoderm differentiation medium - RPMI 1640 containing 1x B27 (Life Technologies) a 100ng/ml Activin A (Peprotech) and 50ng/ml Wnt3a (Peprotech). Medium was changed every 24 hours for a period of 72 hours. After 72 hours, the differentiating cells were transferred to SR-DMSO hepatocyte differentiation medium and were cultured in it for another 5 days.

The medium consisted of KO-DMEM (Life Technologies), Serum Replacement (Life Technologies), 0.5% GlutamMAX (Life Technologies), 1% non-essential amino acids (Life Technologies), 0.2% β-mercaptoethanol (Life Technologies) and 1% dimethyl sulfoxide (Sigma). At day 9, differentiating cells were cultured in hepatocyte maturation medium HepatoZYME (Life Technologies) containing 1% GlutamMAX (Life Technologies), supplemented with 10 ng/ml hepatocyte growth factor (Peprotech) and 20 ng/ml oncostatin M (Peprotech). The process differed a little for iPSCs. hiPSC were cultured on matrigel coated surfaces until 20-50% confluent (depending on the medium). At this point mouse embryonic fibroblast conditioned medium (MEF-CM) or E8 was then replaced with endoderm differentiation medium - RPMI 1640 containing B27 (Life Technologies) a 100 ng/ml Activin A (Peprotech) and 50ng/ml Wnt3a (R&D Systems). Medium was changed every 24 hours for a period of 72 hours. On days 4 and 5 the differentiating cells were cultured in RPMI/B27 medium containing 100ng/ml of Activin A alone. From day 6 the cells were differentiated using hepatocyte specification medium – KO- DMEM (Life Technologies), KO- Serum Replacement (Life Technologies), 0.5% GlutaMAX (Life Technologies), 1% non-essential amino acids (Life Technologies), 0.2% β-mercaptoethanol (Life Technologies) and 1% dimethyl sulfoxide (Sigma). From days 9-14, hepatocyte maturation was directed using HepatoZYME® (Life Technologies) supplemented with 10 uM hydrocortisone 21-hemisuccinate, 10 ng/ml hepatocyte growth factor (Peprotech) and 20ng/ml oncostatin M (Peprotech).

2.3 CHARACTERISATION OF PLURIPOTENT STEM CELLS (PSCs) AND PSCs – DERIVED HEPATOCYTES

2.3.1 IMMUNOCYTOCHEMISTRY

Cell cultures at different points during cellular differentiation were fixed in 100% ice-cold methanol at -20°C for 30 min. Postfixation, cell monolayers were washed twice with PBS at room temperature. After blocking with 0.1% PBS-Tween containing 10% BSA for 1 hour, the cells were incubated with primary antibodies diluted in PBS-0.1% Tween/1% BSA at 4°C overnight. The following day, the primary antibody was removed, and the fixed monolayers were washed three times with PBS-0.1% Tween/1% BSA. Following this, the cells were incubated with the appropriate secondary antibody diluted in PBS-0.1%/Tween/1%BSA for 1 hour at room temperature and washed three times with PBS-0.1%/Tween/1%BSA and subsequently three times with PBS. After washing, the fixed monolayers were incubated with Hoechst 33342 (NucBlue Live Cell Stain Ready Probes; Molecular Probes) diluted in PBS for 20 min at room temperature.

Cultures were subsequently mounted with PermaFluor™ Aqueous Mounting Medium (Thermo Scientific), covered with cover slides and left overnight at 4°C.

The cells were analysed by Olympus TH4-200 microscope and Volocity 4 (alternatively FIJI) software. The percentage of positive cells and standard error were estimated from at least four random fields of view.

2.3.2 ELISA ASSAYS

At days 14, 16, 18, 20, 22, 24, 26 of differentiation, 1ml of each of the medium (L-15, HCM, HZ) was added to hESC - derived hepatocytes and incubated overnight at 37°C in 5% CO_2. After 24 hours, the supernatants were collected (n = 3 per time point and condition) and could be stored at -80°C for later use.

Albumin ELISA assay was measured and carried out as per the manufacturer's (Alpha Diagnostics) instructions. Samples were diluted 1:10 and pipetted (100 ul) in triplicates into a 96-well plate coated with purified anti-human albumin antibodies. Along with standards, the samples were incubated for 1 hour at room temperature. Following incubation and washing, Anti – Human Albumin Horseradish Peroxidase (HRP) was added to each well and incubated for 30 min at room temperature. Subsequently, the colour was developed by adding TMB substrate (chromogenic substrate containing peroxide) to the samples and incubating them in the dark for 15 min. To terminate the reaction, Stop Solution was added (1% sulfuric acid) and the absorbance was read at 450 nm using an MRX II plate reader. The data was normalised to per mg protein as determined by the BCA assay (Pierce, UK).

2.3.3 CYTOCHROME P450 ASSAYS

CYP3A and CYP1A2 activity were measured by pGlo kit from Promega (Madison, WI) and carried out as per the manufacturer's instructions for nonlytic CYP450 activity estimation (http://http://www.promega.com/tbs/tb325/tb325.pdf).

Basic cytochrome P450 activity

At different time points hESC- derived hepatocytes and hiPSC- derived hepatocyte cells were incubated either with CYP3A4 (1:40) or CYP1A2 (1:50) specific luciferin substrate (P450 – Glo™ CYP3A4/CYP1A2 Assay, Promega; UK) and incubated for 5 hours at 37°C. The culture medium was used as a negative control. Following incubation, 50 ul of supernatant from each well (n=3) was pipetted onto the 96-well microplate and mixed with 50 ul of luciferin detection reagent. The plate was left in the dark, at room temperature for 20 min to allow signal stabilisation. The basal activity of the enzymes was measured using luminometer (Promega) and expressed as relative light units (RLU). The data was normalised to per milligram of protein (BCA assay).

Drug- induced cytochrome P450 activity

At day 16 (hESC-derived hepatocytes) and day 12 (hiPSC – derived hepatocytes), cells were incubated with CYP3A and 1A2 inducer, phenobarbital (PB), at 1mM concentration for 48 hours before measurement of CYP3A and CYP1A2 activity. The CYP activity was detected using P450 – Glo ™ Assay and data was normalised to protein concentration as described above.

2.3.4 ANALYSIS OF SINGLE NUCLEOTIDE POLYMORPHISM (SNP) IN PLURIPOTENT STEM CELLS

Human embryonic stem cells (H9, MAN11, MAN12) were maintained for at least three passages in MT medium before collecting samples for SNP analysis.

The genomic DNA of hESCs was extracted using GeneElute™ Mammalian Genomic DNA Miniprep Kit (Sigma- Aldrich) as per manufactures instructions. In brief, cells were released with TrypLE and centrifuged for 5 min at 300 x g. The culture medium (supernatant) was removed and discarded. The pellet was resuspended thoroughly in 200 ul of Resuspension Solution. Subsequently, 20 ul of the Proteinase K solution was added to the sample followed by 200 ul of Lysis Solution C. The lysate was vortexed thoroughly (15 sec), and incubated at 70°C for 10 min. Subsequently, 200 ul of ethanol was added to the lysate and the entire contents of the tube were transferred to the binding column and centrifuged at 6500 x g for 1 minute. Then, the lysate was washed twice using 500 ul Wash Solution Concentrate and centrifuged at 6500 x g for 1-3 min. Finally, the DNA was eluted using 200 ul of the Elution Solution and centrifuged at 6500 x g for 1 minute.

The pure genomic DNA of hESCs was sent to Aros (Denmark) to analyse SNPs of the samples. The samples were examined by Illumina CytoSNP-12 Beadchip Assay. The samples were further analysed by Illumina GenomeViewer software.

2.3.5 FLUORESCENCE ACTIVATED CELL SORTING (FACS)

Staining cells

Fluorescence activated cell sorting (FACS) was used to confirm the cell surface marker expression of hESCs (MT and E8 media) and hiPSCs (CM and E8 media). One well of 6-well plate containing hESCs (iPSC) was treated with TrypLE (Life Technologies) for 5 min at room temperature. Cells were lifted as single cells and transferred to FACs tube containing 1 ml of DMEM/F12 medium. Subsequently, cells were centrifuged at 1000 rpm for 5 min and re-suspended in 1000 ul of 2% FCS in PBS. Cells were centrifuged at 1000 rpm for 5 min and re-suspended in appropriate volume of medium (number of tubes x 100 ul). Cells were aliquotted into 3 tubes, each containing 100 ul of cells and labelled as follows:

Tube 1: 100 ul of unstained cells (just cells, no antibodies)
Tube 2: 100 ul of cells + isotype controls (APC/FITC/PE)
Tube 3: 100 ul of cells + antibodies of interest (APC Tra-1-81; FITC CD15; PE Tra 1-60). All antibodies were diluted 1:50.

The three tubes were incubated for 30-45 min on ice in dark. After incubation, cells were centrifuged at 1000 rpm for 5 min and re-suspended in 500 ul 2% FCS in PBS. Subsequently, cells were centrifuged at 1000 rpm for 5 min and finally re-suspended in 400 ul 2% FCS in PBS. Prior to analysis, cells were left at 4°C.

Compensation controls

Three tubes were prepared as follows:
Tube 1: Positive and negative compensation beads + PE Tra-1-60 antibody (1:50 dilution)
Tube 2: Positive and negative compensation beads + APC Tra-1-81 antibody (1:50 dilution)

Tube 3: Positive and negative compensation beads + FITC CD15 antibody (1:50 dilution)

To each tube was added 400 ul 2% FCS in PBS. All tubes were stored at 4°C prior to analysis.

Unstained cells and compensation beads were used as controls. Dead and apoptotic cells along with debris were not included in the analysis. This was carried out by using and electronic liver gate on forward scatter and side scatter parameters. Data for 5000-100,000 'live' events were acquired for each sample using Fortessa 4- laser and analysed using FlowJo software.

2.4 MOLECULAR TECHNIQUES

2.4.1 RNA ISOLATION AND EXTRACTION

The cells of interest were washed with PBS and 1ml of TRIzol reagent (Life Technologies) was added per well of a 12-well plate and left to incubate for 5 min at room temperature. The cells were scraped, and placed in a 1.5 ml Eppendorf tube (stored at -80° C for later use if required). 0.5 ml of Chloroform was added to the tube and mixed by inverting; this was done in a fume hood. The solution was centrifuged at 13,000 rpm for 15 min at 4°C. The aqueous layer was collected into a clean Eppendorf tube. 1ml of Isopropanol was added to the tube, mixed by inverting and placed for 10 min at room temperature to precipitate RNA. The solution was centrifuged at 13,000 RPM for 20 min at 4°C. The supernatant was aspirated without disturbing the RNA pellet. 0.5 ml of 70% ethanol was used to wash the RNA. Following 5 min incubation at room temperature, the RNA was centrifuged at 8,000 rpm for 5 min at 4°C. The washing step was repeated 3 times. The ethanol was aspirated, and the pellet was left to dry for 5-10 min at room temperature. Once the ethanol evaporated, the RNA pellet was resuspended in 30 ul of deionised water. The RNA quality was assessed by nanodrop.

2.4.2 REVERSE TRANSCRIPTION AND POLYMERASE CHAIN REACTION (PCR)

Total RNA was reverse transcribed using QuantiTect Reverse Transcription kit (QIAGEN; alternatively Superscript III First Strand Synthesis SuperMix kit), as per manufacturer's instructions. A standard RT reaction was as follows:

For Quantitect RT kit

1. *Genomic DNA elimination reaction components* **(Table 2.11)**

Components	Volume / Reaction	Final Concentration
gDNA wipeout Buffer, 7x	2 ul	1x
Template RNA	1ug	
RNase-free water	up to final concentration	
Total volume	14 ul	

2. *Reverse Transcription reaction components* **(Table 2.12)**

Components	Volume / Reaction	Final Concentration
RT Mastermix		
Reverse Transcriptase	1 ul	
RT Buffer, 5x	4 ul	1x
RT Primer Mix	1 ul	
Template RNA		
Entire gDNA elimination reaction	14 ul	

For Superscript III Reverse Transcription kit

1. *One Step cDNA Synthesis* **(Table 2.13)**

Components	Volume/ Reaction
2 x RT Reaction Mix	10 ul
RT Enzyme Mix	2 ul
Template RNA	1ug (x ul)
DEPC- treated water	up to 20 ul final volume

Quantitative polymerase chain reaction (qPCR) was carried out using TaqMan Fast Advance Mastermix and appropriate primers (Applied Biosystems, Foster City, CA http://www.appliedbiosystems.com). The primers are listed in the Table 2.6. A standard qPCR reaction was as follows:

Table 2.14: Volume per reaction of specific qPCR components.

Component	Volume per reaction (384-well plate)
TaqMan Fast Advanced Master Mix (2x)	5 ul
TaqMan Assay primer/probe (20x)	0.5 ul
cDNA template	10 ng (x ul)
Nuclease-free water	up to 10 ul
Total volume per reaction	10 ul

The samples were analysed using Roche LightCycler 480 Real – Time PCR System (the appropriate cycle conditions are specified in Table 2.6) Results were normalised to B2M or GAPDH and expressed as relative expression over the control sample (day 0 either of hESC or hiPSC).

2.4.3 REVERSE TRANSCRIPTION AND RT^2 PROFILER PCR ARRAY (HUMAN DRUG METABOLISM)

The total RNA of hESC-derived hepatocytes (day 18) and Primary Human Hepatocytes (purchased from 3H Biomedical AB) was reverse transcribed using RT^2 First Strand Kit (QIAGEN) as per manufacturer's instructions. The RT reaction was as follows:

1. *Genomic DNA elimination mix* **(Table 2.15)**

Component	Amount
RNA	400 ng (x ul)
Buffer GE	2 ul
RNase-free water	up to 10 ul
Total volume	10 ul final volume

2. *Reverse Transcription mix* **(Table 2.16)**

Component	Volume for 1 reaction
5x Buffer BC3	4 ul
Control P2	1 ul
RE3 Reverse Transcriptase Mix	2 ul
RNase – free water	3 ul
Total volume	10 ul

The qPCR reaction was set up using RT^2 Profiler PCR Array (Human Drug Metabolism Array, Human Drug Metabolism Phase II Enzymes Array, and Human Drug Transporters Array were purchased from QIAGEN) as per manufacturer's instructions. A standard qPCR reaction was as follows:

3. *qPCR components mix* **(Table 2.17)**

Array Format	384 (4 x 96)
2x RT^2 SYBR Green Mastermix (ROX)	650 ul
cDNA synthesis reaction	102 ul
RNase-free water	548 ul
Total volume	1300 ul

The samples were analysed using Applied Biosystems model 7900 HT. The cycle conditions were as follows:

Table 2.18: The qPCR cycle conditions for AF7900 HT machine.

Cycle Conditions (AB 7900 HT)	
Stage	***Temperature/Time/Cycle(s)***
Stage I	95°C / 10 min / 1 cycle
Stage II	95°C / 15 sec / 40 cycles
	60°C / 1 min
Stage III	95°C / 15 sec / 1 cycle
	60°C / 1 min
	95°C / 15 sec

2.4.4 MICRORNA MICROARRAY

Sample processing and microRNA expression were analysed by *Sistemic* (Glasgow). The microRNA profiling was used to compare microRNA expression profile of hESC - derived hepatocytes and primary human hepatocytes.

Cells and Samples

To generate microRNA profiles, two sample sets were used:

- A commercial source (3H Biomedical, Sweden) of total RNA prepared from primary human hepatocytes (a single donor, technical replicates n = 4)
- hESC-derived hepatocytes (cell pellets; n = 4)

Samples were provided as total RNA (primary hepatocytes) and a PBS- washed, frozen cell pellets shipped on dry iced.

Sample processing and quality control

The total RNA from frozen cell pellets was produced using Sistemic's SOP for RNA isolation which preserved the small RNA population (< 200 nucleotides). All total RNA was examined for quantity and quality. RNA concentration was measured following Absorbance ratios at 260/280 and 230/260 nm were determined as indicators of sample yield and purity, respectively. An additional RNA quality control was performed by Agilent 2100 Bioanalyser and the RNA 6000 Nano Kit to determine the RNA integrity number.

Microarray profiling

The samples were analysed on Agilent miRNA platform (using Agilent's SurePrint G3 Human v16 microRNA 8x60K microarray slides; miRBase version 16.0) following Sistemic SOP (SSOP07). One hundred (100) ng of total RNA, from a working solution at 50ng / ul in nuclease-free water, was used as input for each microarray experiment. Each slide contained 8 individual arrays, each array was identified by a unique barcode and contained capture probes for 1349 microRNAs (1205 Human; 144 viral).

The four major key steps of the microarray process were:

1. Labelling of RNA with single-colour, Cy3-based reagent.
2. Hybridisation of the labelled RNA samples to the microarray.
3. Wash steps.
4. Slide scanning, data capture and feature extraction (matching array spots to miRNA IDs) and quality control checks on the resultant image and data files.

Data pre-processing and quality control

The microarray data was normalised using Sistemic's in-house pre-processing and data quality control (QC) methods. Array quality control was performed using outlier testing based on the following metrics:

1. average signal per array
2. average background per array
3. % present (% of miRNAs where expression is detected on each array)
4. principal components 1-3 from PCA (Jackson JE, 1991) of the full normalised sample set

In addition, a sample-to-sample correlation analysis was performed on the normalised data set using Pearson's correlation metric. Outliers were identified using Grubbs' outlier test (Grubbs, 1969) with significant called at $p < 0.05$.

Detection of microRNAs

Detection calls (present or absent) for individual miRNAs were compared across the samples. The detection calls were calculated using the Agilent Feature Extraction (AFE) software version 10.7.3.1. A detailed description of how these calls are made is available in the Feature Extraction Reference Guide on the Agilent website (http://www.genomics.agilent.com).

The differences in miRNA expression between the groups were evaluated by performing t-tests separately for each miRNA. The p-values coming from the t-tests were adjusted for multiple test inflation using the Benjamini-Hochberg method 6

(Benjamini and Hochberg, 1995) and are referred to as pFDR, where FDR is the false discovery rate. The miRNAs with significant differences from hypothesis testing at pFDR < 0.05 as well as having an absolute fold-change (FC) ≥ 1.5 were considered differentially expressed between the drug treatments and vehicle. A p-value cut-off of 0.05 is common practice when analysing microarray data and the use of the fold-change threshold of 1.5 is based on the documented array-to-array variability from the Agilent system.

2.5 PROTEIN BIOCHEMISTRY TECHNIQUES

2.5.1 CELLULAR PROTEIN EXTRACTION

Cells grown in a culture plate were lysed in 150 ul of RIPA Buffer (Life Technologies) for 5 min at room temperature. The cells were sonicated and stored at -80°C for later use.

2.5.2 MEASURING PROTEIN CONCENTRATION

The protein concentration in the cell protein extract samples was quantified using the Pierce™ BCA (bicinchoninic acid; Thermo Scientific/Life Technologies) protein assay. Protein extracts were diluted 1:2 using deionized water (5 ul of sample extract and 5 ul of water) and pipetted in triplicate into a 96 well plate. Reagents A and B were mixed at a 50:1 ratio and a volume of 200 ul was transferred into each sample well and the bovine serum albumin standards (ranging from 20-2000 ug/ml). The plate was incubated at room temperature for 20 min and the absorbance was read at 562nm using FLUOstar Omega (BMG Labtech). The protein concentrations were calculated by linear extrapolation using the standard curve generated from the protein standards. The protocol is based on Zhou *et al* (2012) and Hannoun (2011).

2.5.3 SDS-NUPAGE® POLYACRYLAMIDE GEL ELECTROPHORESIS

The gel electrophoresis (SDS-NuPage®, SDS-PAGE) was used to separate proteins of different molecular weights. The XCell SureLock® Mini-Cell system (Life Technologies, UK) was used to perform the gel electrophoresis. The 4-12% Bis-Tris pre-cast polyacrylamide gel (Life Technologies, UK) was fitted in the chamber and

subsequently filled with 1 x NuPage® MES-SDS running buffer and 0.5 ml of NuPage ® antioxidant (Life Technologies, UK) in the inner chamber. The samples containing 4 x LDS sample Buffer (NuPage ®) and DDT (Sigma – Aldrich) were denatured at 70°C for 10 min. The volume of 10ug of protein and 5 ul of SeeBlue® Plus2 Pre-Stained Standard Markers (Invitrogen) were loaded onto a gel.

A current of 200 V was applied and the samples were run for approximately 90 min. Once the separation of proteins was successful, the gel was carefully removed from the cassette and was used to perform western blot. The protocol is based on Zhou *et al* (2012) and Hannoun (2011).

2.5.4 WESTERN IMMUNOBLOTTING

Protein transfer

In order to detect the presence of specific proteins in sample extracts, western blot was performed using the XCell SureLock® Mini-Cell system, as per manufacturer's instructions. After the protein seperation by SDS – PAGE, the polyacrylamide gel was transferred to the Polyvinylidene fluoride (PVDF) membrane (Millipore, UK) to prevent protein cross over if transfer was over run. The transfer stack was assembled in the following order from cathode to anode: 2-3 x sponge; 2x filter paper soaked in 1x transfer buffer (NuPAGE®); SDS-PAGE gel; PVDF membrane pre-soaked in methanol (15 sec) and then in the transfer buffer; 2x filter paper soaked in transfer buffer; 2-3 x sponge. The stack was assembled in the XCell Blot II module and was tightly sealed and placed into the transfer SureLock® tank containing 1 x transfer buffer in the inner chamber and cold water in the outer chamber. A constant current of 160 mA was applied for 90 min. The protocol is based on Zhou *et al* (2012) and Hannoun (2011).

Immunoblotting

Once proteins have been successfully transferred onto PVDF membrane, the membrane was blocked to prevent nonspecific antibody binding. The membrane was blocked for 1 hour at room temperature with phosphate- buffered saline (PBS)/ 0.1% Tween 20/10% non - fat milk.

Once blocked, the membranes were probed with appropriate primary antibodies (diluted in PBS/0.1% Tween/10% milk at 4°C overnight under constant rotation. Once the primary antibody was incubated, membranes were washed three times in 10 ml of PBS/0.1% Tween. A horseradish peroxide (HRP) – conjugated secondary antibody (diluted in PBS/0.1% Tween; DAKO) was then incubated for 1 hour at room temperature and washed three times in PBS/0.1% Tween. The protocol is based on Zhou *et al* (2012) and Hannoun (2011)

Enhanced chemiluminescence (ECL)

The proteins of interest were detected using enhanced chemiluminescence (Pierce). The signal released was detected by x-ray film due to the chemical interaction of the HRP substrate (DAKO, UK) and conjugated HRP group on the secondary antibody of specific target protein. The chemiluminescence reagents: Peroxide Buffer and Luminol / Enhancer were mixed at a 1:1 ratio and spotted on to the membrane (1ml for each membrane), ensuring it was evenly spread. The membrane was placed in the Kodak x-ray cassette under the transparent foil. In the dark room, the membrane was exposed to BD Biosciences x –ray film for appropriate length of time, typically 1-20 min. The exposed film was developed using a film developer containing the fixative, developer and water solutions. The protocol is based on Zhou *et al* (2012) and Hannoun (2011).

2.6 MODELLING PARACETAMOL TOXICITY *IN VITRO*

Preparation of the paracetamol stock and cell treatment

Paracetamol (Sigma- Aldrich) was diluted in ethanol (Sigma-Aldrich) and prepared at 0.5 mM stock concentration. Different paracetamol concentrations (0 mM, 1 mM, 2 mM, 5 mM, 7 mM, 10 mM, 20 mM, and 50 mM) were prepared by diluting the stock solution in specific volumes of HepatoZYME™ supplemented with factors (HGF, OSM) and 2% Bovine Serum Albumin (BSA; Sigma- Aldrich). At day 17, cells were treated with specific drug concentration and left for 24 hours in the incubator at 37°C. Simultaneously, the same experiment was performed for vehicle control (ethanol + 2% BSA + HGF/OSM).

Measurement of IC50 (Standard Curve)

After 24 hours of incubation with the drug, the paracetamol toxicity was measured by the CellTiter-Glo Luminescent Cell Viability Assay from Promega. Cellular ATP levels were measured as per manufacturer's instructions and the luminescence signal was detected by the luminometer (Promega). In brief, HepatoZYME™ containing HGF (10ng/ml) and OSM (20ng/ml) factors was mixed with CellTitre-Glo® Reagent in ratio 1:1. The medium was aspirated from the cultures and 0.5 ml of the mixture (HepatoZYME™ + CellTitre-Glo® Reagent) was added per well. The cells were left for 2 min on the shaker at room temperature, and for the remaining 28 min were incubated at room temperature in the dark. After 30 min, 100 ul (in duplicates) of the mixture from each well (n=3) was pipetted onto the 96-well microplate and mixed with 100 ul of luciferin detection reagent and left for 10 min at room temperature to stabilise the luminescent signal. The luminescence was recorded by luminometer (Promega). The same experiment was performed for vehicle control (ethanol).
The IC50 of the paracetamol (the concentration of the compound resulting in 50% toxicity) was estimated from the function y = mx +b.

2.7 RNAi TRANSFECTION TECHNIQUES

Precursors and antagomirs stock preparation

Precursors and antagomirs at 5nmol concentration were resuspended in 50 ul of the nuclease-free water to make 100 uM of final concentration. The 10 uM (10 pmol/ul) working stock solution was further prepared by using nuclease-free water, aliquoted in Eppendorf tubes and stored in -20.

Optimisation of transfection

At day 17 of differentiation, cells were transfected with 50 nM Cy3 - labelled precursors and antagomirs at different Lipofectamine RNAiMAX ratios (1:1, 1:2, 1:3) and examined for transfection efficiency after 24 hours of incubation at 37°C.

Cells were analysed by Olympus TH4-200 microscope and Volocity 4 (alternatively FIJI) software.

Table 2.19: The RNAi transfection procedure for 2 wells of a 24-well plate (~2 x 10^5 cells/ well)

Steps	**Procedure Details (adherent cells; 50 nM of miRNA per well)**			
		Ratio		
	Component	**1:1**	**1:2**	**1:3**
Lipofectamine RNAiMAX was diluted in Opti-MEM Medium	Opti-MEM® Medium	45 ul	40 ul	35 ul
	Lipofectamine ® RNAiMAX	5 ul	10 ul	15 ul
miRNA stock was diluted in Opti-MEM medium	Opti-MEM® Medium	45 ul	45 ul	45 ul
	miRNA (10uM)	5 ul	5 ul	5 ul
Diluted Lipofectamine RNAiMAX was added to diluted miRNA (1:1 ratio)	Diluted miRNA	50 ul	50 ul	50 ul
	Diluted Lipofectamine ® RNAiMAX	50 ul	50 ul	50 ul
Incubation	The mix was incubated for 10 min at room temperature.			
miRNA–lipid complex was added to cells	miRNA – reagent complex added per well	50 ul	50 ul	50 ul
	Volume of Opti-MEM medium per well	450 ul	450 ul	450 ul
	Final volume per well	500 ul	500 ul	500 ul
	Final miRNA concentration per well	50 nM	50 nM	50 nM

	Final Lipofectamine RNAiMAX used per well	2.5 ul	5 ul	7.5 ul
Medium changed	After 5 hours of incubation miRNA-lipid-Opti-MEM complex was aspirated and replaced with 0.5 ml of HepatoZYME (no antibiotic) with 20ng/ml OSM and 10ng/ml HGF for remaining time.			
Visualised/ analysed cells	The transfected cells were analysed by Olympus TH4-200 microscope and Volocity 4 software/ FIJI software.			

Transfection efficiency (visualisation)

Transfection efficiency was estimated by live staining. At day 17 of differentiation, cell cultures were transfected with Cy3-labelled precursors/antagomirs (Ambion, Life Technologies) at 50 nM concentration and left for 24 hours in the incubator at 37°C. At day 18, the transfected cells were washed twice with PBS. After washing, the Hoechst 33342 (NucBlue® Live Cell Stain Read Probes; Life Technologies) diluted in HepatoZYME™ medium was added to the culture and incubated at 37°C for 10-15 min. Subsequently, the medium with Hoeschst 33342 was removed and the fresh medium was added. The cells were analysed by Olympus TH4-200 microscope and Volocity 4 (alternatively FIJI) software. The percentage of positive cells and standard deviation were estimated from at least four random fields of view and quoted as ± standard error.

2.8 MODULATING PARACETAMOL TOXICITY

At day 17, cells were transfected with precursors and inhibitors of Cy3-labelled controls, miR-148, miR-24, and miR-324 and incubated for 24 hours at 37°C. Once transfected, hESC-derived hepatocytes were exposed to the concentration of paracetamol resulting in 50% toxicity (IC50) for another 24 hours. The toxic effect of the drug was measured using CellTiter – Glo® Luminescent Cell Viability Assay, and GSH/GSSG-Glo™ Assay (all from Promega).

CellTiter – Glo® Luminescent Cell Viability Assay

See section 2.6 for details. Cellular ATP levels (n=6) were measured as per manufacturer's instructions and the luminescence signal was detected by the luminometer (Promega).

GSH/GSSG-Glo™ Assay

GSH/GSSG activity was measured by pGlo kit from Promega (Madison, WI) and carried out as per the manufacturer's instructions. The activity was measured in treated (paracetamol treatment) and non-treated (ethanol treatment; control) cells. In brief, the Total and Oxidized Glutathione Reagents were prepared as instructed and either of these reagents was added per well at 100 ul volume (n=6 for Total Glutathione Reagent and n=6 for Oxidized Glutathione Reagent). Subsequently, plates were left for 5 min on the shaker to lyse the cells. The 100 ul of luciferin generation reagent was added per well and cells were incubated for 30 min at room temperature in the dark. After 30 min, 100 ul of luciferin detection reagent was added per each well and left for another 15 min at room temperature to stabilise the luminescent signal. The luminescence was recorded by luminometer (Promega).

2.9 PLASMA SAMPLE COLLECTION, PROCESSING, PATIENT INFORMATION

Ethical approval for the study was from the Scotland 'A' Research and Ethics Committee and written informed consent was obtained. Three female donors or their nominated next of kin consented to blood sampling. Paracetamol hepatotoxicity was prospectively defined as previously described (Craig *et al*, 2009). Peripheral blood samples were obtained on the day of admission to the Scottish Liver Transplantation Unit. Serum was collected after centrifuged of blood samples at 1000g for 15 min and 4°C within 1 hour following collection, immediately aliquoted and stored at -80°C until thawing for the experiments.

2.10 FULMINANT PLASMA EXPERIMENTS

hESC (H9) - derived hepatocytes were transfected with the antagomir to miR-324-5p. Twenty four hours post transfection hESC – hepatocytes were exposed to to the fulminant plasma of the three paracetamol overdose patients (20% of plasma diluted in HepatoZYME^{TM} + growth factors) for a further 24 hours (Patient 1, 8, 58) (n=4). ATP levels were measured using CellTitre – Glo® Luminescent Cell Viability assay (as described in section 2.6) and Caspase 3/7 acitvity was measured as described below.

Caspase- Glo 3/7® Assay

Caspase 3/7 activity were measured by pGlo kit from Promega (Madison, WI) and carried out as per the manufacturer's instructions. In brief, HepatoZYME™ containing HGF (10ng/ml) and OSM (20ng/ml) factors was mixed with Caspase-Glo® Reagent in ratio 1:1. The medium was aspirated from the cultures and 0.4 ml of the mixture (HepatoZYME™ + Caspase-Glo® Reagent) was added per well. The cells were left for 2 min on the shaker at room temperature, and for the remaining 58 min were incubated at room temperature in the dark. After 1 hour, 100 ul (in duplicates) of the mixture from each well (n=3) was pipetted onto the 96-well microplate and mixed with 100 ul of luciferin detection reagent and left for 10 min at room temperature to stabilize the luminescent signal. The luminescence was recorded by luminometer (Promega).

2.11 COMPOUND INCUBATION (DILI ASSAYS)

Compounds were dissolved in Hybri-Max dimethyl sulfoxide (DMSO) from Sigma – Aldrich. The 20 mM stock solutions were made and further diluted in DMSO before being added to HepatoZYME^{TM} culture medium (hESC-derived hepatocytes) or in *InVitroGRO* HI medium (cryoplateable hepatocytes), so that a consistent final concentration of 1% DMSO was maintained. Medium was aspirated from 96-well plates and replaced with 100 ul of medium containing the appropriate concentration of compound (vehicle control, 0, 0.1, 1, 10, 25, 50, 100, or 200 uM) in triplicate.

Plates were placed in a humidified 37°C, 5% CO_2 incubator for 6 hours or 24 hours for the Apo-ONE Homogenious Caspase 3/7 Assay (Promega), and 24 hours, 4 days, or 7 days for the CellTitre – Glo Luminescent Cell Viability Assay. Old medium was aspirated, and fresh medium – containing compound was added to the remaining plates on day 4. Fluorescence (Caspases) and luminesce (ATP) were detected using an EnVision plate reader (PerkinElmer), and expressed as a percentage of vehicle control.

Concentration – response curves were plotted using the mean of the three replicates for each of the cell lines, and the concentration corresponding to a 50% viability on the four – parameter logistic regression line (50% inhibition/inhibitory concentration [IC50]) was determined using XLfit model 205.

2.12 STATISTICAL ANALYSIS

2.12.1 STUDENT'S T –TEST

The levels of significance were measured using Student's *t*-test. Significance levels were donated by one, two, three, and four asterisks to indicate $p < 0.05$, $p < 0.01$, $p < 0.001$, and $p < 0.0001$, respectively.

2.12.2 MULTI – GROUP COMPARISON OF DIFFERENT CELL TYPES

Principal Component Analysis (PCA)

The PCA overview plot was generated by *Sistemic* (Glasgow).

Principal Component Analysis (PCA) extracts the main effects from high-dimensional data such as microarray datasets, which for each sample have expression measurements from hundreds of miRNA. These main effects (principal components) were displayed in a simplified graphical representation which retained the main properties of the data. Samples which were similar clustered in the same space on the PCA plot.

2.12.3 RT² PROFILER PCR ARRAY DATA ANALYSIS

The PCR Array gene expression was analysed using PCR Array Data Analysis Web portal (www.SABiosciences.com/pcrarraydataanalysis.php). At the PCR Array Data Analysis Web Portal, Ct data was entered and the Web-based software automatically performed quantification using ΔΔ Ct method.

2.13 miR – mRNA BINDING ANALYSIS

TargetScan Human 6.2 (www.targetscan.org) is an online tool that predicts microRNA binding sites at the 3' UTR of the biological target. The programme focuses on the presence of conserved and non-conserved sites that match the seed region of each of the microRNA (Lewis *et al*, 2005). The predictions were ranked based on the predicted efficacy of targeting as calculated using the context score + scores (Friedman *et al*, 2009 and Grimson *et al*, 2007).

CHAPTER THREE

PLURIPOTENT STEM CELL MAINTENANCE AND HEPATOCELLULAR DIFFERENTIATION USING A NOVEL AND SERUM -FREE APPROACH

3.1 INTRODUCTION

3.1.1 PROPERTIES AND CHARACTERISTICS OF PLURIPOTENT STEM CELLS

Pluripotent stem cells (PSCs) demonstrate an inexhaustible source of supply of human somatic cell types (Donovan and Gearhart, 2001). Therefore, their use in different applications, such as modelling human biology 'in a dish' or cell therapy, is very attractive. While PSCs are an enabling resource, their robust characterisation is essential prior to cellular differentiation. PSCs are usually characterised by the expression of stem cell surface specific markers (e.g SSEA4, Tra-1-60, Tra-1-81) and stem cell specific transcription factors (e.g Oct 3/4, Nanog, Sox2). Appropriate PSCs morphology is characterised by tightly packed colonies with defined edges, displaying high nuclear cytoplasmic ratio and prominent nucleoli (Thomson *et al*, 1998; Carpenter *et al*, 2004). In addition to this, examination of the appropriate chromosome number (karyotype) is essential. Although useful, methods such as 'virtual karyotyping' that mostly consist of comparative genomic hybridization (arrayCGH), single nucleotide polymorphism (SNP), DNA microarrays, and short tandem repeats provide higher resolution than conventional cytogenetics (e.g giemsa banding or FISH). Following their characterisation for PSC markers, PSC pluripotency must be assessed. This is usually measured by the ability of cells to form embryoid bodies (EBs) that can be further differentiated to three germ layers: ectoderm, mesoderm and endoderm indicated by the expression of β-tubulin III, α smooth muscle actin, and α – fetoprotein respectively. In addition to EBs, teratoma or PluriTest assays are also used as diagnostic criteria for bona fide pluripotent stem cells *in vivo* (Evans and Kaufman, 1981; Müller *et al*, 2012). Although PSCs should maintain appropriate genomic stability and express specific stem cell markers, their microenvironment such as cell : cell and cell : matrix interactions should be considered. In order to stabilise healthy environment for PSCs adhesion and growth, research previously employed different cell feeder layers. Initially, mouse embryonic fibroblasts (MEFs) were used to support hESC growth (Thomson *et al*, 1998), however their xenogenic nature has forced researchers to replace them with feeders of human origin such as foreskin cells (Amit *et al*, 2003) or bone marrow cells (Cheng *et al*, 2003).

As hESCs were required to be cultured in scalable manner, feeders - free systems were developed, where major focus was on the development of new cell matrices. The first matrix used was Matrigel ™, the protein mixture extracted from Englebreth – Holm-Swarm sarcoma (Xu *et al*, 2001). Although it provided necessary attachment for cell support and growth, its animal origin and batch – batch variation led to develop more defined matrices such as fibronectin (Wang *et al*, 2005; Amit *et al*, 2004), vitronectin (Braam *et al*, 2008), and laminins (Rodin *et al*, 2009; Rodin *et al*, 2011). However, in order to use PSCs in industrial settings and the clinic, defined culture conditions and SOPs are required.

3.1.2 DEFINED CULTURE SYSTEMS FOR PLURIPOTENT STEM CELLS

Although pluripotent stem cells have a great potential in regenerative medicine, their progress strictly depends on well – characterised stem cell systems that would allow proper stem cell growth and differentiation. Since the first human embryonic stem cell isolation by Thomson *et al* (1998), most of the research has been focused on culturing cells on mouse embryonic fibroblasts (MEFs) in the presence of fetal calf serum (FCS). Although animal – derived components have been widely accepted by researchers to successfully maintain and passage both hESCs and hiPSCs, products of animal origin are problematic. First, the nonhuman components found in serum or from feeder cell layers may elicit unknown biological effects on the cells, especially as significant variability is observed in serum, and feeder cells. Additionally, animal products used in the stem cell experimentation could potentially transmit pathogens to the cultured cells, therefore limiting use of pluripotent stem cells and their derivatives in cell-therapy and bio-artificial devices (Akopian *et al*, 2010). In order to overcome these issues, researchers and companies have focused on developing defined, xeno–free, and serum-free media formulations, where major components are based on the signalling required for hESC/hiPSC self – renewal (for reviews see Chase and Firpo, 2007; Unger *et al*, 2008). Currently, there is a number of commercially available serum – free media for hESC and hiPSC culture such as Nutristem (StemGent), PluriStem (Millipore), StemPro (Life technologies), X-Vivo (Lonza), ESF (Cell Science and Technology), TesR1 (StemCell Technologies), TeSR2 (StemCell Technologies),

mTeSR1 (Stem Cell Technologies), TESR – E8 (StemCell Technologies), and E8 (Life Technologies). Although these media are considered as 'serum-free', some of them contain a fraction of bovine (BSA) or human (HSA) serum albumin in order to prevent the toxic effects of β – mercaptoethanol that plays a major role as an antioxidant (Chen *et al*, 2011). In addition to this, the formulation of these media contains different supplements (i.e insulin, transferrin, selenium) and growth factors (i.e bFGF, TGFβ; Nodal/Activin), therefore affecting different signalling pathways that are responsible for cell pluripotency, and long-term stability in culture (Wang *et al*, 2005; Beattie *et al*, 2005; James *et al*, 2005; Vallier *et al*, 2005; Xiao *et al*, 2006; Greber *et al*, 2007; Xu *et al*, 2008). Therefore, choice of the pluripotent stem cell medium for cell maintenance, expansion and differentiation should be researched thoroughly, especially if a clinical endpoint is desired. Akopian *et al* (2010) examined eight different serum-free media formulations in five different laboratories and concluded that StemPro and mTesR1 were the only formulations which supported stem cells for at least ten passages. The researchers attributed these positive results not only to FGF and TGFβ signalling that are mostly used in stem cell media but also to agonists to GABA receptors (Wang *et al*, 2008) and ErbB2 (Wang *et al*, 2007) which are considered to play a major role in hESC maintenance. Although mTeSR1 is widely successful in propagation of pluripotent stem cells, Chen *et al* (2011) pointed out that the StemCell Technologies 'TeSR' media are quite complex in terms of their formulation and even a fraction of either animal or human serum may cause batch variability. In order to overcome these problems, Chen *et al* along with Life Technologies as first have produced Essential 8 (E8) medium that is only based on eight components and is free from any serum or animal products. Therefore, we decided to examine the effects of E8 versus mTeSR1 on different pluripotent stem cell lines and on their derivate hepatocyte function. This was done with a view to lock down the 'best' stem cell system with which to generate hepatocytes for modelling purposes in Chapters 4 and 5.

3.2 RESULTS

In this chapter, the pluripotent properties of three human embryonic stem cell lines and one human induced pluripotent stem cell line were successfully characterised by embryoid body formation and flow cytometry.

Their DNA sequence variations were analysed by examining single nucleotide polymorphism (SNP) using Illumina Genome Viewer. We have established a new serum-free hepatic differentiation protocol and used it to successfully differentiate three human embryonic stem cell lines (two of them derived under GMP conditions) and one human induced pluripotent stem cell line. These lines were efficiently differentiated to hepatocytes when cultured in three different stem cell media: mTeSR1 (Stem Cell Technologies), Essential 8 (Life Technologies) and MEFs-conditioned medium (R&D). Differentiated status was measured by quantitative PCR (qPCR), immunocytochemistry, and cytochrome P450 functional assay. Additionally, stem cell – derived hepatocytes were externally validated by industry. In those experiments, human embryonic stem cell (H9)-derived hepatocytes were exposed to 20 well characterised hepatotoxicants and displayed similar level of toxicity as primary human hepatocytes, hence proving their potential use in drug predictive studies and cell-based therapies in the future.

3.2.1 CHARACTERISATION OF PLURIPOTENT STEM CELLS IN CULTURE

A research grade, human embryonic stem cell line (H9), and two human embryonic stem cell lines derived under GMP conditions (female MAN11 and male MAN12) were characterised in two commercially available serum free pluripotent media (mTeSR1(MT) and Essential 8 (E8)). Additionally, a human induced pluripotent stem cell line (33D6) was characterised in mouse embryonic fibroblast conditioned medium (MEF - CM) as originally reported (Sullivan *et al*, 2010) and E8.

Single nucleotide polymorphisms (SNPs) of stem cells

A single nucleotide polymorphism (SNP) is a variation at a single position in a DNA sequence among individuals. Any SNPs occurring within a gene may lead to variations in amino acid sequence, and therefore may potentially change the property of the coded protein. In order to study genetic abnormalities in hESC populations, genomic DNA samples were analysed by SNPs by Illumina HumanCytoSNP-12 v 2.1 Assay. The samples were further analysed by Illumina GenomeViewer software. The analysis was done by analysing log R ratio (log_2 (signal intensities for allele A + allele B) and B allele frequency (calculated from signal intensity for allele B / signal intensities for allele A + B). Each blue dot represents the log_2 ratio of one marker. A log ratio of 0 (~ +/- 0.5) corresponds to normal, diploid copy number. Increased and decreased log_2 ratios correspond to either gained or deleted regions respectively. A value of 0.5 on B allele frequency (BAF) plot corresponds to heterozygous SNPs (AB genotype), whereas SNPs of value 0 or 1 correspond to homozygous changes (AA or BB genotype). Gain of one copy will increase log R ratio and will change B allele frequency to values of 0, ~ 0.33, ~ 0.67 and 1.0 indicating AAA, AAB, ABB, BBB potential genotypes respectively.

Analysis of human embryonic stem cell line H9 cultured in mTeSR1 (MT) demonstrated two potential SNPs indicated as duplications on chromosome 7 (Figure 3.1) and chromosome 14 (Figure 3.2). Figure 3.1A and Figure 3.1B revealed that potential SNPs were located at the chromosome 7 (q11.21) between positions 62,113,011 - 62,699,114. Further inside to the positions 62,113,011 - 62,699,114 revealed no particular gene sequence (Figure 3.1C), therefore the potential microduplication could have occurred in a non-coding region of the genome. The second SNP was detected on chromosome 14 (q23.2) between positions 63,577,228 – 63,785,655 (Figure 3.2A and Figure 3.2B). Figure 3.2C revealed a potential duplication in Ras Homolog Family Member J (RHOJ) gene (chr 14, q23.2, exact position: 63,671,080 - 63,760,230) that is responsible for regulating different processes such as cell motility, focal adhesion and invasion (Wilson *et al*, 2014).

Although the software demonstrated the exact gene position using GRCh37 assembly (human genome housed at Genome Reference Consortium), the position of RHOJ has been recently updated in current assembly release GRCh38 where new location has been revealed (chr 14, q23.2, 63,204,114 – 63,292,219). Therefore the analysis of the SNP of this particular gene was not analysed any further. In addition to present SNPs, H9s did not demonstrate any potential DNA variances in genes, including HNF4a, CYP3A4, or CYP1A2 (Supplementary Figures 1.1 and 1.2). What is more, for the purpose of this project H9s were examined for potential SNPs in SULT2A1, UGT1A1, and GSTT1 enzymes and no potential single-based variances were revealed (Supplementary Figure 1.3). No particular SNPs have been detected in MAN11 and MAN12 cell lines (Supplementary Figures 1.4 and 1.5). All human embryonic stem cell lines (H9, MAN11, MAN12) demonstrated appropriate alignment of DNA satellites (repetitive non-coding DNA that is the main component of centromeres) at all chromosomes except of chromosomes 13, 14, 15, 21, and 22. The DNA satelites are indicated by no signal in both log R ratio and B allele frequency (Supplementary Figures 1.1, 1.4 and 1.5) as they possess different (usually lower) density than bulk DNA. The other chromosomes presented (13, 14, 15, 21, and 22) are acrocentric as indicated by short (almost invisible) p arms (no log R ratio present). In this project, SNP analysis was not performed for human induced pluripotent stem cells.

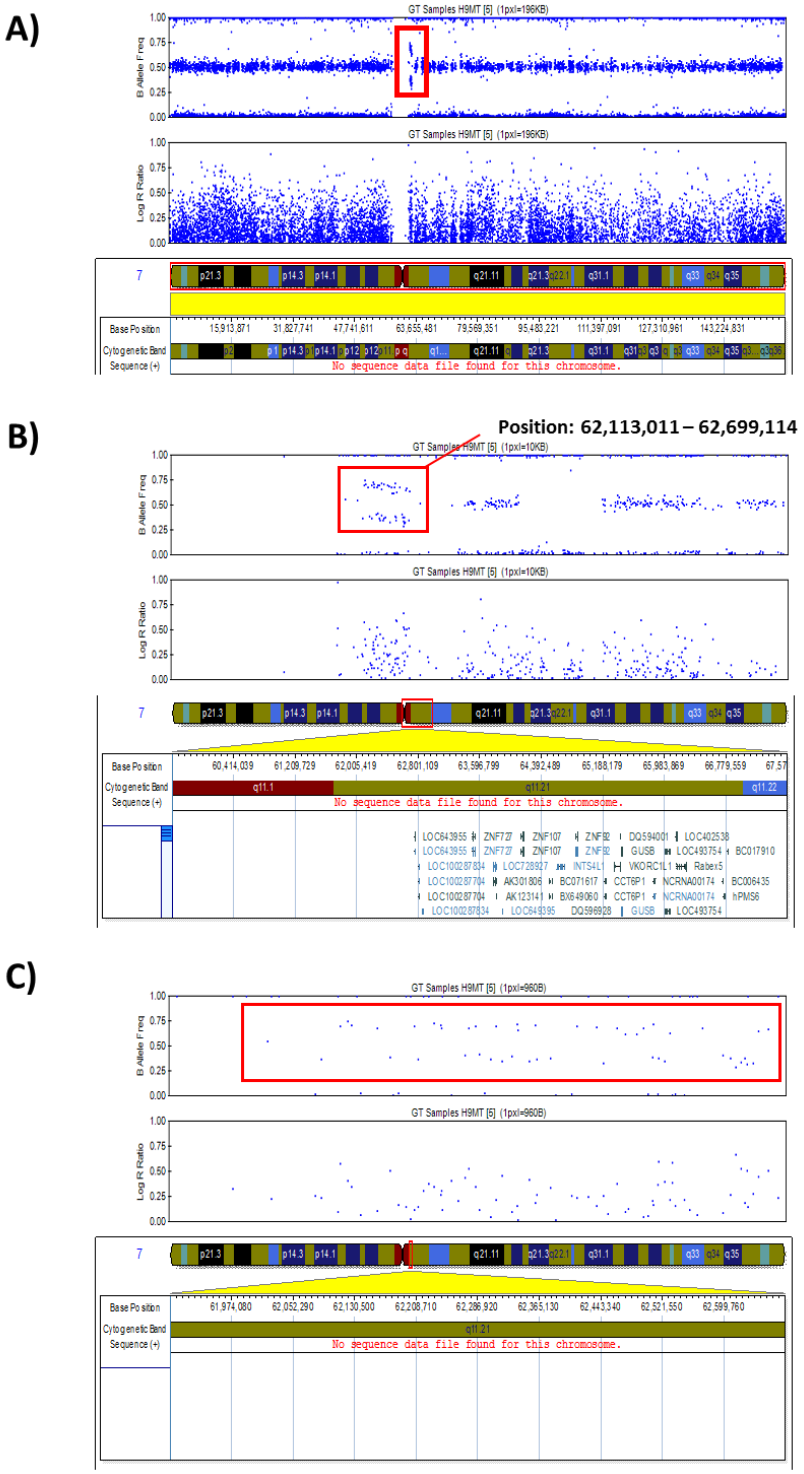

Figure 3.1: SNP analysis of H9s cultured in mTeSR1 conditions (chromosome 7). A) Potential SNP found on chromosome 7. B) Closer look to the SNP. Microduplication found on chromosome 7, q11 (position: 62,113,011-62,699,114). C) Closer look to the SNP. No sequence found on chromosome 7, q11.21, position: 62,113,011-62,699,114). Samples were analysed by Illumina GenomeViewer software. Abbreviation: SNP, short nucleotide polymorphism.

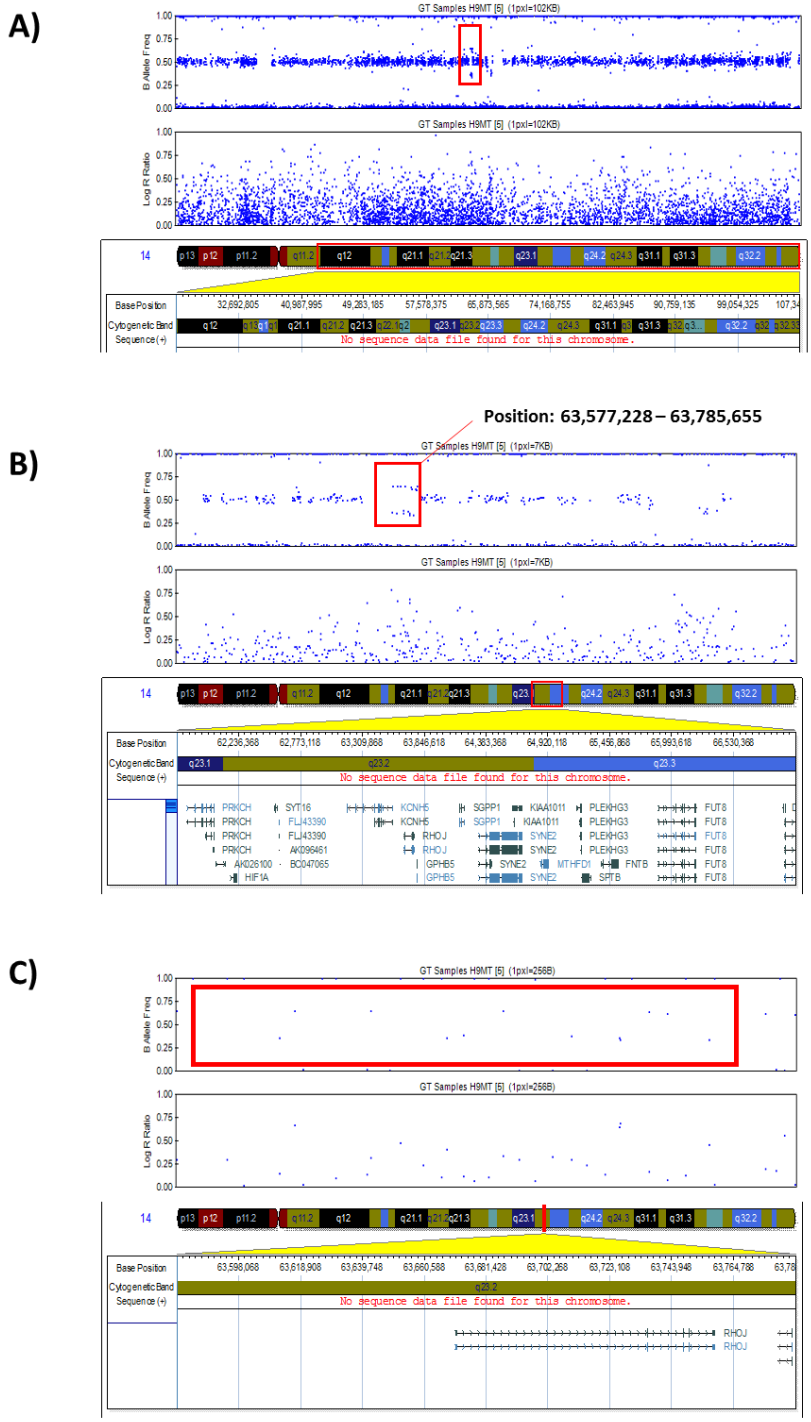

Figure 3.2: SNP analysis of H9s cultured in mTeSR1 conditions (chromosome 14). A) Potential SNP found on chromosome 14. B) Closer look to the SNP. Microduplication found on chromosome 14, q23 (position: 63,577,228 – 63,785,655). C) Closer look to the SNP. Potential SNP found in RHOJ gene located on chromosome 14, q23.2, exact position: 63,671,080 - 63,760,230 (GRCh37 assembly). Samples were analysed by Illumina GenomeViewer software. Abbreviation: SNP, short nucleotide polymorphism; RHOJ, Ras Homolog Family Member J.

Fluorescence Activated Cell Sorting (FACS)

In order to characterise and examine the level of pluripotency of selected stem cell lines, fluorescence activated cell sorting (FACS) was used that analyses pluripotent stem cell surface markers. In this project, antibodies such as SSEA-4, TRA-1-60, and TRA-1-81 (all from eBioscience) were used to identify human pluripotent stem cell markers, and SSEA-1 was selected as a negative control as it uniquely marks stem cell differentiation. Table 3.1 represents the percentage of positive cells for each of the surface markers in a particular cell line and conditions.

		PLURIPOTENT STEM CELL MARKERS			
		SSEA-1 FITC % +ve cells	SSEA-4 PE % +ve cells	TRA-1-60 PE % +ve cells	TRA-1-81 APC % +ve cells
CELL LINE (MEDIUM)	**PASSAGE**				
H9 (MT)	44	2.65	97.7	96	91.1
	47	0.79	99.7	98	93.7
	50	0.65	98.4	90.4	99.9
	53	9.72	99.5	95	99.4
H9 (E8)	56	1.8	-	85.9	12.2
	60	2.1	-	87.4	15
MAN11 (MT)	52	1.13	97.82	97.42	92.63
	55	2.5	98.8	96.5	90.4
	58	1.8	96.5	98.9	93.7
MAN11(E8)	54	4.5	-	93.1	35.7
	61	3.2	-	91.5	40.1
MAN12 (MT)	48	0.52	98.12	94.52	97.39
	53	0.99	98.58	96.2	97.86
	57	1.5	97.5	95.5	96.3
MAN12 (E8)	56	2.4	-	81.7	15.9
	61	1.2	-	84	20.1
33D6 (CM)	51	16.2	-	96.2	81.3
	62	11.5	-	94.5	79.8
33D6 (E8)	53	8.6	-	73.5	17.4
	61	6.1	-	80.1	23.5

Table 3.1: Flow cytometry. Human embryonic stem cell lines (H9, MAN11, MAN12) and human induced pluripotent stem cell line (33D6) are high for human pluripotent surface markers expression (SSEA-4, Tra-1-60, Tra-1-81), and low for the differentiation marker SSEA-1. The percentage of positive cells was taken from at least two passages. Abbreviations: MT, mTeSR1; E8, Essential 8; CM, MEFs-Conditioned Medium.

The levels of Tra-1-60 for all human embryonic stem cell lines in both conditions was above 90%, whereas for human induced pluripotent stem cells was ~80%. Surface marker Tra-1-81 was positive in more than 90% of human embryonic cells in MT condition, however the expression of this marker was much lower in E8 medium than expected. Similarly, to human ES cells, iPSC line 33D6 displayed low expression (~20%) of this marker in E8 medium, however high expression (~80%) was observed in cells cultured in CM medium. Although, both human embryonic and induced pluripotent stem cells expressed Tra-1-81 at low levels in E8 medium, this was probably due to insufficient amount of the antibody and not cells *per se*. SSEA4 was expressed in more than 96% of human embryonic stem cell lines in MT conditions, however it was not optimised in both CM and E8 medium. The stem cell differentiation marker, SSEA1, was expressed at low levels (~ 0.5-17%) in all cell lines as expected. The representative histograms of surface marker expression of hESC (H9; passage 47) cultured in MT are demonstrated in Supplementary Figure 1.10.

Embryoid body formation

Embryoid bodies (EBs) are three-dimensional aggregates formed in suspension by pluripotent stem cells (PSCs). Ability to form EBs by PSCs and to differentiate them further to three lineages is a standard method to assess the level of pluripotency. In this project, human embryonic and induced pluripotent stem cells were scraped to low cluster plate to promote aggregation. After seven days, when aggregates were well defined and vacuolated, cells were transferred to gelatin-coated chamber slides to allow for spontaneous differentiation. After fourteen days, cells were stained for three markers that characterise each of the germ layers: α smooth muscle actin (αSMA) for mesoderm, α-fetoprotein (AFP) for endoderm, and B-tubulin III for ectoderm. These data demonstrates that all three hESC (H9, MAN11, MAN12) and hiPSC (33D6) lines were able to spontaneously differentiate as indicated by positive expression of all linage markers (Figure 3.3).

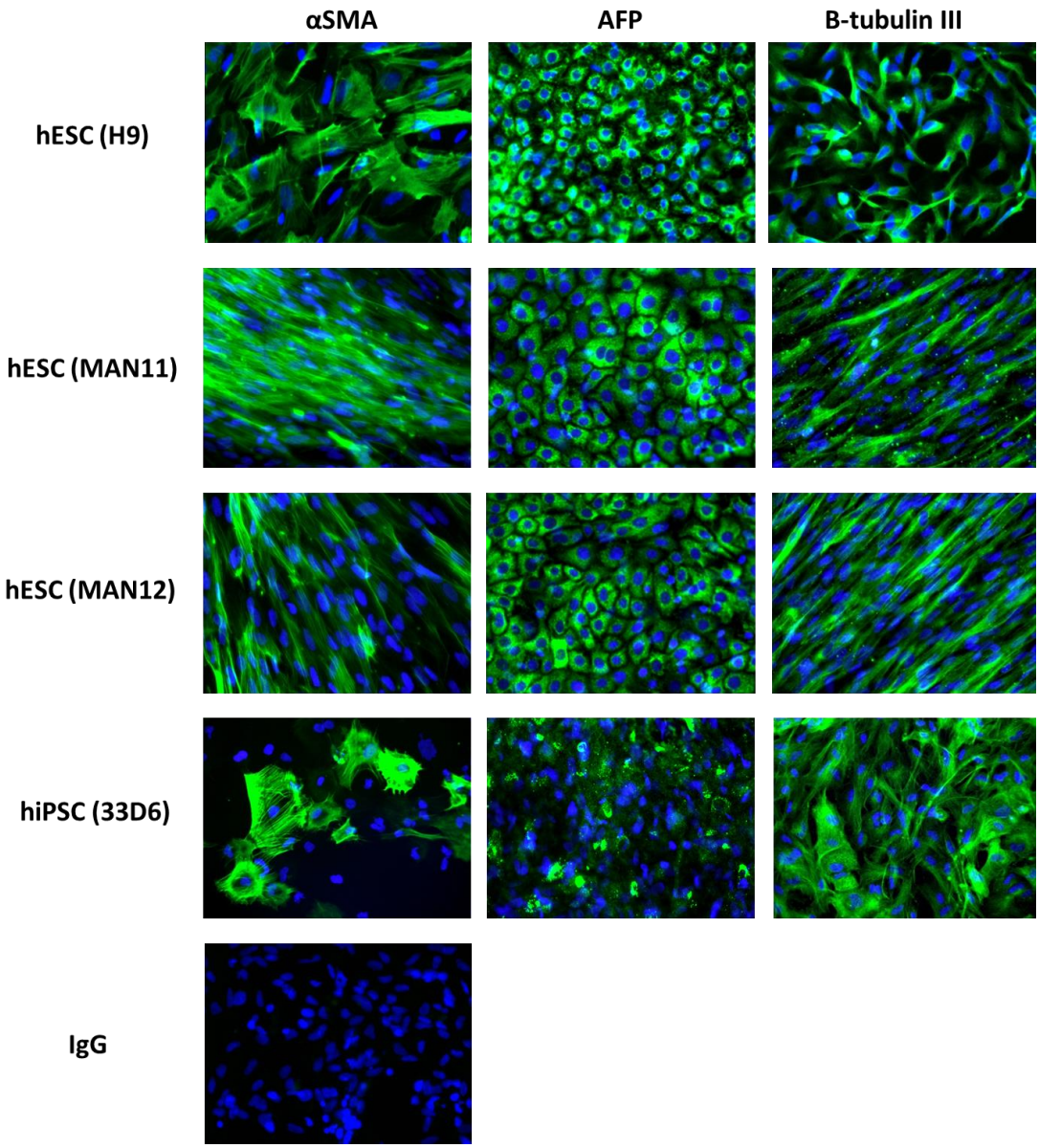

Figure 3.3: Embryoid body (EB) formation. Three human embryonic stem cell lines (H9, MAN11, MAN12) and one human induced-pluripotent stem cell line (33D6) successfully formed EBs. The EBs were able to spontaneously differentiate to all three germ layers as represented by expression of smooth muscle actin (αSMA; mesoderm), α-fetoprotein (AFP; endoderm), and B-tubulin III (ectoderm). The images were taken at x 40 magnification.

3.2.2 CHARACTERISATION AND OPTIMISATION OF HEPATOCYTE DIFFERENTIATION

The new serum – free model for pluripotent stem cell (PSCs) – derived hepatic differentiation

In order to circumvent the problems connected with animal-derived products and L-15 medium (Hay *et al*, 2007, 2008a), we examined commercially available serum-free hepatocyte maturation media: Hepatocyte Culture Medium (HCM, Lonza) and HepatoZYME (HZ, Life Technologies). In order to optimise the hepatic differentiation protocol, we focused on human embryonic H9 cell line as it was the most studied type of line in our laboratory. hESCs were differentiated to definitive endoderm and hepatoblasts up to day 8 as previously published (Hay *et al*, 2007 and 2008a). At day 8 of differentiation, early hepatocytes were transferred to three media (L-15; HCM; HZ) supplemented with specific growth and maturation factors (see Materials and Methods for details). From day 15 of differentiation, cell supernatant was collected every second day to examine metabolic functionality of cells by cytochrome P450 (CYP3A and CYP1A2) activity and albumin production.

Figure 3.4 demonstrates that over a time course CYP3A activity of hepatic cells was substantially increasing in HZ conditions, displaying the highest activity at day 21 of differentiation. In comparison with other media, cells cultured in HZ medium demonstrated ~12 fold increase in the enzyme production at day 21 ($p < 0.0001$).

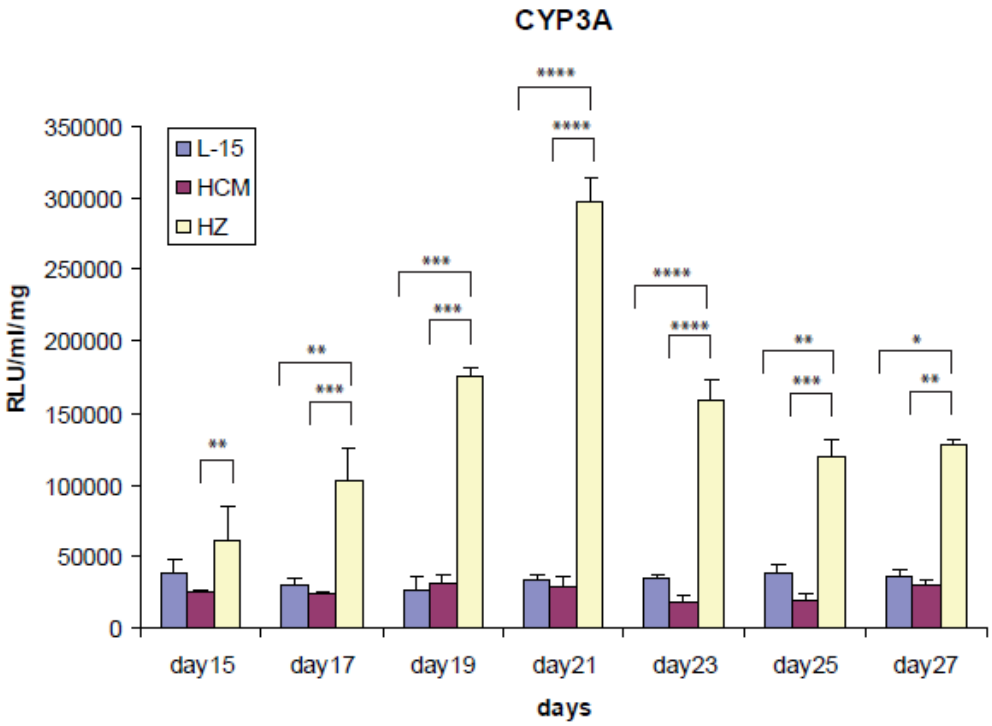

Figure 3.4: Cytochrome 3A activity (L-15, HCM, HZ). Cytochrome 3A activity was measured over a time course in Leibovitz's (L-15), Hepatocyte Culture (HCM), and HepatoZYME™ (HZ) media. Levels of significance are quoted over the bars and measured by Student's t test: *p-values*: *(<0.05); ** (<0.01); *** (<0.001); **** (<0.0001)

Figure 3.5 demonstrates that similarly to CYP3A, the levels of hepatic CYP1A2 activity was increasing during differentiation process. CYP1A2 displayed ~ 16 fold higher activity at day 25 in comparison with other media ($p < 0.0001$).

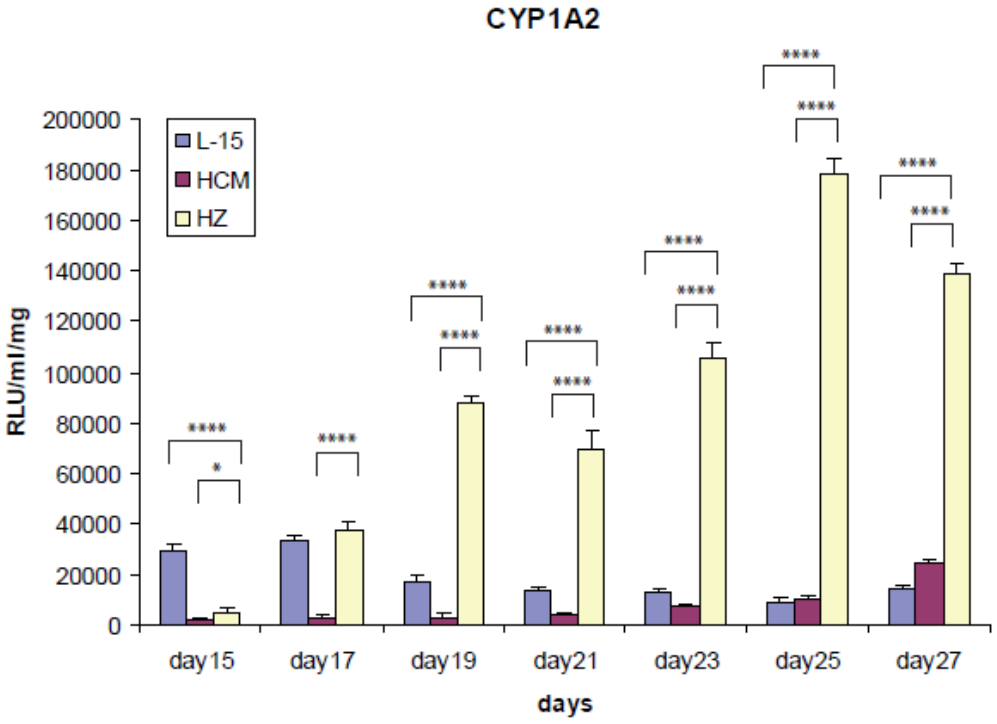

Figure 3.5: Cytochrome 1A2 activity (L-15, HCM, HZ). Cytochrome 1A2 activity was measured over a time course in Leibovitz's (L-15), Hepatocyte Culture (HCM) and HepatoZYME™ (HZ) media. Levels of significance are quoted over the bars and measured by Student's t test: p-values: *(<0.05); ** (<0.01); *** (<0.001);****(<0.0001).

In addition to cytochrome activity, the production of albumin, the major serum protein of the liver, was examined by Enzyme – Linked Immunosorbent Assay (ELISA). Figure 3.6 demonstrates that hESC-derived hepatocytes displayed the highest protein production at days 21, 23, 25 when cultured in HZ conditions. In comparison with other media, the level of albumin at these days in this particular conditions was ~ 2 fold ($p < 0.0001$; $p < 0.001$; $p < 0.01$) and ~14 fold ($p < 0.0001$) higher than in HCM and L-15 media respectively.

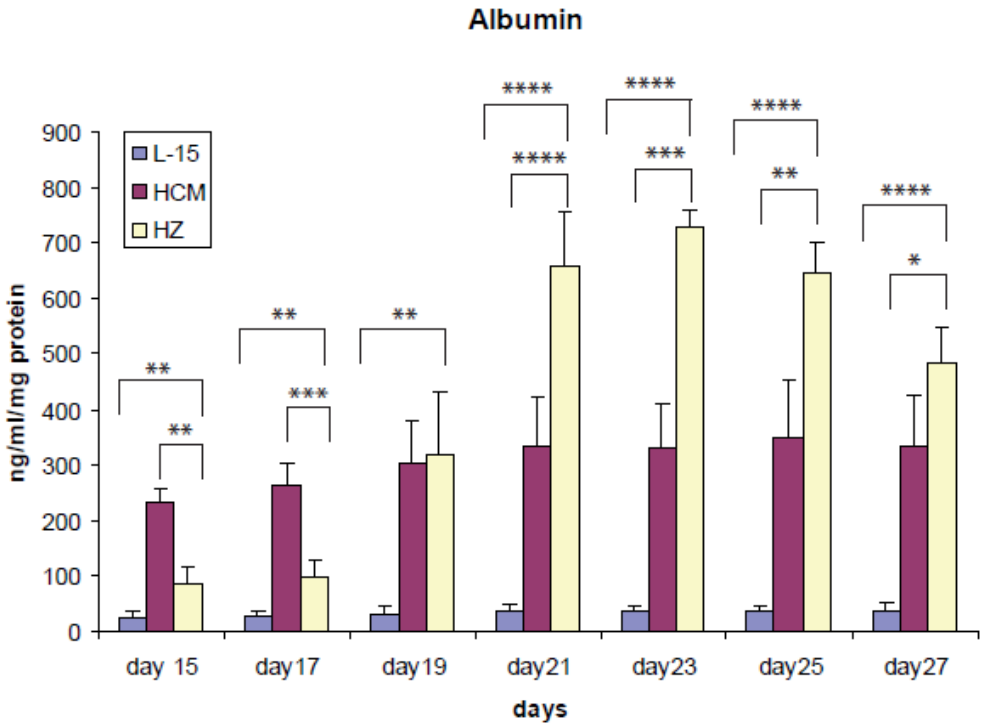

Figure 3.6: Albumin production (L-15, HCM, HZ). Albumin production was measured over a time course in Leibovitz's (L-15), Hepatocyte Culture (HCM), and HepatoZYME™ (HZ) media. Levels of significance are quoted over the bars and measured by Student's t test: p-values: *(<0.05); ** (<0.01); *** (<0.001); **** (<0.0001).

Morphological changes during hepatic differentiation using a serum-free approach

Taking into consideration that hESC-derived hepatocytes significantly produced cytochromes P450 (CYP3A/ CYP1A2) and albumin as well as were free from any animal products in HepatoZYME™ conditions, we decided to apply this medium in our current protocol and create fully functional serum-free *in vitro* hepatocyte differentiation procedure. Figure 3.7 demonstrates the schematic overview of the re-optimised protocols for human embryonic stem cell lines (i) and human induced pluripotent stem cell lines (ii) that were based on initial Hay *et al* (2007; 2008a) and Sullivan *et al* (2010) procedures respectively.

i)

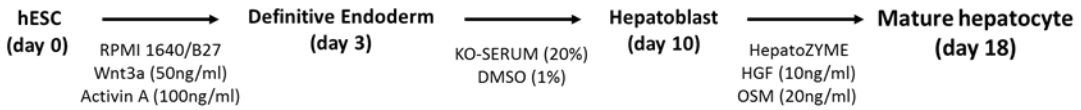

ii)

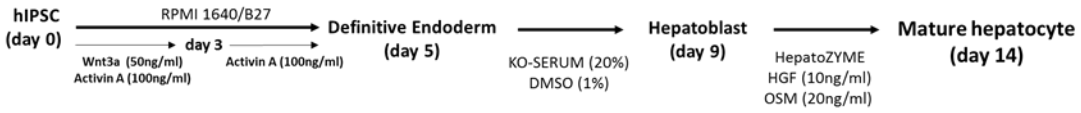

Figure 3.7: Hepatocyte differentiation protocol. Step – wise protocol for the differentiation of human embryonic (i) and human induced (ii) pluripotent stem cells to hepatocytes using a serum-free system. Abbreviations: RPMI 1640, Roswell Park Memorial Institute Medium 1640; KO – SERUM, Knockout Serum Replacement; DMSO, dimethyl sulfoxide; HGF, hepatocyte growth factor; OSM, oncostatin M.

Once the last stage of the hepatic differentiation protocol was optimised, we decided to examine whether the procedure could be applied to different human embryonic and induced pluripotent stem cell lines and whether different pluripotent serum free culture conditions would affect phenotype, gene expression and functionality of hepatic cells. In order to investigate that, hESCs mentioned above were cultured either in mTeSR1 or E8 for at least three passages before starting hepatocyte differentiation. hiPSC line 33D6 was chosen and cultured in CM conditions as reported previously (Sullivan *et al*, 2010). Similarly, the 33D6 line was passaged at least three times before differentiation. In addition, hiPSCs were cultured in E8 medium to examine the effect of animal-free components on hiPSC- derived hepatocyte activity.

Figure 3.8 demonstrates that hESC line H9 cultured either in MT or E8 underwent a series of morphological changes. hESC morphology changed as cells exited pluripotency (day 0) and transited through definitive endoderm (day 3) and upon hepatic specification (hepatoblast day 10; hepatocyte day 18). H9s in both serum - free conditions displayed dome-like colonies at day 0 as expected. Addition of Wnt3a and Activin A stimulated cells to loosen up, proliferate and form definitive endoderm that is characterised by spike/triangle –like shape. Upon hepatic specification (day 10), cells acquired more defined polygonal shape to finally form hexagonal shape with well - defined larger nuclei and canaliculi - like structures surrounding them at day 18 of maturation. Figure 3.9 and Figure 3.10 demonstrate two hESCs lines derived under GMP conditions, female MAN11 and male MAN12 that efficiently underwent sequential morphological changes when initially cultured either in MT or E8 medium. Although the differentiation was successful in both lines, MAN11 displayed morphologically less defined definitive endoderm structure in both conditions in comparison with MAN12, where cells at day 3 demonstrated similar phenotype to H9 cell line. Similarly to hESC lines, hiPSC line 33D6 demonstrated appropriate morphology at all four stages of differentiation (Figure 3.11). It is important to mention that hiPSCs cultured in CM were much bigger in size and less compacted in comparison with E8 medium (day 0).

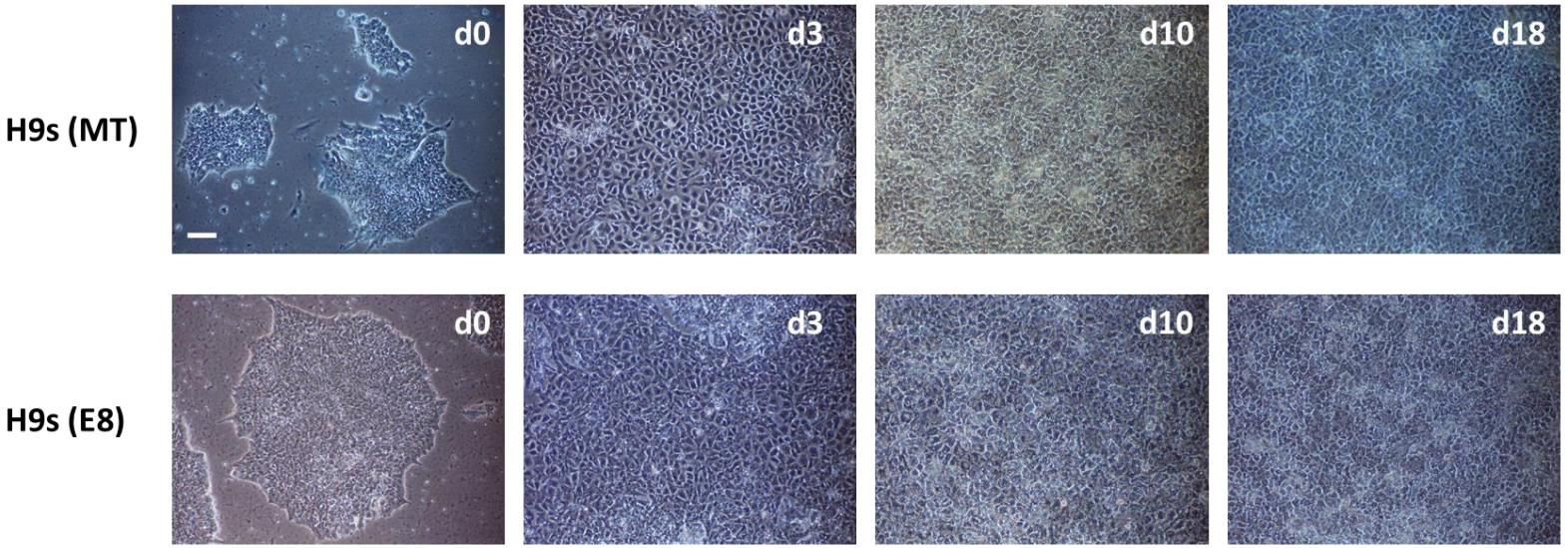

Figure 3.8: Cell morphology during hepatic differentiation (H9s). Phase-contrast imaging demonstrated the human embryonic stem cells (H9) were undergoing sequential morphological changes during transit from stem cell (day 0), to definitive endoderm (day 3), to hepatoblast (day 10), to hepatocyte (day18) in two different serum-free media mTeSR (MT) and Essential 8 (E8). Scale bar represents 100 um.

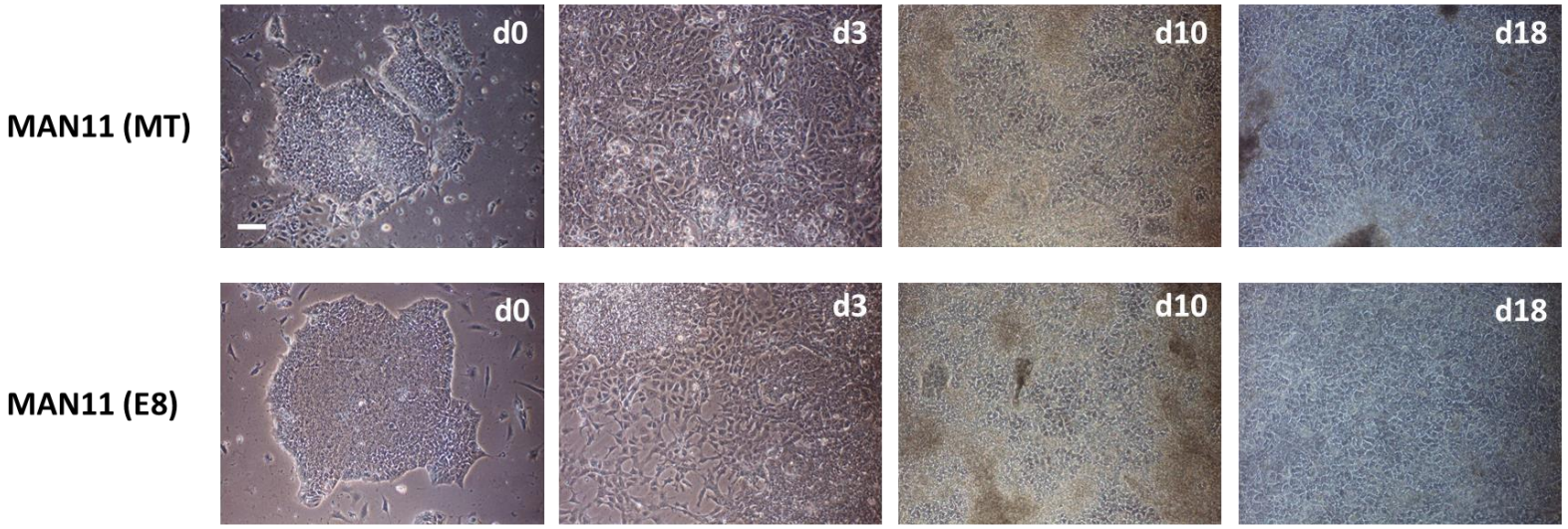

Figure 3.9: Cell morphology during hepatic differentiation (MAN11). Phase-contrast imaging demonstrated the human embryonic stem cells (MAN11) were undergoing sequential morphological changes during transit from stem cell (day 0), to definitive endoderm (day 3), to hepatoblast (day 10), to hepatocyte (day18) in two different serum-free media mTeSR (MT) and Essential 8 (E8). Scale bar represents 100 um.

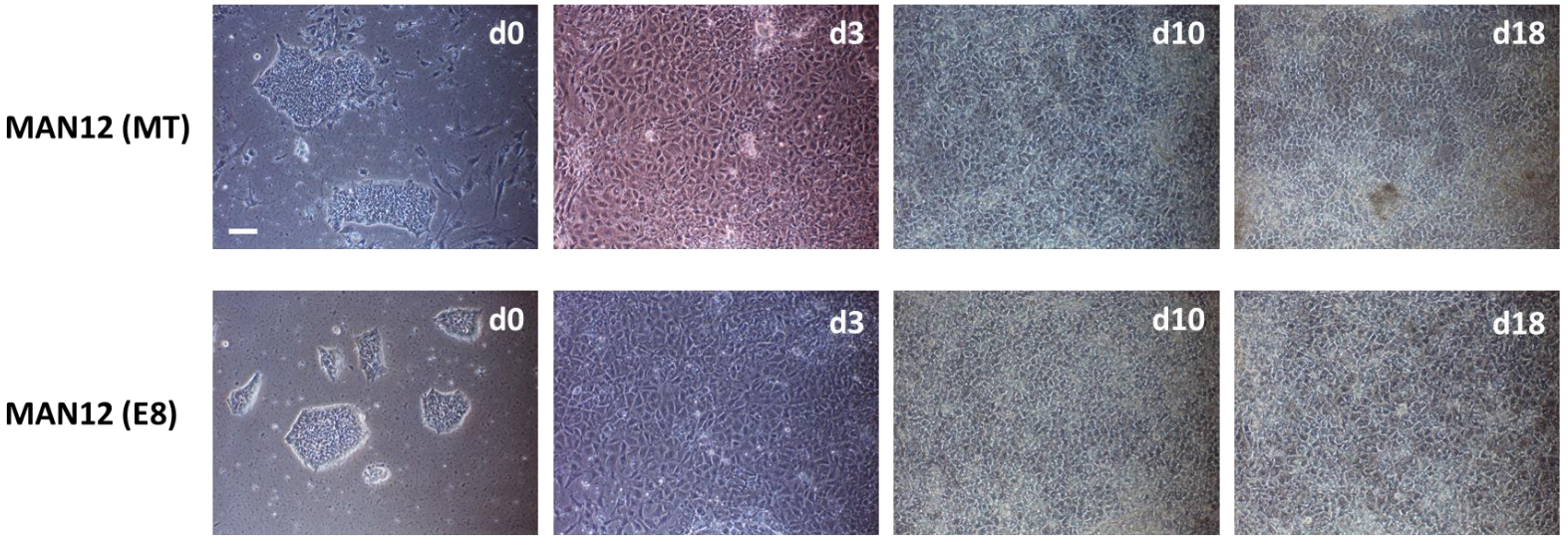

Figure 3.10: Cell morphology during hepatic differentiation (MAN12). Phase-contrast imaging demonstrated the human embryonic stem cells (MAN12) were undergoing sequential morphological changes during transit from stem cell (day 0), to definitive endoderm (day 3), to hepatoblast (day 10), to hepatocyte (day18) in two different serum-free media mTeSR (MT) and Essential 8 (E8). Scale bar represents 100 um.

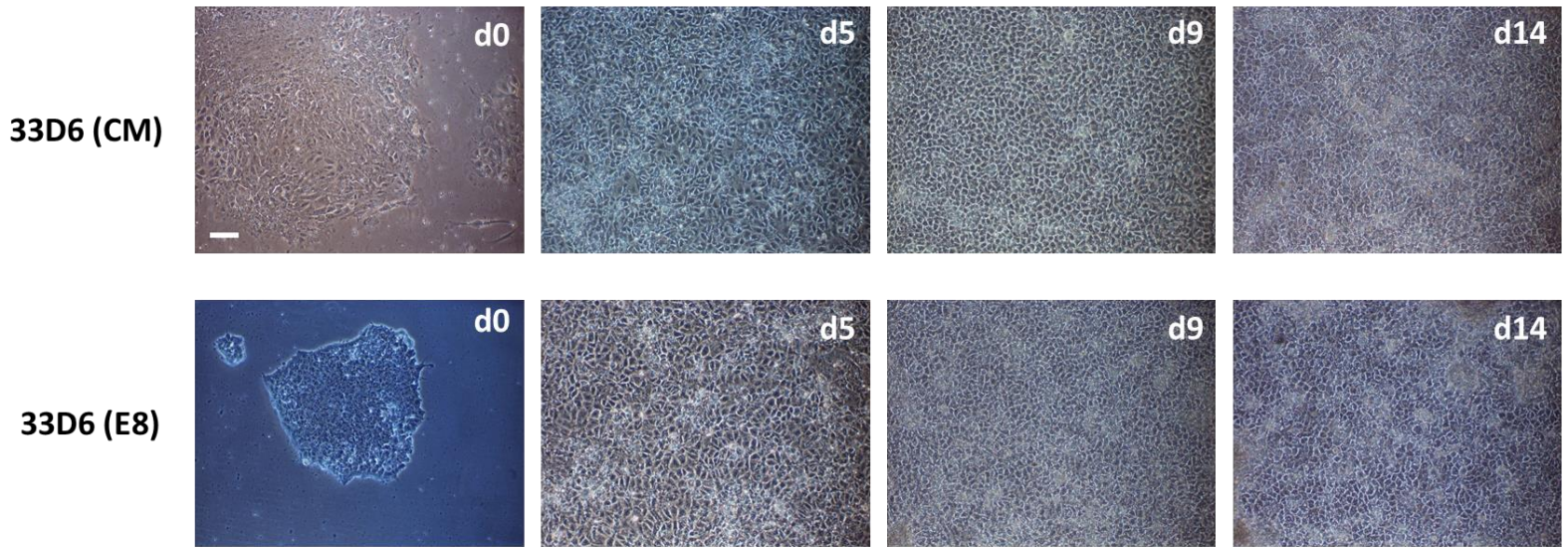

Figure 3.11: Cell morphology during hepatic differentiation (33D6). Phase-contrast imaging demonstrated the human induced pluripotent stem cells (33D6) were undergoing sequential morphological changes during transit from stem cell (day 0), to definitive endoderm (day 5), to hepatoblast (day 9), to hepatocyte (day 14) in Conditioned medium (CM) and serum - free Essential 8 (E8). Scale bar represents 100 um.

Gene and protein expression changes during hepatic differentiation using a serum – free approach

In line with changes in cell morphology, changes in gene expression throughout cellular differentiation were observed in all cell lines presented. In this project, hESCs and hiPSCs were examined for major pluripotent stem cell (OCT 3/4, NANOG), definitive endoderm (SOX17, CXCR4, NODAL) and hepatic (HNF4a, HNF1B, AFP, ALB, ECAD) markers by quantitative PCR (qPCR). The genes were normalised to B2M housekeeping gene, however appropriate gene expression was also observed when normalised to GAPDH (Supplementary Figures 1.6 and 1.7). Figure 3.12 demonstrates gene expression changes over a time course in H9s cultured either in MT or E8 medium prior to differentiation. At day 3 postdifferentiation, Oct and Nanog significantly decreased by 5- and 2.5 fold in comparison with day 0 in MT conditions. Surprisingly, H9s cultured in E8 displayed 3 fold higher expression of Nanog at day 3. hESCs cultured in E8 demonstrated significantly higher levels of endodermal markers at day 3 than in MT, as indicated by changes in CXCR4, and Nodal expression by ~5 -, and ~ 4 fold respectively. Contrary to this, Sox17 was expressed 1.5 fold higher in MT conditions. The marker of the fetal liver α-fetoprotein (AFP) was expressed at the similar gene levels (Supplementary Table 1.1A). The major hepatic transcriptional factor HNF4a was expressed in E8 conditions ~ 25 -, ~11 -, and 60-fold higher at days 3, 10, and 18 respectively in comparison with MT medium. Hepatic progenitor marker HNF1B was expressed 1.5 fold higher in E8 medium at day 10, whereas the marker of mature hepatocyte albumin (ALB) was expressed 2 fold lower at day 18 in comparison with MT conditions. E-cadherin, a marker of epithelial cell adhesion was upregulated by ~ 2.4 fold in E8 medium at day 10 in comparison with MT (Supplementary Table 1.1B).

In order to confirm efficient hepatic differentiation, immunocytochemistry was performed (Figures 3.13 and 3.14). At day 3 postdifferentiation, Oct 3/4 was downregulated to 1.4% (SE ± 0.84) and 0% for MT and E8 respectively. Sox 17 was similarly expressed at endodermal stage in both media, as indicated by 93% (SE ± 2.32) and 91% (SE ± 1.18) for MT and E8 respectively.

Upon hepatic specification, 94% (SE ± 2.73) and 88% (SE ± 4.14) of cells were positive for HNF4a expression at day 10 in MT and E8 respectively. AFP was positive in 99% of cells at day 10 and remained at the same level till day 18 in both media. Albumin was expressed by ~25% more in MT than in E8 medium at day 18 (97% (SE ± 1.1) and 72% (SE ± 3.92) respectively). E-cadherin was highly expressed both in day 0 and day 18 in both media (80-100%). Appropriate expression of markers during differentiation of H9s (MT) to hepatocytes was also confirmed by Western blot (Supplementary Figure 1.8A).

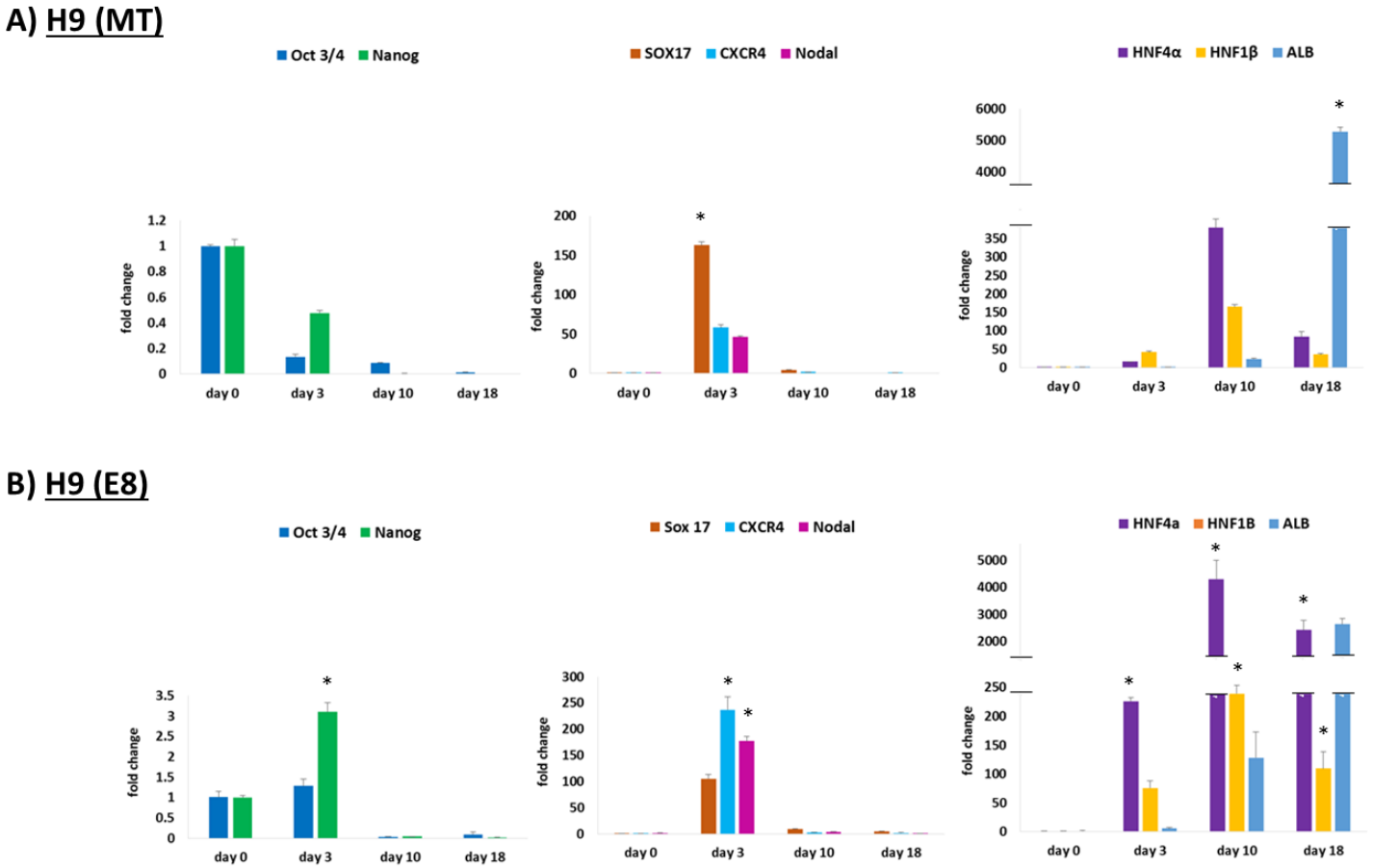

Figure 3.12: Expression of specific markers during hepatic differentiation (H9s). The quantitative polymerase chain reaction (qPCR) gene expression demonstrates over a time course downregulation of pluripotent genes (Oct3/4; Nanog), upregulation of endodermal markers (Sox17, CXCR4, Nodal), and hepatic markers (HNF4a, HNF1B, ALB) in hESC cell line H9 when cultured in mTeSR1 (A) or E8 (B) medium. Significant variances in gene expression between the two media are labelled with an asterix ($p<0.05$) as determined by Student's *t-test*.

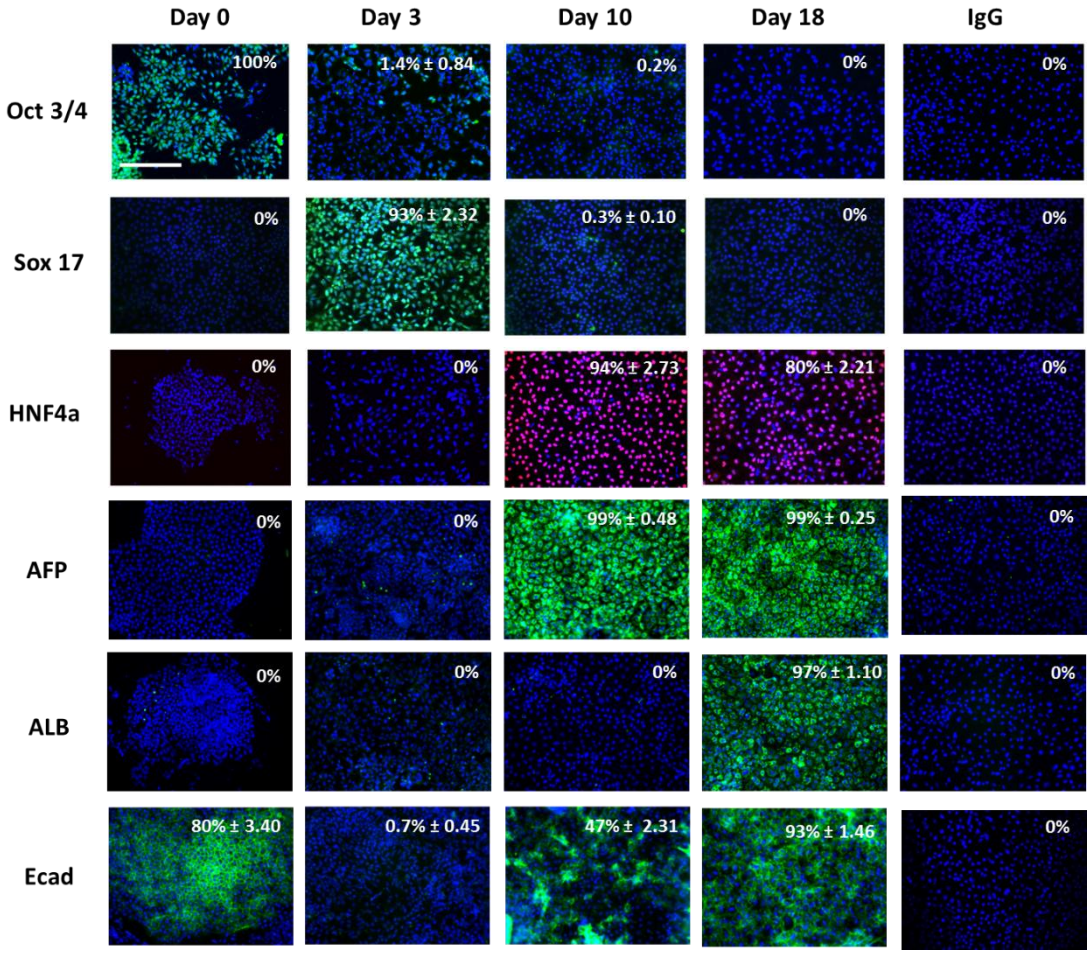

Figure 3.13: Protein expression during hepatic differentiation (H9s in MT) Stagewise hESC (H9 cell line) differentiation to the hepatocyte lineage. H9 cell line cultured in mTeSR (MT) was differentiated in a stagewise fashion toward the hepatocyte lineage. Immunocytochemistry showing downregulation of pluripotency marker Oct 4, as the cells expressed endodermal transcripts (Sox 17). Upon hepatic specification, HNF4a, AFP and ALB expression increased. Ecad expression was significantly downregulated at the definitive endoderm specification. IgG controls demonstrated the specificity of immunostaining. The percentage of positive cells is provided in the top right of each panel. This was calculated from four random fields of view and is quoted as ± standard error. The images were taken at x 20 magnification. Abbreviations: Oct 4, Octamer 4; Sox 17, SRY-box 17; HNF4a, hepatic nuclear factor 4a; AFP, alpha-fetoprotein; ALB, albumin; Ecad, E-cadherin.

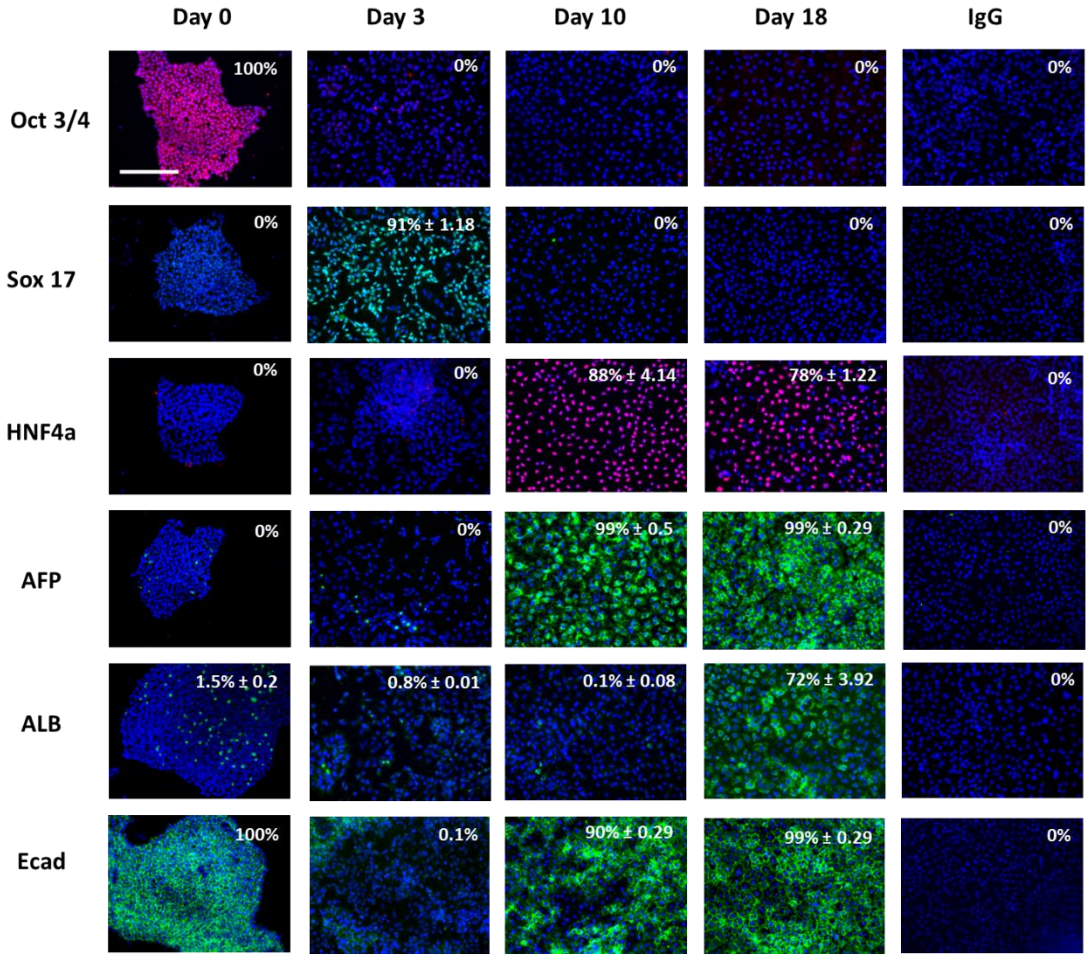

Figure 3.14: Protein expression during hepatic differentiation (H9s in E8). Stagewise hESC (H9 cell line) differentiation to the hepatocyte lineage. H9 cell line cultured in Essential 8 (E8) was differentiated in a stagewise fashion toward the hepatocyte lineage. Immunocytochemistry showing downregulation of pluripotency marker Oct 4, as the cells expressed endodermal transcripts (Sox 17). Upon hepatic specification, HNF4a, AFP and ALB expression increased. Ecad expression was significantly downregulated at the definitive endoderm specification. IgG controls demonstrated the specificity of immunostaining. The percentage of positive cells is provided in the top right of each panel. This was calculated from four random fields of view and is quoted as ± standard error. The images were taken at x 20 magnification. Abbreviations: Oct 4, Octamer 4; Sox 17, SRY-box 17; HNF4a, hepatic nuclear factor 4a; AFP, alpha-fetoprotein; ALB, albumin; Ecad, E-cadherin.

Similarly to H9s, Oct 3/4 and Nanog were downregulated in female GMP-hESC line MAN11 at day 3 of differentiation in MT conditions by 2.5 and 2 fold respectively. In E8 conditions, the gene expression of Oct remained similar in comparison with day 0, whereas Nanog expression increased by 1.6 fold. In comparison with MT, cells in E8 displayed significant upregulation of Sox17, CXCR4, and Nodal by ~450, ~ 40 -, and 30 fold change. AFP was upregulated by ~3 fold at day 10 in MT conditions in comparison with E8, whereas downregulated by ~7 fold at day 18 (Supplementary Table 1.1A). HNF4a was significantly upregulated in E8 by ~30 -, ~45 -, and ~100 fold at days 3, 10, and 18 respectively in comparison with MT medium. HNF1B demonstrated higher expression by 2 fold at day 10 in E8 medium, whereas albumin was expressed higher by ~ 14 fold in the same medium when compared with MT conditions (Figure 3.15).

Immunocytochemistry demonstrated downregulation of Oct 3/4 by ~50 fold at day 3 (2% (SE±1.86)) in MT conditions, however ~ 53.3% (SE ± 8.0) of cell remained positive for this gene in E8 at the same day. Endodermal Sox 17 was expressed at ~58 % (SE ± 5.53) in MT and ~ 98% (SE ± 0.58) in E8 at day 3 of differentiation. The master hepatic regulator HNF4a was expressed in ~84% (SE ± 1.06) and 87% cells (SE ± 1.16) at day 10 and 18 respectively in MT, whereas ~54% (SE ± 4.9) and 72% (SE ± 3.83) were positive at the same days in E8. AFP protein expression was present in ~ 63% (SE ± 2.47) at day 10, and increased up to 90% (SE ± 2.05) by day 18. The same serum protein was expressed at 99% (SE ± 0.58) at day 10 in E8, and remained stable till day 18 as indicated by 99% (SE ± 0.48). Albumin was similarly expressed in both media at day 18, as demonstrated by 95% (SE ± 2.14; MT) and 98% (SE ± 0.71; E8). E - cadherin similarly to ALB was expressed at 96% (SE ± 2.40) and 98% (SE ± 1.0) at day 18 in MT and E8 respectively (Figures 3.16 and 3.17).

A) MAN11 (MT)

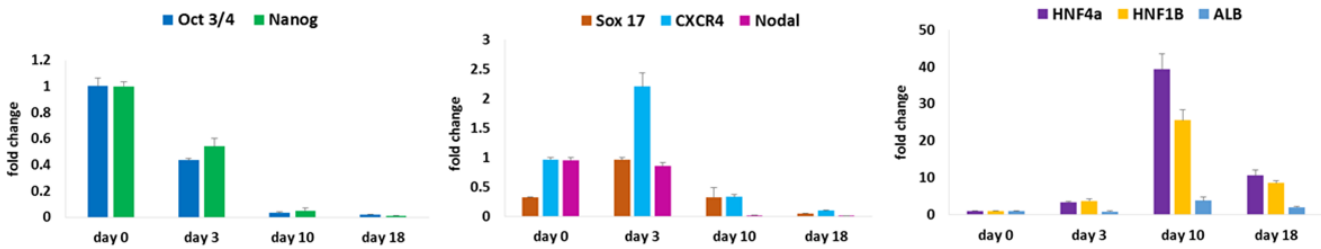

B) MAN11 (E8)

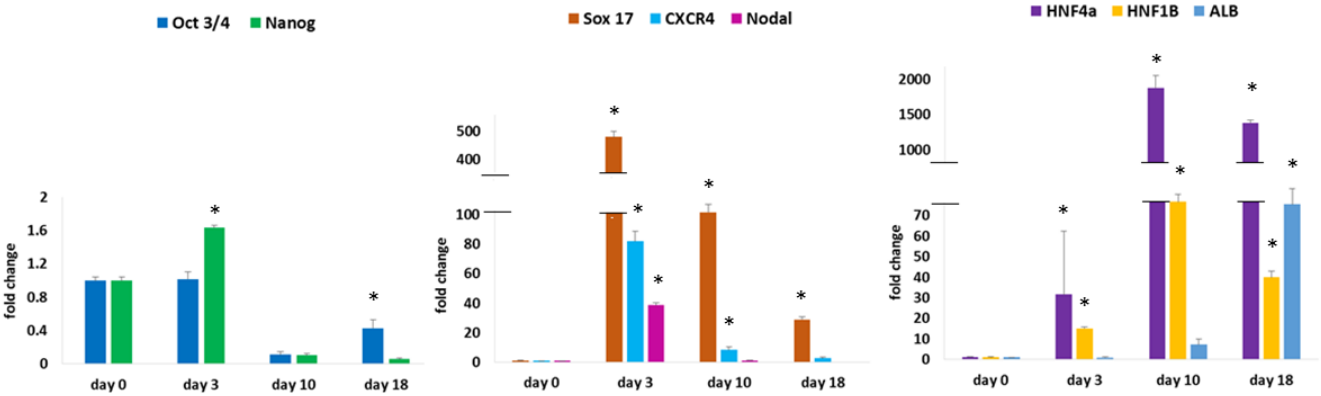

Figure 3.15: Expression of specific markers during hepatic differentiation (MAN11). The quantitative polymerase chain reaction (qPCR) gene expression demonstrates over a time course downregulation of pluripotent genes (Oct3/4; Nanog), upregulation of endodermal markers (Sox17, CXCR4, Nodal), and hepatic markers (HNF4a, HNF1B, ALB) in GMP-hESC cell line MAN11 when cultured in mTeSR1 (A) or E8 (B) medium. Significant variances in gene expression between the two media are labelled with an asterix ($p<0.05$) as determined by Student's *t-test*.

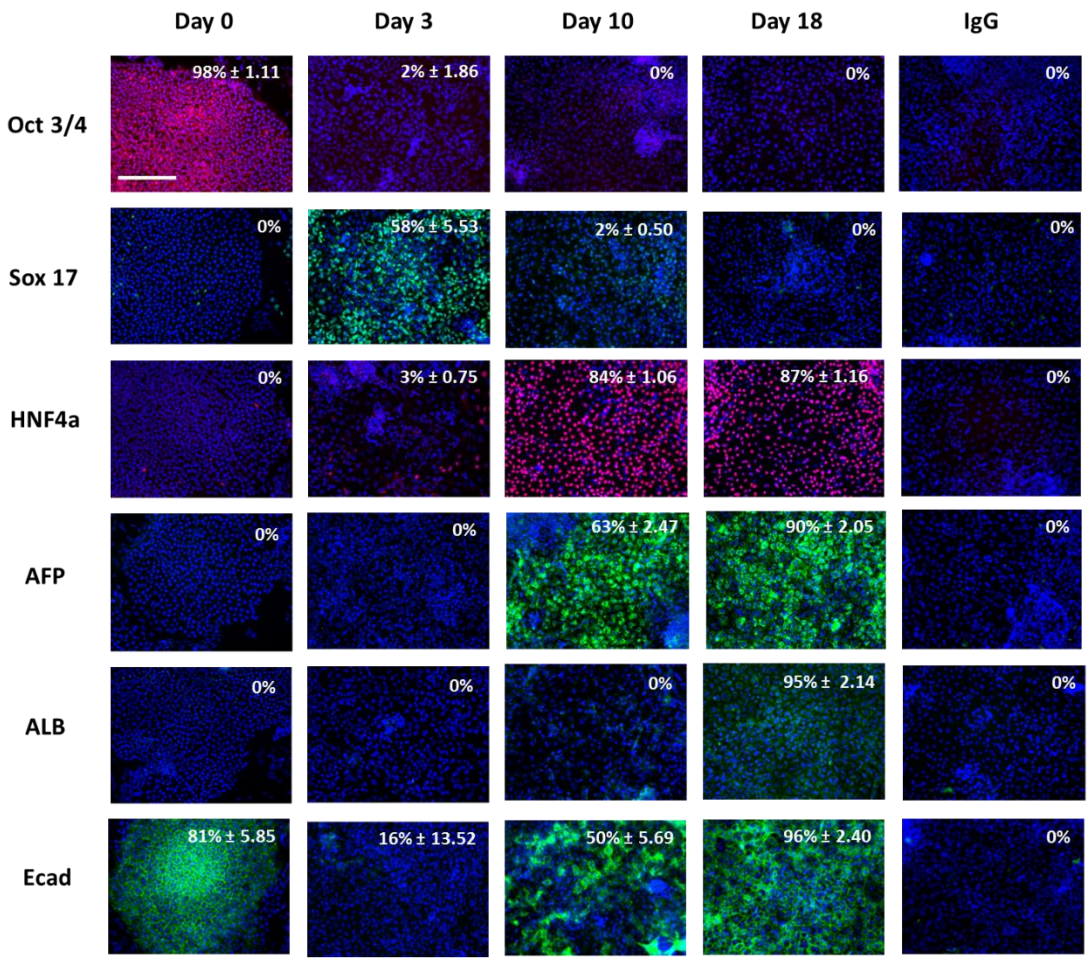

Figure 3.16: Protein expression during hepatic differentiation (MAN11 in MT). Stagewise GMP - hESC (MAN11 cell line) differentiation to the hepatocyte lineage. MAN cell line cultured in mTeSR (MT) was differentiated in a stagewise fashion toward the hepatocyte lineage. Immunocytochemistry showing downregulation of pluripotency marker Oct 4, as the cells expressed endodermal transcripts (Sox 17). Upon hepatic specification, HNF4a, AFP and ALB expression increased. Ecad expression was significantly downregulated at the definitive endoderm specification. IgG controls demonstrated the specificity of immunostaining. The percentage of positive cells is provided in the top right of each panel. This was calculated from four random fields of view and is quoted as ± standard error. The images were taken at x 20 magnification. Abbreviations: Oct 4, Octamer 4; Sox 17, SRY-box 17; HNF4a, hepatic nuclear factor 4a; AFP, alpha-fetoprotein; ALB, albumin; Ecad, E-cadherin.

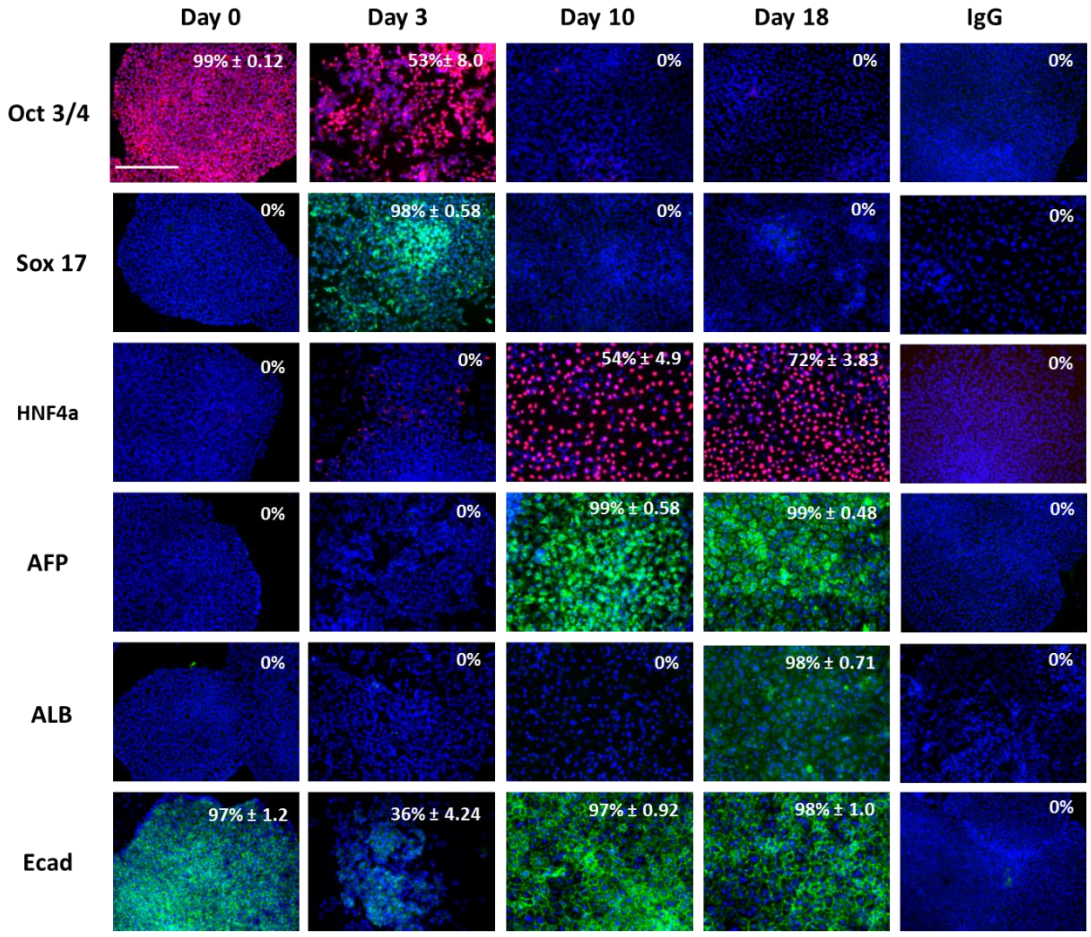

Figure 3.17: Protein expression during hepatic differentiation (MAN11 in E8). Stagewise GMP - hESC (MAN11 cell line) differentiation to the hepatocyte lineage. MAN11 cell line cultured in Essential 8 (E8) was differentiated in a stagewise fashion toward the hepatocyte lineage. Immunocytochemistry showing downregulation of pluripotency marker Oct 4, as the cells expressed endodermal transcripts (Sox 17). Upon hepatic specification, HNF4a, AFP and ALB expression increased. Ecad expression was significantly downregulated at the definitive endoderm specification. IgG controls demonstrated the specificity of immunostaining. The percentage of positive cells is provided in the top right of each panel. This was calculated from four random fields of view and is quoted as ± standard error. The images were taken at x 20 magnification. Abbreviations: Oct 4, Octamer 4; Sox 17, SRY-box 17; HNF4a, hepatic nuclear factor 4a; AFP, alpha-fetoprotein; ALB, albumin; Ecad, E-cadherin.

Male GMP-hESC line MAN12 displayed increase in Oct and Nanog by 2.5 fold and 1.5 fold at day 3 in MT medium respectively (Figure 3.18). Similarly, Nanog was upregulated by ~1.5 fold in E8 medium at the endodermal stage, whereas Oct levels remained the same at day 3. The upregulated Oct expression at endodermal stage in both media was confirmed by immunostaining where ~ 55% and 86% of cells remained positive for this gene in MT and E8 conditions respectively

(Figures 3.19 and 3.20). Cells cultured in E8 medium demonstrated a significant increase in Sox17, CXCR4, and Nodal by ~125-, ~28-, and ~ 22 fold in comparison with MT conditions. AFP gene and protein expression was similarly expressed in both media at days 10 and 18 (Supplementary Table 1.1A). Although HNF4a displayed increase in gene expression by ~30, ~ 60, ~900 fold at days 3, 10, and 18 in E8 medium when compared to MT, the protein expression was similarly expressed at hepatoblast and hepatocyte stage in both media (Figures 3.18, 3.19 and 3.20). HNF1B was increased by ~10 fold in E8 medium at day 10 in comparison with other conditions. Contrary to other genes, albumin expression increased by ~10 fold in MT medium in comparison with E8.

Gene expression results were further confirmed by immunocytochemistry (Figures 3.19 and 3.20). Oct 3/4 protein expression was downregulated at day 3, however remained still highly expressed at day 3 as indicated by ~ 55% (SE ± 4.0) and 86% (SE ± 5.20) of cell being positive for this protein in MT and E8 respectively. Although results at day 3 were different as expected, the Oct expression was not present from day 10 onwards in both conditions. Sox17 protein expression was present in both media at ~ 85% (SE ± 1.29; MT) and 89% (SE ± 4.09; E8) at the definitive endoderm stage. Upon hepatic specification, HNF4a was present at ~ 82% (SE ± 4.66) and 88% (SE ± 6.40) at day 10 in MT and E8 respectively, whereas the expression of this protein was downregulated to ~ 68% (SE ± 3.05) in MT and in E8 remained constant (88%; SE ± 0.49) by day 18 of differentiation. In MT conditions, AFP was expressed at 100% at day 10 and remained stable till day 18 (99%; SE ± 0.48). The same protein was expressed in ~ 99% (SE ± 0.33) of cells at the hepatoblast stage, and was slightly decreased to ~ 82% (SE ± 6.57) by hepatocyte stage. Both conditions demonstrated similar expression of albumin at day 18 of differentiation, as indicated by 99% (SE ± 0.58; MT) and 97% (SE ± 1.15; E8) of cells being positive for this protein. E – cadherin was similarly expressed in both media at 99% (SE ± 0.33) and 91% (SE ± 2.50) at day 18.

A) MAN12 (MT)

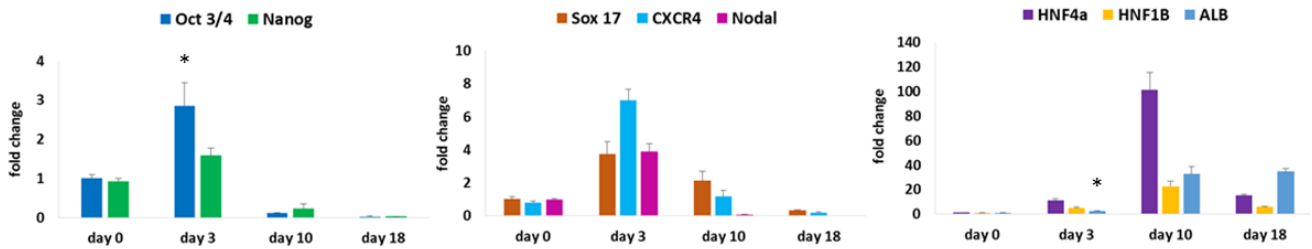

B) MAN12 (E8)

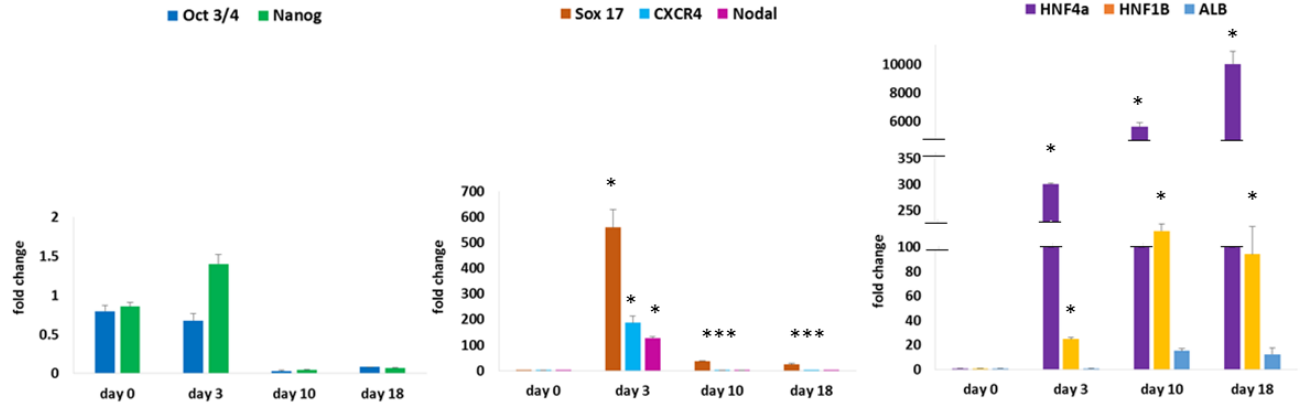

Figure 3.18: Expression of specific markers during hepatic differentiation (MAN12). The quantitative polymerase chain reaction (qPCR) gene expression demonstrates over a time course downregulation of pluripotent genes (Oct3/4; Nanog), upregulation of endodermal markers (Sox17, CXCR4, Nodal), and hepatic markers (HNF4a, HNF1B, ALB) in GMP-hESC cell line MAN12 when cultured in mTeSR1 (A) or E8 (B) medium. Significant variances in gene expression between the two media are labelled with an asterix ($p<0.05$) as determined by Student's *t-test*.

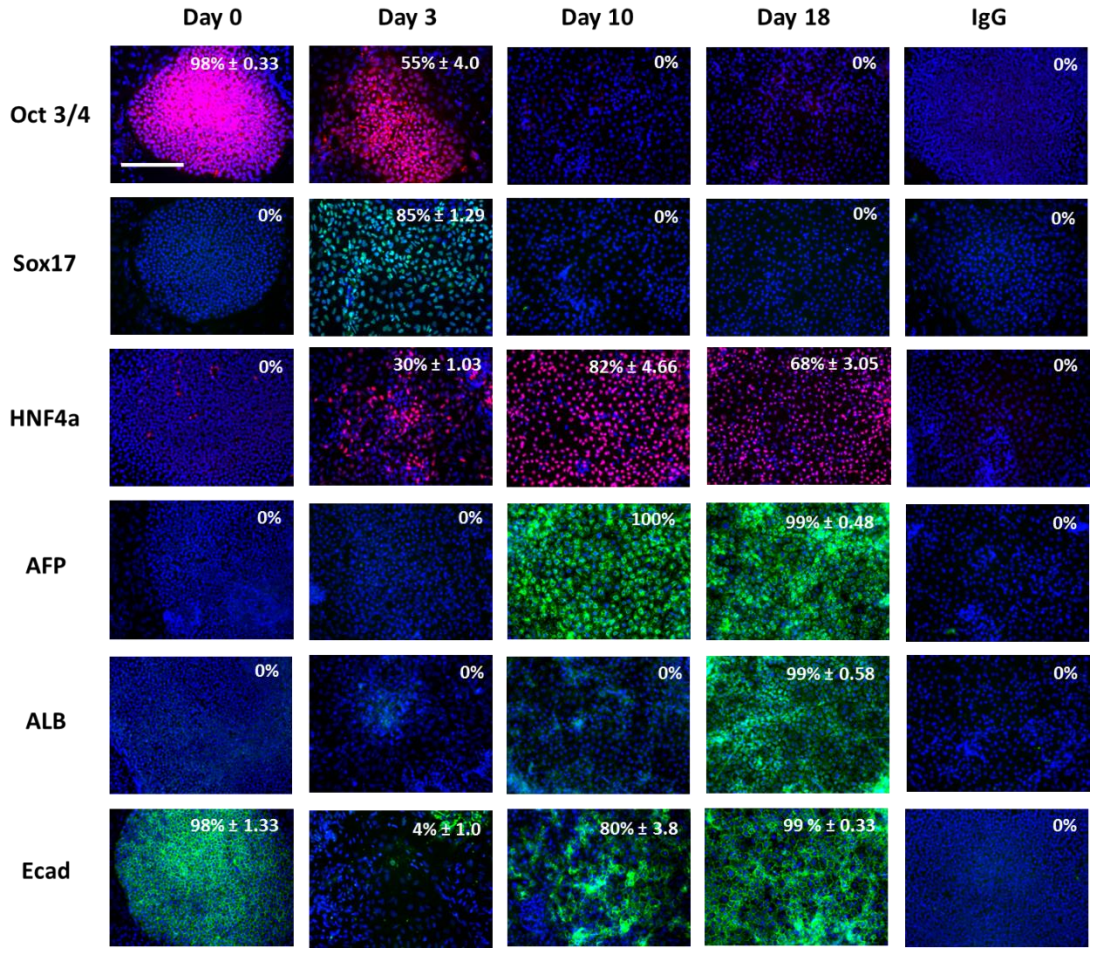

Figure 3.19: Protein expression during hepatic differentiation (MAN12 in MT). Stagewise GMP-hESC (MAN12 cell line) differentiation to the hepatocyte lineage. MAN12 cell line cultured in mTeSR (MT) was differentiated in a stagewise fashion toward the hepatocyte lineage. Immunocytochemistry showing downregulation of pluripotency marker Oct 4, as the cells expressed endodermal transcripts (Sox 17). Upon hepatic specification, HNF4a, AFP and ALB expression increased. Ecad expression was significantly downregulated at the definitive endoderm specification. IgG controls demonstrated the specificity of immunostaining. The percentage of positive cells is provided in the top right of each panel. This was calculated from four random fields of view and is quoted as ± standard error. The images were taken at x 20 magnification. Abbreviations: Oct 4, Octamer 4; Sox 17, SRY-box 17; HNF4a, hepatic nuclear factor 4a; AFP, alpha-fetoprotein; ALB, albumin; Ecad, E-cadherin.

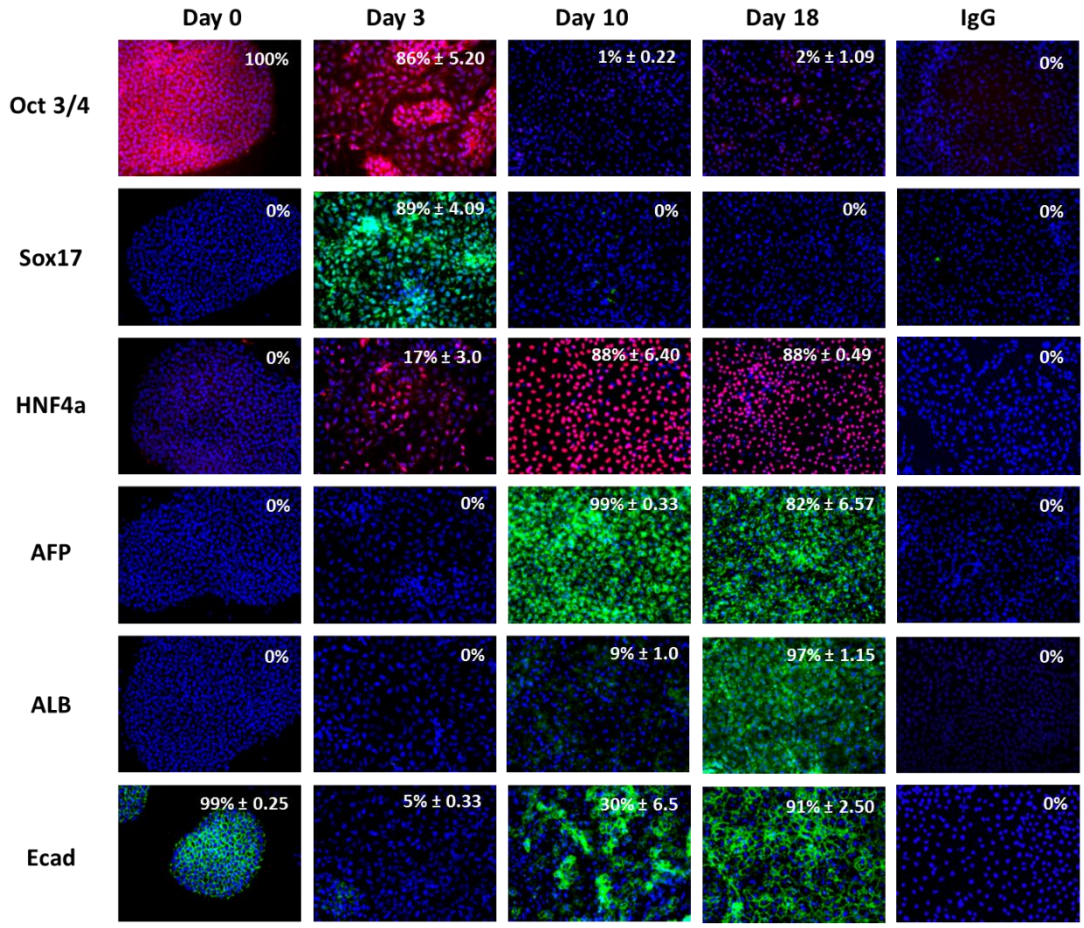

Figure 3.20: Protein expression during hepatic differentiation (MAN12 in E8) Stagewise GMP - hESC (MAN12 cell line) differentiation to the hepatocyte lineage. MAN12 cell line cultured in Essential 8 (E8) was differentiated in a stagewise fashion toward the hepatocyte lineage. Immunocytochemistry showing downregulation of pluripotency marker Oct 4, as the cells expressed endodermal transcripts (Sox 17). Upon hepatic specification, HNF4a, AFP and ALB expression increased. Ecad expression was significantly downregulated at the definitive endoderm specification. IgG controls demonstrated the specificity of immunostaining. The percentage of positive cells is provided in the top right of each panel. This was calculated from four random fields of view and is quoted as ± standard error. The images were taken at x 20 magnification. Abbreviations: Oct 4, Octamer 4; Sox 17, SRY-box 17; HNF4a, hepatic nuclear factor 4a; AFP, alpha-fetoprotein; ALB, albumin; Ecad, E-cadherin.

Figure 3.21 demonstrates that hiPSC line 33D6 initially cultured in CM displayed downregulation of Oct and Nanog by 2.5 and 10 fold respectively by day 5 of differentiation. In E8 conditions at day 5, Oct expression remained the same, whereas Nanog increased by ~ 2 fold. Similarly to other lines, endodermal genes were significantly upregulated at day 5 in E8 medium in comparison with alternative conditions.

This was indicated by increase in Sox17, CXCR4, and Nodal gene expression by ~16, ~66-, and ~45 fold change in E8 medium. HNF4a increased by ~13-, ~122-, and ~500 fold at days 5, 9, and 14 in E8 medium in comparison with CM. HNF1B transcription factor was similarly expressed in both media at day 5, whereas at day 9 it increased by ~47 fold in E8 medium when compared with CM. AFP gene expression increased ~521 fold in E8 in comparison with CM, whereas E-cad increased by ~12 fold in E8 (Supplementary Table 1.1 A and B). Albumin was upregulated by ~3 fold at day 14 in E8 medium in comparison with CM conditions.

Successful differentiation of hiPSC line 33D6 was confirmed by immunocytochemistry (Figures 3.22 and 3.23). The pluripotent marker Oct 3/4 was significantly decreased by day 3, as indicated by 0.8% (SE ± 0.2) and 0.1% in MT and E8 media respectively. HNF4a hepatic marker was similarly expressed in MT and E8 conditions at day 10, as indicated by ~98% (SE ± 0.47) and ~97% (SE ± 0.48) respectively. By day 18 the hepatic transcription marker expression decreased to ~65% (SE ± 0.40) in MT, whereas in E8 conditions the expression remained constant (~91%; SE ± 4.18). At day 10, AFP protein expression was significantly upregulated in MT conditions as indicated by 100% of cells being positive for this marker, whereas only 42% (SE ± 0.63) of cell were expressing this protein in E8. By day 18, the expression of AFP was similar in both conditions (~98%, SE ± 0.3 for MT and 100% for E8). At the hepatocyte stage, E – cadherin was present in ~98% (SE ± 0.33) and 95% (SE ± 0.58) cells in MT and E8 respectively. Appropriate expression of markers during differentiation of 33D6s (CM) to hepatocytes was also confirmed by Western blot (Supplementary Figure 1.8B).

A) 33D6 (CM)

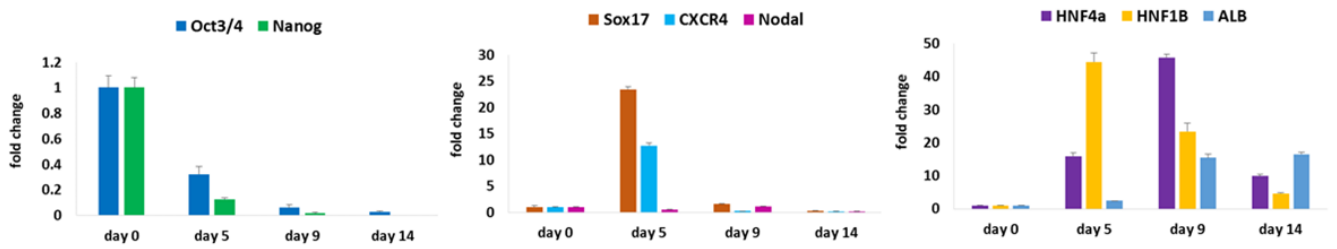

B) 33D6 (E8)

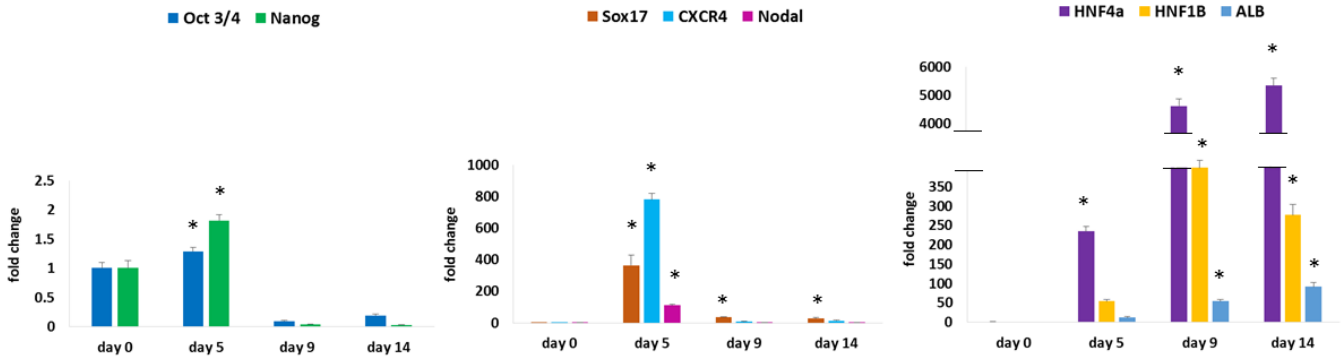

Figure 3.21: Expression of specific markers during hepatic differentiation (33D6). The quantitative polymerase chain reaction (qPCR) gene expression demonstrates over a time course downregulation of pluripotent genes (Oct3/4; Nanog), upregulation of endodermal markers (Sox17, CXCR4, Nodal), and hepatic markers (HNF4a, HNF1B, ALB) in hIPSC cell line 33D6 when cultured in CM (A) or E8 (B) medium. Significant variances in gene expression between the two media are labelled with an asterix ($p<0.05$) as determined by Student's *t-test*.

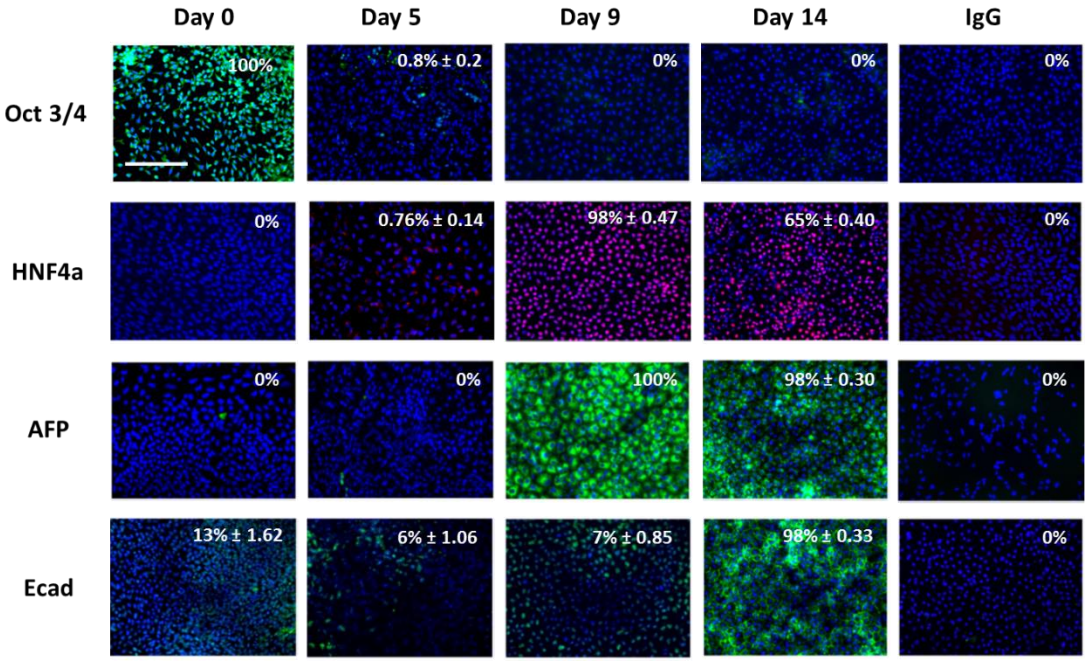

Figure 3.22: Protein expression during hepatic differentiation (33D6 in CM). Stagewise hiPSC (33D6 cell line) differentiation to the hepatocyte lineage. 33D6 cell line cultured in Conditioned Medium (CM) was differentiated in a stagewise fashion toward the hepatocyte lineage. Immunocytochemistry showing downregulation of pluripotency marker Oct 4. Upon hepatic specification, HNF4a and AFP expression increased. Ecad expression was significantly downregulated at the definitive endoderm specification. IgG controls demonstrated the specificity of immunostaining. The percentage of positive cells is provided in the top right of each panel. This was calculated from four random fields of view and is quoted as ± standard error. The images were taken at x 20 magnification. Abbreviations: Oct 4, Octamer 4; HNF4a, hepatic nuclear factor 4a; AFP, alpha-fetoprotein; Ecad, Ecadherin.

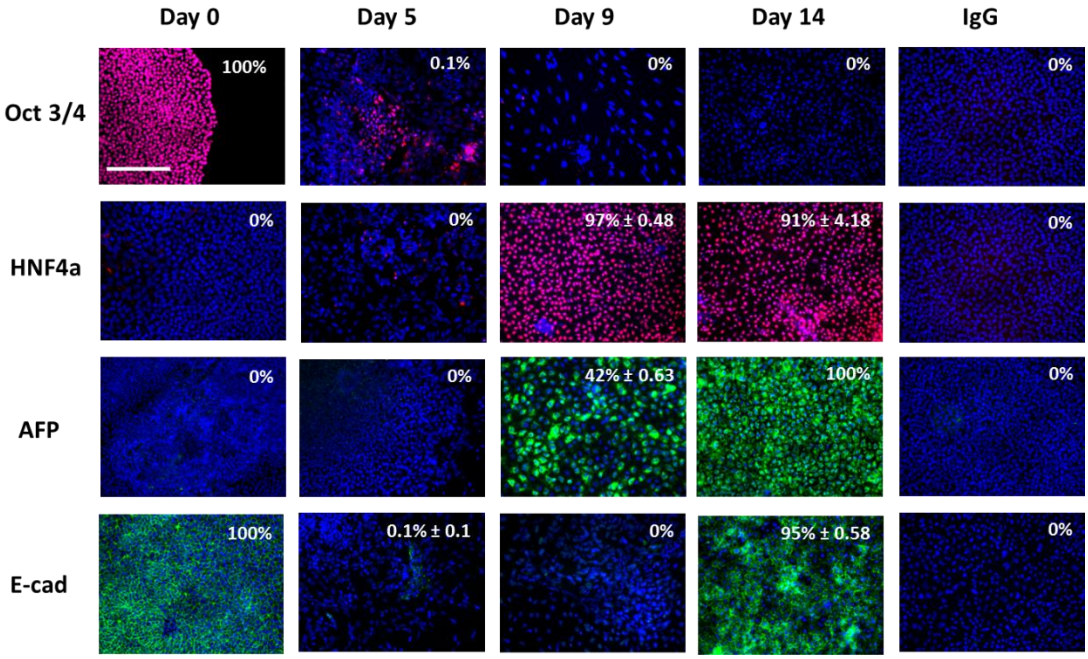

Figure 3.23: Protein expression during hepatic differentiation (33D6 in E8). Stagewise hiPSC (33D6 cell line) differentiation to the hepatocyte lineage. 33D6 cell line cultured in Essential 8 (E8) was differentiated in a stagewise fashion toward the hepatocyte lineage. Immunocytochemistry showing downregulation of pluripotent marker Oct 4. Upon hepatic specification, HNF4a, AFP and AFP expression increased. Ecad expression was significantly downregulated at the definitive endoderm specification. IgG controls demonstrated the specificity of immunostaining. The percentage of positive cells in provided in the top right of each panel. This was calculated from four random of fields of view and is quoted as ± standard error. The images were taken at x 20 magnification. Abbreviations: Oct 4, Octamer 4; HNF4a, hepatic nuclear factor 4a; AFP, alpha-fetoprotein; Ecad, Ecadherin.

Metabolic function of PSC-derived hepatocytes using a serum-free approach

The liver plays a central role in many biochemical processes. In this project, the interest was specifically in drug metabolism and how stem cell – derived models could be used to study compound pharmacology and hepatotoxicity. The first step was to assess which, if any, cell based assay was suitable to for large-scale screening within the pharmaceutical industry. In order to progress to large – scale manufacture and industrial screening, stem cell –derived hepatocytes had to exhibit inducible cytochrome P450 activity. Using our serum – free process, hESCs (H9 lines) and hiPSCs demonstrated significantly improved metabolic capacity and were more stable in character, when compared with previous approaches using serum-containing medium (Hay *et al*, 2008a; Sullivan *et al*, 2010). Whereas basal activities of the cytochrome P450 enzymes provided important background information, we were keen to assess whether PSC-derived hepatocytes were drug – inducible, a hallmark of more mature hepatocyte. To assess this, pleiotropic P450 inducer, phenobarbital (PB), was used. Human ES and iPS cells selected in this project were induced with 1 mM PB for 48 hours before the assessment of P450 activity.

Hepatocytes derived from H9 line cultured in MT medium exhibited inducible CYP3A (~ 5 fold) and CYP1A2 (~ 4 fold) activity (Figure 3.24). Contrary to MT, hepatic cells derived from H9 line cultured in E8 demonstrated no induction of CYP3A enzymes, however CYP1A2 was induced by ~4 fold (Figure 3.24). Hepatocytes derived from GMP-hESC female MAN11 line initially cultured in MT displayed induction of CYP3A by ~2 fold, whereas no significant induction of CYP1A2 was observed (Figure 3.25). Similarly, neither CYP3A nor CYP1A2 was induced in E8 medium by phenobarbital (Figure 3.25). Hepatic cells derived from GMP-hESCs male MAN12 line cultured either in MT or E8 conditions did not display any CYP3A induction (Figure 3.26). CYP1A2 in MAN12-derived hepatocytes in both media was induced but not significantly (p>0.05). Although, somatic cells derived from hiPSC line 33D6 demonstrated activity of both enzymes in two different media conditions, no drug induction was observed (Figure 3.27).

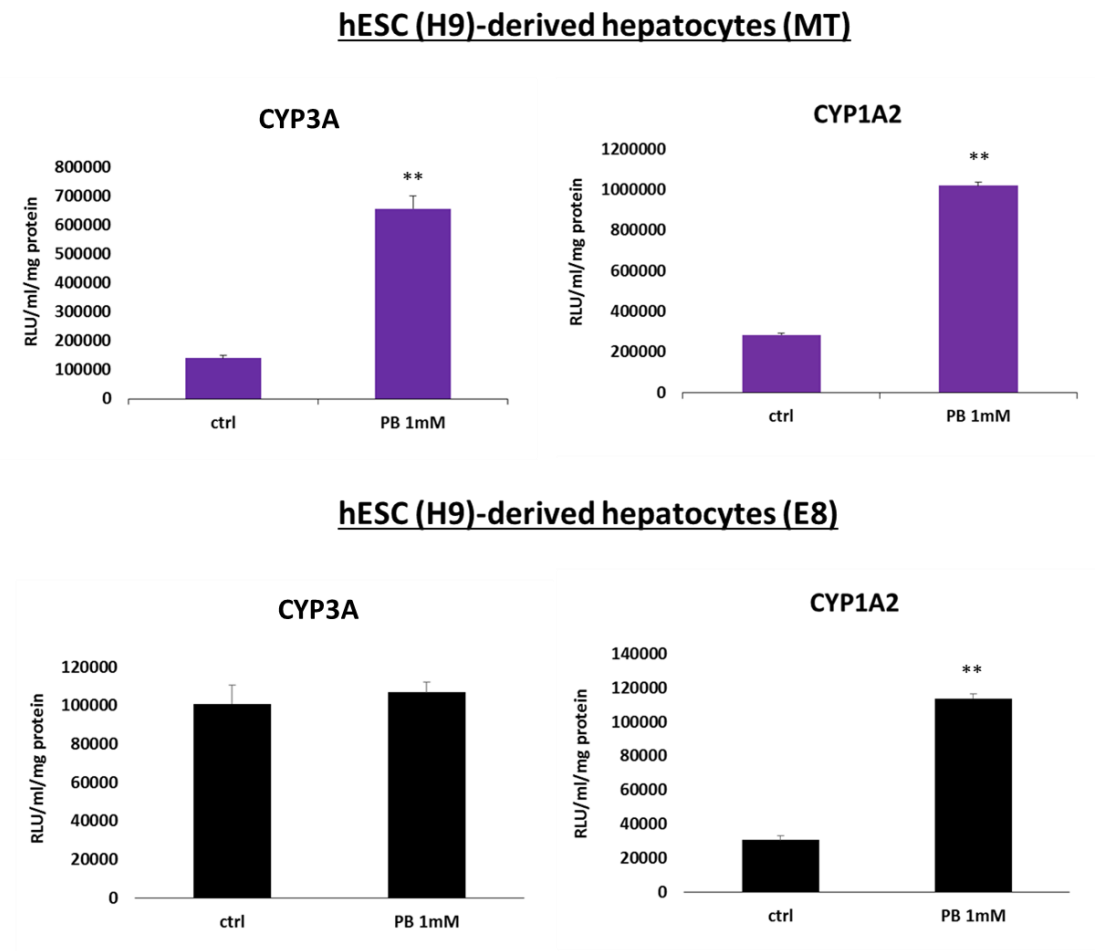

Figure 3.24: Cytochrome P450 activity of hESC (H9)-derived hepatocytes. Human hESC-derived hepatocytes display Cytochrome P450 drug metabolism (CYP3A and CYP1A2). The top panel demonstrates hepatocytes displaying both basic and inducible Cytochrome P450 3A and 1A2 drug metabolism when derived from ES cells cultured in mTeSR (MT) medium. The lower panel demonstrates hepatocytes displaying both basic Cytochrome P450 3A and 1A2 activity when derived from ES cells cultured in Essential 8 (E8) medium, however only CYP1A2 was induced. Phenobarbital drug induction was carried out from day 16 for 48h, changing medium and phenobarbital on the daily basis. The CYP3A and CYP1A2 activity were measured using the nonlytic pGLO™ System (Promega) at day 18 (hESC-derived hepatocytes). At 5h post treatment, CYP3A and CYP1A2 activity were measured on a luminometer (Promega). Units of activity are expressed as relative light unit (RLU) ml^{-1} mg^{-1} protein (n=3). Level of significance are quoted and measured by Student's *t-test*. Significance levels are denoted ** ($P < 0.01$). Abbreviations: PB, Phenobarbital; Ctrl, Control; ml, millilitre; mg, milligram; mM, millimolar.

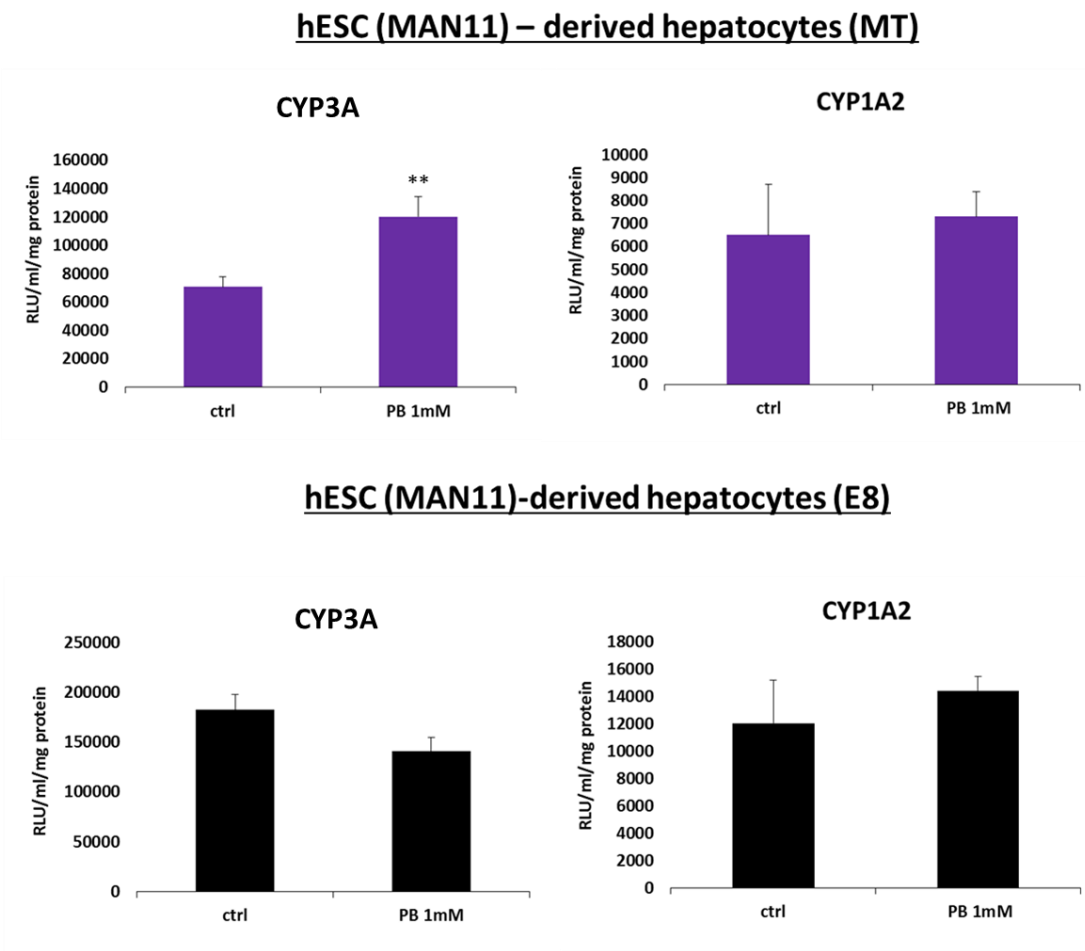

Figure 3.25: Cytochrome P450 activity of hESC (MAN11)-derived hepatocytes. Human hepatocytes derived from female GMP-grade hESC MAN11 line display Cytochrome P450 drug metabolism (CYP3A and CYP1A2). The top panel demonstrates hepatocytes displaying basic Cytochrome P450 3A and 1A2 when derived from ES cells cultured in mTeSR (MT) medium, however only inducible is 3A. The lower panel demonstrates hepatocytes displaying basic Cytochrome P450 3A and 1A2 activity when derived from ES cells cultured in Essential 8 (E8) medium. No drug induction was observed for both enzymes. Phenobarbital drug induction was carried out from day 16 for 48h, changing medium and phenobarbital on the daily basis. The CYP3A and CYP1A2 activity were measured using the nonlytic pGLO^{TM} System (Promega) at day 18 (hESC-derived hepatocytes). At 5h post treatment, CYP3A and CYP1A2 activity were measured on a luminometer (Promega). Units of activity are expressed as relative light unit (RLU) ml^{-1} mg^{-1} protein (n=3). Level of significance are quoted and measured by Student's *t-test*. Significance levels are denoted ** ($P < 0.01$). Abbreviations: PB, Phenobarbital; Ctrl, Control; ml, millilitre; mg, milligram; mM, millimolar.

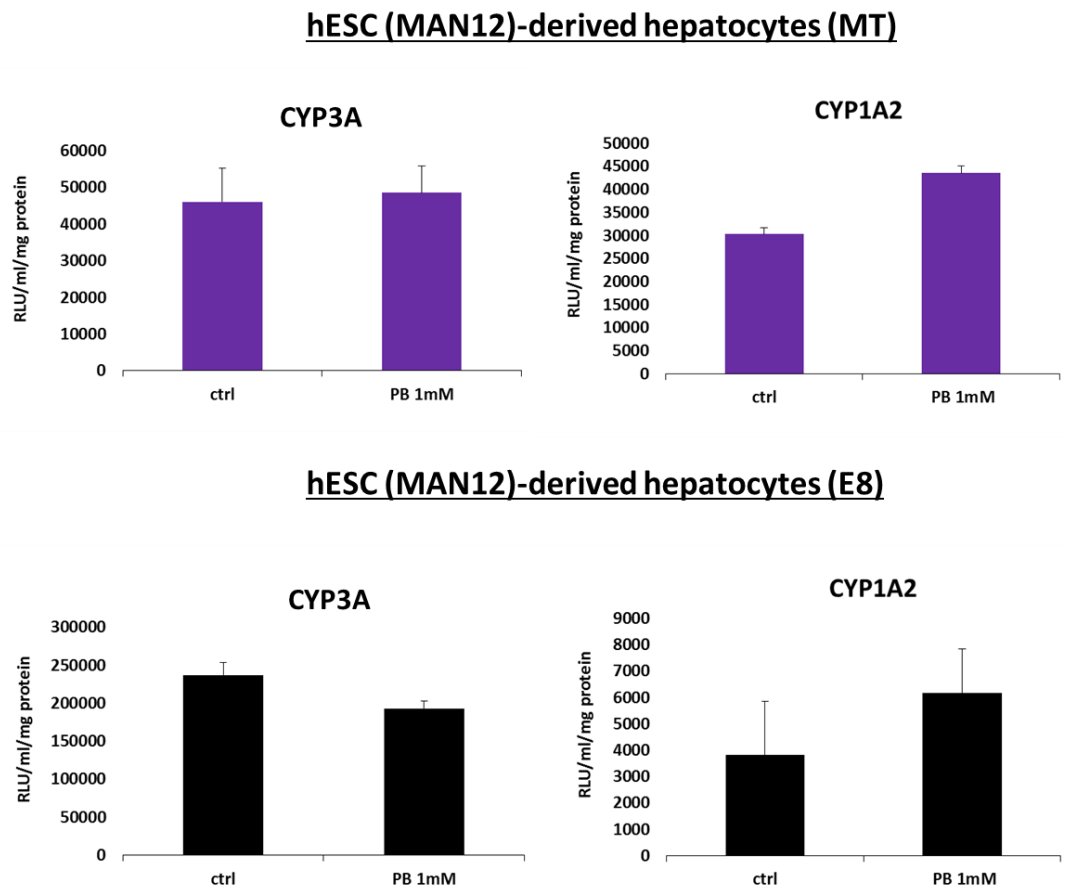

Figure 3.26: Cytochrome P450 activity of hESC (MAN12)-derived hepatocytes Human hepatocytes derived from male GMP-grade hESC MAN12 line display Cytochrome P450 drug metabolism (CYP3A and CYP1A2). The top panel demonstrates hepatocytes displaying basic Cytochrome P450 3A and 1A2 when derived from ES cells cultured in mTeSR (MT) medium. The lower panel demonstrates hepatocytes displaying basic Cytochrome P450 3A and 1A2 activity when derived from ES cells cultured in Essential 8 (E8) medium. No drug induction was observed for both enzymes in neither of the medium. Phenobarbital drug induction was carried out from day 16 for 48h, changing medium and phenobarbital on the daily basis. The CYP3A and CYP1A2 activity were measured using the nonlytic pGLO™ System (Promega) at day 18 (hESC-derived hepatocytes). At 5h post treatment, CYP3A and CYP1A2 activity were measured on a luminometer (Promega). Units of activity are expressed as relative light unit (RLU) ml^{-1} mg^{-1} protein (n=3). Abbreviations: PB, Phenobarbital; Ctrl, Control; ml, millilitre; mg, milligram; mM, millimolar.

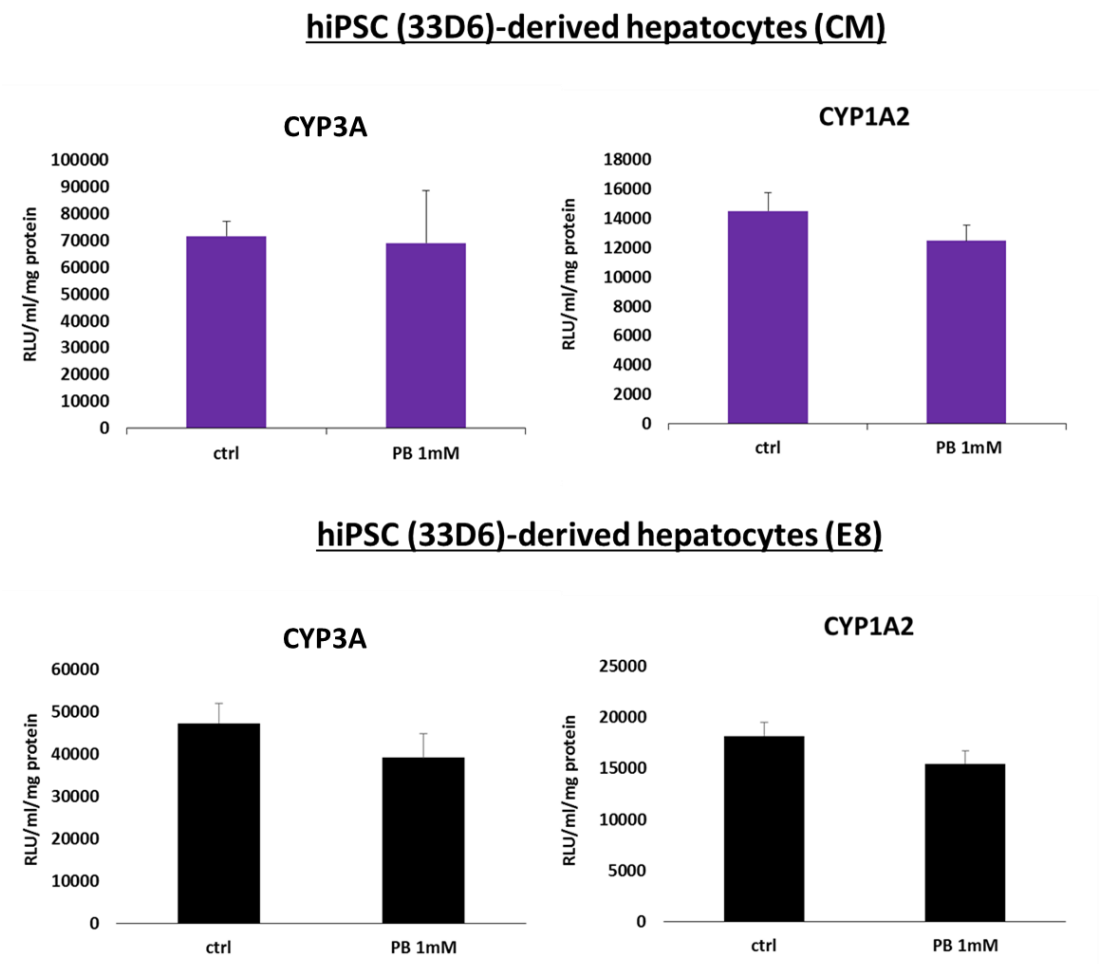

Figure 3.27: Cytochrome P450 activity of hiPSC (33D6)-derived hepatocytes. Human hepatocytes derived from hiPSC line (33D6) display Cytochrome P450 drug metabolism (CYP3A and CYP1A2). The top panel demonstrates hepatocytes displaying basic Cytochrome P450 3A and 1A2 when derived from hiPCS cells cultured in MEFs Conditioned Medium (CM) medium. The lower panel demonstrates hepatocytes displaying basic Cytochrome P450 3A and 1A2 activity when derived from hiPSC cells cultured in Essential 8 (E8) medium. No drug induction was observed for both enzymes in neither of the medium. Phenobarbital drug induction was carried out from day 12 for 48h, changing medium and phenobarbital on the daily basis. The CYP3A and CYP1A2 activity were measured using the nonlytic pGLO^{TM} System (Promega) at day 14 (hESC-derived hepatocytes). At 5h post treatment, CYP3A and CYP1A2 activity were measured on a luminometer (Promega). Units of activity are expressed as relative light unit (RLU) ml^{-1} mg^{-1} protein (n=3). Abbreviations: PB, Phenobarbital; Ctrl, Control; ml, millilitre; mg, milligram; mM, millimolar.

3.2.3 HESC-DERIVED HEPATOCYTES AS A RELIABLE MODEL TO PREDICT DRUG-INDUCED LIVER INJURY

As it was clear that hepatocytes derived from the H9 cell line exhibited the highest basal and drug inducible cytochrome P450 activity, we elected to use hESC-derived hepatocytes to examine their potential for future large-scale manufacture and industrial application. hESC - derived hepatocytes, chosen on their basis of metabolic competence, were compared to a well-characterised batch of cryoplatable human hepatocytes (referred as primary hepatocytes). hESCs were scaled up and differentiated in 96-well plate format. In collaboration with Bristol-Myers-Squibb (USA) twenty known hepatotoxins were screened using primary and stem cell-derived hepatocytes (Table 3.2). Each cell type was incubated with specific compound for 1, 4, or 7 days. In general, toxicity increased with time of exposure and eventually all compounds identified as toxic (IC_{50} < 200 uM) in primary human hepatocyte cultures were also toxic in hESC hepatocytes. Initially (day 1), fewer compounds were toxic to hESC hepatocytes (45%) as compared with primary hepatocytes (60%), but by day 4 hESC hepatocytes displayed increased sensitivity (65%) over primary hepatocytes (60%). One compound, benzobromarone, was substantially more toxic in hESC hepatocytes cultures than in primary hepatocytes, but most compounds (8 of 20) were more toxic in primary hepatocyte cultures. By day 7, both assays identified 75% of the hepatotoxins as toxic *in vitro*.

	hESC hepatocytes		
Test Articles	Day 1 IC50 (μM)	Day 4 IC50 (μM)	Day 7 IC50 (μM)
Amiodarone	171.13	64.77	20.25
Benzbromarone	174.66	74.41	42.57
Isoniazid	>200	>200	>200
Bicalutamide	>200	112.55	33.86
Danazol	>200	>200	56.61
Diclofenac	>200	>200	>200
Dantrolene	>200	>200	189.76
Dacarbazine	>200	>200	>200
Felbamate	>200	>200	>200
Hycanthone	63.34	5.35	1.83
Ketoconazole	131.10	62.60	32.06
Perhexiline	23.08	21.22	6.46
Nitrofurantoin	>200	51.89	24.09
Puromycin	9.71	0.86	0.27
Flutamide	>200	45.49	18.74
Simvastatin	>200	7.23	6.63
Tolcapone	92.37	47.73	47.34
Valproic Acid	>200	>200	>200
Troglitazone	198.53	101.06	85.74
Nefazodone	105.67	42.38	28.49

	Cryoplateable hepatocytes		
Test Articles	Day 1 IC50 (μM)	Day 4 IC50 (μM)	Day 7 IC50 (μM)
Amiodarone	103.55	59.15	25.00
Benzbromarone	>200	>200	186.42
Isoniazid	>200	>200	>200
Bicalutamide	87.48	54.44	67.32
Danazol	36.78	21.80	41.24
Diclofenac	>200	>200	>200
Dantrolene	>200	>200	58.54
Dacarbazine	>200	>200	>200
Felbamate	>200	>200	>200
Hycanthone	0.28	0.06	0.07
Ketoconazole	24.46	2.51	12.09
Perhexiline	5.28	2.00	1.01
Nitrofurantoin	40.48	1.36	8.55
Puromycin	1.19	0.10	1.06
Flutamide	50.76	8.77	13.72
Simvastatin	100.60	9.57	13.52
Tolcapone	170.85	78.20	54.75
Valproic Acid	>200	>200	>200
Troglitazone	>200	>200	37.93
Nefazodone	11.25	2.11	11.52

Table 3.2: Prediction of drug – induced liver injury. IC50 for 20 human hepatotoxicants cultured with hESC-derived hepatocytes and cryopreserved human hepatocytes for 1, 4, or 7 days. Cellular ATP levels were measured and used to calculate IC50 (the concentration of the compound resulting in 50% toxicity). Wells were plated in triplicate for each concentration and each compound tested. If a compound failed to generate IC50 with the maximum concentration tested (200 uM), it was expressed as > 200. In general, toxicity increased with time of exposure. All compounds eventually were identified as toxic (e.g, an IC50 < 200 uM) in primary (cryopreserved) hepatocyte cultures were also toxic in hESC hepatocytes. Abbreviations: hESC, human embryonic stem cell. The experiment and analysis was performed by Dr Sarah Farnworth and Bristol-Myers-Squibb (BMS; USA). The results are published in Szkolnicka *et al*, 2014b.

As drug-induced liver injury is a complex process, it was important not only to assess cell viability (ATP production) but also the mechanism of cell death. In order to examine this, caspase 3/7 activity was measured by fluorescence using the Apo-ONE Homogenous Caspase 3/7 assay (Promega). The results demonstrated that nine of the fifteen toxic compounds induced increases in caspase 3/7 production over the same range of concentrations that reduced ATP (Figure 3.28). The remaining six toxic compounds did not induce caspase activity (Figure 3.29). Of the five compounds that were not toxic, concentration – related increases in hESC hepatocyte ATP were observed for dacarbazine, felbamate, and valproic acid, indicative of hormesis (Figure 3.30). Of note, troglitazone also induced a substantial increase in hESC hepatocyte ATP on day 7, at lower concentrations, before sustaining a complete loss of cell ATP between 10 and 100 uM (Figure 3.28).

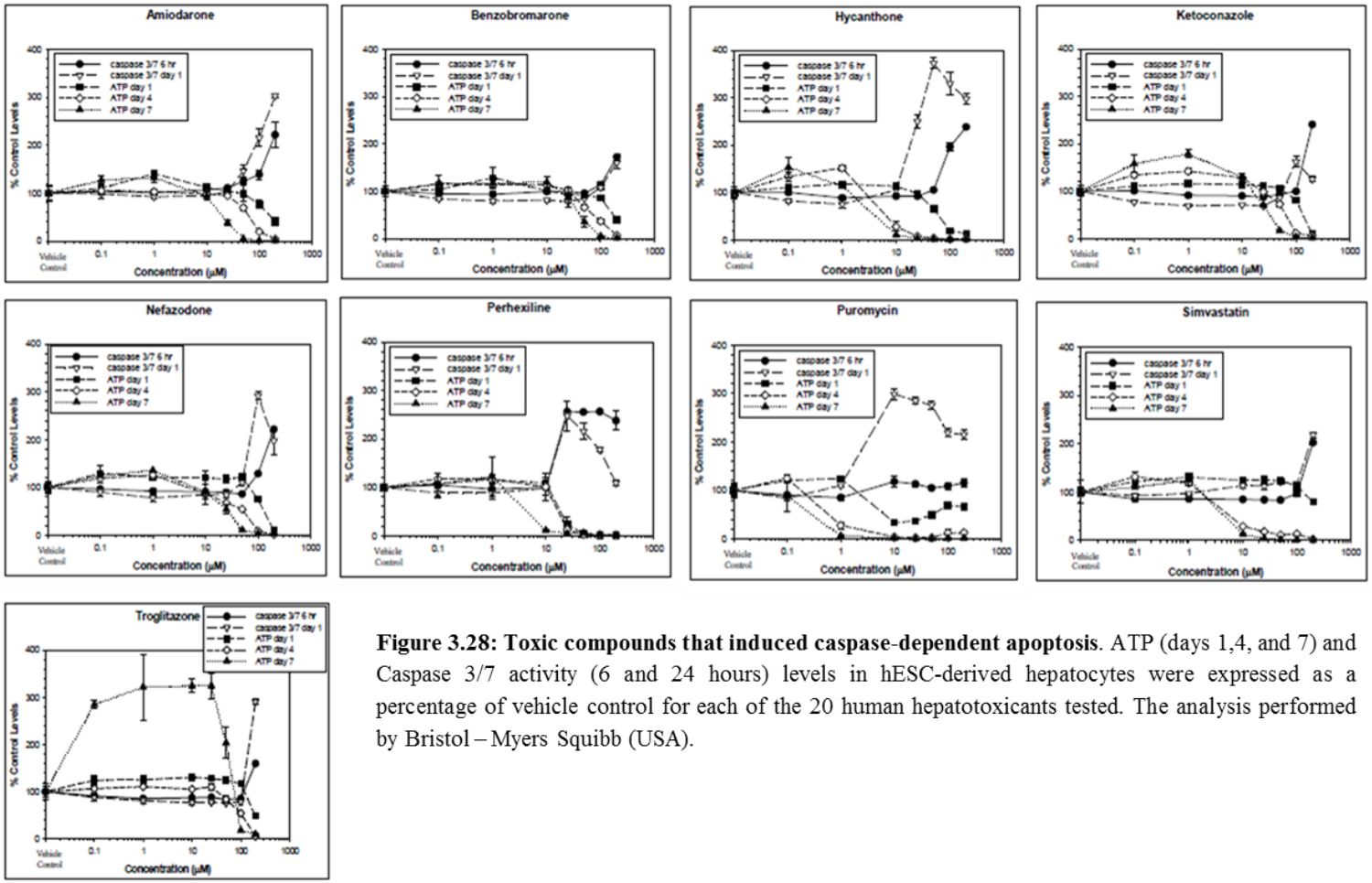

Figure 3.28: Toxic compounds that induced caspase-dependent apoptosis. ATP (days 1,4, and 7) and Caspase 3/7 activity (6 and 24 hours) levels in hESC-derived hepatocytes were expressed as a percentage of vehicle control for each of the 20 human hepatotoxicants tested. The analysis performed by Bristol – Myers Squibb (USA).

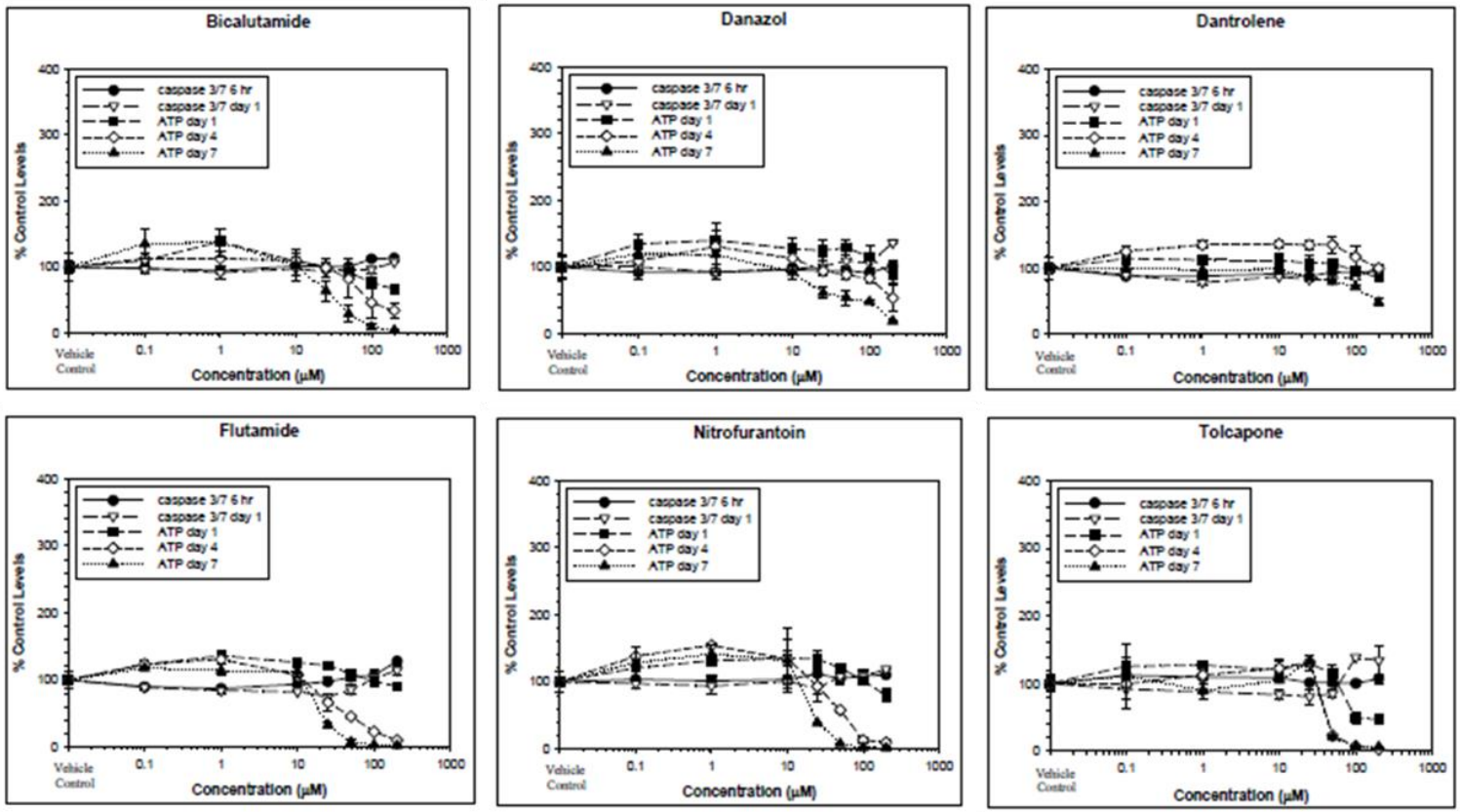

Figure 3.29: Toxic compounds that induced caspase –independent necrosis. ATP (days 1, 4, and 7) and Caspase 3/7 activity (6 and 24 hours) levels in hESC-derived hepatocytes were expressed as a percentage of vehicle control for each of the 20 human hepatotoxicants tested. The analysis performed by Bristol-Myers Squibb (USA).

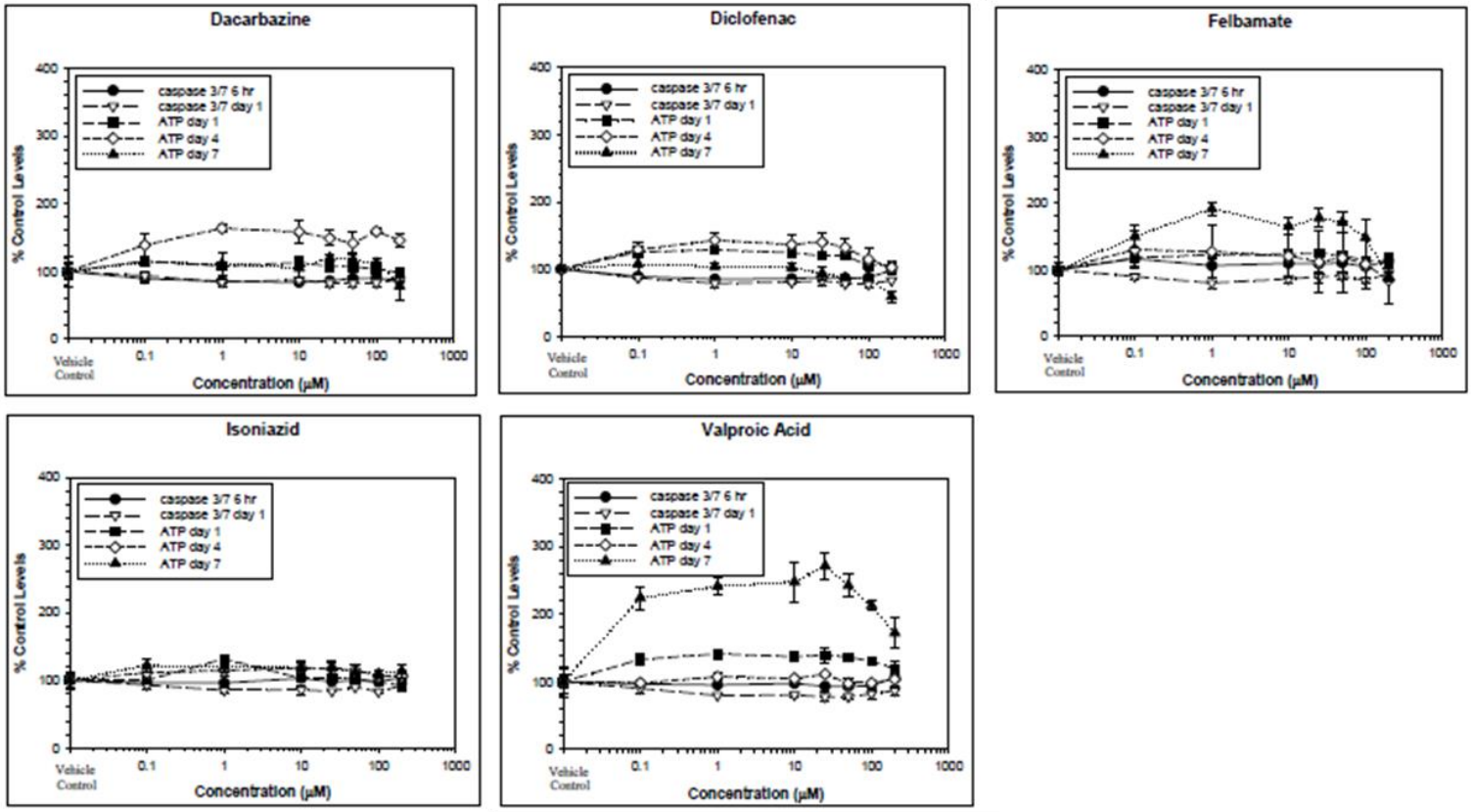

Figure 3.30: Compounds that did not induce any of the mechanism of toxicity. ATP (days 1, 4, and 7) and Caspase 3/7 activity (6 and 24 hours) levels in hESC-derived hepatocytes were expressed as a percentage of vehicle control for each of the 20 human hepatotoxicants tested. The analysis performed by Bristol-Myers Squibb (USA).

3.3 DISCUSSION

The liver plays an important role in human physiology. It has been estimated to perform over 500 functions *in vivo*. Liver disease leads to decompensated organ function and results in the derangement of normal bodily functions. Therefore, it is important that early diagnosis and intervention take place. In this vein, defined human hepatocyte models from hESCs and iPSCs were developed during this project. Importantly, the novel serum-free approach that has been established in our laboratory, drives efficient hepatic differentiation in a format suitable for high throughput screening. In addition to this, we have demonstrated that culturing pluripotent stem cells (PSCs) in different serum-free media (here MT and E8) may affect the gene expression during differentiation stages. For instance, PSCs cultured in E8 medium displayed an increase in Nanog gene expression at day 3 (definitive endoderm specification) of differentiation in comparison with MT. Although unexpected, Teo *et al* (2011) demonstrated that Nanog is necessary to initiate the expression of Eomesodermin (EOMES) transcriptional factor, which in turn cooperates with SMAD2/3 to activate transcriptional network directing definitive endoderm formation. Although the specific reason is unknown, it has been hypothesized that much higher concentrations of Nodal and TGFβ in E8 medium contrary to MT medium results in the activation of Nanog, and therefore stimulation of its activity on endodermal genes at day 3 (Xu *et al*, 2008).

Interestingly, hESC hepatocytes derived from H9s cultured in mTeSR1 exhibited greater metabolic and drug-inducible activity when compared with hepatocytes derived from MAN lines that were derived under GMP conditions and hiPSC hepatocytes. What is more, hepatic cells derived from pluripotent stem cells that were initially cultured in Essential 8 medium demonstrated lower cytochrome P450 activity when compared with MT (Figures 3.24 – 3.27). Although the exact reason is unknown, it is potentially suggested that higher levels of bFGF and TGFβ in E8 than in MT may influence the level of hepatic differentiation and metabolic activity.

What is more, early studies in our laboratory demonstrated that use of bFGF inhibitor (at 1uM concentration, StemCell Technologies) in E8 medium for 24 hours prior to differentiation results in regained cytochrome P450 activity to the levels comparable with MT. In order to approach issues such as weak embryoid body formation or differentiation, both StemCell Technologies and Life Technologies companies have produced commercially available Essential 6 medium (E6) that does not contain bFGF and TGFβ.

Contrary to embryonic lines, induced pluripotent stem cell line 33D6 did not demonstrate any induced levels of the cytochromes P450 (CYP3A and CYP1A2) by phenobarbital (Figure 3.27). The reason for this is unknown, and we do not claim that this is a generic iPSC trait, but merely that it is evident in our best performing retrovirally derived iPSC line. The failure to respond to phenobarbital may be attributable to a number of factors, including stresses inherent with cellular reprogramming, genetic background, epigenetic modifications, and/or retroviral DNA insertion, and those should be the focus of future investigation.

On the basis of metabolic competence, hESC hepatocytes were selected for scale-up and evaluated as a tool for hepatotoxicity studies (Table 3.2). hESC hepatocyte populations were robust, survived transit, and accurately predicted human compound toxicity, which was comparable to cryopreserved human hepatocytes. Within the group of 20 compounds tested, 15 were determined as toxic. Two mechanisms of cytotoxicity appeared to be involved, caspase-dependent apoptosis (9 compounds) (Figure 3.28) and caspase-independent necrosis (6 compounds) (Figure 3.29). Of note, ATP synthesis was induced at lower compound concentrations in response to some compounds (Figure 3.30). This is an example of hormesis, which is associated with cellular stress. Of note, there was clear evidence of hormesis in hESC-derived hepatocytes postexposure to valproic acid, felbamate, and dacarbazine. Interestingly, these three compounds were not detected as cytotoxic, and further investigation of stress-related endpoints, for example, reactive oxygen species, heat shock proteins, and unfolded protein-response transcription factors, will most likely be useful in defining the mechanism of toxicity associated with these compounds.

The two remaining compounds, isoniazid and diclofenac, did not induce toxicity in either primary or hESC hepatocytes. Isoniazid hepatotoxicity appears to be immune mediated, whereas diclofenac toxicity in human patients appears over weeks to months, making it possible that models of short duration or lacking immune components do not reveal the cumulative effects of these compounds.
These data support that hESC hepatocytes performed on a par with gold standard assays, promising in the future that they may serve as a partial or full replacement for primary cells in safety screening.

In conclusion, it is important to use well characterised pluripotent stem cell lines and it is feasible to construct serum - free models. It has been demonstrated that it is possible to model the potential for human drug-induced liver injury using stem cell-derived hepatocytes. This is an important step to using stem cell-derived somatic cells in tailoring human medicines for different genetic backgrounds and improving the efficiency of drug development. In the future, it may also be possible to use such a resource for developing cell-based therapies. Whereas current models are equivalent to primary hepatocytes, there is a requirement to improve their sensitivity and prediction rates of drug toxicity. Therefore, in the future it will be important to sophisticate cell-based models and end point measurements to deliver better success in predicting human liver injury.

CHAPTER FOUR

IDENTIFICATION OF NOVEL NON-CODING RNAs WHICH ARE PREDICTED TO REGULATE HUMAN PHASE II DRUG METABOLISM

4.1 INTRODUCTION

4.1.1 PSC-DERIVED HEPATOCYTES FOR MODELLING DRUG METABOLISM

Currently, drug development takes more than 12 years, has high attrition rate, and costs between U.S $800 million and $2 billion (Orloff *et al*, 2009; Kola and Landis, 2004; Medine *et al*, 2013). As a result there has been a significant reduction in new drug candidates. One of the major reasons for compound attrition is drug induced liver injury (DILI) and accounts for approximately 50% of acute liver-failure cases in the United States (Ostapowicz *et al*, 2002; Chalasani and Björnsson, 2010). Current approaches to detect DILI employ a range of human cell lines and primary hepatocytes both of which are limited by scarcity, poor function, species specific readouts and batch to batch variation. Therefore in recent years there has been a focus on deriving hepatocytes from renewable stem cell populations isolated from defined genetic backgrounds (for a review see Szkolnicka *et al* 2013).

Human embryonic stem cells (hESCs) and induced pluripotent stem cells (iPSCs) are examples of pluripotent stem cells (PSCs) which offer an unlimited supply of human soma when coupled with an efficient differentiation procedure. Both PSC populations have been shown to efficiently differentiate to hepatocytes using defined factors (Lavon et al, 2004; Cai *et al*, 2007; Duan *et al*, 2007; Hay *et al* 2007 ; Hay *et al* 2008ab; Agarwal *et al*, 2008; Basma *et al* 2009; Hay *et al* 2011; Hannan *et al*, 2013; Medine *et al* 2013; Szkolnicka *et al*, 2014). Stem cell derived somatic cells are being developed and, which more closely reflect hepatocyte physiology, will undoubtedly provide new biomarkers of disease; more accurate prediction of human liver toxicity and may lead to the development of safer and more effective drugs in the future.

Drug metabolising enzymes (DMEs) are divided into three major phases and play central roles in the metabolism, elimination, and/or detoxification of xenobiotics or exogenous compounds introduced into the body (Meyer, 1996). In phase I, a variety of enzymes acts to introduce reactive and polar groups into their substrates, and these reactions may occur by oxidation, reduction or hydrolysis.

The Cytochrome P450 superfamily is the major player in the process of oxidation. It is found abundantly in the liver, gastrointestinal tract, lung and kidney (Lewis, 2003b). The reduction and hydrolysis of the drug is mainly carried out by nitro-reductases and esterases respectively. Phase II DMEs are often termed conjugation enzymes and they include different subfamilies such as: Sulfotransferases (SULT), UDP-glucuronosyltransferases (UGT), and Glutathione S-Transferases (GST). Conjugation of phase I metabolites with phase II enzymes increases hydrophilicity of the compound resulting in the enhanced excretion in the bile, the urine, mediated via bile secretion and sweat (Hinson and Forkert, 1995). Conjugates and their metabolites can be excreted from cells by Phase III transporters which majorly include ATP-binding cassette (ABC) transporters and solute – carrier transporters (SLC) (Xu *et al*, 2005b) (Figure 4.1).

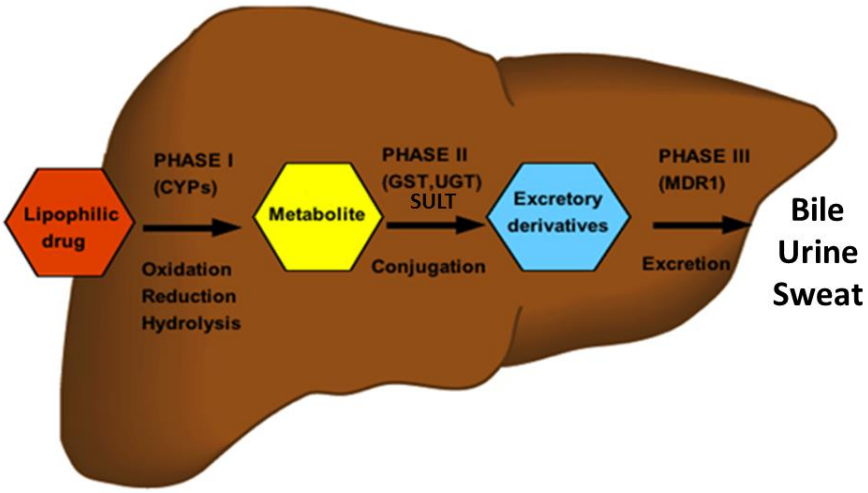

Figure 4.1: Phases of drug metabolism (I, II, III). Drugs are metabolised by Phase I enzymes (e.g CYPs) to form highly reactive metabolites that are detoxified by Phase II conjugating enzymes (e.g GST, UGTs, SULTs) and excreted by Phase III transporters (e.g MDR1) to bile, urine or sweat. Abbreviations: CYPs, Cytochromes P450; GST, glutathione S-transferases; UGT, UDP-glucuronosyltransferases, SULT, sulfotransferases; MDR1, multidrug-resistance protein 1.

4.1.2 MICRORNAs IN DRUG METABOLISM

MicroRNAs (miRs) are a class of small, non-coding RNAs which major role is to inhibit gene expression at translational level (Friedman *et al*, 2009), however recently studies have demonstrated that the RNA molecules increase transcriptional and translational activity (Vasudevan and Steitz, 2007b; Fabian *et al*, 2010). MicroRNAs can also inhibit gene expression at transcriptional level by recruiting different epigenetic factors (e.g DNA methyltransferases) or by interacting with the pre-initiation complex at the transcription start site blocking the binding of RNA polymerase II and basal transcriptional factors. (Pastori *et al*, 2010).

Recently, some microRNAs have been shown to directly or indirectly control the drug metabolising enzymes or nuclear receptors, and consequently, affect the capacity of drug metabolism and disposition, and influence the sensitivity of cells to xenobiotic agents (Yu, 2009; Nakajima and Yokoi, 2011; Yokoi and Nakajima, 2013; Yu and Pan, 2012). Therefore, dysregulation of specific microRNAs which control the expression of drug metabolising enzymes or drug transporters, might lead to considerable change in the pharmacokinetic and pharmacodynamics property of a drug (Figure 4.2). Improved understanding of the regulatory pathways of these enzymes will provide novel insights into adverse drug reactions, drug resistance and drug-drug interaction in clinical pharmacotherapy. Identification of microRNA – enzyme interactions would help to develop new microRNA –based therapeutics such as miRNA antagonists or mimics that block toxic metabolite formation and cell death (Bader *et al*, 2010).

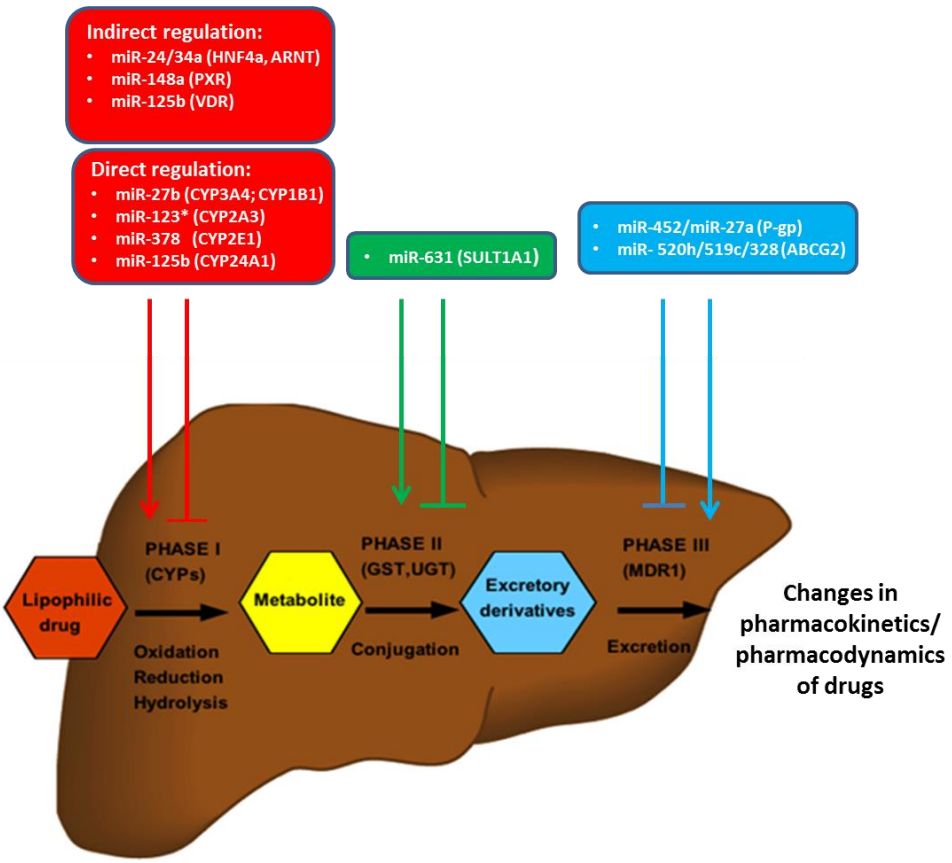

Figure 4.2: MicroRNA regulation of drug metabolism. MicroRNAs can directly regulate drug metabolising enzymes (direct regulation) or indirectly by controlling transcriptional factors (indirect regulation). Such regulation may cause changes in pharmacokinetics/dynamics of drugs leading to a therapeutic failure. MicroRNAs shown have been demonstrated to regulate specific genes (in brackets) at different metabolic stages. Adapted from Yokoi and Nakajima (2013), and Yu (2009). Abbreviations: HNF4a, hepatic nuclear factor 4a; ARNT, aryl hydrocarbon receptor nuclear translocator; PXR, pregnane X receptor; VDR, vitamin D receptor; CYP, cytochrome P450; SULT1A1, sulfotransferase 1A1; P-gp, P-glycoprotein; ABCG2, ATP-binding cassette sub-family G member 2.

4.2 RESULTS

In this chapter, we examined microRNA and drug metabolism gene expression in stem cell - derived hepatocytes. Firstly, the metabolic gene expression profile was examined in hESC - derived hepatocytes and compared with primary human hepatocytes profile. Once the commonly expressed metabolic genes were identified, the metabolic pathways that were intact in both systems were determined. After pathway identification (paracetamol), microRNA expression profile was examined both in hESC – derived hepatocytes and primary human hepatocytes. Once the commonly microRNAs were determined in both systems, we identified number of microRNAs that could modulate specific metabolic pathways of interest. The microRNA-mRNA binding interactions were predicted using TargetScan Human 6.2 software. This programme was chosen in this study as it is considered to have one of the highest precision and sensitivity of all current computational tools (Witkos *et al*, 2011). In addition, its total context score that is assigned to each result correlates with protein downregulation (Witkos *et al*, 2011).

4.2.1 METABOLIC GENE EXPRESSION PROFILE

As regulation of all three phases of drug metabolising enzymes has a significant impact on metabolism, elimination and pharmacokinetics of a particular drug, it was important to assess what metabolic genes were expressed in both stem cell - derived (day 18 of differentiation) and freshly isolated primary human hepatocytes derived from one particular batch lot. In order to examine gene expression profile, three RT^2 Profiler PCR Arrays of Phase I, II and III (Qiagen) were employed. Each array contained 96 genes in 4 replicates (384 – well plate). Phase I array included enzyme families such as alcohol dehydrogenases (ADH1/4/5/6), aldehyde dehydrogenases (ALDH1), arachidonate lipoxygenases (ALOX5/12/15), cytochromes P450 (CYP1/2/3/11/17/19), carboxylesterases (CES1/2/3), epoxide hydrolases (EPHX1), and hydroxysteroid dehydrogenases (HSD17). Phase II array contained glutathione S-transferases families (alpha, GSTA; mu, GSTM; pi, GSTP; omega, GSTO; theta, GSTT), catechol–O-methyltransferases (COMT), N-acetyltransferases (NAT1 and NAT2), sulfotransferases (SULT1/2/4/6) and UDP-glucuronyltransferases

(UGT1/2/3/8). The Phase III array included two major influx transporters: solute carrier transporters (SLC2/10/15/16/19/22/28/29/38) and solute carrier organic anion transporters (SLCO1/2/3/4) and one superfamily of efflux transporters: ATP- binding cassette transporters (subfamily A/B/C). All arrays were normalised to five housekeeping genes (B actin, ActB; beta-2-microglobulin, B2M; glyceraldeyhyde-3-phosphotase dehydrogenase, GAPDH; hypoxanthine phosphoribosyltransferase 1, HPRT1; and ribosomal protein P0, RPLP0). In the analysis, the three-fold difference was taken into consideration. Fold differences larger than 3 fold threshold were representing up-regulated genes, fold differences narrower than 3 fold threshold were indicating down-regulated genes, whereas fold differences between -3 to +3 boundary were representing genes similarly expressed. From these studies it was demonstrated that stem cell derived hepatocyte expressed transcript for Phase I drug metabolism with ~ 32% similarity to primary hepatocytes (Figure 4.3; Supplementary Table 1.2). Phase II drug metabolism with ~ 35% (Figure 4.3; Supplementary Table 1.3) and Phase III drug metabolism with ~ 29% similarity to primary hepatocytes (Figure 4.3; Supplementary Table 1.4).

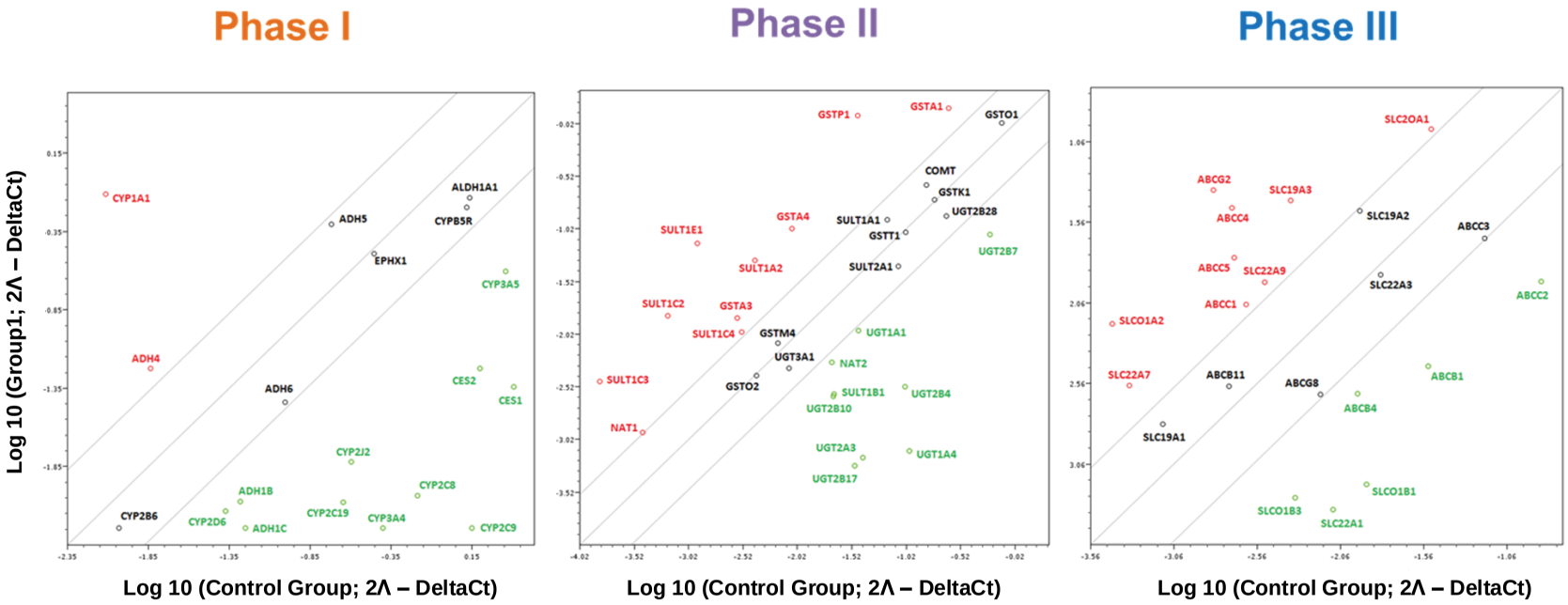

Figure 4.3: Stem cell –derived (day 18) and primary human hepatocyte gene expression. The scatter plots represent expression of the major metabolic genes involved in Phase I (A), Phase II (B), and Phase III (C) drug metabolism. Gene expression was performed using Human Drug Metabolism RT^2 Profiler PCR Array (QIAGEN) according to the manufacture instructions. The gene expression was analysed by RT2 Profiler PCR Array Data Analysis version 5.0 (QIAGEN). The scatter plot represents 3 fold change in gene expression. The graph plots the $\log_{10}$ of normalized gene expression levels in a control condition (x-axis) versus an experimental condition (y-axis). Symbols outside the boundary area indicate fold – differences larger than a threshold (3 fold). The red symbols in the upper - left corner readily identify up-regulated genes, and the green symbols in the lower-right corner readily identify down-regulated genes. The human primary hepatocyte total RNA was purchased from 3H Biomedical (Sweden).

Phase I gene expression data (Figure 4.3; Supplementary Table 1.2) demonstrates that in comparison with primary human hepatocytes, stem cell derived hepatocytes displayed higher expression of CYP1A1 (upregulated by ~ 99.74 fold), similar expression of CYP2B6 and CYB5R3 reductase (downregulated by -1.63 and -2.05 fold), and lower expression of the major hepatic cytochromes P450 involved in drug metabolism such as CYP3A4, CYP2C9, CYP2C19, and CYP2D6 (downregulated by -69.31, -246.36, -27.11, and -5.80 fold respectively). The Phase I array also measured alcohol (ADH) and aldehyde (ALDH) dehydrogenases that play a significant role in drug-drug/ drug-alcohol interactions. Class 4 of alcohol dehydrogenase (ADH4) was upregulated in stem cell derived hepatocytes by ~ 4.07 fold in comparison with the primary human hepatocyte model. The other classes of alcohol dehydrogenases (ADH5, ADH6) and aldehyde dehydrogenase class 1A1 (ALDH1A1) were similarly expressed in both hepatic systems, and their fold change is indicated as 2.60, -2.71, -1.87 respectively. In addition, epoxide hydrolase (EPHX1) was similarly expressed in both models (downregulated by – 1.08 fold), whereas carboxylesterase 1 and 2 (CES1, CES2) were downregulated in hepatocyte-like cells by -56.19 and -26.53 fold respectively in comparison with the primary system.

Phase II expression data (Figure 4.3; Supplementary Table 1.3) demonstrates that in comparison with the gold standard model, glutathione S – transferases GSTP1, GSTA1, GSTA3, GSTA4 were upregulated in stem cell hepatocytes by 33.14, 5.68, 5.09, and 11.26 fold respectively. Glutathione S - transferases of other classes, GSTT1, GSTK1, GSTM4, GSTO1, GSTO2 were similarly expressed in both models as indicated by – 1.06, 1.05, 1.25, 1.34 and – 1.04 fold respectively. Neither of the GST enzymes that play an important role in drug metabolism were downregulated. Different polypeptides of sulfotransferases family 1 such as SULT1A2/ 1E1/ 1C2/1C4/1C4 demonstrated higher expression in stem cell derived hepatocytes than primary hepatocytes, with increase in expression measured at by 12.29, 59.55, 23.14, 23.14, 3.40 fold respectively. Two sulfotransferases, SULT1A1 and SUL2A1 were expressed at the same levels in two models (fold change: 1.84 and -1.92 respectively).Whereas SULT1B1 was downregulated in stem cell derived hepatocytes by -8.05 fold in comparison to primary human hepatocytes.

Neither of the UDP-glucuronosyltransferase (UGT) genes was upregulated in the stem cell derived hepatocytes. Enzymes UGT3A1 and UGT2B28 were similarly expressed in both models (fold change – 1.78), whereas other families of UGTs such as UGT1A1/ 1A4 and UGT2A3/ 2B4/ 2B7/ 2B10/ 2B17 were downregulated by – 3.35 / -137.61 and -59.49 / -30.73 / -6.65 / -8.33 / -59.46 fold respectively. UGT1A9 gene was not expressed in the stem cell derived hepatocytes (Ct> 35; data not shown) and therefore it was not analysed in further detail. Other enzymes such as N-acetyltransferase 1 (NAT1) was upregulated in stem cell derived hepatocytes by 3.09 fold, catechol-O-methyltransferase (COMT) was similarly expressed (fold change: 1.69) in both models, whereas NAT2 was downregulated by -3.83 fold in stem cell derived hepatocytes.

Phase III expression data (Figure 4.3, Supplementary Table 1.4) demonstrates that stem cell derived hepatocytes expressed higher gene expression of ABC transporters such as ABCG2 (fold change: 29.17) and different members of ABCC family: ABCC1 (fold: 3.58), ABCC4 (fold: 17.42) and ABCC5 (fold: 8.28) in comparison with primary human hepatocytes. Other ABC transporters such as ABCB11, ABCC3, and ABCG8 were expressed similarly as primary hepatocytes (1.41, -2.93, -2.83 fold change respectively). ABCB1, ABCB4, and ABCC2 transporters were downregulated in the stem cell derived hepatocyte model (fold change: -8.38; -4.68; -11.92 respectively). Influx transporters such as solute carrier transporters (SLC) were also analysed in the array. Membrane transport proteins such as SLCO1A2 (fold change: 17.38), SLC19A3 (fold change: 8.59), SLCO2A1 (fold change: 49.01), and the two membrane transporters responsible for organic cation/anion/zwitterion transport such as SLC22A7 (fold change: 5.70) and SLC22A9 (fold change: 3.82) were upregulated in stem cell-derived hepatocytes in comparison with primary human hepatocytes. Two folate/thiamine influx transporters, SLC19A1 (fold change: 2.07) and SLC19A2 (fold change: 2.85) as well as SLC22A3 (fold change: -1.18) were similarly expressed in both models. Two solute organic anion transporters that are mainly expressed in the liver such as SLCO1B1 (fold change: -19.9) and SLCO1B3 (fold change: -8.69) as well as SLC22A1 (fold change: -17.46) were downregulated in stem cell-derived hepatocytes in comparison with primary human hepatocytes.

As the Phase II qPCR array did not include three important phase II metabolic genes (UGT2B15, UGT1A6, and SULT1A3), the expression of these genes was analysed by qPCR (Figure 4.4) and compared with the primary human hepatocytes (PHH). As Figure 4.4A demonstrates, UGT2B15 gene expression was downregulated by 67-fold in hESC - derived hepatocytes in comparison with primary human hepatocyte, whereas UGT1A6 enzyme was downregulated in hepatocyte - like cells by ~ 7 fold (Figure 4.4B). SULT1A3 was upregulated in HLCs by ~ 9 fold when compared with PHHs (Figure 4.4C).

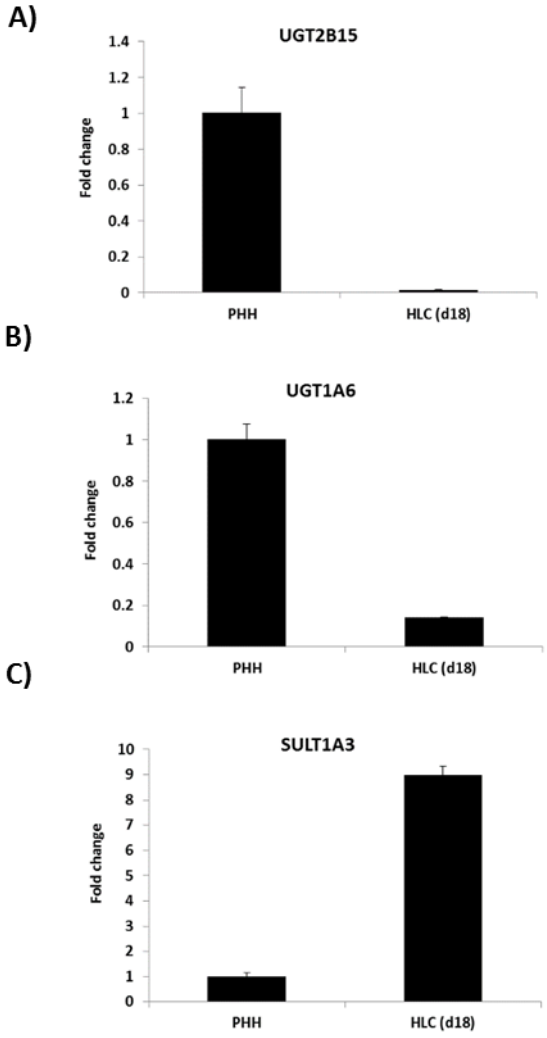

Figure 4.4: Gene expression of UGT2B15, UGT1A6, and SULT1A3. Gene expression of UGT2B15, UGT1A6, and SULT1A3 in Primary Human Hepatocytes (PHH) and in hepatocytes (d18) derived from human embryonic stem cell line H9. The gene expression was normalised to B2M housekeeping gene and expressed as fold change relative to PHH. Abbreviations: UGT2B15/UGT1A6, UDP-glucuronosyltransferases 2B15/1A6; SULT1A3, Sulfotransferase 1A3, B2M, beta2-microglobulin.

4.2.2 PARACETAMOL (APAP) METABOLIC PATHWAY

Having identified commonly expressed metabolic genes in both models, it was important to determine which drug metabolic pathways were intact. To search for candidate metabolic pathways, Pharmacogenomics Knowledge Base (PharmGKB; www.pharmgkb.org) was used. From these studies we determined that both stem cell - derived and primary human hepatocytes exhibited an intact paracetamol metabolic pathway by gene expression. Paracetamol (APAP) is a common analgesic drug, and it is majorly produced from the phenacetin precursor by phase I enzymes: CYP1A2 and 1A1 (Huang *et al*, 2012). When taken in therapeutic doses, greater than 90% of paracetamol is metabolized to phenolic glucuronide (APAP-glucuronide) and sulphate (APAP-sulfate) in the liver by glucuronosyltransferases (UGTs) and sulfotransferases (SULTs) and subsequently excreted in the urine by ABC transporters (Bessems and Vermeulen, 2001; Adjei *et al*, 2008). Of the remaining paracetamol, ~ 2% is excreted in the urine unchanged, ~ 5-10% is metabolized by cytochrome P450 (CYP) to N-acetyl-p-benzoquinone imine (NAPQI), a highly reactive, electrophilic molecule that causes harm by formation of covalent bonds with other intracellular proteins (Chun *et al*, 2009; Larson, 2007; Rumack, 2002; Nelson, 1990). This reaction is prevented by conjugation with glutathione (GSH) and subsequent reactions generate a water-soluble product that is excreted into bile (APAP – cysteine; Jaeshke and Bajt, 2006). With paracetamol overdose, UGTs and SULTs are saturated, diverting the drug to be metabolized by CYP and generating NAPQI in amounts that can deplete intracellular glutathione. If glutathione is not replenished or GSTs do not function properly, NAPQI begins to accumulate in the hepatocytes, leading to hepatotoxicity and eventually liver failure (Lee, 1995; Hinson *et al*, 2010) (Figure 4.5).

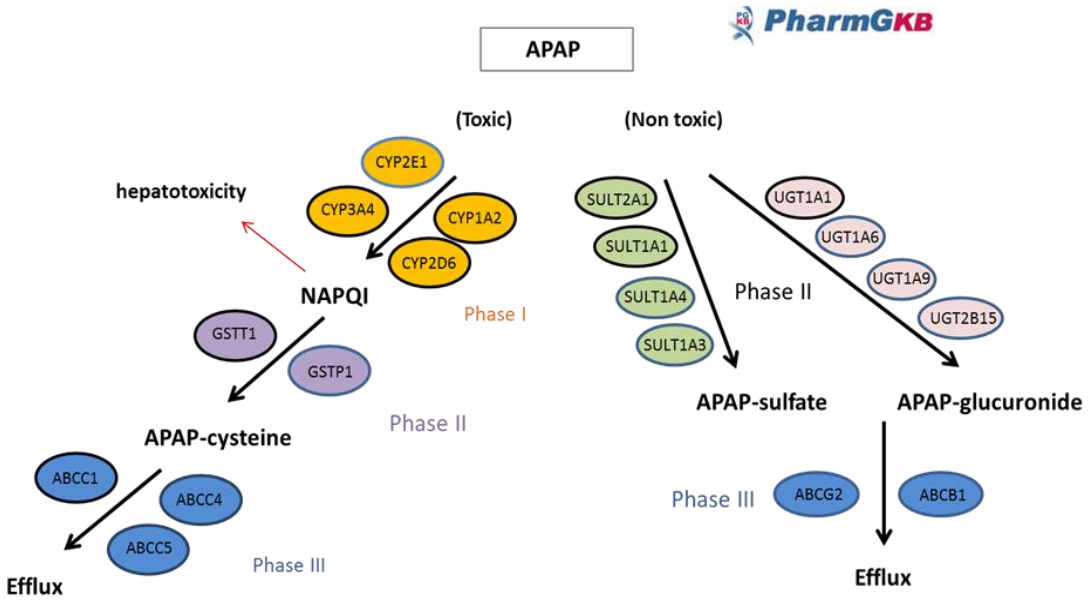

Figure 4.5: APAP (paracetamol) metabolism (based on Pharmacogenomics Knowledge Base PharmGKB; www.pharmgkb.org). At normal doses it is conjugated by two major families of phase II enzymes: Sulfotransferases (SULTs) and UDP-glucuronosyltransferases (UGTs). This leads to the production of two metabolites: APAP-sulfate and APAP-glucuronide, which are further effluxed from the cell by one of the ABC transporters. At higher doses than recommended, APAP (paracetamol) is metabolised by Cytochrome P450 enzymes. This leads to the formation of a reactive metabolite, N-acetyl-p-benzoquinone imine (NAPQI), which is further transformed to a non-toxic APAP- cysteine and mercapturic acid by Glutathione S- transferases (GSTT1,GSTP1). The metabolite is effluxed from the cell by one of the phase III transporters.

4.2.3 PROTEIN EXPRESSION OF MAJOR METABOLIC GENES

In order to validate the results generated from the PCR array experiments, immunostaining focusing on phase II and phase III protein expression was performed. Figure 4.6 and Figure 4.7 represent protein expression of the major phase II metabolic enzymes and phase III transporters of paracetamol processing during differentiation of human embryonic stem cells (hESCs; day 0) to definitive endoderm (DE; day 3), to hepatoblast (HBL; day 10) and to hepatocyte (HLC; day 18).

The top panel of Figure 4.6 demonstrates high expression of glutathione S-transferase p1 (GSTP1) throughout the whole hepatic differentiation process. At day 0 (hESCs), GSTP1 was expressed at approximately 99% (SE±0.4) and the percentage of positive cells remained relatively constant at all stages of differentiation, as indicated by 98% (SE±0.48) in DE, 90% (SE±0.85) in HBL, and 96% (SE±0.4) in HLC. Glutathione S-transferase theta 1 (GSTT1) demonstrated stable expression at 98% at all stages of differentiation (SE for hESCs: ±0.25; DE: ±0.65; HBL ± 0.48; HLC ± 0.25). The protein expression of sulfotransferase 1A1 (SULT1A1) was not detected at day 0, however at day 3 postdifferentiation it was significantly increased (98% ± 0.5) and remained constant at HBL (97% ± 0.4) and HLC (98% ± 0.63) stages. Contrary to SULT1A1, sulfotransferase 2A1 (SULT2A1) expression was not detected at pluripotent and definitive endoderm stages. During hepatic specification, 90% (± 0.65) of cells were positive for SULT2A1, whereas the expression of this enzyme was reduced by ~ 1.5 fold in stem cell derived hepatocytes (59% ± 2.85).

UDP-glucuronosyltransferase 1A1 (UGT1A1) protein expression was not detected at the pluripotent, endodermal and hepatoblast stage (Figure 4.7). The expression of this protein significantly increased at the final stage of differentiation, as indicated by hepatocytes expressing 54% (± 4.3) cells positive for this marker. The ATP-binding cassette G2 (ABCG2) transporter was not expressed at the early stages of the differentiation, with increasing levels at the hepatic specification (HBL: 9% ± 0.63) and hepatocyte formation (HLC: 52% ± 1.55). The ATP-binding cassette C1 (ABCC1) transporter demonstrated high expression at day 0 (99% ± 0.48), day 3 (99% ± 0.48), and day 10 (99% ± 0.4) with decreasing levels by ~ 1.3 fold at day 18 of differentiation (77% ± 1.1) (Figure 4.7).

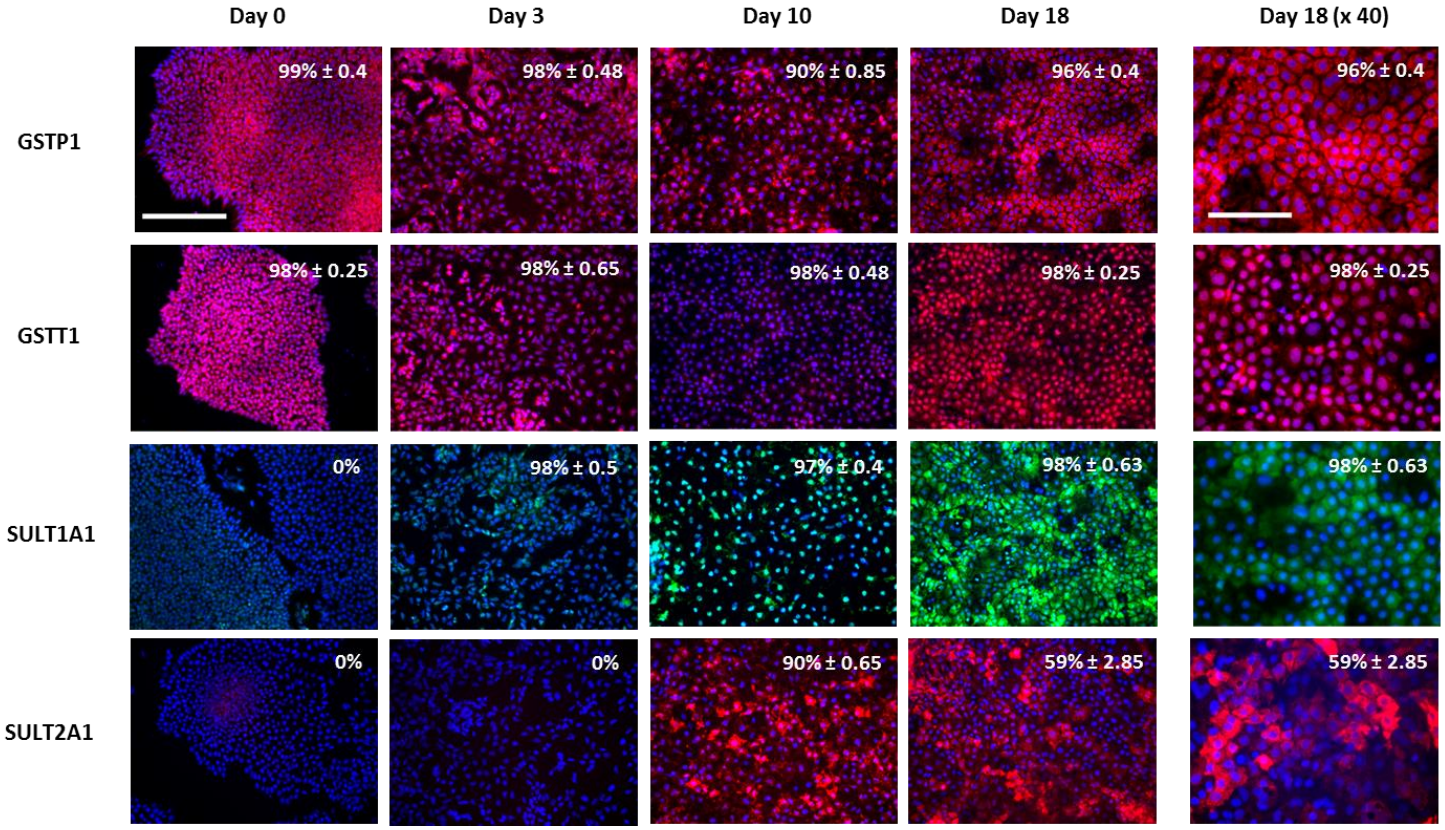

Figure 4.6: GSTs and SULTs protein expression. Stagewise human embryonic stem cell (hESC) differentiation to the hepatocyte lineage. Immunocytochemistry represents protein expression of phase II metabolic enzymes: GSTs (GSTP1, GSTT1) and SULTs (SULT1A1, SULT2A1) at different stages of hepatic differentiation. The percentage of positive cells is provided in the top right of each panel. This was calculated from four random fields of view and is quoted as ± standard error. The images were taken at x20 magnification. The last column of images was taken at x40 magnification. All scale bars represent 100um. The IgG controls that demonstrated specificity of the immunostaining are presented in Figure. Abbreviations: GSTP1/GSTT1, glutathione S-transferase pi 1/theta 1; SULT1A1/SULT2A1, sulfotransferase 1A1/ 2A1.

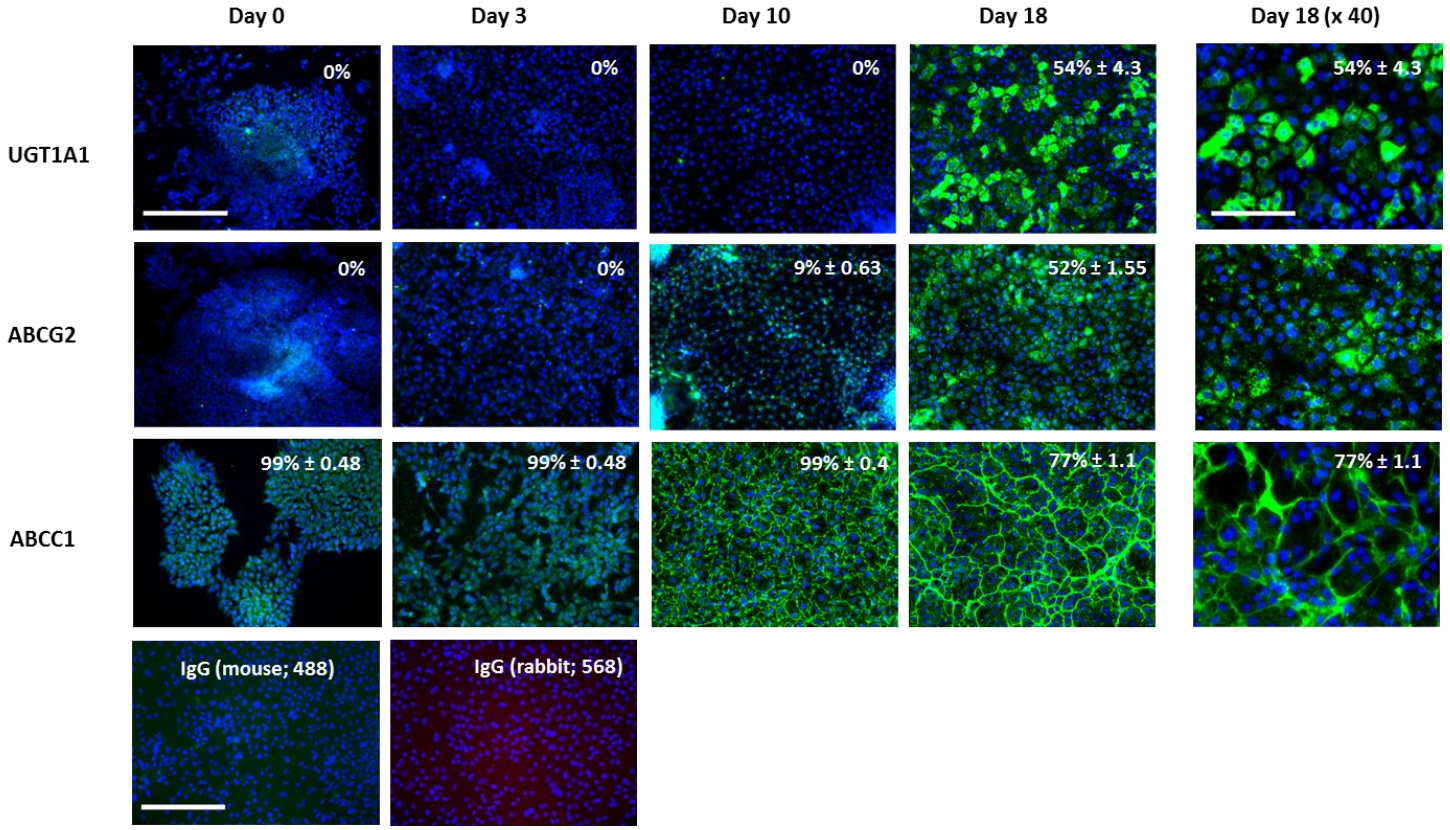

Figure 4.7: **UGTs and ABCs protein expression**. Stagewise human embryonic stem cell (hESC) differentiation to the hepatocyte lineage. Immunocytochemistry represents the protein expression of phase II metabolic enzyme UGT1A1 and ABC transporters (ABCG2, ABCC1) at different stages of hepatic differentiation. The percentage of positive cells is provided in the top right of each panel. This was calculated from four random fields of view (each field had at least 300 cells) and is quoted as ± standard error. The images were taken at x20 magnification. The last column of images was taken at x40 magnification. All scale bars represent 100um. Immunoglobulin G controls demonstrated specificity of immunostaining. Abbreviations: UGT1A1, UDP-glucuronosyltransferase 1A1; ABCG2/ABCC1, ABC-binding cassette transporters G2/C1.

After validating the expression of the major phase II enzymes and phase III transporters involved in paracetamol detoxification, we decided to select and focus on three phase II enzymes that were similarly expressed in both models and played a major role in toxic (GSTT1) and non- toxic (SULT2A1, UGT1A1) processing of the drug (Figure 4.8). Once the genes were selected, we firstly examined microRNAs that were commonly expressed in both stem cell derived hepatocytes and primary human hepatocytes (Figure 4.8), and used the TargetScan Human 6.2 programme to identify novel targets.

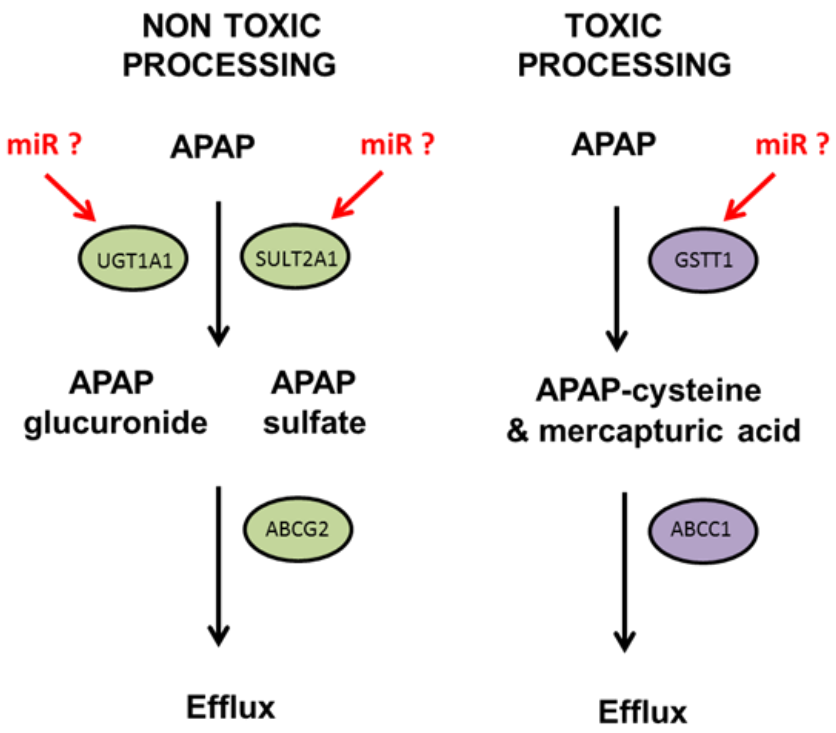

Figure 4.8: APAP metabolism and microRNA/target prediction. The expression of enzymes and transporters involved in APAP metabolism and potential microRNA-target prediction. Phase II enzymes (GSTT1, SULT2A1, UGT1A1) and Phase III transporters (ABCG2, ABCC1) play major role in toxic and non-toxic pathways of APAP metabolism. In the non-toxic pathway APAP is metabolised by SULT2A1 enzymes and UGT1A1 to produce APAP sulfate and APAP glucuronide metabolite respectively that are effluxed from the cell by ABCG2 transporter. In a toxic pathway, APAP (paracetamol) is metabolised by GSTT1 enzyme to produce APAP cysteine and mercapturic acid metabolites that are effluxed from the cell by ABCC1 transporter. Abbreviations: GSTT1, glutathione S-transferase theta 1; SULT2A1, sulfotransferase 2A1; ABCG2, ATP-Binding Cassette Transporter Subfamily G member 2; ABCC1, ATP-Binding Cassette Transporter Subfamily C member 1; miR, microRNA.

4.2.4 MICRORNA EXPRESSION PROFILE

In order to study miR regulation in toxicity studies, it is important that hESC-derived hepatocytes reflect partially the miR expression profile of the current gold standard model, primary human hepatocytes. Therefore, we compared the level of microRNA expression in stem cell derived and primary human hepatocytes. To generate microRNA expression profile, the RNAs from four replicates of primary human hepatocytes (a single donor) and from four experimental samples of hESC-derived hepatocytes (day 18) were used. The differences in miRNA expression between the two groups (PHH and HLCs) were evaluated firstly by performing ANOVA and then t-tests separately for each miRNA. The p-values coming from the t-tests were adjusted for multiple test inflation using the Benjamini-Hochberg method 6 (Benjamini Y and Hochberg Y, 1995) and are referred to as pFDR, where FDR is the false discovery rate. The miRNAs with significant differences from hypothesis testing at pFDR < 0.05 as well as having an absolute fold-change (FC) ≥ 1.5 were considered differentially expressed. A p-value cut-off of 0.05 is considered as a common practice when analysing microarray data and the use of the fold-change threshold of 1.5 is based on the documented array-to-array variability from the Agilent system. The microRNAs that had p-value > 0.05 and FC ≤ 1.5 were considered to be similarly expressed. A summary representation of the expression data was produced using Principal Component Analysis (PCA) (Jackson JE, 1991). PCA extracts the main effects from high-dimensional data such as microarray datasets, which for each sample have expression measurements from hundreds of miRNA. These main effects (principal components) were displayed in a simplified graphical representation which retained the main properties of the data. In the PCA, samples that were similarly expressed clustered in the same space on the PCA plot.

Principal Component Analysis overview plot, generated using 367-reliably detected miRNAs revealed very strong clustering by cell type (using pFDR < 0.05 and FC ≥ 1.5) (Figure 4.9A). The statistical analysis of the microRNA Array demonstrated that ~60% of reliably detected microRNAs were expressed at the same level both in primary human hepatocytes and hESC-derived hepatocytes, whereas ~ 40% were differentially expressed in both of these systems (Figure 4.9B; Supplementary Tables 1.6a/b/c and 1.7a/b/c).

Of note the major microRNA found in the hepatocyte, miR-122 (Lagos-Quintana *et al*, 2002), was expressed at the same level in hESC-derived hepatocytes as in primary human hepatocytes (Figure 4.9C).

A

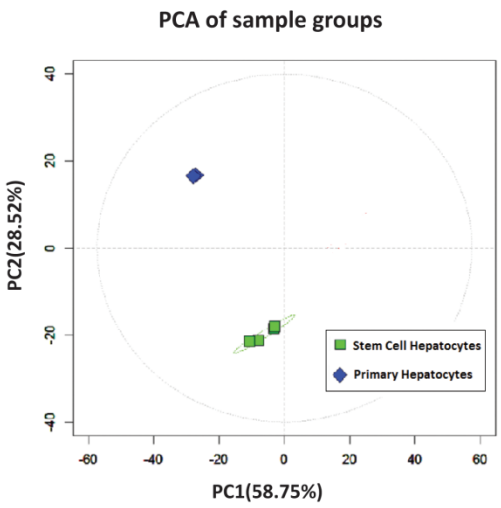

C

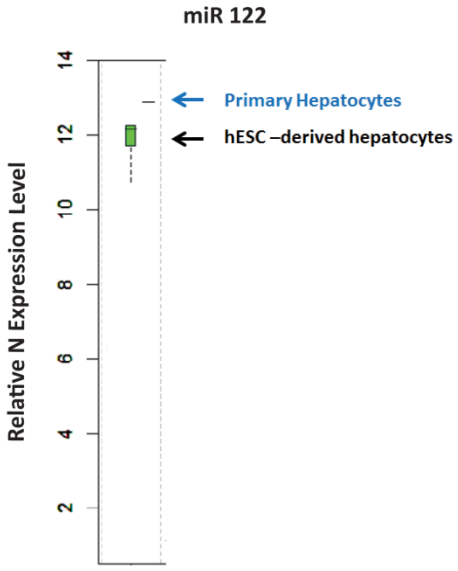

B

Primary Hepatocytes versus hESC- derived hepatocytes	
Total (common) number of expressed miRs	367
Number of the same miRs	220 (60 %)
Number of differentially-expressed miRs	147 (40 %)

Figure 4.9: MicroRNA expression profile. Stem cell - derived hepatocytes (HLCs) and primary human hepatocytes (PHH) microRNA expression profile. (A) Principle Component Analysis overview plot demonstrates strong clustering by cell type. (B) Statistical analysis of the microRNA Array demonstrates 367-reliably detected microRNAs in both HLCs and PHH; 220 microRNAs have a similar expression in both systems, and 147 microRNAs are differentially-expressed. (C) microRNA 122 (miR-122) is expressed in HLCs at the same level as in PHH. The microRNA Array was carried out by Sistemic (Glasgow). The RNA samples (4 replicates of PHH and 4 experimental samples of hESC-derived hepatocytes) were run on Agilent miRNA platform.

Table 4.1 represents expression of microRNAs of interest that are expressed at similar levels in both stem cell - derived hepatocytes and primary human hepatocytes (for the whole microRNA array see Supplementary Table 1.6a/b/c).

miR name	Mean log_2 intensity	Interpretation
hsa-miR-23b-3p	7.85	Similar
hsa-miR-24-3p	8.31	Similar
hsa-miR-27b-3p	7.76	Similar
hsa-miR-122-5p	10.08	Similar
hsa-miR-148a-3p	7.71	Similar
hsa-miR-148b-3p	5.16	Similar
hsa-miR-324-5p	4.49	Similar

Table 4.1: MicroRNAs commonly expressed in both systems. Expression of selected microRNAs in stem cell - derived hepatocytes in comparison with primary human hepatocytes. Human miRs: 23b, 27b, 122, 148a/b, 324 are similarly expressed in both cell based models. Abbreviations: HLC, hepatocyte-like cells; PHH, primary human hepatocytes; hsa, human; miR, microRNA.

4.2.5 MICRORNA TARGET PREDICTIONS

It has been proven that microRNAs may interact with essential drug metabolizing enzymes which may result in pharmacokinetic and pharmacodynamic changes of a drug and may lead to therapeutic failure (Yu, 2009). Recent studies have shown an extensive work on miR regulation in Phase I drug metabolism, however the role of miRs in Phase II and Phase III is still poorly understood (Yu and Pan, 2012). Therefore the aim of the experiments was to identify miR candidate regulators of Phase II and Phase III activity, in the context of paracetamol metabolism.

In order to predict potential microRNA binding sites, TargetScan Human 6.2 (www.targetscan.og) software was used. The software analysed 3'UTR of the target gene and the results were based on the online context score. The context score takes into consideration type of seed matching, 3' pairing outside of the seed region and adenine/uracil (AU) content upstream and downstream of predicted site. These parameters are important as they verify how accessible the site is for the miR/RISC complex to fine tune gene expression. The potential microRNA binding sites were also examined by the other tools available online, however they were not as efficient in predicting miR/mRNA interactions as TargetScan Human 6.2 (see Supplementary Table 1.8 for details).

In case of a non-toxic paracetamol metabolism, two microRNAs: hsa-miR-324-5p (context score 96%; 8mer seed match type) and hsa-miR-148a/b-3p (context score 93%; 8mer seed match type) were predicted to regulate SULT2A1 and UGT1A1 respectively (Figure 4.10). In case of a toxic paracetamol metabolism, a commonly expressed hsa-miR-24-3p (context score 84%; 7mer-m8 seed match type) demonstrated a potential high binding affinity for glutathione S - transferase theta 1 (GSTT1) (Figure 4.11; Supplementary Table 1.5).

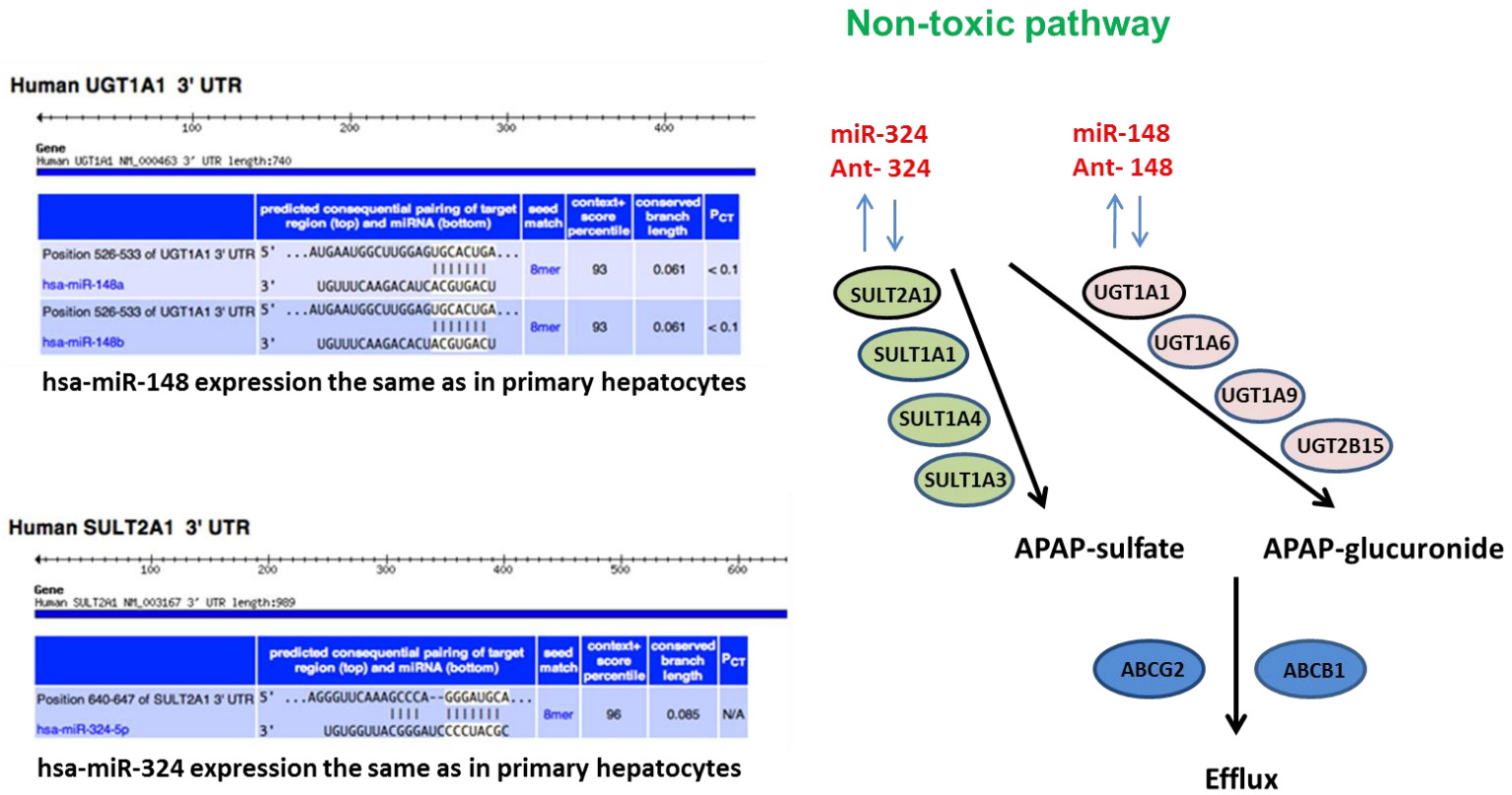

Figure 4.10: MicroRNA target predictions for non-toxic pathway of paracetamol. In a non-toxic pathway hsa-miR-324 and hsa- miR-148 demonstrate high binding affinity for SULT2A1 and UGT1A1 respectively. Inhibitors (Ant) of these microRNAs may also change expression of SULT2A1 and UGT1A1. All results are based on online context score using TargetScan Human 6.2 (www.targetscan.org). Abbreviations: SULT2A1/1A1/1A4/1A3, Sulfotransferase 2A1/1A1/1A4/1A3; UGT 1A1/1A6/1A9/ 2B15, UDP-glucuronosyltransferase 1A1/1A6/1A9/ 2B15; ABCB1/ABCG2; ATP-binding cassette transporter B1/G2; Ant, Antagomir; ↑↓ positive/negative gene expression.

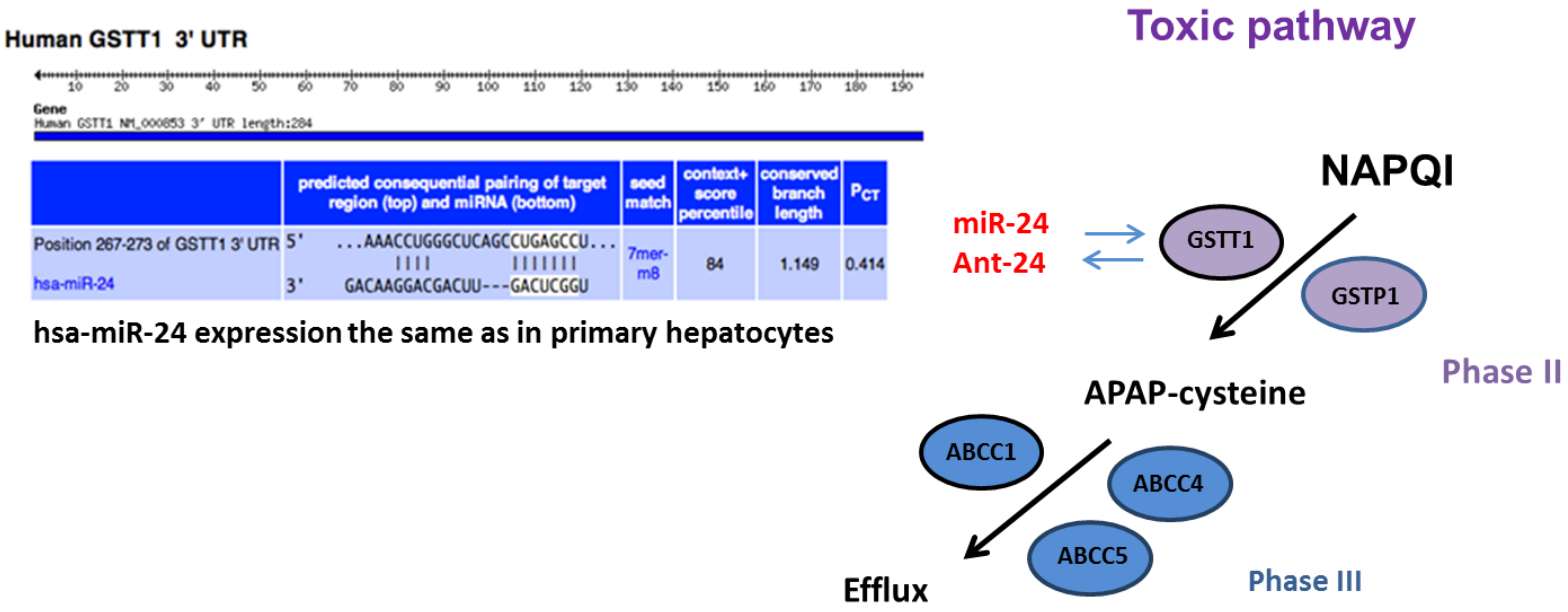

Figure 4.11: MicroRNA target predictions for toxic pathway of paracetamol. Hsa-miR-24 is predicted to bind GSTT1. Inhibitor (Ant) of this microRNA may also change expression of GSTT1. All results are based on online context score using TargetScan Human 6.2 (www.targetscan.org). Abbreviations: GSTT1/GSTP1, Glutathione S-transferase T1/P1; ABCC1/ABCC4/ABCC5, ATP-binding cassette transporter C1/C4/C5; Ant, Antagomir; ←/→ positive/negative gene expression.

4.3 DISCUSSION

MicroRNAs are known to play an important role in regulating human drug metabolism. Therefore, the identification of microRNAs and their metabolic targets in pluripotent stem cell derived hepatocytes will allow us to elucidate their function *in vivo*. These findings will provide better understanding of the biology underlying human drug metabolism and may shed light on human DILI.

Metabolic gene expression array and immunocytochemistry of particular proteins of interest revealed different expression patterns. RT^2 Profiler PCR expression array (Figure 4.3) demonstrated that cytochrome P450 1A1 (CYP1A1) was highly upregulated (~ 99 fold) in stem cell derived hepatocytes in comparison with the gold standard model. It has been demonstrated that CYP1A1 is a gene expressed at low levels in most adult liver samples and is more likely expressed in fetal cells (Hines, and McCarver, 2002; Marongiu *et al*, 2011). What is more, Jozefczuk *et al* (2011) transcriptomic analysis showed that hESC-derived hepatocytes demonstrated higher expression of CYP1A1, CYP11A1, CYP19A1, while hiPSC-derived hepatocytes had enriched CYP46A1 and CYP26A1. Although CYP2B6 that plays a significant role in phenobarbital metabolism (Liu *et al*, 2015) was similarly expressed at gene level in both cell-based systems, most of the drug metabolising cytochromes were downregulated in hepatocyte-like cells. Several studies have reported cytochrome expression in hESC-derived hepatocytes, in particular CYP3A4 isoform activity has been shown to vary considerably from 0-90% of the primary human hepatocytes used as comparators (Ek *et al*, 2007; Basma *et al*, 2009; Duna *et al*, 2010; Yildirimman *et al*, 2011). Potential cytochrome expression differences could be connected with the hESC starting population epigenetics, hepatic differentiation procedures or variability in primary hepatocyte donors (Wobus and Loser, 2011; Robinton and Daley, 2012; Kia *et al*, 2012).

Figure 4.3 and Figure 4.6 demonstrated that the two major enzymes of glutathione S-transferase family, namely GSTP1 and GSTT1 that play an essential role in paracetamol metabolism were either upregulated or similarly expressed in stem cell derived hepatocytes in comparison to primary human hepatocytes.

Although both are considered as markers of fetal and mature hepatocytes, this was corroborated by the immunostaining studies with protein expression detected at the early stages of differentiation.

Several papers have demonstrated that phase II detoxifying GST enzymes could be expressed in embryonic stem cells and definitive endoderm (Raijimakers *et al*, 2001; Funakoshi *et al*, 2011; Nair *et al*, 2013; Acharaya *et al*, 2010). Since standard culture techniques maintain mammalian cells *in vitro* under an artificial physicochemical environment such has ambient air and 5% CO_2, GST enzymes could have been increased in order to protect cells from oxidative damage and prevent mutagenesis (Ishii and Mann, 2014).

The qPCR and protein expression data (Figure 4.3) demonstrate that the two major liver sulfotransferases, namely SULT1A1 and SULT2A1 that are responsible for different sulfation processes, were expressed at the same level in both cell based systems. This was highly efficient with cells expressing ~ 98% for SULT1A1 and ~59% SULT2A1 in stem cell- derived hepatocytes. Despite similarities, a number of sulfotransferases (e.g SULT1A2, SULT1A3, SULT1E1, SULT1C2) were upregulated in hepatocyte - like cells in comparison with primary human hepatocyte (Figures 4.3 and 4.4). Alcorn and McNamara (2002) reported that investigation of hepatic sulfotransferase activity in the fetus and neonates revealed high activity of this enzymatic pathway suggesting an essential role in homeostasis and detoxification in the fetus and neonate. What is more, it has been demonstrated that in neonates and up to the age of 9, paracetamol sulfate is the major metabolite, whereas above this age paracetamol glucuronide is the major metabolic product (Levy *et al*, 1975; Grijalva *et al*, 2013). Similar pattern of paracetamol detoxification was observed in 2D and 3D stem cell derived hepatocytes, where sulfates were a dominating product over glucuronides in comparison with primary human hepatocytes potentially suggesting immaturity of *in vitro* cell models (Sengupta *et al*, 2014). Therefore in this project, sulfotransferases were examined in particular due to immaturity of hESC-derived hepatocytes.

With the exception of UDP glucuronosyltransferase 1A1 (UGT1A1), that is exclusively expressed in adult liver (Strassburg *et al*, 2002) and plays one of the major roles in bilirubin/ drug metabolism (Wang *et al*, 2006; Tukey and Strassburg, 2000), the remaining UGT families were significantly downregulated in the stem cell derived model (UGT1A4/1A6/2A3/2B4/2B7/2B10/2B15/2B17) (Figures 4.3 and 4.4). Enzymes such as UGT1A4/1A6 as well as UGT2s (2B being the most studied due to its abundance) catalyse the glucuronidation of endogenous compounds, namely steroid hormones, bile acids, retinoids, fatty acids and thyroid hormones (Mackenzie *et al*, 1997; Radominska-Pandya *et al*, 1999).

It has been reported that UGT enzymes were expressed at low levels during fetal and early postnatal human development. These phase II enzymes increase after birth, reaching about 25% of adult levels by 3 months of age (Coughtrie *et al*, 1988; Grijalva and Khashayar, 2013). Studies by Mikkelsen *et al* (1994) observed that infants demonstrated reduced and variable morphine clearance secondary to immature glucuronidation pathway. What is more, impaired chloramphenicol – UGT dependant conjugation in neonates has resulted in the 'gray baby' syndrome, a cause of neonatal deaths in the 1960s and 1970s (Weiss *et al*, 1960; Craft *et al*, 1974).

PCR array (Figure 4.3) demonstrated similar expression of phase III transporters such as ABCG8 and ABCB11 that play an important role in cholesterol and bile acid transport respectively (Yu *et al*, 2002; Henkel *et al*, 2013). The two major ABC transporters of non-toxic (ABCG2) and toxic (ABCC1) pathways of paracetamol metabolism were upregulated in stem cell derived hepatocytes by 29.17 and 3.58 fold, with cells positively expressing these enzymes at ~ 52% and ~ 77% respectively at day 18 of differentiation (Figures 4.3 and 4.7). Leslie *et al* (2005) reported that these two protective efflux systems (ABCC1 and ABCG2) located in the different sides of polarized cells cooperate to serve as physiologic protection. Contrary to ABCG2, ABCC1 (MRP1) protein was expressed at all stages of differentiation, potentially suggesting that ABCC1 role is protecting differentiating cells not only from toxic effects of xenobiotics but also from endogenous toxic metabolites and oxidative stress (Leslie *et al*, 2005).

Glutathione, a three amino acid peptide (gamma glutamyl-cysteinylglycine), is an abundant antioxidant found in eukaryotic cells (Sies, 1999). Most of the time, this peptide exists in reduced form (GSH) in which the sulfhydryl group of the cysteine is not linked in a disulphide linkage to a second glutathione. A small percentage of the glutathione is oxidised and present as a dimer of two of the peptide elements connected by a disulphide bond between the cysteines present in both molecules. Oxidised glutathione (GSSG) is an indicator of cell health and oxidative stress (Ballatori *et al*, 2009). It has been proven that certain chemicals react with GSH to form adducts or to increase the GSSG levels, decreasing the ratio of reduced to oxidised GSH (GSH/GSSG). In connection with that, two studies (Hirrlinger *et al*, 2001 and Mueller *et al*, 2005) suggested that glutathione disulphide (GSSG), the oxidised form of glutathione, is a substrate of ABCC1, which enables ABCC1 to extrude GSSG from the cells during oxidative stress, therefore protecting from the cytotoxic effects.

A certain number of microRNAs were similarly expressed in both of the cell-based models such as: hsa-miR-23b-3p; - 24-3p; -27b-3p; - 122-5p; -148a/b-3p; -324-5p (Table 4.1). Two microRNAs, miR-23b and miR-27b that belong to the miR-23b cluster (comprised fully of miRs 23b, 27b, and 24-1) have been demonstrated to be highly expressed in hepatocytes compared to developing bile ducts in fetal mouse liver (Rogler *et al*, 2009). What is more, Tzur *et al* (2009) studies demonstrated that human miR-23b is highly more expressed in adult liver than in embryonic liver and may be capable of inhibiting cell proliferation and mediate cell cycle arrest in mature hepatocytes (Tong *et al*, 2008). Specification and maturation of hepatocytes primarily depends on hepatic nuclear 4a (HNF4a) transcription factor that regulates various numbers of genes involved in synthesis/metabolism of fatty acid, cholesterol, glucose, urea and drug metabolism (Gonzalez, 2008; Kamiyama *et al*, 2007). In connection to that, it has been demonstrated that microRNA 24 (miR-24) directly inhibits HNF4a at both coding and 3'UTR region playing an important role in the regulation of bile acid production (Takagi *et al*, 2010). Similarly to HNF4a, pregnane X receptor (PXR) along with retinoid X receptor a (RXRa) regulate drug metabolism and elimination by binding to response elements of target genes such as cytochromes P450, UDP-glucuronosyltransferases, sulfotransferases and ABC transporters (MDR1 and MPR2) (Meijerman *et al*, 2006).

The microRNA array demonstrated that miR-148a that has been confirmed to negatively control pregnane X receptor (PXR) (Takagi *et al*, 2008), was expressed at the same level in both cell based models.

Comparable expression was also detected for microRNA 122-5p, the most abundant microRNA in the liver tissue (Lagos-Quintana *et al*, 2002) that is involved in the regulation of cholesterol metabolism (Elmen *et al*, 2008; Esau *et al*, 2006; Esau, 2008; Krützfeldt *et al*, 2005) and hepatitis C virus replication (Jopling *et al*, 2005; Lanford *et al*, 2010) (Figure 4.9C) . Similarly to miR-122, expression of miR-324-5p in stem cell - derived hepatocytes was not significantly different from primary human hepatocytes. This particular small non-coding RNA has been described to play a regulatory role in Hedgehog signalling in cerebellar neuronal progenitors (Feretti *et al*, 2008; Xu *et al*, 2014), however its role in liver is not well studied.

Target prediction strictly depends on the effectiveness of miR-mRNA interactions (Witkos *et al*, 2011). The levels of these interactions depend on different factors such as the 'seed' match. The 'seed' is a site located at 5' part of microRNA (positions 2-7) and its complete pairing within the 3' target mRNA region (canonical site) determines the certainty of interaction (Figure 4.12). There are four canonical sites: the 8mer having matched adenine in position 1 and an additional match in position 8; the 7mer1A that has an adenine in position 1 at the 5' end of miRNA, the 7merM8 that has adenine match in position 8; the 6mer that has no adenine match either in 1 or 8 position.

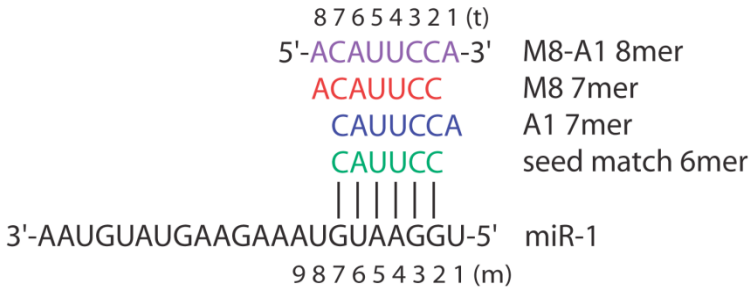

Figure 4.12: Seed match types. 8mer (M8-A1 8mer) having matched adenine in position 1 and an additional match in position 8, the M8-7mer that has adenine match in position 8; the 1A-7mer that has an adenine in position 1 at the 5' end of miRNA; the 6mer that has no adenine match either in 1 or 8 position. Adapted from TargetRank (http://hollywood.mit.edu/targetrank).

In this study, the level of mRNA/miR interactions is high for UGT1A1/miR-148a; SULT2A1/miR-324-5p and GSTT1/miR-24-3p, as indicated by 93%, 96% and 84% context score respectively (Figures 4.10 and 4.11). In addition, UGT1A1/miR-148a and SULT2A1/miR-324-5p interactions have been predicted to be stronger in comparison with GSTT1/ miR-24-3p. The first two interactions represent 8mer seed match (Figure 4.10) that represent the most efficient type of canonical site. What is more, they have an additional pairing with 3' part of microRNA (3'– supplementary sites) and corresponding nucleotides what may potentially enhance the binding. The SULT2A1/miR-324-5p interaction as the only one in this study demonstrated at least 3-4 nucleotides consecutively paired at 13-16 positions of mRNA that are considered to be required to facilitate target prediction.

In conclusion, microRNA and metabolism gene array identified important microRNA/mRNA interactions in stem cell derived hepatocytes that would allow us to understand the regulation of paracetamol metabolism and drug-induced liver injury in more details. What is more, metabolic gene and protein expression data revealed that hESC-derived hepatocytes exhibited upregulated sulfotransferases as well as downregulated cytochromes and UDP-glucuronosyltransferases in comparison with primary human hepatocytes, potentially suggesting immaturity of the stem cell *in vitro* model that should be studied further.

CHAPTER FIVE

MODELLING AND MODULATING PARACETAMOL TOXICITY IN HESC – DERIVED HEPATOCYTES USING NON - CODING RNAS

5.1 INTRODUCTION

5.1.1 CELL-BASED *IN VITRO* MODELS FOR PREDICTING PARACETAMOL TOXICITY

The liver is a multi-functional and highly regenerative organ. While resilient, the liver is susceptible to organ damage and failure. In both the acute and chronic settings liver disease has dire consequences for health. A common cause of liver damage is adverse reactions to drugs which can lead to drug induced liver injury (DILI). This creates major problems for patients, clinicians, the pharmaceutical industry and regulatory authorities (Olsen and Whalen, 2009). It has been reported that in the United Kingdom (UK) approximately 15% of the hospital in-patients suffer from liver toxicity in response to medicines during admissions, with 20% of these patients readmitted again after one year and a 2% mortality rate (Davies *et al*, 2010; Davies *et al*, 2009). The annual cost to the National Health Service in the UK ~£450 million with the costs growing year by year (Pirmohamed, 2004).

In the context of drug overdose or serious adverse reactions, liver failure can be acute and life threatening, and in some cases require orthotopic liver transplantation. While transplantation is highly successful, such an approach has limitations (Szkolnicka *et al* 2014a) and justifies basic science attempts to develop better human models to study liver injury and scalable intervention strategies. Paracetamol (APAP) is a major cause of drug-induced liver injury and accounts for 50% of cases of acute liver failure (Chun, 2009). Although much progress has been made in order to understand APAP- induced liver injury, most of the present knowledge of APAP hepatotoxicity has been learned from rodent studies *in vivo* and in primary culture. Despite their usefulness, there are significant species differences in the enzymatic activity of specific drug metabolism enzymes (e.g CYP1A, -2C, -2D, -3A) (Martignoni *et al*, 2006) and course of injury between rodents and humans (Nelson, 1990 and Jaeschke and Bait, 2006). In particular, Knight *et al* (2001) and Singer *et al* (1995) have noted that increased aminotransferase activity, the major marker of APAP-induced liver injury, can be detected in the plasma of rodents within 2-6 h of administration of a toxic dose of the drug (peak at 12 h), whereas in humans the activity of this enzyme is not observed before 12-24 h following ingestion and peaks at 48-72 h.

Although species differences such as metabolic rate and body size are important, mechanistic differences should also be taken into consideration. In order to bridge the gap between animals and humans much research has been focused on developing new and more predictable human *in vitro* models for drug toxicity studies. Primary human hepatocytes (PHH) are considered to be the gold standard *in vitro* model, however limited lifespan and donor background of these cells significantly affect the drug response. In order to generate more drug sensitive PHHs, cells are usually immortalized with SV40 T large antigen (Youdim *et al*, 2007), hTERT and E5/E7 (Tsuruga *et al*, 2008) or co-cultured with murine stromal fibroblasts (Khetani *et al*, 2013). Despite initial successes such as improved functional stability after 9 days of repeated drug exposure, the low levels of basal cytochrome P450 activity still limit use of PHH in analytical methods (Sinz *et al*, 2008). There has been much focus on variety of hepatoma cell lines as they demonstrate phenotypic stability and can be produced in large quantities. Hepatic cancer cell line HepG2 has been extensively used in drug toxicity studies, however its resemblance to gold standard model is still low. In paracetamol studies, three independent experiments tried to use adenovirus to induce the activity of CYP2E1 (Bai and Cederbaum, 2004), CYP3A4 (Vignati *et al*, 2005), and CYP2C9 (Iwamura *et al*, 2011) that play an important role in a toxic pathway of APAP metabolism. Although HepG2 cells transiently over-expressing particular enzymes displayed higher sensitivity to paracetamol-induced necrosis or apoptosis and generated higher amounts of reactive metabolites, the nature of viral transduction approach (enzyme of interest is transient) requires a new transfection for each experiment, therefore increasing the level of potential vector-integrated mutations (Godoy *et al*, 2013). What is more, Holmgren *et al* (2014) toxicity studies demonstrated that high proliferation of HepG2 cells in culture makes them impractical for long-term studies. HepaRG cell line, hepatoma – derived bipotent progenitors, demonstrated a positive model to study APAP-induced liver injury. In McGill *et al* (2011) studies, HepaRG cells exposed to different concentrations of the drug displayed APAP (NAPQI)-protein adduct formation, glutathione depletion, mitochondrial dysfunction and lactate dehydrogenase release. Although promising, the role in drug toxicity studies is still disputable due to their cancer origin and low sensitivity to different types of drugs (Gerets *et al*, 2012).

Contrary to models mentioned above, stem cells represent a type of cells that are capable of self-renewal, are genetically-stable and able to differentiate to all tissues. Therefore they are a promising source to generate a variety of cell-based models that can be used for drug development and high-throughput drug screening for different pathologies. Mesenchymal stem cells (MSCs) derived from bone marrow and adipose tissue have been reported to successfully differentiate to hepatocyte-like cells both *in vitro* and *in vivo* (Lysy *et al*, 2008; Lee *et al*, 2004; Aurich *et al*, 2007; Oyagi *et al*, 2006; Banas *et al*, 2007; Kuo *et al*, 2008). Although recent studies have demonstrated that these adult stem cell – derived hepatic cells express liver-specific genes and are able to improve the mouse liver after acute APAP intoxication (Stock *et al*, 2014), their use safety screening is limited due to loss of multipotency after lengthy expansion (Muraglia *et al*, 2000 and Aomatsu *et al*, 2013).

In recent years, functional hepatocytes derived from human embryonic (hESCs) and induced pluripotent (hiPSCs) stem cells have become an attractive toxicity model. Several different research groups (Cai *et al*, 2007; Hay *et al*, 2008; Si-Tayeb *et al*, 2010b, Brolen *et al*, 2010; Touboul *et al*, 2010; Yildrimman *et al*, 2011; Hannan *et al*, 2013; Ulvestadt *et al*, 2013; Medine *et al*, 2013; Szkolnicka *et al*, 2014b) have established functional and of high purity hepatocytes derived from hESCs and hiPSCs. Recent studies demonstrated that stem derived hepatocytes not only expressed proper liver metabolic functions but displayed stability and sensitivity to different drug exposures for more than 2 weeks (Holmgren *et al*, 2014) and demonstrated hepatotoxicity comparable to primary human hepatocytes (Szkolnicka *et al*, 2014b). Although Sengupta *et al* (2014) have demonstrated a potential application of hESC-derived hepatocytes for assessing APAP- induced liver injury, the modified hepatic differentiation procedure required use of bovine serum albumin. Therefore the use of serum-free hepatic differentiation protocol established in this project may become a more stable and reliable model for paracetamol cytotoxicity in the future.

5.1.2 THE IMPORTANCE OF MICRORNAS IN PARACETAMOL TOXICITY

Drug – induced liver injury (DILI) with paracetamol as the major contributor to the cytotoxicity, is a serious clinical problem and is the leading cause of drugs being removed from the market (Chang and Schiano, 2007; Halegoua-De Marzio, and Navarro, 2008). When taken in the appropriate amounts, paracetamol is modified by sulfotransferases (SULTs) and UDP glucuronosyltransferases (UGTs) and removed from the body without organ damage (Chun *et al*, 2009). However, when paracetamol is taken above the recommended dose it is metabolised by phase I enzymes such as cytochromes to generate a toxic intermediate N-acetyl-p-benzoquinone imine (NAPQI), which if untreated can lead to massive hepatocyte cell death and liver failure, placing the patient in a life threatening situation. In order to prevent the first onset of liver failure, identification of reliable and sensitive biomarkers is required. Currently, the major markers for APAP-induced liver injury are serum hepatocellular enzymes such as alanine (ALT) or aspartate (AST) aminotransferases and total bilirubin levels. Although useful, these serum markers are not liver specific, are detected at later injury stage and may be induced during metabolic perturbations such as food starvation (Lindena *et al*, 1986; Wang et al, 2009a; Thulin *et al*, 2014). In order to overcome these issues, new biomarkers for DILI have been discovered such as human leukocyte antigen (HLA), glutamate dehydrogenase (GLDH), high mobility group box protein 1 (HMGB1), and keratin 18 (K18) (Antoine *et al*, 2009; Antoine *et al*, 2012; O'Brien *et al*, 2002). In addition to these, circulating microRNAs have emerged as promising biomarkers for DILI (Wang *et al*, 2009a; Starkey *et al*, 2011). In particular, liver -specific microRNA-122 has been considered as a reliable marker for APAP toxicity as it is evolutionary conserved among species, very abundant, stable and can be detected using small amounts of starting material (Mitchell *et al*, 2008).

Although identification of tissue specific and drug sensitive markers is essential to prevent liver cytotoxicity, APAP overdose usually produces either no immediate symptoms or nonspecific intestinal irritation during the first 24 hours (Wang *et al*, 2009a). Therefore, much of research should be focused on finding new therapeutic methods to treat patients who suffered from sudden idiosyncratic or intrinsic DILI.

Currently, the most effective is N-acetylcysteine (NAC), an amino acid derivative that can be quickly converted into intracellular reduced glutathione in order to detoxify NAPQI. However, NAC is effective only if administered within 8-10 h after the initial ingestion which may not correlate with the APAP-induced liver injury symptoms (after 24 h) (Chong, 2007). As microRNAs have been demonstrated to play an important role in regulating drug metabolism and liver functions (see the discussion for details), there is a high potential for these non-coding RNAs to use them for therapeutic purposes against liver injury. Several studies have proven that microRNAs are able to regulate Phase I enzymes and Phase III transporters (Pan *et al*, 2009a; Tsuchiya *et al*, 2006; Yu, 2009; Yu and Pan, 2012), however the second phase of drug metabolism, drug conjugation, has not been studied in detail. Drug conjugation is a crucial stage part in human drug metabolism, and any alternations in this process can lead to changes in compound pharmacology, including therapeutic dose and clearance from the body. Therefore identification of microRNAs that may control expression of phase II enzymes that are responsible for APAP detoxification could be the next step to discover new treatment for DILI. What is more, studying phase II-miR interactions in stem cell – derived model would be more reflective to primary human hepatocytes. This would allow for better cytotoxicity prediction and identification of potential new microRNAs as biomarkers for paracetamol-induced liver injury.

5.2 RESULTS

In this chapter, we were interested to examine whether inhibition or delivery of microRNAs to hESC-derived hepatocytes would reduce paracetamol cytotoxicity *in vitro*. We identified a novel anti-microRNA of miR-324-5p which regulated the phase II SULT2A1 enzyme, reduced paracetamol induced hepatotoxicity and glutathione depletion. Additionally, we also demonstrated a supportive role for anti-microRNA-324 in response to fulminant plasma collected from paracetamol overdose patients.

5.2.1 MODELLING PARACETAMOL TOXICITY *IN VITRO*

In Chapter 4 the results generated from the array experiments were validated by immunostaining, focussing on phase II and phase III drug metabolism and excretion. Phase II proteins from the normal (SULT2A1, UGT1A1) and toxic (GSTT1) pathways were expressed in 59%, 54% and 98% respectively (Chapter 4; Figures 4.6 and 4.7) Importantly, stem cell –derived hepatocytes also expressed phase III drug transporters important in each pathway, in 52% (ABCG2) and 77% (ABCC1) of cells (Chapter 4; Figures 4.7). Therefore, it has been hypothesised that stem cell-derived hepatocytes possess the correct machinery to process paracetamol (APAP) in a normal and toxic manner. To test this, stem cell –derived hepatocytes were exposed to a range of concentrations of APAP (range 0 to 50 mM) for 24 hours. The cell morphology was examined and the cell viability was monitored by ATP production. Phase-contrast imaging demonstrated dose dependent toxicity on cell viability indicated by increasing cell death (Figure 5.1). The morphology results were in line with the cell viability assay. The studies demonstrated that hESC-derived hepatocytes responded to APAP in a dose dependent fashion, with an IC50 value (concentration that causes 50% of the cell death) of 12.85 mM (Figure 5.2; Supplementary Figure 1.9).

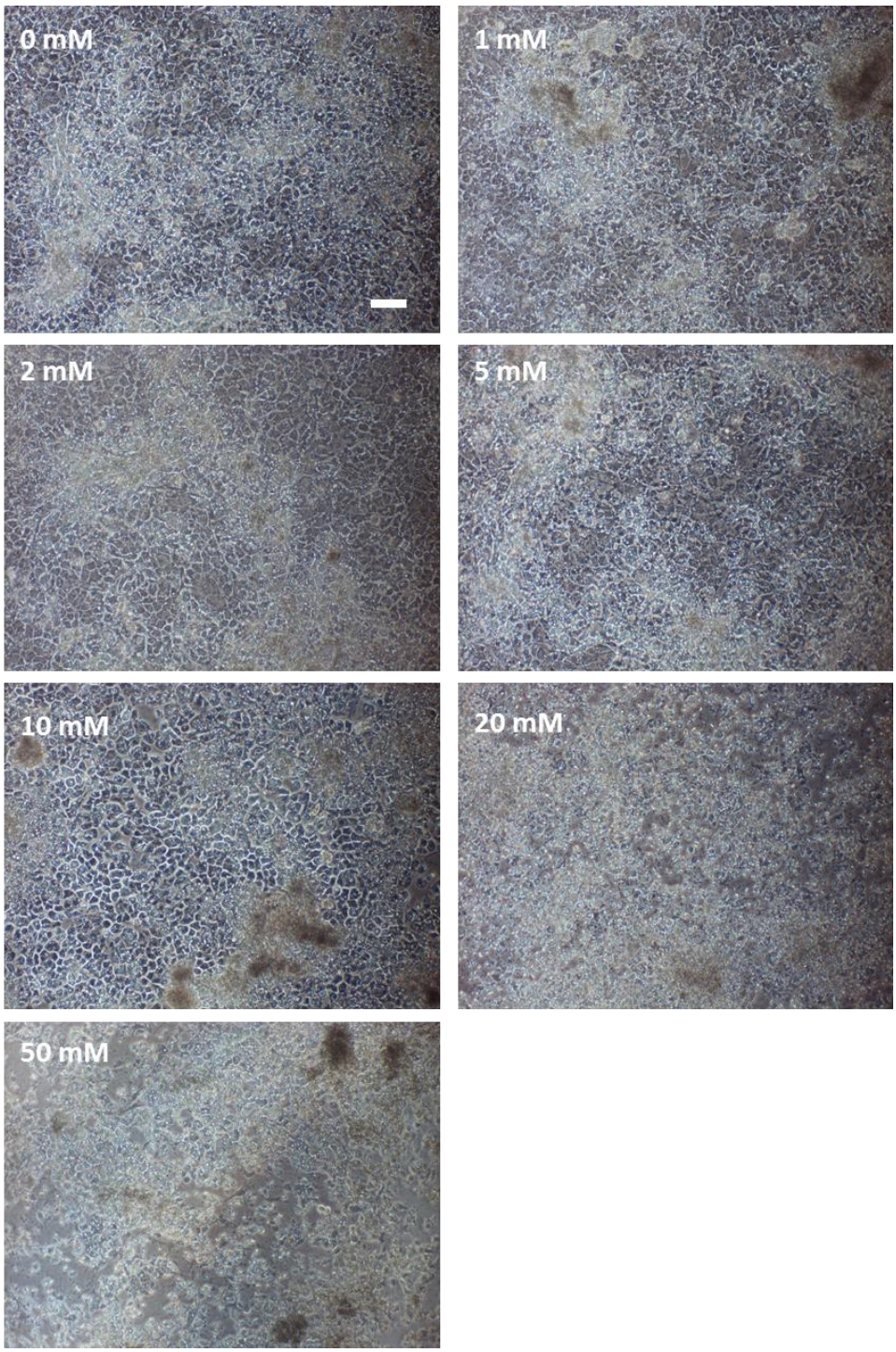

Figure 5.1: Morphology of hESC-derived hepatocytes after exposure to paracetamol. Morphological change of hESC-derived hepatocytes (day 17) exposed to different concentrations of paracetamol (APAP) (0-50 mM) for 24 hours. Contrary to the other concentrations, cells exposed to 20 and 50mM APAP demonstrated significant apoptosis. Scale bar represents 100 um. Abbreviations: mM; millimolar.

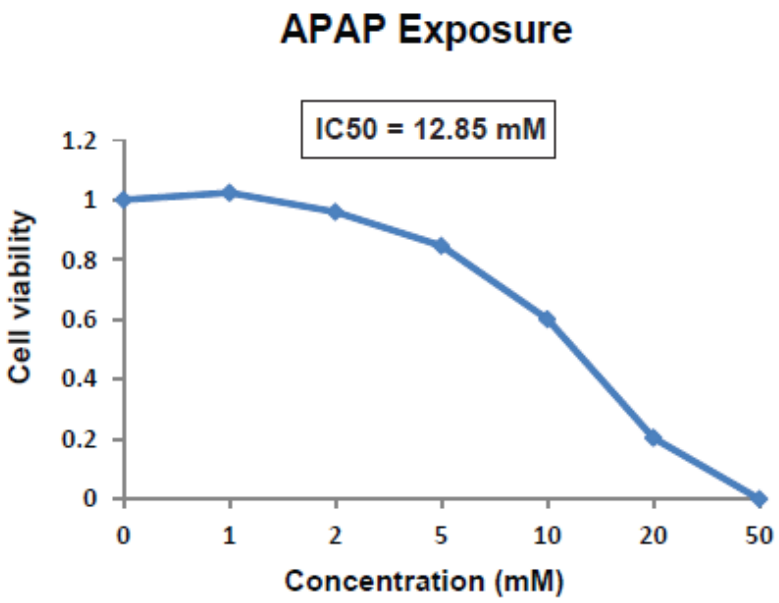

Figure 5.2: Paracetamol (APAP) *in vitro* toxicity in stem cell –derived hepatocytes. At day 17, hESC-hepatocytes were induced with different concentrations of APAP (0-50 mM) for 24 hours. The CellTitre- Glo® Luminescent Cell Viability Assay (Promega) was used to measure the ATP levels. The IC50 (12.85 mM) was calculated from the function f(x) = ax + b. n=3, biological replicates. The graph represents fold change in cell viability.

5.2.2 OPTIMISATION OF TRANSFECTION EFFICIENCY

In order to test the hypothesis that stem cell – derived hepatocyte susceptibility to APAP overdose (IC50 = 12.85 mM) could be regulated by microRNAs, the synthetic RNAs were introduced in to the cells by lipophilic based transfection (Lipofectamine RNAiMAX; Life Technologies). In these experiments precursors and corresponding antagomirs were used. Stem cell – derived transfection was optimised (Figure 5.3). hESC - derived hepatocytes transfected with Cy3-labelled precursors (Ambion; Life Technologies) and Cy3-labelled antagomirs (Ambion; Life Technologies) at 50 nM concentration displayed efficient levels of transfection. Cy3-labelled precursors transfected at the 1:1, 1:2, and 1:3 lipofectamine ratio resulted in 81% (SE±6.4), 90% (SE±3.2), and 97% (SE±1.2) of positive cells respectively. Transfection with Cy3-labelled antagomirs at 1:1, 1:2, and 1:3 lipofectamine ratio resulted in 21% (SE±3.4), 47% (SE±5.49) and 33% (SE±2.3) of positive cells respectively (Figure 5.3).

The immunostaining demonstrated that the most efficient transfection ratio for precursors at 50 nM concentration was 1:3, whereas for the corresponding antagomirs at the same concentration was 1:2.

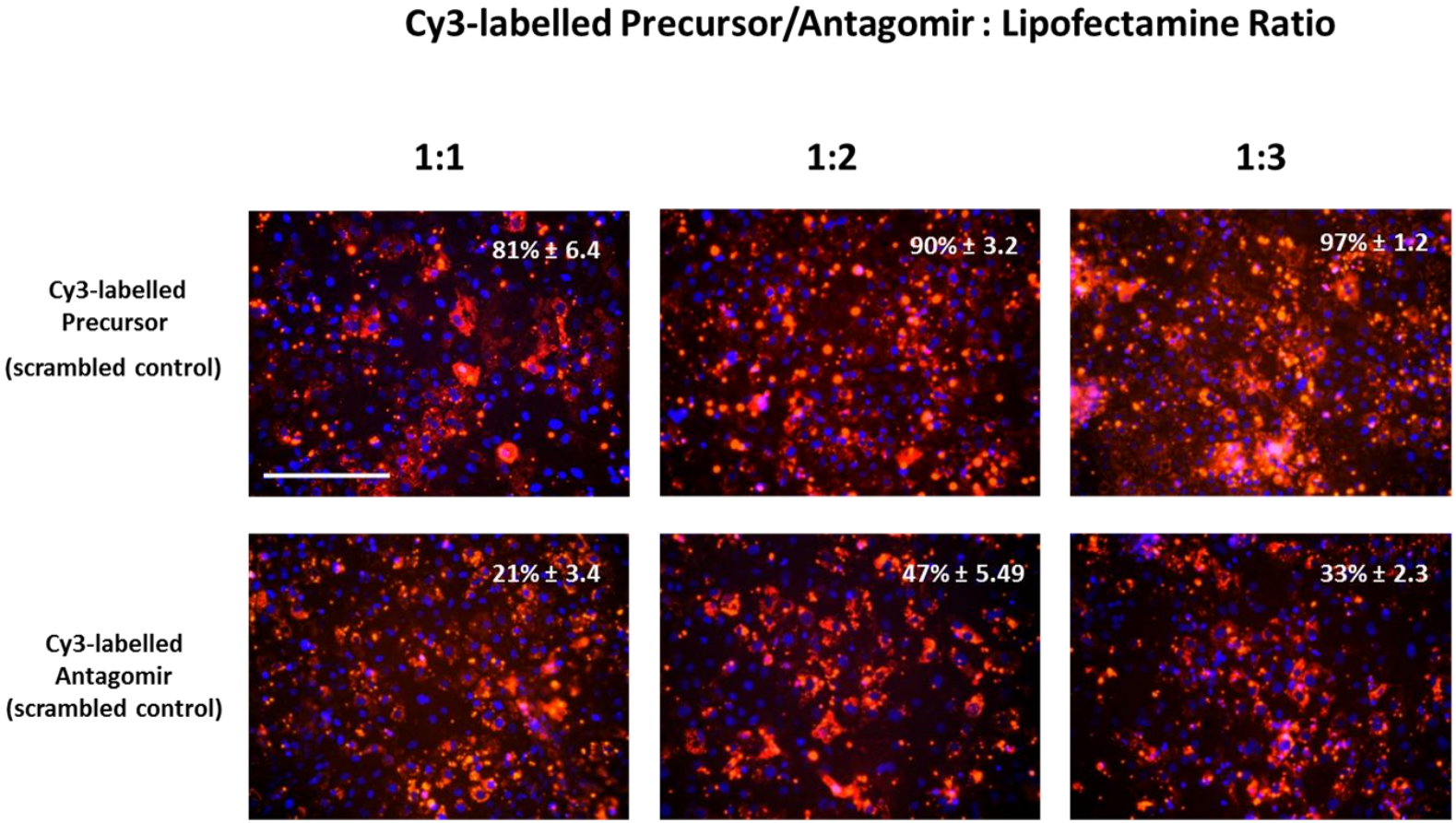

Figure 5.3: Transfection efficiency. hESC - derived hepatocytes were transfected with Cy3-labelled scrambled precursors and antagomirs (50nM) at different lipofectamine RNAiMAX ratios (1:1; 1:2; 1:3) for 24 hours. The percentage of positive cells is provided in the top right of each panel. This was calculated from fields of view and is quoted as ± standard error. Scale represents 100um.

In order to further validate the transfection ratio efficiency and cell viability for both precursors and antagomirs, the well - established microRNA liver controls were used. In this experiment, precursors and antagomirs of miR-122-5p (marker of adult liver, Chang *et al*, 2004; Barad *et al*, 2004) and miR-483-3p (marker of fetal liver, Fu *et al*, 2005) were transfected at both 1:2 and 1:3 lipofectamine ratio to determine the level of potential cell toxicity caused by lipophilic-based approach. The results demonstrated that transfection of both scrambled (Pre/Ant Ctrl) and liver (Pre/Ant of miR-122 and miR-483) microRNA controls did not significantly affect the viability of stem cell-derived hepatocytes as indicated by similar production of cellular ATP (Figure 5.4).

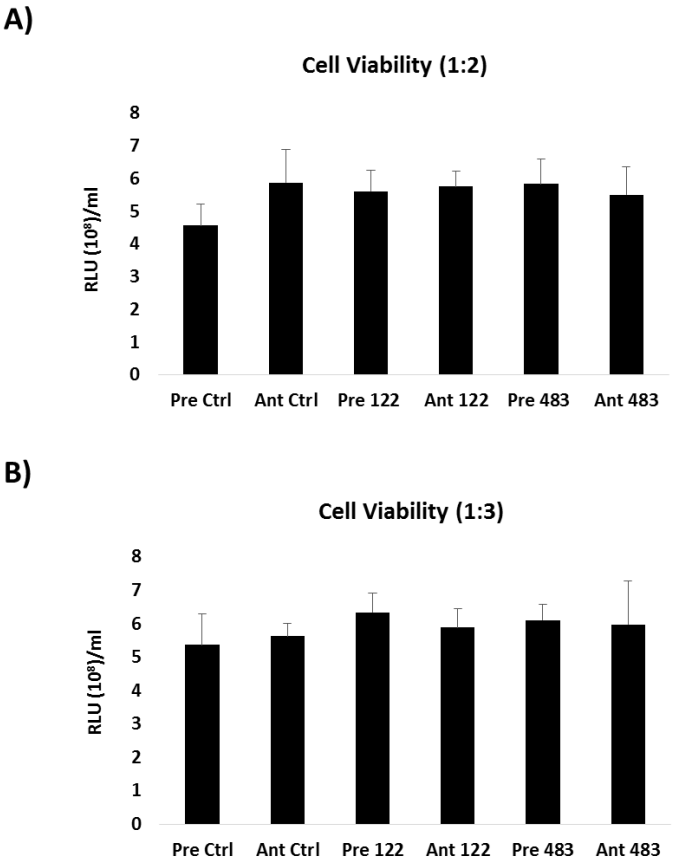

Figure 5.4: Cell viability and microRNA transfection. hESC - derived hepatocytes transfected with precursors and antagomirs (both at 50 nM) of the scrambled control, miR-122-5p and miR-483-3p for 24 hours. Cell viability (ATP production) did not significantly change either at 1: 2 (A) or 1:3 (B) lipofectamine RNAiMAX ratios. Cell viability was measured by CellTitre – Glo® Luminescent Cell Viability Assay (Promega). Abbreviations: Pre Ctrl, precursor scrambled control; Ant Ctrl, antagomir scrambled control; Pre/Ant 122, precursor/antagomir of miR-122-5p; Pre/Ant 483, precursor/antagomir of miR-483-3p; RLU/ml, relative light units/ml.

5.2.3 MODULATION OF PARACETAMOL METABOLISM USING PRECURSORS AND ANTAGOMIRS

In order to examine whether precursors / antagomirs of miR-24-3p, miR-148a, and miR-324-5p had any direct effect on the regulation of mRNA of GSTT1, UGT1A1, and SULT2A1, stem-cell derived hepatocytes were transfected with the microRNA activators and inhibitors at day 17 of differentiation for 24 hours and subsequently examined for gene expression by qPCR.

The results demonstrated that transfection with the precursor of miR-24-3p and miR-324-5p did not have any significant effect on the gene expression of GSTT1 and SULT2A1 enzyme respectively in comparison with the scrambled control (Figure 5.5). Transfection with precursor of miR-148a resulted in decreased UGT1A1 gene expression as indicated by ~ 2 (SD± 0.02) fold change (Figure 5.5). Transfection with the antagomir of miR-24-3p did not have any significant effect on the gene expression of GSTT1 enzyme in comparison with the scrambled control (Figure 5.6). Contrary to this result, transfection with the antagomirs of miR-148a and miR-324-5p resulted in increased gene expression of UGT1A1 and SULT2A1 enzymes as indicated by ~ 2.4 (SD±0.23) and ~ 2.04 (SD±0.12) fold change respectively (Figure 5.6).

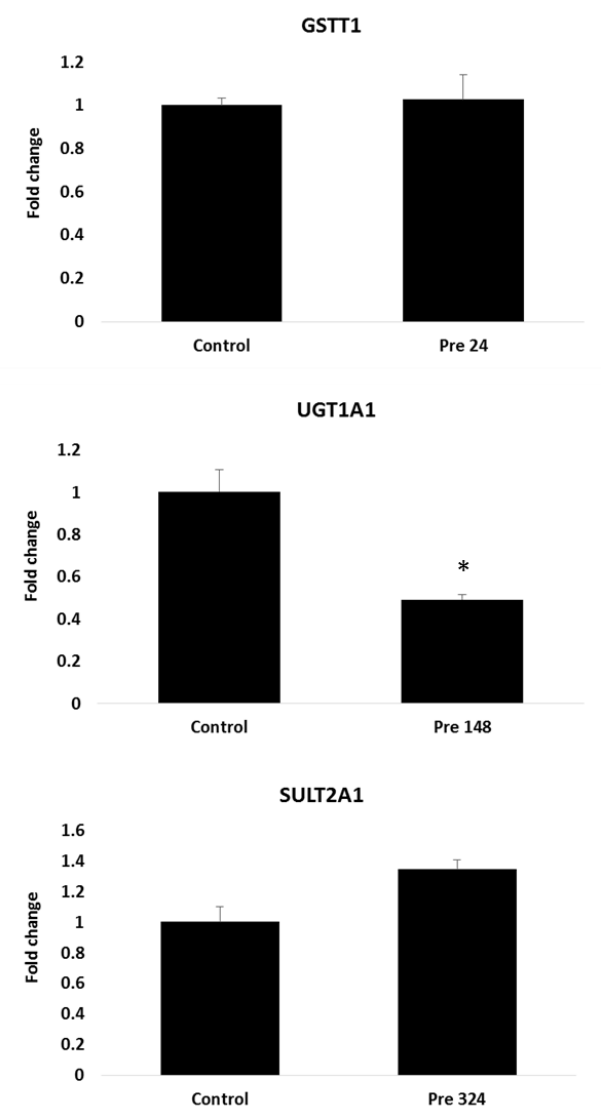

Figure 5.5: Gene expression of Phase II enzymes after transfection with miR precursors. Gene expression of GSTT1, UGT1A1, and SULT2A1 after transfection with precursors of scrambled control, miR-24-3p, miR-148a, and miR-324-5p respectively. The gene expression was normalised to housekeeping gene B2M and scrambled control. Levels of significance were measured by Student's *t test*, where $p < 0.05$ and $p < 0.01$ were indicated by one and two asterix respectively. Abbreviations: GSTT1, glutathione S-transferase theta 1, UGT1A1, UDP-glucuronosyltransferase 1A1; SULT2A1, sulfotransferase 2A1; Pre 24/148/324; precursor of miR-24-3p, miR-148a, miR-324-5p; B2M, B-microglobulin.

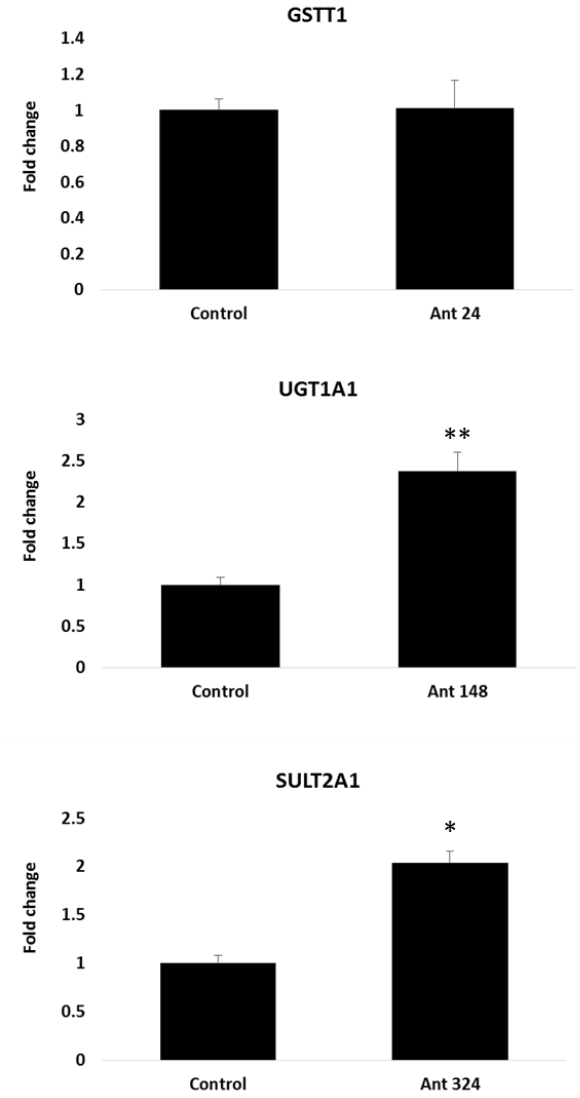

Figure 5.6: Gene expression of Phase II enzymes after transfection with miR antagomirs. Gene expression of GSTT1, UGT1A1, and SULT2A1 after transfection with antagomirs of scrambled control, miR-24-3p, miR-148a, and miR-324-5p respectively. The gene expression was normalised to housekeeping gene B2M and scrambled control. Levels of significance were measured by Student's *t test*, where $p < 0.05$ and $p < 0.01$ were indicated by one and two asterix respectively. Abbreviations: GSTT1, glutathione S-transferase theta 1, UGT1A1, UDP-glucuronosyltransferase 1A1; SULT2A1, sulfotransferase 2A1; Ant 24/148/324; antagomir of miR-24-3p, miR-148a, miR-324-5p; B2M, B-microglobulin.

In order to validate the regulatory effect of selected microRNAs on GSTT1, UGT1A1 and SULT2A1 gene expression, the protein expression of these specific enzymes was also examined by immunocytochemistry. hESC-derived hepatocytes transfected with precursors of miR-24-3p, miR-148a, and miR-324-5p expressed 99% (SE±0.29), 18% (SE±2.30), and 63% (SE±0.55) of cells positive for GSTT1, UGT1A1, and SULT2A1 respectively, suggesting no potential regulatory effect on the protein expression of these particular enzymes (Figure 5.7).

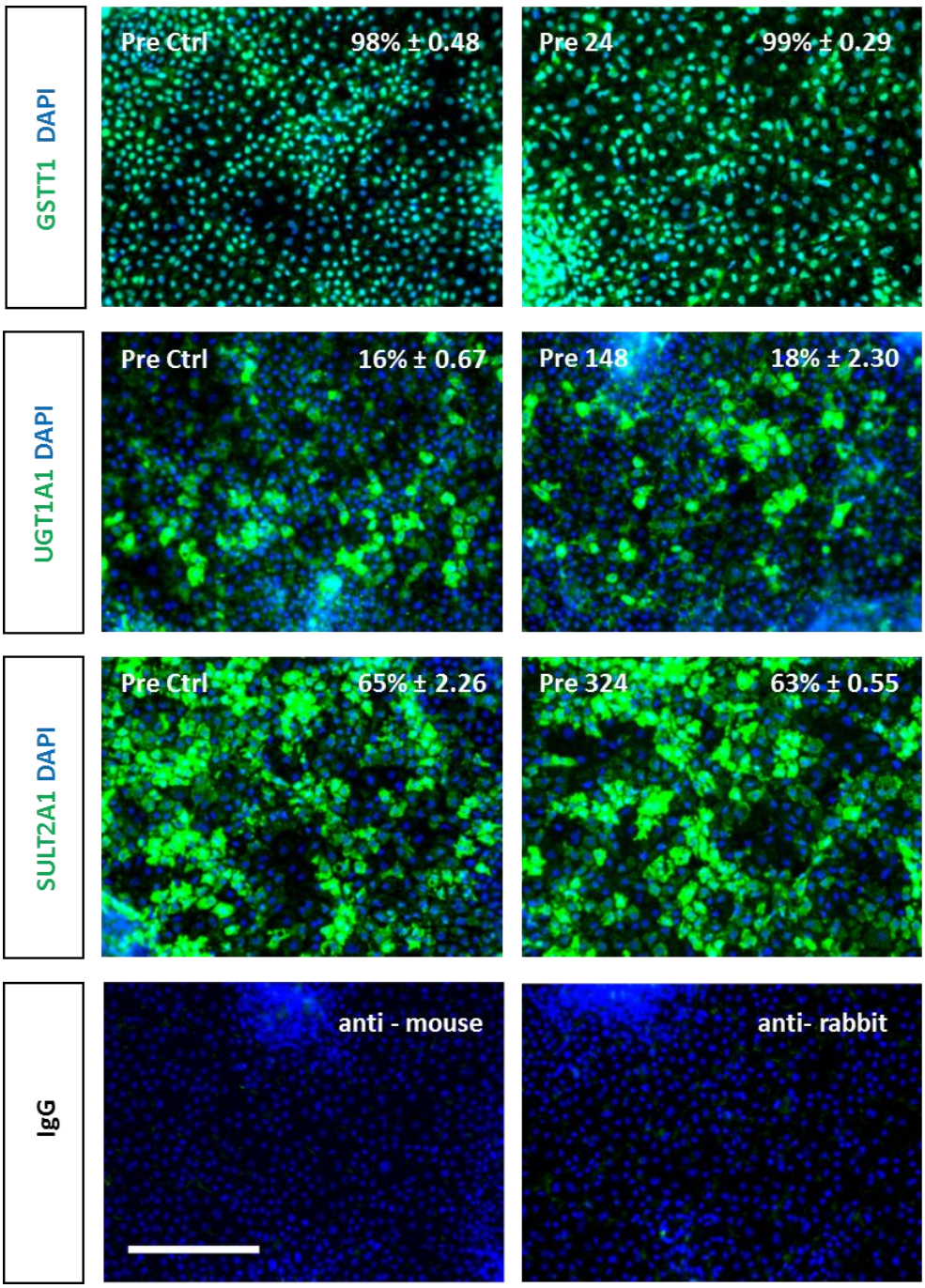

Figure 5.7: Protein expression of Phase II enzymes after transfection with precursors. Protein expression of GSTT1, UGT1A1, SULT2A1 after 24h transfection with either precursor scrambled control or relevant precursor of miR-24-3p, miR-148a; miR-324-5p. The percentage of positive cells is provided in the top right of each panel. This was calculated from four random fields of view and is quoted as ± standard error. Immunoglobulin G controls demonstrated the specificity of immunostaining. Scale bar represent 100um. Abbreviations: Pre Ctrl; precursor scrambled control; Pre 24/148/324; precursor of miR-24-3p; miR-148a; miR-324-5p.

Once it was established that phase II enzyme expression could be modulated for the non-toxic pathway (UGT1A1 and SULT2A1), the cell viability and reduced glutathione production (glutathione depletion) were measured in response to APAP incubation. Stem cell-derived hepatocytes were transfected with precursors of miR-24-3p, miR-148a, and miR-324-5p for 24 hours prior to APAP incubation (IC50) for another 24 hours. The results demonstrated that transfection with precursors of miR-24-3p and miR-148a slightly reduced cell viability in comparison with scrambled control, whereas transfection with precursor of miR-324-5p significantly reduced ATP production in stem cell derived hepatocytes (1.9 x 10^8 RLU/ml; p = 0.007) (Figure 5.8). Similarly to cell viability, transfection with precursors of miR-24-3p, miR-148 and miR-324-5p resulted in decreased generation of reduced glutathione (Figure 5.9).

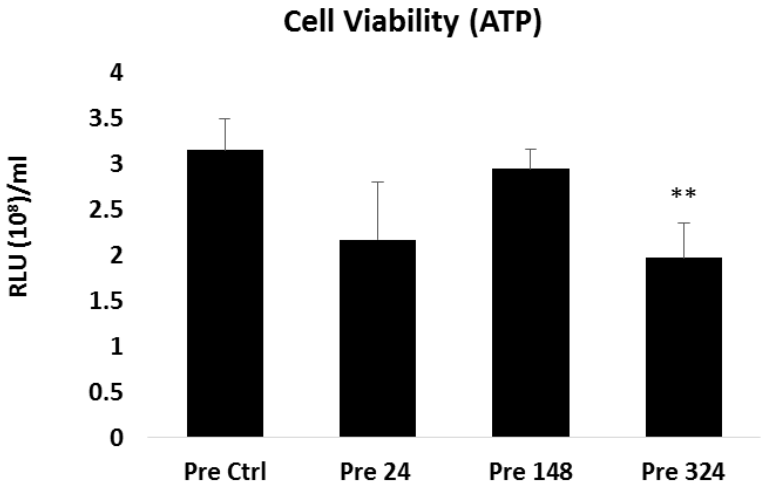

Figure 5.8: Cell viability after transfection with precursors. hESC - derived hepatocytes (d17) were transfected with precursors at 50nM concentration for 24 hours. At day 18, the transfected cells were exposed to paracetamol concentration that causes 50% of the cell death (IC50=12.85 mM) for another 24 hours. At day 19, the cell viability was measured using CellTiter – Glo® Luminescent Cell Viability Assay (Promega). Abbreviations: Pre Ctrl, precursor scrambled control; Pre 24/148/324; precursor of miR-24-3p. miR-148a, miR-324-5p. Levels of significance were measured by Student's *t test*, where $p < 0.01$ was indicated as two asterix.

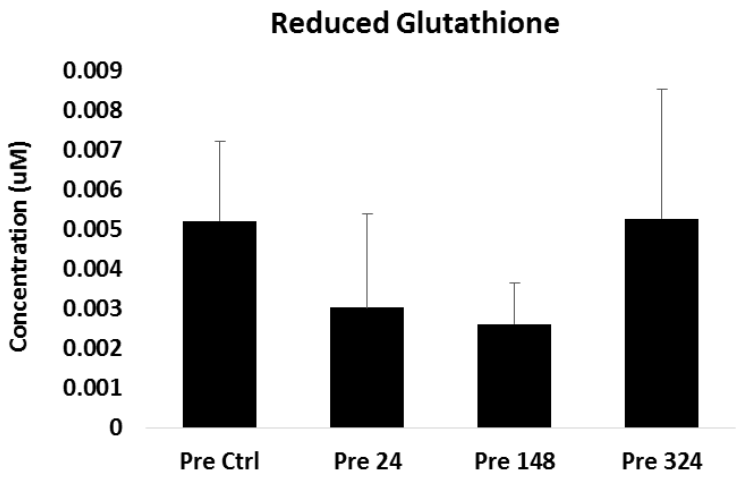

Figure 5.9: Reduced glutathione production after transfection with precursors. hESC - derived hepatocytes (d17) were transfected with precursors at 50nM concentration for 24 hours. At day 18, the transfected cells were exposed to paracetamol concentration that causes 50% of the cell death (IC50=12.85 mM) for another 24 hours. At day 19, the glutathione reduction was measured using GSH/GSSG-Glo™ Assay (Promega). Abbreviations: Pre Ctrl, precursor scrambled control; Pre 24/148/324; precursor of miR-24-3p. miR-148a, miR-324-5p. Levels of significance were measured by Student's *t test*, where $p < 0.01$ was indicated as two asterix.

Stem cell – derived hepatocytes transfected with antagomirs of miR-24-3p, and miR-148a expressed 99% (SE±0.25) and 17% (SE±0.60) of cells positive for GSTT1 and UGT1A1 respectively, potentially suggesting no regulatory effect of these microRNAs on the protein expression of selected enzymes. Contrary to the precursor, hESC-derived hepatocytes transfected with the antagomir of miR-324-5p expressed 95% (SE±1.09) of cells positive for SULT2A1, therefore suggesting inhibitory role of miR-324 on SULT2A1 expression by ~ 20% (Figure 5.10).

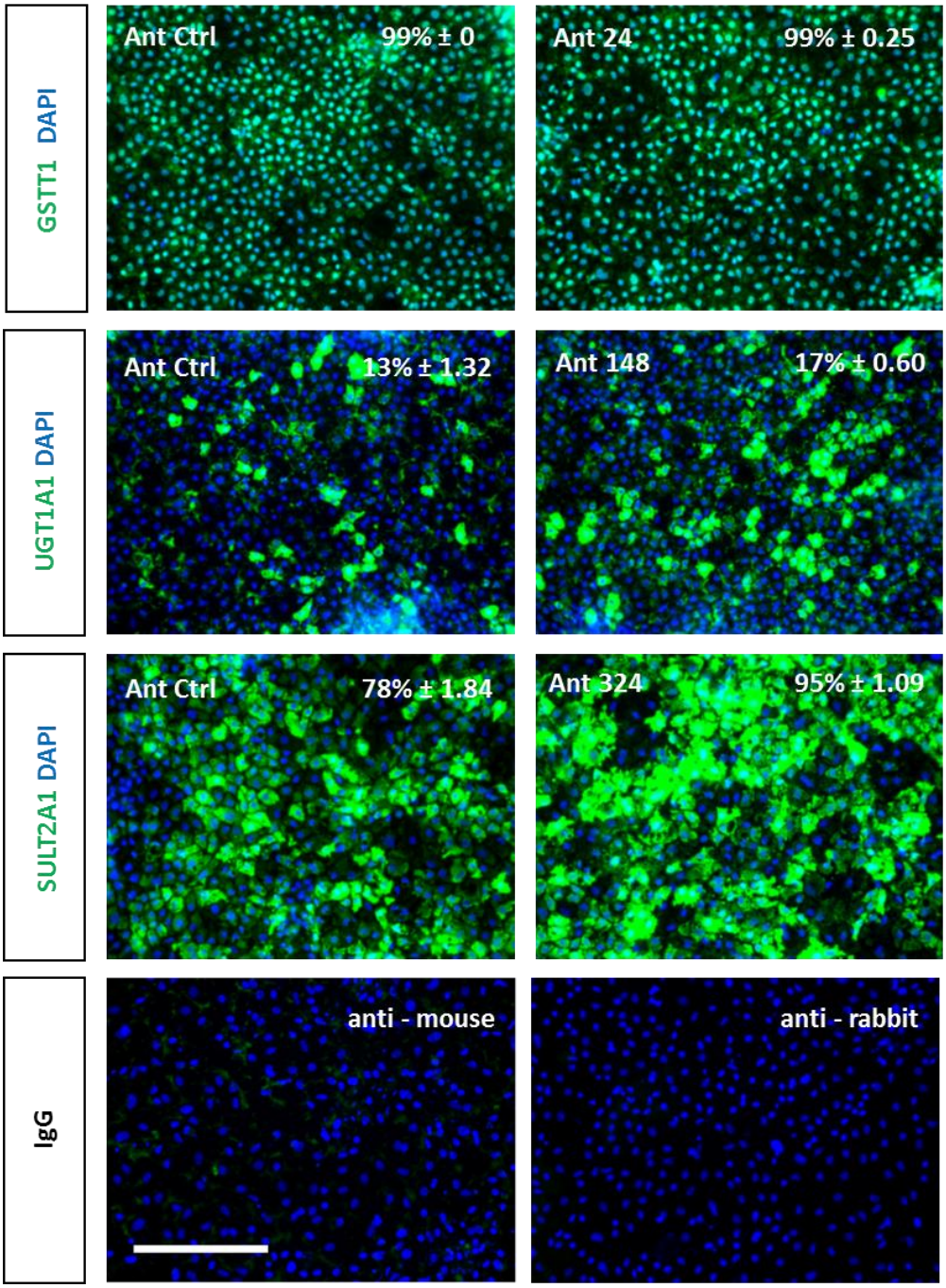

Figure 5.10: Protein expression of Phase II enzymes after transfection with antagomirs. Protein expression of GSTT1, UGT1A1, SULT2A1 after 24h transfection with either antagomir scrambled control or relevant precursor of miR-24-3p, miR-148a; miR-324-5p. The percentage of positive cells is provided in the top right of each panel. This was calculated from four random fields of view and is quoted as ± standard error. Immunoglobulin G controls demonstrated the specificity of immunostaining. Scale bar represent 100um. Abbreviations: Ant Ctrl; antagomir scrambled control; Ant 24/148/324; antagomir of miR-24-3p; miR-148a; miR-324-5p.

Transfection with the antagomirs of miR-24-3p and miR-148a did not increase the cell viability and generation of reduced glutathione in response to toxic concentration of APAP in comparison with scrambled control (Figure 5.11). Contrary to the antagomirs of miR-24-3p and miR-148a, inhibition of miR-324-5p in stem cell – derived hepatocytes resulted in a significant increase of ATP production (3.12 x 10^8 RLU/ml; p = 0.04) and reduced oxidative stress as indicated by 2-fold increase in reduced glutathione (0.008023 uM; *p* =0.03) (Figure 5.12)

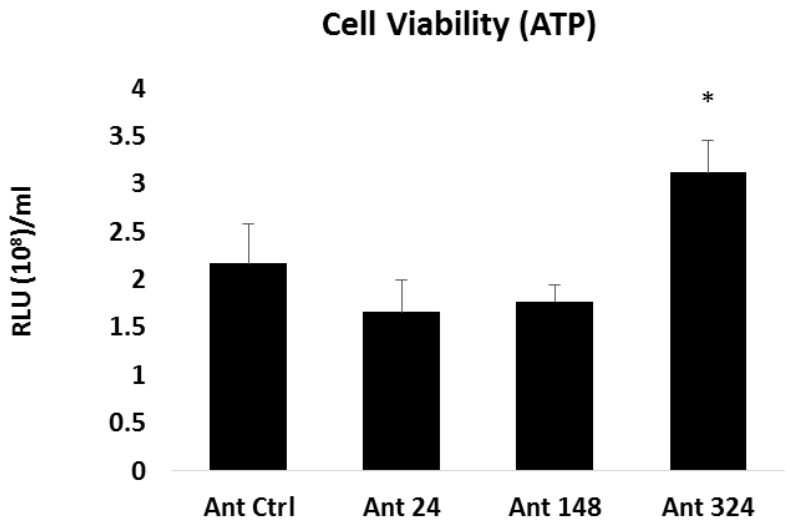

Figure 5.11: Cell viability after transfection with antagomirs. hESC - derived hepatocytes (d17) were transfected with antagomirs at 50nM concentration for 24 hours. At day 18, the transfected cells were exposed to paracetamol concentration that causes 50% of the cell death (IC50=12.85 mM) for another 24 hours. At day 19, the cell viability was measured using CellTiter – Glo® Luminescent Cell Viability Assay (Promega). Abbreviations: Ant Ctrl, antagomir scrambled control; Ant 24/148/324; antagomir of miR-24-3p. miR-148a, miR-324-5p. Levels of significance were measured by Student's *t test*, where $p < 0.05$ was indicated as one asterix.

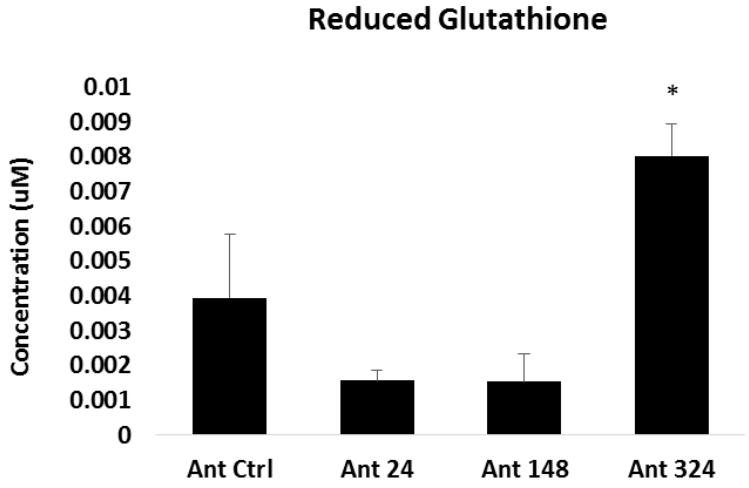

Figure 5.12: Reduced glutathione production after transfection with antagomirs. hESC - derived hepatocytes (d17) were transfected with antagomirs at 50nM concentration for 24 hours. At day 18, the transfected cells were exposed to paracetamol concentration that causes 50% of the cell death (IC50=12.85mM) for another 24 hours. At day 19, the glutathione reduction was measured using GSH/GSSG-Glo™ Assay (Promega). Abbreviations: Ant Ctrl, antagomir scrambled control; Ant 24/148/324; antagomir of miR-24-3p. miR-148a, miR-324-5p. Levels of significance were measured by Student's *t test*, where $p < 0.05$ was indicated as one asterix.

5.2.4 CELL PROTECTIVE EFFECT OF THE ANTAGOMIR 324-5P AFTER EXPOSURE TO PLASMA OF THE PARACETAMOL OVERDOSE PATIENTS

As the inhibition of miR-324-5p in stem cell – derived hepatocytes resulted in increased gene and protein expression of SULT2A1 enzyme as well as significantly increased cell viability and reduced glutathione (GSH) in response to APAP incubation, we were interested to examine whether the antagomir of miR-324-5p could increase cell viability after exposure to the sera of paracetamol overdose female patients. In this experiment, stem cell –derived hepatocytes were exposed to the inhibitor of miR-324-5p for 24 hours and subsequently exposed to 20% of patient's specific serum for another 24 hours. In this study, cell viability and caspase 3/7 activity were measured (Figures 5.13 and 5.14). Interestingly, hESC-derived hepatocytes showed significant increase in cell viability following exposure to Patient 1 (3.29×10^8 RLU/ml; $p = 0.016$) and Patient 58 serum (3.54×10^8 RLU/ml; $p = 0.0017$) in comparison with scrambled controls (2×10^8 RLU/ml and 2.08×10^8 RLU/ml respectively). Cell exposure to Patient 8 serum did not demonstrate any significant increase in cell survival in comparison with scrambled controls as indicated by

3.72 x 10^8 RLU/ml and 3.67 x 10^8 RLU/ml respectively (Figure 5.13). In line with ATP production, exposure to Patient 1 and Patient 58 sera resulted in increased caspase 3/7 activity as indicated by 2.3 x 10^7 RLU/ml (p =0.008) and 2.6 x 10^7 RLU/ml (p=0.0103) respectively and compared to scrambled controls (1.6 x 10^7 RLU/ml and 1.4 x 10^7 RLU/ml respectively). Exposure to Patient 8 serum did not significantly increase caspase 3/7 activity in comparison with the scrambled control as indicated by 2.8 x 10^7 RLU/ml and 2.9 x 10^7 RLU/ml respectively (Figure 5.14).

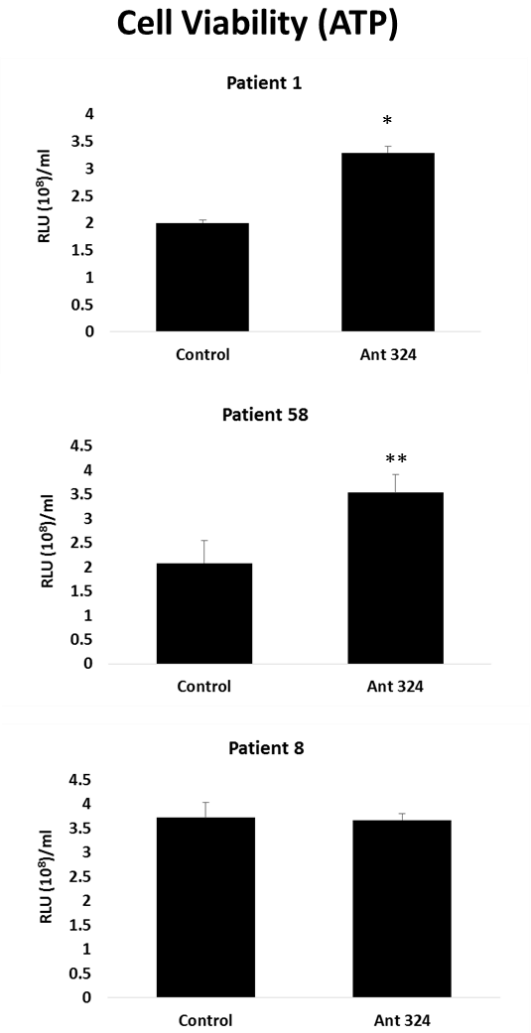

Figure 5.13: **Cell viability after exposure to the fulminant plasma.** hESC - derived hepatocytes were transfected with the antagomir to miR-324-5p. Twenty four hours post transfection hESC – hepatocytes were exposed to the fulminant plasma of the three paracetamol overdose patients for a further twenty four hours (Patients 1, 8, 58). The cellular ATP was measured on a luminometer (Promega). Units of activity are expressed as relative light units (RLU) ml^{-1} (n=4). Levels of significance are quoted and measured by Student's *t*-test. Significance levels are denoted by one and two asterisks to indicate $p < 0.05$ and $p < 0.01$ respectively.

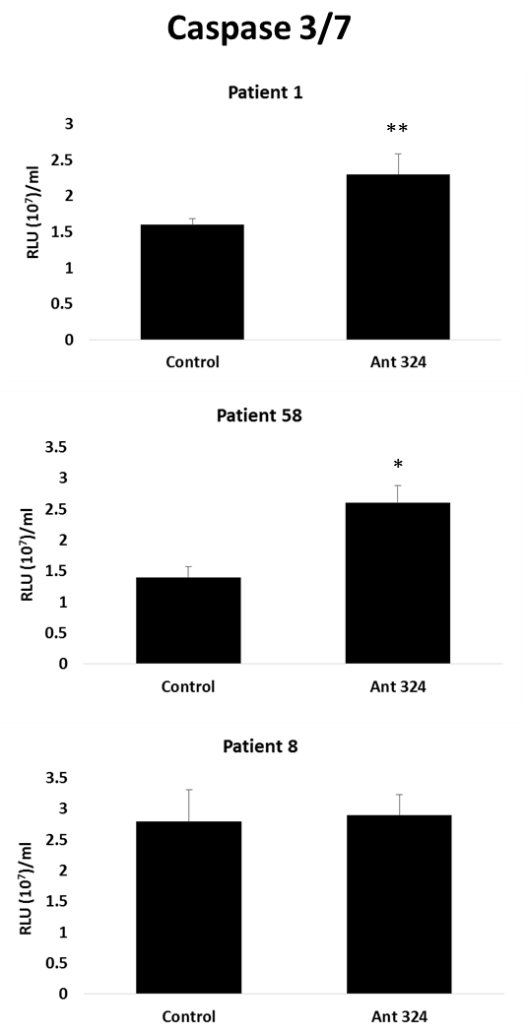

Figure 5.14: **Caspase 3/7 activity after exposure to the fulminant plasma.** hESC - derived hepatocytes were transfected with the antagomir to miR-324-5p. Twenty four hours post transfection hESC – hepatocytes were exposed to the fulminant plasma of the three paracetamol overdose patients for a further twenty four hours (Patients 1, 8, 58). The Caspase 3/7 activation was measured on a luminometer (Promega). Units of activity are expressed as relative light units (RLU) ml^{-1} (n=4). Levels of significance are quoted and measured by Student's *t*-test. Significance levels are denoted by one and two asterisks to indicate $p < 0.05$ and $p < 0.01$ respectively.

5.3 DISCUSSION

Despite major progress in the knowledge and management of human liver injury, there are approximately 2000 cases per year of acute liver failure (ALF) in the United States (Hoofnagle, 1995; Polson *et al* 2005; Fontana, 2008). Paracetamol overdose is a major factor in ALF, with critical damage done to the hepatocyte compartment of the liver, and accounts for approximately 50% of cases (Nourjah *et al*, 2006; Bari and Fontana, 2014). Although hepatocyte cell death occurs in large numbers, the manner in which the cells die following overdose remains complicated and controversial (Jaeschke *et al* 2012). Current medical treatments for paracetamol overdose include gastric lavage, activated charcoal ingestion and administration of cimetidine (Underhill *et al*, 1990; Burkhart *et al*, 1995). Agents such as methionine, N-acetylcysteine (NAC), and cysteamine are also used to detoxify the liver toxic effects of NAPQI, with NAC considered as the most effective intervention to prevent liver failure (Brok *et al*, 2006). Although successful, these treatments may cause side effects, including the inhibition of key metabolic functions of the liver (Makin *et al*, 1995; Kozer and Koren, 2001), as well as negatively effects on pulmonary, gastrointestinal and central nervous systems (Chun *et al*, 2009; Schmidt and Dalhoff *et al*, 2001). In the absence of notable effect and at the onset of severe liver decompensation and failure, liver transplant is the only effective approach to treat patients. While highly successful, this is not considered to be an 'off the shelf' or scalable alternative. Therefore, other treatments are being explored to improve patient outcome. MicroRNAs are potent non-coding RNAs which can alter mammalian gene expression and therefore represent promising candidates for treating human disease. Several studies have shown that regulation of different microRNAs may potentially serve as effective therapeutics. Currently, antisense oligonucleotides to miR-122 (RG-101; preclinical stage and Miravirsen (SPC3649); clinical stage) and miR-21 (RG-012; preclinical stage) are being developed to treat chronic hepatitis C virus (HCV) or Alport Syndrome respectively (Thong *et al*, 2014; Heidet and Gubler, 2009). More recently, the systemic delivery of miR-34a has been shown to reduce liver tumour growth (Daige *et al*, 2014) and miR-33 promotes clearance of excess cholesterol and is useful in treating atherosclerosis (Rayner *et al* 2011).

In the recent years there has been a focus on miR regulation of phase I enzymes involved in human drug metabolism. Studies have demonstrated that miR-27b regulates CYP3A4 and CYP1B1 and miR-126* controls CYP2A3 expression (Pan *et al*, 2009a; Tsuchiya *et al*, 2006; Kalscheuer *et al*, 2008). Other studies have also focused on microRNA regulation of drug transporters such as P-glycoprotein and breast cancer resistant protein (BCRP) (Kovalchuk *et al*, 2008; Zhu *et al*, 2008; Liao *et al*, 2008; To *et al* 2008, Pan *et al*, 2009b). While phase I and phase III of drug metabolism have been studied, there is still little known about regulation of phase II enzymes by microRNAs. Phase II enzymes, such as glutathione S - transferases and sulfotransferases, are essential to sufficiently detoxify different xenobiotics, therefore these enzymes serve as important clinical targets.

In this study, three potential microRNAs (miR-24-3p, miR-148a, miR-324-5p) have been predicted by TargetScan Human 6.2 (see Chapter 4 for details) to regulate three important phase II enzymes that play an essential role both in toxic and non-toxic pathways of paracetamol metabolism: GSTT1, UGT1A1 and SULT2A1. In order to validate these interactions and examine their protective effect from toxic concentrations of paracetamol, induction of those two pathways was required. Using IC50 value of paracetamol in stem-cell derived model would allow to stimulate enzymes of interest under toxic conditions, however would not lead to complete cell death. Contrary to *in vitro* primary human and mouse hepatocytes that have been reported to show paracetamol IC50 value of 5-8 mM (Viollon *et al*, 1991), hESC-derived hepatocytes displayed slightly less sensitivity as indicated by IC50 at 12.85 mM (Figure 5.2). Although the value of stem cell model has been comparable with HepG2 IC50 at 12.34 mM (Kostrubsky *et al*, 2005; Wang *et al*, 2002; Li *et al*, 2013), the cell culture company Reinnervate did not observe IC50 even above 20 mM after 24 hours of drug exposure in HepG2 (application note: Toxicity assessment using HepG2 liver cell lines; www.reinnervate.com). Therefore it proves that our hESC – hepatocytes are potentially still a better model to study the sensitivity of drugs than cancer-derived models.

In order to test the hypothesis that stem cell –derived hepatocyte susceptibility to APAP overdose could be regulated by microRNAs, synthetic RNAs were introduced in to the cells by lipophilic based transfection. hESC - hepatocytes transfected with Cy3-labelled precursors and Cy3-labelled antagomirs at 50nM concentration displayed efficient levels of transfection at miR/lipofectamine ratios 1:3 and 1:2 respectively (Figure 5.3). It is assumed that higher amount of lipofectamine was required for efficient precursors transfection as the oligonucleotides were long (~70nt) and double-stranded, whereas antagomirs were short (~23 nt) and single-stranded. In addition, transfection with precursors/antagomirs of well-known liver microRNAs (miR-122 and miR-483) demonstrated that transfection at both ratios did not affect cell viability, proving that lipofectamine did not induce any cytotoxic effect *per se* (Figure 5.4).

Following optimisation, hESC-derived hepatocytes were transfected with appropriate microRNA precursors and inhibitors for 24 hours in order to examine whether oligonucleotides had any direct effect on mRNA transcript changes in the enzymes of interest. As demonstrated in Figure 5.5 and Figure 5.6, neither precursor nor antagomir had any effect on GSTT1 transcript. There are two potential suggestions for it. First, the 50 nM concentration of the oligonucleotides could have been too low to stimulate changes in this enzymes, and therefore further studies are required to examine whether higher concentrations of these molecules would be effective. Secondly, the level of miR-24/GSTT1 interaction, indicated by 7merM8 'seed' match (see Chapter 4 for details) was less effective than for other interactions studied in this project, therefore more specific binding should be taken into consideration when analysing results on TargetScan. What is more, Swart and Dandara (2014) demonstrated that neither of the computational algorithms used in their study confirmed the results of miR-631/SULT1A1 interaction reported by Yu *et al* in 2010, therefore proving that better tools for microRNA/gene binding specificity should be developed. Contrary to miR-24/GSTT1 interaction, transfection with either precursor or antagomir of miR-148a significantly downregulated or upregulated UGT1A1 mRNA respectively, therefore suggesting that the miR is involved in mRNA degradation of this enzyme.

Apart of high level of binding (‘seed’ match - 8mer), the same microRNA has been demonstrated to regulate the activity of PXR transcription factor (Takagi *et al*, 2008) that also controls the activity of UGT1A1. Therefore, it is suggested that one microRNA may interact with similar genes that have similar metabolic functions. hESC - derived hepatocytes transfected with the inhibitor of miR-324-5p demonstrated a significant increase in SULT2A1 transcripts, potentially suggesting high and valid interaction between this particular microRNA and target. Similarly to the antagomir, precursor 324-5p upregulated the gene transcription rather than downregulated as would be expected, therefore further studies are required to understand this phenomenon.

In order to validate qPCR results, examination of protein expression was performed. Immunocytochemistry (Figure 5.7) has revealed that pre miR-24/GSTT1 and pre miR324/SULT2A1 interactions do not decrease protein expression. Protein expression confirms qPCR results for these genes, therefore further studies, especially of Drosha and Dicer mechanisms should be investigated. Although transfection with precursor miR-148a significantly downregulated UGT1A1 gene expression (Figure 5.5), the immunofluorescence did not confirm that (Figure 5.7). Recently, Dluzen *et al* (2014) have reported that next to miR-491-3p, miR-148a was selected as one of the top candidates to target UGT1A1, however luciferase activity assay did not show any repressed luciferase activity *in vitro* in Huh7 cell line. This confirms lack of protein change in our study, however the research group did not examine whether microRNA had any effect on the stability or on the degradation of the mRNA. What is more, the same group has reported that miR-491-3p did not have any effect on UGT1A1 expression in HepG2 cells, probably due to low levels of this enzyme expressed in this line. Therefore, further overexpression of this microRNA had little effect due to already saturating levels of the enzyme. This potentially suggests that ratio of miR/enzyme in the cell is important to exert the inhibitory effect.

In case of antagomirs (Figure 5.10), transfection with miR-24 inhibitor did not upregulate GSST1 protein expression in comparison with scrambled control, what has been confirmed by qPCR results (Figure 5.6), therefore as mentioned before, higher concentrations of oligonucleotides could be required. Although, qPCR results demonstrated that inhibition of miR-148a significantly upregulated UGT1A1 gene expression (Figure 5.6), immunofluorescence demonstrated only increase by 4% in protein expression in comparison with scrambled control (Figure 5.10). This again suggests that UGT1A1 expression could be under post-translational modification**.**

Contrary to other interactions, inhibition of miR-324 resulted in ~ 20% increase in SULT2A1 protein expression, what has been confirmed by qPCR results (Figures 5.6 and 5.10). This may potentially suggest that miR-324 regulates this enzyme not only by inhibiting translation at 3' UTR but may also degrade transcripts by deadenylation process (Djuranovic *et al*, 2012), however further research is required to prove that.

Once the miR/target interactions were examined and validated, stem cell - derived hepatocytes were transfected with precursors and inhibitors of microRNAs for 24 hours and subsequently exposed to paracetamol IC50 concentration for another 24 hours. This allowed to examine whether modulation of particular enzymes by specific microRNAs was sufficient to rescue cells from toxic effects of this drug. Despite the differences in gene and protein expression, transfection with precursors for all three enzymes demonstrated reduced cell viability and glutathione production (Figures 5.8 and 5.9) after exposure to paracetamol. Although the result was expected, investigation of other mechanisms that may interfere with ATP production and oxidative stress should be examined. Figure 5.11 and Figure 5.12 demonstrate that only inhibition of miR-324 resulted in significant increase in cell viability and glutathione reduction after paracetamol exposure. This potentially suggests that inhibition of this microRNA, promotes 'switch' from toxic pathway to non-toxic pathway by increasing levels of SULT2A1, hence rescuing cells from death and decreasing oxidative stress.

The (initial) positive results with antagomir 324 against SULT2A1 pushed us to examine whether inhibition of this microRNA would increase cell viability after exposure to the sera of paracetamol-poisoned patients. Figure 5.13 and Figure 5.14 demonstrate that the antagomir of miR 324 increased not only cell viability but also caspase 3/7 activity after exposure to Patient 1 and Patient 58 sera in comparison with scrambled control. As necrosis (metabolic perturbation with ATP depletion) and apoptosis (execution of ATP-dependant death program via caspases) represent an alternate outcomes of the same cellular pathways (through mitochondrial permeabilization), there has been a lot of controversies whether APAP-induced liver injury is caused by first or the second death mechanism (Bechmann *et al*, 2008; Kon *et al*, 2004; Ray *et al*, 1996; El Hassan *et al*, 2003; Gujral *et al*, 2002). As necrosis process is still considered as the dominant mechanism induced in paracetamol cytotoxicity, higher amount of ATP and caspase 3/7 activity in this study suggests 'switch' from necrosis to apoptosis, indicating slower cell death. To further confirm that, Malhi *et al* (2006) have reported that apoptosis may develop in damaged cells that survive the injurious stresses that would otherwise cause necrotic cell death effect. Contrary to Patient 1 and Patient 58, transfection with the miR-324 inhibitor followed by exposure to Patient 8 serum had no effect on cell survival and increase in apoptosis, therefore further analysis of the individual profiles of these females is required to identify potential factors affecting these differences.

In conclusion, it was demonstrated that stem cell based models are essential to developing a better understanding of human drug metabolism and its regulation. In this study, it has been demonstrated that a novel miR inhibitor, antagomir to miR-324, plays a major role in the regulation of phase II enzyme SULT2A1 in the context of acute paracetamol injury and fulminant plasma from overdose patients. Notably, inhibition of this microRNA led to an increase in SULT2A1 expression, improving cell survival, reducing glutathione depletion and ultimately cell necrosis. These findings offer a serious promise to reduce the toxic effects of paracetamol overdose. What is more, these findings are novel and provide proof of concept, exemplifying the power of stem cell based models to identify new approaches to treating human liver damage.

CHAPTER SIX

GENERAL CONCLUSIONS AND PERSPECTIVES

6.1 DISCUSSION

6.1.1 IMPROVEMENT OF CURRENT *IN VITRO* MODELS IN DILI STUDIES

Drug – induced liver injury (DILI) is currently a major concern as it is not predictable from pre-clinical safety assessment studies due to lack of predictive models (Williams *et al*, 2012). Despite extensive work, up to date there is no universally accepted biomarker for DILI and *in vivo* systems often fail to predict serious cases of DILI caused by both intrinsic (predictive) and idiosyncratic (unpredicted) reactions occurred in man. Therefore it is required to improve an understanding of DILI mechanism that will allow to design drugs that have low risk of causing potential adverse drug reactions in the patient population. Currently, due to concerns about poor performance and animal welfare, *in vitro* hepatocyte models have been in demand. What is more, *in vitro* models have enabled investigation of many chemicals entities in short time frame. Contrary to standard hepatic models (e.g primary hepatocytes, cancer-derived cell lines), pluripotent stem cells have opened new opportunities to obtain unlimited amount of genetically defined hepatocytes. Although promising, most of the stem cell-derived hepatic cells are cultured in serum - and xeno - containing conditions that limit their scale up and application. Therefore, current research in the stem cell field is focused on developing *in vitro* systems that are defined and are derived to clinical grade.

During my project, I have established an efficient and serum-free protocol to successfully differentiate pluripotent stem cells to hepatocytes (Szkolnicka *et al*, 2014; Szkolnicka *et al*, 2014b). In this project (Chapter 3), I have been able to use this procedure to differentiate human embryonic stem cells (hESCs), including hESC lines that were derived under GMP standards, as well as human induced pluripotent stem cells. What is more, recent publications demonstrated that our hepatic model is scalable, shippable and can be successfully used to study drug toxicity and virus-host interactions in line with current gold standards (Medine *et al*, 2013; Szkolnicka *et al*, 2014a, Szkolnicka *et al*, 2014b, Zhou *et al*, 2014).

In regards to advanced drug toxicity studies in 2D models, recent research has been focused on developing *in vitro* assays not only to model intrinsic but idiosyncratic drug-induced liver injury (DILI). Derivation of hepatocytes from functional induced pluripotent stem cells of patients who develop DILI could allow study of idiosyncratic reactions in DILI - affected patients compared with treated controls (Jozefczuk *et al*, 2011; Fontana, 2014). What is more, Faulkner *et al* (2012) have expanded T cells (in the presence of dendritic cells) *in vitro* from peripheral blood of patients with allergic drug reactions. As antigens are presented on HLA molecules of antigen – presenting cells to the T cell receptors, additional studies of T cell physiology could be conducted. Such studies would allow studying drug hypersensitivity (e.g T cell proliferation, T cell change from 'naïve' to 'memory' type, cytokine production) in individuals in more depth.

Although two dimensional hepatic assays have been efficient, they still demonstrate low cellular polarity, diffused liver zonation or limited utility under standard culture conditions for certain types of toxicity testing. In order to overcome these issues and mimic native tissue architecture, stem cell field has been focused on the development of new *in vitro* platforms such as 3D culture/tissue models and microfluidic systems. Much research has been focused on the development of natural and synthetic 3D scaffolds (Hay *et al*, 2011; Skardal *et al*, 2012; Lucendo – Villarin *et al*, 2014), where cells have ability to proliferate, migrate and properly differentiate in order to regain phenotypic stability and all necessary metabolic functions. Recently, it has been demonstrated that the use of defined biopolymer substrate in conjunction with serum-free hepatic differentiation, revealed a unique gene signature (MMP13, CTNND2, and THBS2) that predicts stable hepatocyte performance (Lucendo – Villarin *et al*, 2015). Therefore, this and future similar studies may identify gold standard parameters for somatic cell quality control. Use of different matrices and addition of scaffolds has paved the way for more advanced co-culture systems, where human cells are composed of two to three primary cell types (Khetani and Bhatia, 2008; Ishii *et al*, 2010; Tuleuova *et al*, 2010; Enosawa *et al*, 2011; Takebe *et al*, 2013; Ware *et al*, 2015).

Although co – culture models allow to mimic *in vivo* environment and intercellular signalling, a lot of these models do not contain the appropriate proportions of supporting cells to resemble the whole liver. What is more, development of different synthetic scaffolds to hold cells together may introduce nonhuman and non-native aspect to the system what may effect drug toxicity assessment in the future (Visk, 2015). In order to overcome issues connected with application of foreign materials, much focus has been on self-forming hepatocyte spheroids, often called hepatospheres. It has been reported that contrary to 2D models, 3D spheroids either of primary cells or stem cell – derived hepatocytes prolonged the expression of phase I enzymes such as CYP1A1, CYP1A2, CYP2B9, CYP2B10 (Nemoto and Sakurai, 1992; Nemoto *et al*, 1995; Shen *et al*, 2006), phase II UGT1A1, NNMT (Gieseck III *et al*, 2014) and were more sensitive to acetaminophen-induced hepatotoxicity (Du *et al*, 2006). Although hepatospheres have been considered to hold a great promise as an *in vitro* system, optimisation of their size and oxygen/nutrition diffusion is still required. These issues have been recently approached by incorporation of fluid flow devices (microfluidics) such as HuREL® Biochip (Chao *et al*, 2009), Hollow – Fibre Reactor (Shmelzer *et al*, 2009) or Single – and Multi – Well Perfused Bioreactor (Sivaraman *et al*, 2005) that mimic blood flow, shear stress and supply cells with appropriate amounts of oxygen and nutrition. A more recent approach to generate 3D systems involves bioprinting, a method that allows for automated production of structures composed of living cells that possess critical attributes of specific tissue. Bioprinted 3D models such as Organovo's exVive3D liver tissue (Organovo®; USA) recently has been reported to secrete fibrinogen, albumin and transferrin proportional to levels in whole liver and demonstrate *in vivo*-like responses to acetaminophen, ethanol or diclofenac (Visk, 2015). Three - dimensional bioprinting holds a great promise to fill the gaps between lead optimization and drug discovery phases, however use of this method is still fairly premature and therefore further developments are required.

Although efficient 2D and 3D models have been established for accurate drug toxicity prediction or future cell –based therapies, the large variability has been reported both on markers expression and key enzymes activities in PSC-derived hepatocytes. Such differences limit the application of these cells in safety pharmacology and toxicology assessment.

One of the reason for it is lack of agreed endpoints of hepatic differentiation and maturation along with lack of standardized comparators for differentiated PSC-derived hepatocytes (Kia *et al*, 2012; Wobus and Loser, 2011). Recently, it has been demonstrated that the degree of 'hepatic differentiation' is controversial and needs further studies. Godoy *et al* (2015) genome - wide study has demonstrated that hepatocytes derived from human embryonic and induced pluripotent stem cells *in vitro* possess high expression of colon-associated transcriptional factors (e.g KLF5, CDX2, NKX2), colon – enriched genes (e.g MEP1A, CDH17) and fibroblast – enriched genes (e.g TWIST1 and SNAIL2). Therefore, it has been suggested that in order to further differentiate PSC-derived hepatocytes to pure mature populations, suppression of factors responsible for colon development and hepatic dedifferentiation is required. Such whole-genome analysis would open new opportunities to understand the transcriptional regulatory networks controlling the differentiation program, and would potentially eliminate 'unwanted' genes both in 2D and 3D systems. What is more, Avior *et al* (2015) studies demonstrated that looking at liver *per se* may not be sufficient to find answers on how to drive maturation of drug metabolic enzymes. Research of this group has revealed that vitamin K_2 and litocholic acid, that is the byproduct of intestinal flora, stimulate the activity of PXR transcription factor that controls CYP3A4 and CYP2C9 expression in hPSC-derived hepatocytes. Avior *et al* studies demonstrated that microbial-derived cues were responsible for maturing cytochromes post-partum, and therefore future focus should be both on liver development and gut colonization.

6.1.2 PHARMACOGENOMICS OF PARACETAMOL

In this project (Chapter 4), hepatocytes derived from hESCs under serum-free conditions displayed comparable expression of metabolic enzymes and transporters to human primary hepatocytes. The major focus was on SULT2A1, SULT1A1, UGT1A1, GSTT1 and GSTP1 enzymes as these play an essential role in paracetamol metabolism. Although our *in vitro* model along with other stem cell systems reported previously (McGill *et al*, 2011; Gunnes *et al*, 2013; Sengupta *et al*, 2014, Ware *et al*, 2015) demonstrate a promising platform to study APAP-induced hepatotoxicity, recent studies call to focus on pharmacogenomics of paracetamol and ontogenesis of the regulatory pathways (Krasniak *et al*, 2014). A various number of research groups have reported that APAP pharmacokinetics (PK) and pharmacodynamics (PD) may widely differ between individuals and populations. Zuppa *et al* (2011) have reported that APAP PK varies with age from birth to adulthood. The authors have reported that the clearance (L/hr) of APAP increased two fold at 1 year of age (~4.09 L/hr) in comparison with 1 month old (~2.02 L/hr), whereas adolescent demonstrated the drug clearance at ~14.27 L/hr. Such differences are inseparably connected with various levels of metabolic enzymes in different age populations. Vieira *et al* (1996) analysed more than 238 livers, and discovered that CYP2E1 expression was increasing within the age (neonate < infant < child). Various levels of CYP2E1 would explain why younger infants have a decreased risk of paracetamol hepatotoxicity. What is more, it has been demonstrated that ethnicity may influence the cytochrome expression. Johnsrud *et al* (2003) have reported that CYP2E1 protein expression was higher in Northern European – Americans and Hispanic – Americans than in African – Americans. In case of phase II enzymes, glutathione S - transferases (GST) and UDP-glucuronosyltransferases (UGT) have also been reported to increase within the age (Strassburg *et al*, 2002; Zuppa *et al*, 2011). Although some papers (Grijalva *et al*, 2013; Levy *et al*, 1975) have reported that up to age of 9 paracetamol sulfate is the major metabolite, Zuppa *et al* (2011) reported that APAP – sulfation is likely constant among ages (28 days to > 12 years of age). Such information may be favourable in the context of studying SULT2A1 regulation in this project as Ant -324 -5p may be effective in all age populations, therefore acting as a universal therapeutic in the future.

Except of PK and PD of APAP, polymorphism of metabolic genes and microRNAs that regulate their expression should be taken into consideration (often referred to as miRSNPs). It has been reported that genetic variations of 3'UTR of CYP1A2, CYP2B6, CYP2E1, PXR, UGT1A1, and UGT2B7 (Hu *et al*, 1997; Matimba *et al*, 2009; Warnich *et al*, 2011; Wei *et al*, 2012; Dandara *et al*, 2014; Court *et al*, 2013; Swart and Dandara, 2014) as well as SNPs in microRNAs *per se* may interfere with miR-mRNA interactions, therefore influencing capacity of an individual to properly metabolise and excrete drugs, including paracetamol.

Although pharmacogenomic data is very useful in predicting potential effects of APAP on metabolic genes in individuals, inflammatory responses have recently been taken into consideration when preventing hepatotoxicity. Garcia *et al* (2014) injected female Balb/c mice with Freund Complete Adjuvant (FCA) and boosted with Freund's Incomplete Adjuvant (FIA) before administering a toxic dose (360 mg/kg) of paracetamol for three days. Injection of adjuvants resulted in an increase in pro-inflammatory cytokines, α- 1- acid glycoprotein, lactate dehydrogenase and reduced CYP2E1 enzyme that is primarily responsible for producing hepatotoxic metabolite (NAPQI). Although the study revealed that inflammatory responses could decrease hepatotoxicity caused by paracetamol, the phenomenon is very complex due to potential activation of Kupffer cells or other immune-mediated molecular pathways that may cause overall tissue injury. Therefore, further research of this aspect is required.

In the context of developing new reliable stem cell derived *in vitro* models for drug toxicity assays, it is essential to study large number of stem cells derived from individuals where age, ethnicity, microbiome and immune mechanisms are examined in more details.

6.1.3 IMPROVEMENT OF MICRORNA TARGET IDENTIFICATION

In the last two chapters of this project (Chapter 4 and 5), I identified three potential microRNAs (miR-24, miR-148a, miR-324) that bind to specific targets of phase II drug metabolism (GSTT1, UGT1A1, and SULT2A1). Further investigation using precursors and antagomirs allowed us to discover that inhibition of miR-324 may potentially regulate SULT2A1 enzyme at both gene and protein expression and significantly decrease APAP-induced toxicity in hESC – derived hepatocytes. Although the results have been promising in *in vitro* system, there are couple of aspects that should be taken into consideration in the future. Firstly, examination of the function of antagomir for miR -324 (Ant-324) *in vivo* would be very useful to further confirm the effects of this microRNA in more complex systems. Since, miR-324-5p has been conserved in most of the species (based on miRBase; gene family ID: MIPF0000165), inhibition of this non-coding RNA for instance in APAP-injured mice would give additional information on its precise location (using fluorescence *in situ* hybridization; FISH). Additionally, it would be important to examine whether ALT/AST/bilirubin levels decrease or any changes in the size of mitochondria are observed.

In this project, TargetScan Human 6.2 has been used to identify miR-mRNA interactions as this tool comparing to others (e.g miRanda, PicTar, Diana-microT, PITA) is highly precise and sensitive (Witkos *et al*, 2011) However, it has been reported that due to our poor understanding of miR - mRNA interactions beyond 'seed' pairing, the prediction of most of the current algorithms have low sensitivity and specificity what in a results creates ~ 40% of false-positives (Zampetaki and Mayr, 2012; Swart and Dandara, 2014). Therefore, all potential miR - mRNA interactions should be confirmed by functional validation. Recent experimental strategies to identify direct miRNA targets include use of microRNA precursors/antagomirs and luciferase – based assays. Although these methods are very useful, they are based on the hypothesis that reduced protein synthesis by microRNAs is the destabilization of target mRNAs.

Unfortunately, microRNAs and mRNAs levels not always correlate, therefore detecting changes at the messenger level to predict microRNA targets is not always reliable. In order to overcome these problems, new high- throughput methods have been developed such as Labelled miRNA Pull-Down (LAMP) Assay, High – Throughput Sequencing by Cross – Linking and Immunoprecipitation (HITS-CLIP), Cell-Based Cross-Linking and Immunoprecipitation (CLIP), and Immunoprecipitation of Tagged Components of the RISC Complex (RISC-IP) (Zampetaki and Mayr, 2012).

Since microRNAs not only regulate their target by mRNA degradation but by protein translation, study of proteomics should be essential. Methods such as use of pulsed stable isotope labelling by amino acids (pSILAC) in cell culture may help to identify newly synthesized proteins that are pulsed-labelled with different isotopes of amino acids from the already existing ones (Zampetaki and Mayr, 2012).

What is more, studies have also proven that different chemical designs of microRNA inhibitors may demonstrate inconsistencies in the results, therefore use of different types of inhibitors (e.g locked nucleic acid or 2'-O'-methyl nucleotides) should be examined.

6.1.4 CONCLUSION

The studies demonstrate that hESC – derived hepatocytes are a useful tool to dissect the effects of miRs on gene regulation. These studies are enabling and may have significant translational potential.

SUPPLEMENTARY FIGURES AND TABLES

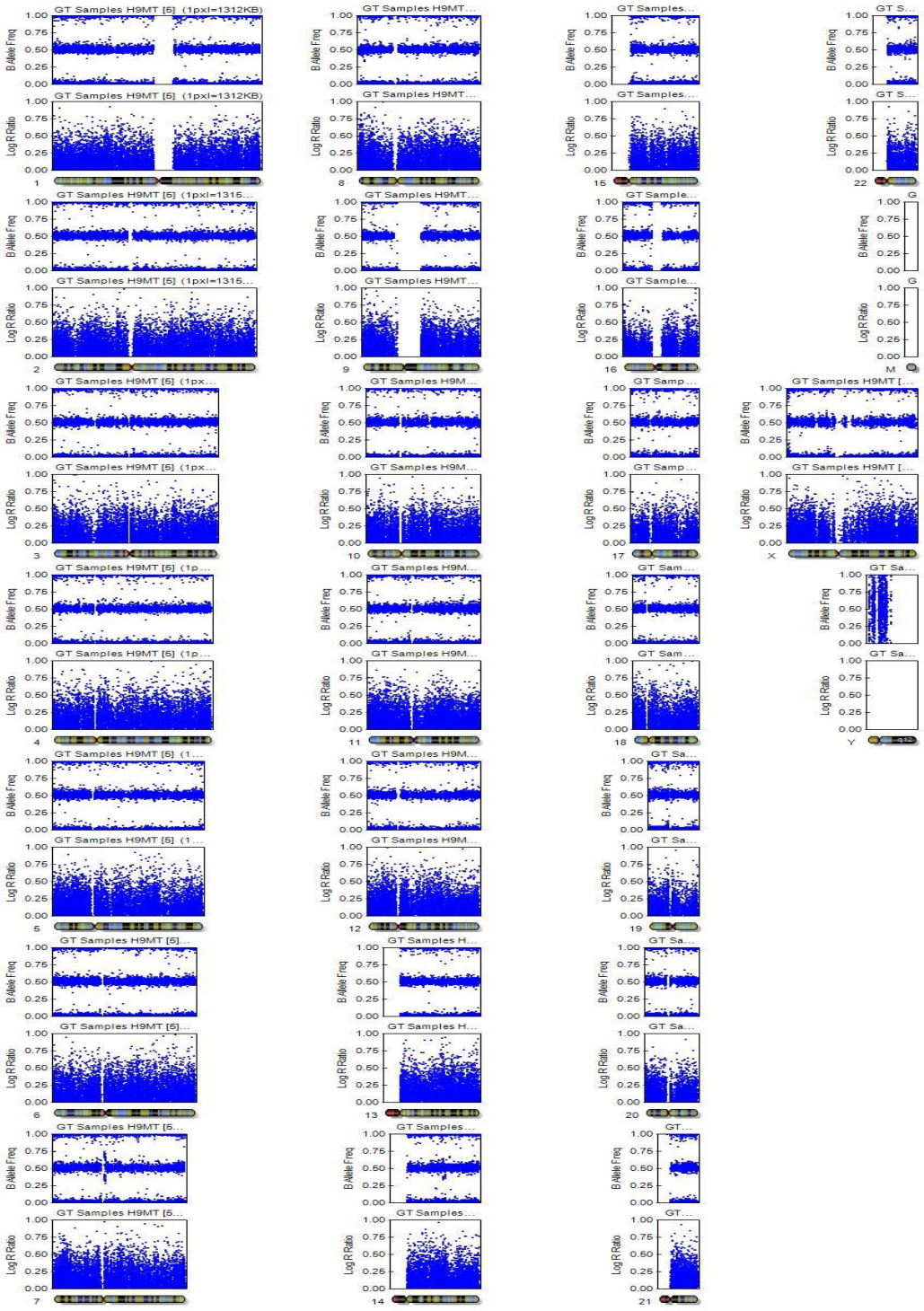

Supplementary Figure 1.1: SNP analysis of H9 cell line cultured in MT. The analysis was done using Illumina GenomeViewer software. Abbreviations: SNP, single nucleotide polymorphism; MT, mTeSR1.

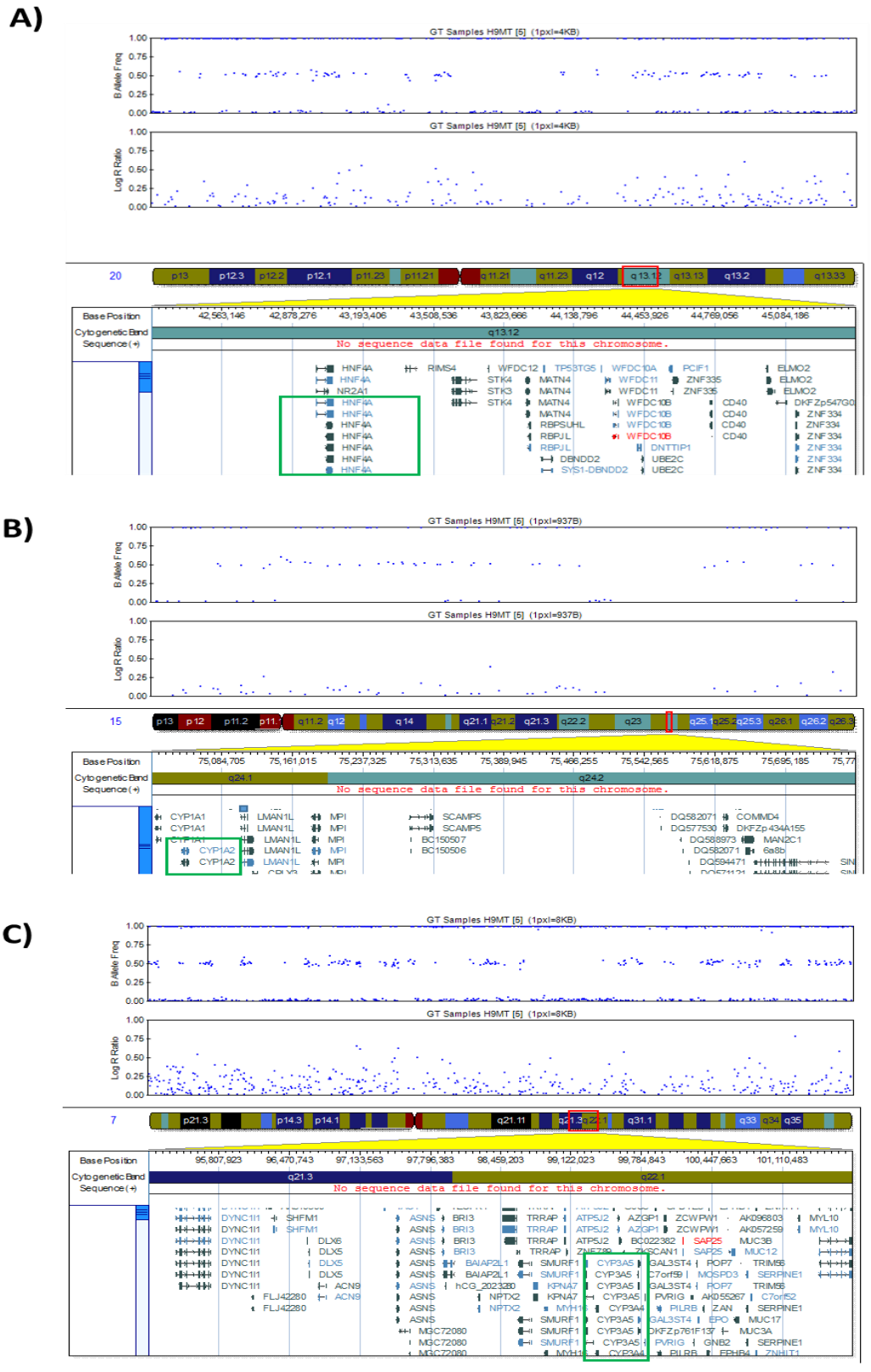

Supplementary Figure 1.2: SNP analysis of HN4a (A), CYP1A2 (B), and CYP3A4 (C) in H9 cell line cultured in MT. SNPs were analysed by Illumina GenomeViewer software. Abbreviations: SNP, single nucleotide polymorphism; HNF4a, hepatic nuclear factor 4a; CYP3A4/CYP1A2, cytochrome P450 3A4 and 1A2; MT, mTeSR1.

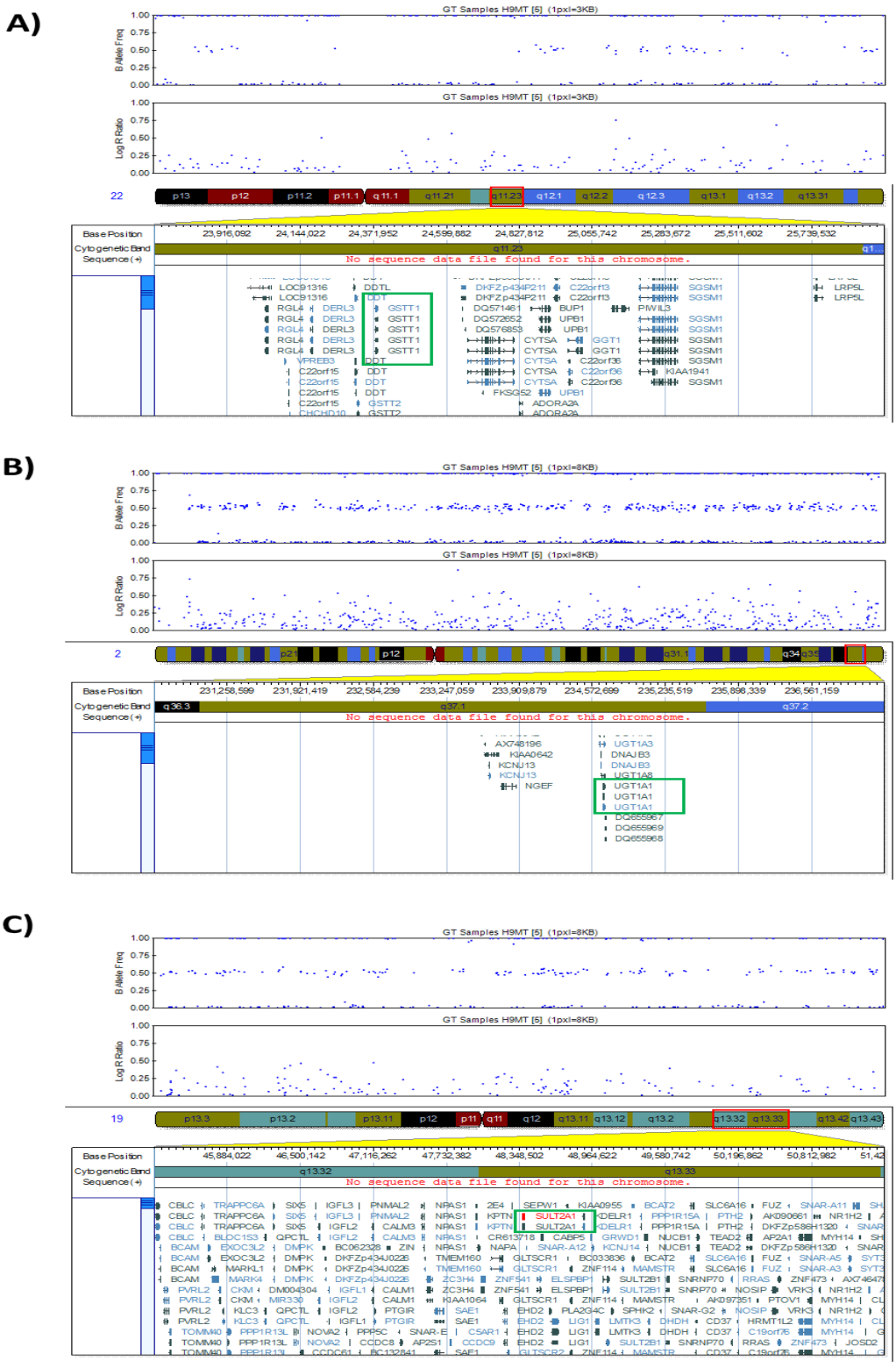

Supplementary Figure 1.3: SNP analysis of GSTT1 (A), UGT1A1 (B), and SULT2A1(C) in H9 cell line cultured in MT. SNPs were analysed by Illumina GenomeViewer software. Abbreviations: SNP, single nucleotide polymorphism; GSTT1, glutathione S-transferase; UGT1A1, UDP-glucuronosyltransferase 1A1; SULT2A1, sulfotransferase 2A1; MT, mTeSR1.

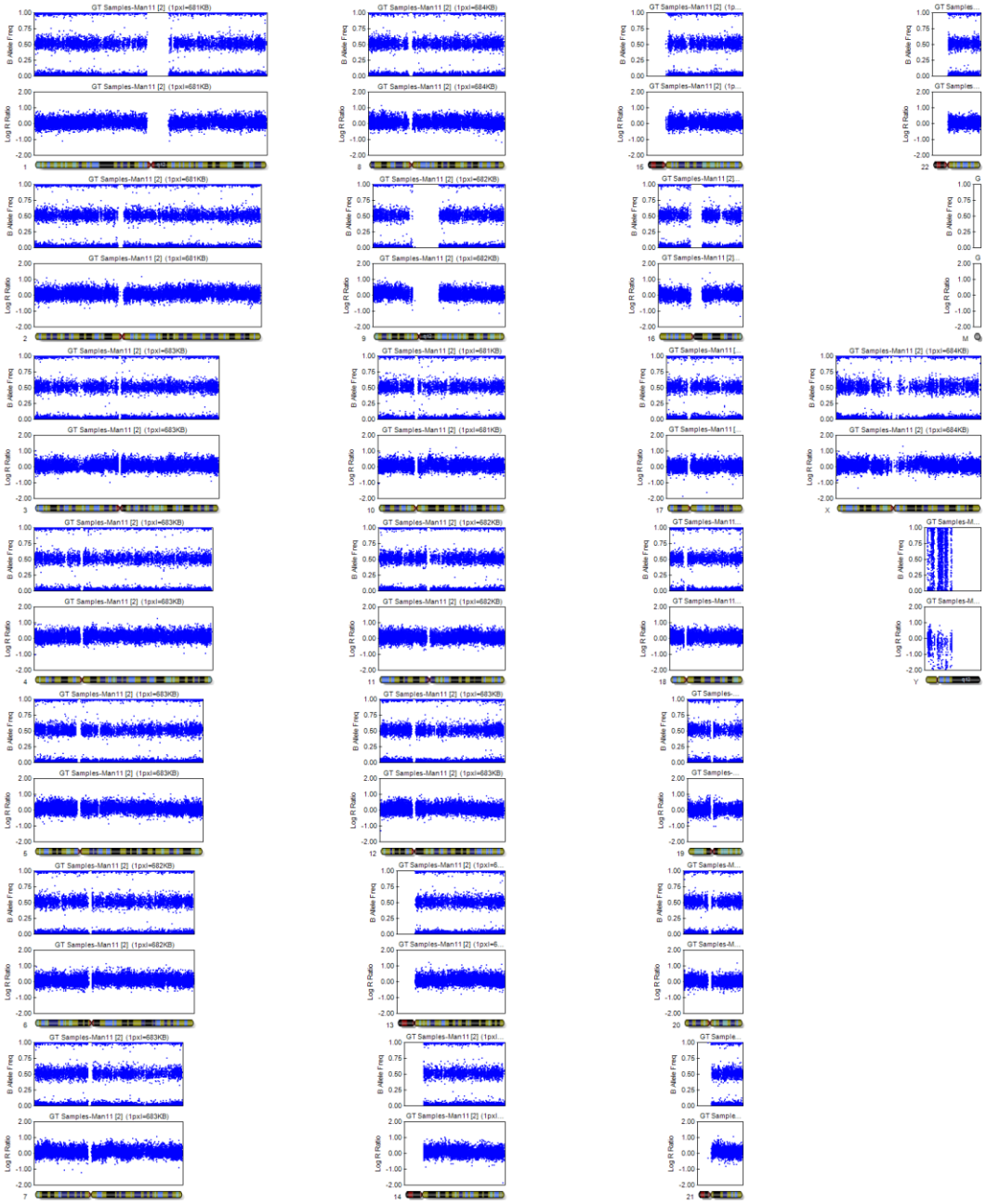

Supplementary Figure 1.4: SNP analysis of MAN11 cell line cultured in MT. The analysis was done using Illumina GenomeViewer software. Abbreviations: SNP, single nucleotide polymorphism; MT, mTeSR1.

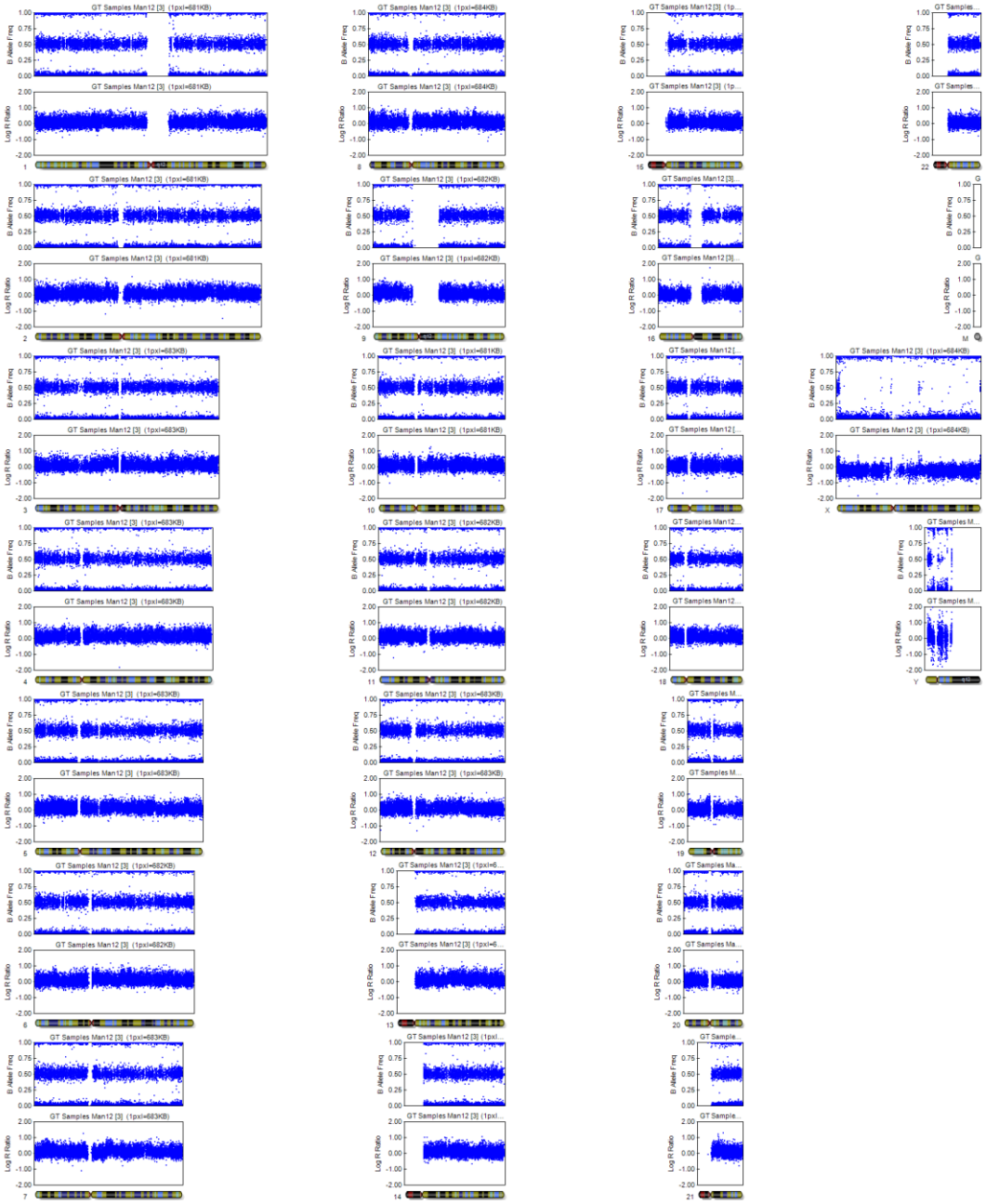

Supplementary Figure 1.5: SNP analysis of MAN12 cell line cultured in MT. The analysis was done using Illumina GenomeViewer software. Abbreviations: SNP, single nucleotide polymorphism; MT, mTeSR1.

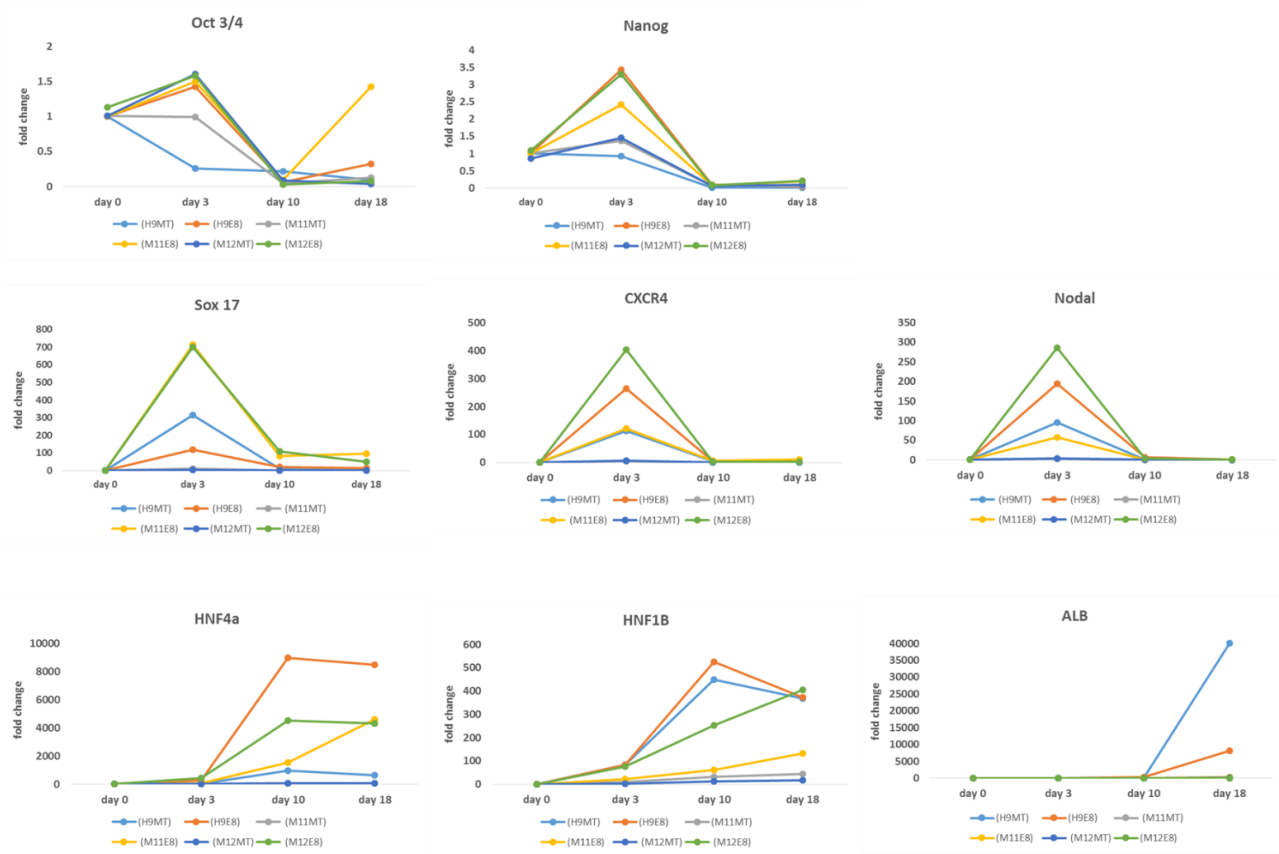

Supplementary Figure 1.6: Gene expression of selected markers at different stages of hepatic differentiation (hESCs in MT and E8). Genes were normalised to housekeeping gene GAPDH and relatively to day 0. Abbreviations: MT, mTeSR1; E8, Essential 8; Oct 3 / 4, Octamer 3 / 4; Sox17, SRY-determining region Y; CXCR4, chemokine CXC motif receptor 4; HNF4a/HNF1B, hepatic nuclear factor 4a/1B; ALB, albumin.

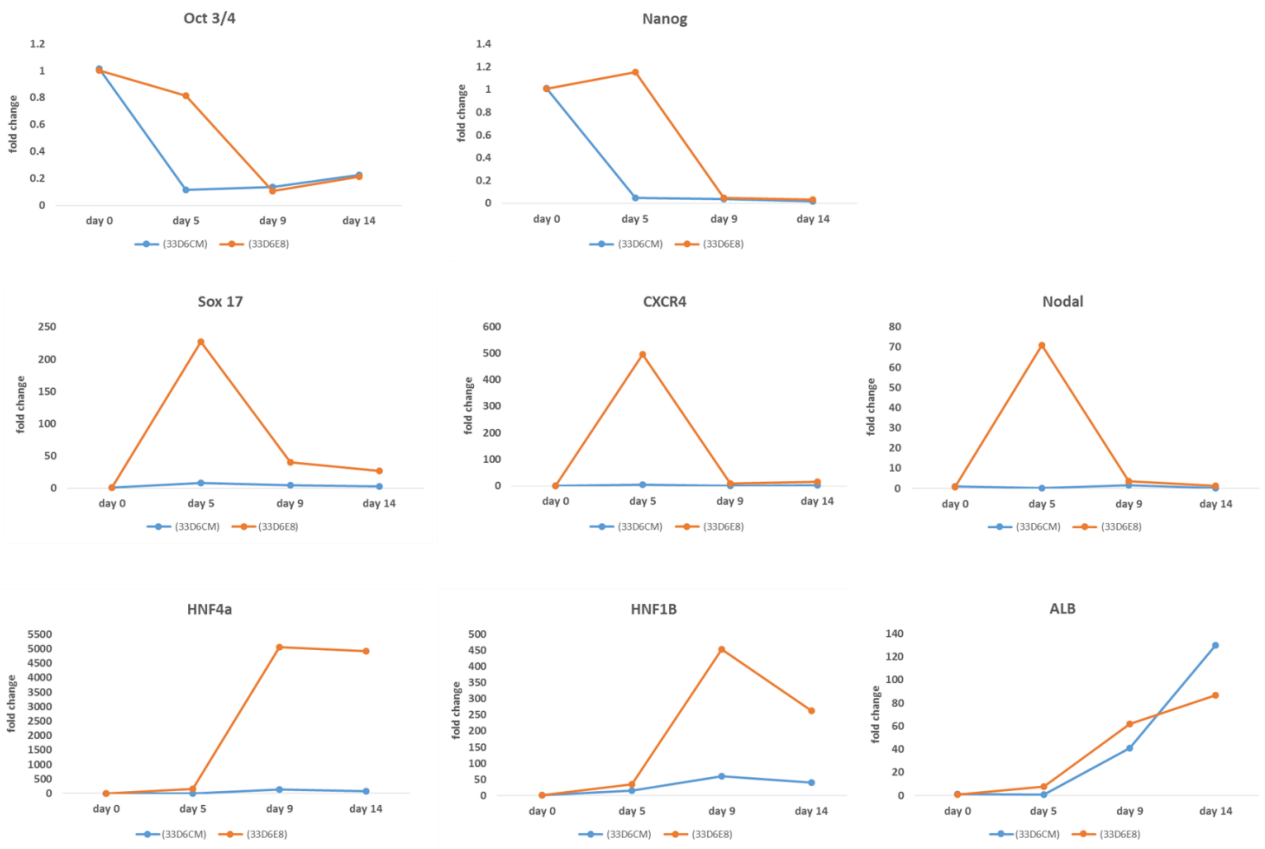

Supplementary Figure 1.7: Gene expression of selected markers at different stages of hepatic differentiation (hiPSCs in CM and E8). Genes were normalised to housekeeping gene GAPDH and relatively to day 0. Abbreviations: CM, Conditioned Medium; E8, Essential 8; Oct 3 / 4, Octamer 3 / 4; Sox17, SRY-determining region Y; CXCR4, chemokine CXC motif receptor 4; HNF4a/HNF1B, hepatic nuclear factor 4a/1B; ALB, albumin.

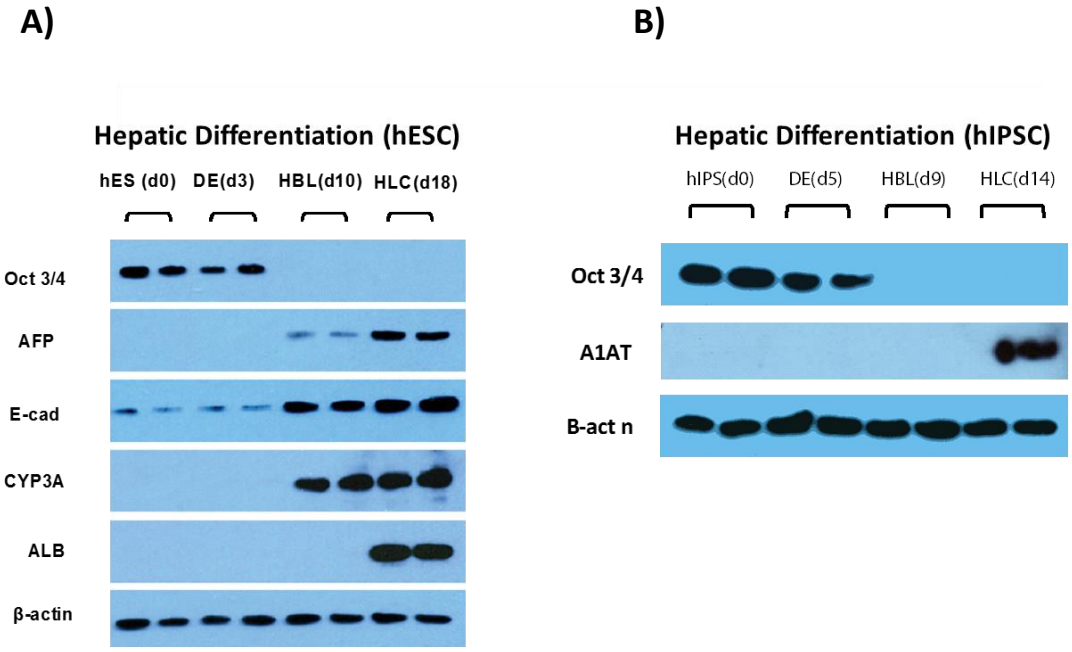

Supplementary Figure 1.8: Protein expression assessed by Western blots. Western blots demonstrate protein expression of appropriate markers at each stage of hESC (H9) (A) and hiPSC (33D6) (B) hepatic differentiation. Abbreviations: Oct 3/4, Octamer 3/4; AFP, α-fetoprotein; E-cad, E-cadherin; CYP3A, cytochrome P450 3A; ALB, albumin; A1AT, α1-antitrypsin; hESC/hIPSC, human embryonic/human induced pluripotent cell.

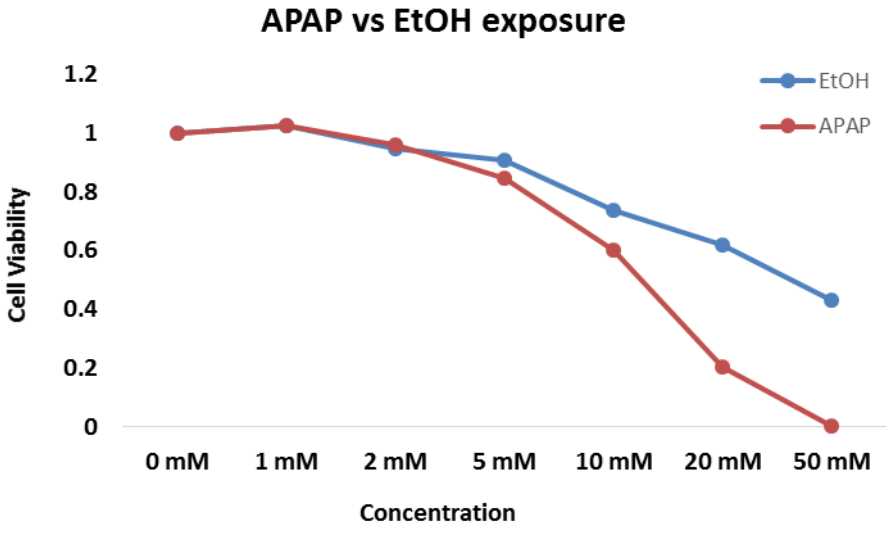

Supplementary Figure 1.9: APAP/EtOH *in vitro* toxicity in stem cell- derived hepatocytes. APAP was more toxic to cells than EtOH. At day 17, hESC-hepatocytes were induced with different concentrations of APAP (0-50 mM) and Ethanol (vehicle control) for 24 hours. The CellTitre- Glo® Luminescent Cell Viability Assay (Promega) was used to measure the ATP levels.The graph represents fold change in cell viability. Abbreviations: APAP, Acetaminophen (Paracetamol); EtOH, Ethanol.

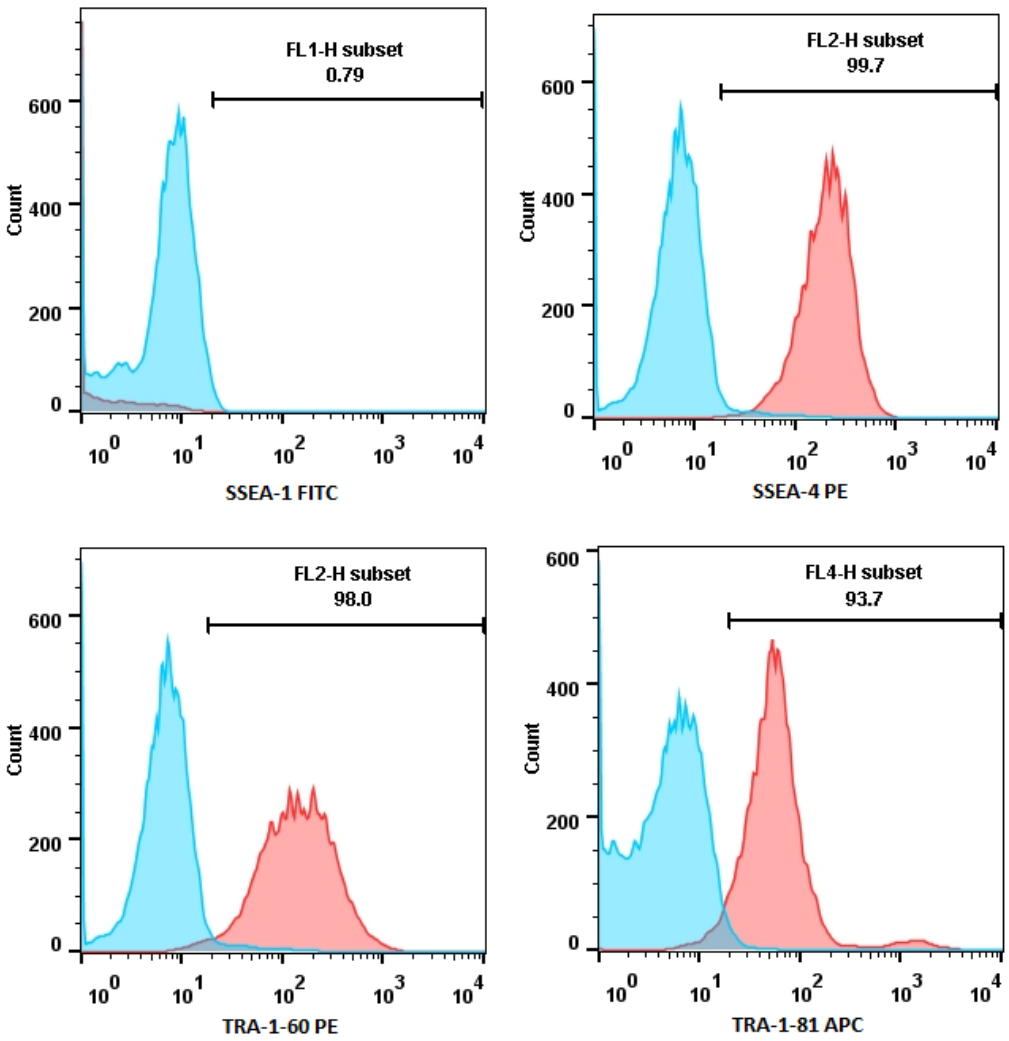

Supplementary Figure 1.10: Surface marker expression of hESC (H9) cultured in MT medium. The histograms demonstrate hESC surface marker expression levels as expected, including stage specific embryonic antigens (SSEA) and tumour rejection antigens (Tra). The marker of differentiation SSEA1 was expressed at 0.79%, whereas the pluripotency markers SSEA4, Tra-1-60 and Tra-1-81 were expressed at 99.7%, 98%, and 93.7% respectively. The blue colour indicates unstained cells and the red colour represents stained cells with particular fluochrome-conjugated antibodies.

A)

CELL LINE (MEDIUM)	AFP FOLD CHANGE OVER A TIME COURSE (NORMALISED TO B2M AND DAY0)			
	DAY 0	**DAY 3**	**DAY 10**	**DAY 18**
H9 (MT)	1.00	0.17	170523.3	41633.41
H9 (E8)	1.20	1.26	88282.83	16540.69
MAN 11(MT)	1.00	0.17	11473.98	6742.89
MAN 11 (E8)	1.00	1.38	3880.68	964.57
MAN 12 (MT)	0.93	2.24	15926.52	12346.79
MAN 12 (E8)	0.88	0.77	58835.32	13211.28
	DAY 0	**DAY 5**	**DAY 9**	**DAY 14**
33D6 (CM)	1.00	0.26	123.71	526.68
33D6 (E8)	0.60	7.77	10115.78	274675.1

B)

CELL LINE (MEDIUM)	E-CADHERIN FOLD CHANGE OVER A TIME COURSE (NORMALISED TO B2M AND DAY0)			
	DAY 0	**DAY 3**	**DAY 10**	**DAY 18**
H9 (MT)	0.03	0.01	0.80	0.03
H9 (E8)	1.00	0.45	1.95	1.53
MAN 11(MT)	1.00	0.49	2.63	1.25
MAN 11 (E8)	1.02	0.33	4.44	2.29
MAN 12 (MT)	1.00	2.28	8.94	2.55
MAN 12 (E8)	1.05	0.15	0.73	1.47
	DAY 0	**DAY 5**	**DAY 9**	**DAY 14**
33D6 (CM)	1.00	0.35	0.13	0.24
33d6 (E8)	1.05	0.54	1.07	3.01

Supplementary Table 1.1: Gene expression of AFP (A) and Ecad (B) at different stages of hESC and hiPSC differentiation. Gene expression was measured using qPCR and normalised to housekeeping gene B2M and relatively to day 0. Abbreviations: AFP, α – fetoprotein; Ecad, E-cadherin; B2M, Beta -2- Microglobulin; MT, mTeSR1; E8, Essential 8.

RT² PROFILER PCR ARRAY - Human Drug Metabolism Phase I (QIAGEN; PAHS-002Z)						
Gene Symbol	AVG ΔCt		2^ - ΔCt		Fold Change	Fold Up – or Down-Regulation
	Group1 (HLC)	Control Group (PHH)	Group1 (HLC)	Control Group (PHH)	Group 1/ Control	Group 1/ Control
CYP1A1	0.38	7.02	0.768483	0.007705	99.74	99.74
ADH4	4.08	6.10	0.059302	0.014562	4.07	4.07
ADH5	1.01	2.39	0.495439	0.190431	2.60	2.60
EPHX1	1.64	1.52	0.321538	0.347956	0.92	-1.08
ADH6	4.78	3.34	0.036387	0.098713	0.37	-2.71
ALDH1A1	0.45	-0.45	0.729565	1.363349	0.54	-1.87
CYPB5R	0.65	-0.38	0.636322	1.303635	0.49	-2.05
CYP2B6	7.46	6.75	0.005694	0.009309	0.61	-1.63
CYP3A5	2.01	-1.18	0.248204	2.272074	0.11	-9.15
CYP2J2	6.06	1.98	0.015040	0.252693	0.06	-16.80
CYP2C8	6.76	0.63	0.009224	0.647110	0.01	-70.16
CYP2C9	7.46	-0.49	0.005694	1.402808	0.00	-246.36
CYP3A4	7.46	1.34	0.005694	0.394672	0.01	-69.31
CYP2C19	6.91	2.15	0.008323	0.225670	0.04	-27.11
CYP2D6	7.09	4.56	0.007318	0.042426	0.17	-5.80
CES1	4.46	-1.36	0.045546	2.559360	0.02	-56.19
CES2	4.07	-0.66	0.059552	1.579842	0.04	-26.53
ADH1B	6.89	4.26	0.008442	0.052291	0.16	-6.19
ADH1C	7.46	4.16	0.005694	0.056056	0.10	-9.84

Supplementary Table 1.2: **Phase I drug metabolism (PCR Array).** Fold-Change (2^(- Delta Delta Ct)) is the normalized gene expression (2^(- Delta Ct)) in the Test Sample divided the normalized gene expression (2^(- Delta Ct)) in the Control Sample. Fold-Regulation represents fold-change results in a biologically meaningful way. Fold-change values greater than one indicate a positive- or an up-regulation, and the fold-regulation is equal to the fold-change. Fold-change values less than one indicate a negative or down-regulation, and the fold-regulation is the negative inverse of the fold-change. Up-regulated genes (fold differences larger than a 3 fold threshold) are indicated in red, down-regulated genes (fold differences narrower than 3 fold treshold) are indicated in green. Genes similarly expressed for the Group 1 and Control (fold differences between -3 to +3 boundary) are indicated in black. Abbreviations: HLC, hepatocyte-like-cells; PHH, primary human hepatocytes.

RT² PROFILER PCR ARRAY - Human Drug Metabolism Phase II (QIAGEN; PAHS-069Z)						
Gene Symbol	AVG ΔCt		2^ - ΔCt		Fold Change	Fold Up – or Down-Regulation
	Group1 (HLC)	Control Group (PHH)	Group1 (HLC)	Control Group (PHH)	Group 1/ Control	Group 1/ Control
GSTP1	-0.20	4.85	1.148277	0.034646	33.14	33.14
GSTA1	-0.42	2.08	1.341208	0.236264	5.68	5.68
GSTA4	3.37	6.86	0.096681	0.008588	11.26	11.26
GSTA3	6.20	8.55	0.013622	0.002677	5.09	5.09
SULT1E1	3.85	9.74	0.069583	0.001166	59.66	59.66
SULT1A2	4.37	7.98	0.048511	0.003948	12.29	12.29
SULT1C2	8.20	12.73	0.003411	0.000147	23.14	23.14
SULT1C3	8.20	12.73	0.003411	0.000147	23.14	23.14
SULT1C4	6.63	8.40	0.010075	0.002967	3.40	3.40
NAT 1	9.80	11.43	0.001118	0.000362	3.09	3.09
GSTO1	0.04	0.46	0.971041	0.724547	1.34	1.34
GSTO2	8.00	7.95	0.003893	0.004040	0.96	-1.04
GSTT1	3.47	3.39	0.089944	0.095282	0.94	-1.06
GSTK1	2.45	2.52	0.182812	0.174788	1.05	1.05
GSTM4	6.98	7.30	0.007905	0.006338	1.25	1.25
UGT2B28	2.98	2.15	0.126827	0.225954	0.56	-1.78
UGT3A1	7.78	6.94	0.004559	0.008118	0.56	-1.78
SULT1A1	3.08	3.96	0.117951	0.064148	1.84	1.84
SULT2A1	4.55	3.61	0.042611	0.081891	0.52	-1.92
COMT	2.01	2.76	0.249051	0.147120	1.69	1.69
UGT1A1	6.58	4.83	0.010486	0.035145	0.30	-3.35
UGT1A4	10.39	3.28	0.000746	0.102607	0.01	-137.61
UGT2B4	8.36	3.41	0.003054	0.093826	0.03	-30.73
UGT2B7	3.56	0.83	0.084852	0.564152	0.15	-6.65
UGT2B10	8.65	5.59	0.002489	0.020726	0.12	-8.33
UGT2A3	10.59	4.69	0.000649	0.038640	0.02	-59.49
UGT2B17	10.85	4.95	0.000543	0.032289	0.02	-59.46
NAT2	7.58	5.64	0.005230	0.020051	0.26	-3.83
SULT1B1	8.60	5.59	0.002579	0.020766	0.12	-8.05

Supplementaty Table 1.3: Phase II drug metabolism (PCR Array). Fold-Change (2^(- Delta Delta Ct)) is the normalized gene expression (2^(- Delta Ct)) in the Test Sample divided the normalized gene expression (2^(- Delta Ct)) in the Control Sample. Fold-Regulation represents fold-change results in a biologically meaningful way. Fold-change values greater than one indicate a positive- or an up-regulation, and the fold-regulation is equal to the fold-change. Fold-change values less than one indicate a negative or down-regulation, and the fold-regulation is the negative inverse of the fold-change. Up-regulated genes (fold differences larger than a 3 fold threshold) are indicated in red, down-regulated genes (fold differences narrower than 3 fold treshold) are indicated in green. Genes similarly expressed for the Group 1 and Control (fold differences between -3 to +3 boundary) are indicated in black. Abbreviations: HLC, hepatocyte-like-cells; PHH, primary human hepatocytes.

RT² PROFILER PCR ARRAY - Human Drug Transporters Phase III (QIAGEN; PAHS-070Z)						
Gene Symbol	AVG ΔCt		2^ - ΔCt		Fold Change	Fold Up – or Down-Regulation
	Group1 (HLC)	Control Group (PHH)	Group1 (HLC)	Control Group (PHH)	Group 1/ Control	Group 1/ Control
ABCC1	6.89	8.73	0.008423	0.002350	3.58	3.58
ABCC4	4.89	9.01	0.033689	0.001934	17.42	17.42
ABCC5	5.93	8.98	0.016410	0.001982	8.28	8.28
ABCG2	4.52	9.39	0.043502	0.001491	29.17	29.17
SLCO1A2	7.29	11.41	0.006390	0.000368	17.38	17.38
SLCO2A1	6.64	12.26	0.009994	0.000204	49.01	49.01
SLC19A3	4.75	7.85	0.037173	0.004328	8.59	8.59
SLC22A7	8.55	11.07	0.002659	0.000466	5.70	5.70
SLC22A9	6.43	8.37	0.011561	0.003030	3.82	3.82
ABCC3	5.53	3.98	0.021683	0.063471	0.34	-2.93
ABCB11	8.58	9.07	0.002616	0.001859	1.41	1.41
ABCG8	8.74	7.25	0.002338	0.006587	0.35	-2.82
SLC19A1	9.35	10.40	0.001529	0.000738	2.07	2.07
SLC19A2	4.95	6.46	0.032350	0.011345	2.85	2.85
SLC22A3	6.28	6.05	0.012855	0.015105	0.85	-1.18
ABCB1	8.16	5.09	0.003490	0.029260	0.12	-8.38
ABCB4	8.73	6.51	0.002351	0.011003	0.21	-4.68
ABCC2	6.42	2.84	0.011709	0.139434	0.08	-11.91
SLCO1B1	10.59	6.34	0.000648	0.012367	0.05	-19.09
SLCO1B3	10.88	7.76	0.000532	0.004626	0.12	-8.69
SLC22A1	11.12	7.00	0.000448	0.007829	0.06	-17.46

Supplementary Table 1.4: Phase III drug metabolism (PCR Array). Fold-Change (2^(- Delta Delta Ct)) is the normalized gene expression (2^(- Delta Ct)) in the Test Sample divided the normalized gene expression (2^(- Delta Ct)) in the Control Sample. Fold-Regulation represents fold-change results in a biologically meaningful way. Fold-change values greater than one indicate a positive- or an up-regulation, and the fold-regulation is equal to the fold-change. Fold-change values less than one indicate a negative or down-regulation, and the fold-regulation is the negative inverse of the fold-change. Up-regulated genes (fold differences larger than a 3 fold threshold) are indicated in red, down-regulated genes (fold differences narrower than 3 fold treshold) are indicated in green. Genes similarly expressed for the Group 1 and Control (fold differences between -3 to +3 boundary) are indicated in black. Abbreviations: HLC, hepatocyte-like-cells; PHH, primary human hepatocytes.

microRNA/ Gene (symbol)	Accession Number (miRBase)	
hsa-miR-324-5p	MI0000813 / MIMAT0000761	
hsa-miR-24-3p	MI0000080 / MIMAT0000080	
hsa-miR-148a	MI0000253 / MIMAT0000243	
	UniGene	**GeneBank**
SULT2A1	Hs.515835	NM_003167
GSTT1	Hs.268573	NM_000853
UGT1A1	Hs.554822	NM_000463

Supplementary Table 1.5: **miRBase ID and NCBI of selected microRNAs and genes**. Abbreviations: hsa, human; miR, microRNA, ID, identification; NCBI, National Centre for Biotechnology Information.

miRNA	Mean log2 intensity	Relative mean intensity (%)	Max. log2 intensity	Relative max. intensity (%)	Times detected (%)	Chromosome Band
hsa-let-7b-3p	2.167553914	15.39758566	4.759083184	33.80695194	54.54545455	22q13.31
hsa-let-7e-5p	4.315044314	30.65264676	5.195762764	36.90897916	90.90909091	19q13.41
hsa-let-7f-1-3p	1.45060131	10.30459164	3.752587461	26.65713942	18.18181818	9q22.32
hsa-miR-1	1.562493903	11.09943959	4.033989956	28.65612962	18.18181818	20q13.33 /// 18q11.2
hsa-miR-107	8.445884654	59.99676945	9.20038125	65.35646358	100	10q23.31
has-miR-1202	6.624326485	47.05702306	9.080396756	64.50413344	100	6q25.3
hsa-miR-1207-5p	8.276057831	58.79037591	10.36982484	73.66380382	100	8q24.21
hsa-miR-122-5p	10.08319276	71.62766441	12.88839682	91.55490564	100	18q21.31
hsa-miR-1224-5p	4.619021262	32.8119984	6.317471652	44.87722788	100	3q27.1
hsa-miR-1225-3p	3.997769591	28.39883213	5.235933105	37.19433597	100	16p13.3
hsa-miR-1225-5p	7.302618353	51.87538401	9.080396756	64.50413344	100	16p13.3
hsa-miR-1226*	2.73590075	19.4349335	6.432835079	45.69673148	36.36363636	3p21.31
hsa-miR-1228-3p	4.737513176	33.65372574	6.047606994	42.96019866	100	12q13.3
hsa-miR-1228-5p	2.336520334	16.59786719	5.533498506	39.3081421	36.36363636	12q13.3
hsa-miR-1234	5.018803171	35.65191678	6.517331819	46.29696836	100	8q24.3
hsa-miR-1237	3.113032203	22.11395052	4.222428371	29.99473375	90.90909091	11q13.1
hsa-miR-1238	4.283605841	30.42931826	5.402617074	38.37840372	100	19p13.2
hsa-miR-1246	9.203731352	65.38026159	12.88839682	91.55490564	100	2q31.1
hsa-miR-1249	1.710712988	12.15233891	3.779902166	26.85117404	36.36363636	22q13.31
hsa-miR-1258	1.366140729	9.704611618	3.652512778	25.94624199	9.090909091	2q31.3
hsa-miR-125a-3p	3.718808154	26.4171824	5.533498506	39.3081421	81.81818182	19q13.41
hsa-miR-125b-5p	6.907149701	49.06610558	8.24897089	58.59795924	100	11q24.1 /// 21q21.1
hsa-miR-126-3p	4.453699943	31.63761046	6.745973602	47.92116392	72.72727273	9q34.3
hsa-miR-1260b	8.739559616	62.08293919	9.951193434	70.68998485	100	11q21
hsa-miR-1268b	6.897900491	49.00040226	8.914241059	63.32381836	100	17q25.3
hsa-miR-1275	7.082825486	50.31404822	9.543230472	67.79195098	100	6p21.31
hsa-miR-128	4.867008714	34.57361919	5.863396753	41.65163006	100	2q21.3 /// 3p22.3
hsa-miR-1281	4.906137632	34.85157807	7.000447289	49.72886077	100	22q13.2
hsa-miR-1288	3.126365697	22.20866726	4.382662349	31.1329829	81.81818182	17p11.2
hsa-miR-1290	6.649179186	47.23356842	9.685937919	68.80569746	100	1p36.13
hsa-miR-1296	1.866800635	13.2611339	3.836693986	27.25460434	45.45454545	10q21.3
hsa-miR-1305	4.957477645	35.21628054	6.488825654	46.09447	100	4q34.3
hsa-miR-133b	1.767910763	12.55865298	4.191590285	29.7756702	27.27272727	6p12.2
hsa-miR-135a-3p	3.580095563	25.43181406	5.333142011	37.88487587	100	3p21.1 /// 12q23.1
hsa-miR-140-5p	3.713856714	26.38200901	5.333142011	37.88487587	81.81818182	16q22.1
hsa-miR-1471	2.371194554	16.84418138	5.108433596	36.28862165	36.36363636	2q37.1
hsa-miR-148a-3p	7.715908631	54.81126137	9.34381318	66.37535654	100	7p15.2
hsa-miR-148b-3p	5.16186919	36.66821043	6.317471652	44.87722788	100	12q13.13
hsa-miR-150-3p	4.834592275	34.34334353	7.181437537	51.0145556	100	19q13.33
hsa-miR-151a-3p	4.160489957	29.55474376	5.468096887	38.84355064	90.90909091	8q24.3
hsa-miR-151a-5p	6.759415776	48.01665268	7.908331533	56.17816998	100	8q24.3
hsa-miR-155-5p	2.817584404	20.01518714	4.174217694	29.65226106	63.63636364	21q21.3
hsa-miR-16-5p	8.507873725	60.4371193	9.685937919	68.80569746	100	13q14.2 /// 3q25.33
hsa-miR-17-3p	3.717872965	26.41053913	5.605092098	39.81671929	90.90909091	13q31.3
hsa-miR-181a-5p	6.125048032	43.51031416	7.000447289	49.72886077	100	1q32.1 /// 9q33.3
hsa-miR-181b-5p	4.149834728	29.47905254	4.97754762	35.35885099	90.90909091	1q32.1 /// 9q33.3
hsa-miR-1825	4.717609699	33.51233803	6.609645511	46.95273427	100	20q11.21
hsa-miR-183-5p	3.26200335	23.17219225	5.2540446	37.32299404	81.81818182	7q32.2
hsa-miR-185-5p	3.599703802	25.5711045	4.964394851	35.26541808	90.90909091	22q11.21
hsa-miR-186-5p	3.107641947	22.07565993	4.576235395	32.50806176	81.81818182	1p31.1
hsa-miR-188-5p	5.832657074	41.43326556	9.2666837	65.82745424	100	Xp11.23
hsa-miR-1909-5p	1.881355523	13.36452701	4.082699416	29.0021455	36.36363636	19p13.3
hsa-miR-191-3p	4.106883242	29.1739394	4.949522624	35.1597707	100	3p21.31
hsa-miR-1910	1.56203899	11.09620803	4.204958561	29.87063401	18.18181818	16q24.1
hsa-miR-1914-3p	4.204836624	29.8697678	5.120226753	36.37239634	100	20q13.33
hsa-miR-1915	8.285328163	58.85622928	10.65447387	75.6858563	100	10p12.31
hsa-miR-193a-5p	4.085079479	29.01905268	5.605092098	39.81671929	100	17q11.2
hsa-miR-197-3p	5.426277098	38.5464767	7.888192297	56.03510751	100	1p13.3
hsa-miR-1973	5.804181369	41.23098357	6.891326276	48.95370121	100	4q26
hsa-miR-198	2.236101149	15.88452253	5.2540446	37.32299404	36.36363636	3q13.33
hsa-miR-203	3.126895637	22.21243177	4.798541198	34.08724862	72.72727273	14q32.33
hsa-miR-205-3p	1.96851625	13.98368797	4.713406887	33.48248264	36.36363636	1q32.2
hsa-miR-20a-3p	2.765103481	19.64238003	4.366871399	31.02080922	72.72727273	13q31.3
hsa-miR-21-5p	12.09963664	85.95181434	12.88839682	91.55490564	100	17q23.1
hsa-miR-210	5.877366952	41.75086974	8.351444508	59.32589791	90.90909091	11p15.5
hsa-miR-211-5p	1.376709151	9.779686194	3.768765425	26.77206232	9.090909091	15q13.3
hsa-miR-218-5p	4.947405224	35.14472939	7.814426908	55.5111026	90.90909091	4p15.31 /// 5q34
hsa-miR-22-5p	2.71668992	19.29846611	4.156098562	29.52354874	63.63636364	17p13.3

Supplementary Table 1.6 (a): The list of 220 microRNAs commonly expressed in stem cell (H9) – derived hepatocytes (day 18) and primary human hepatocytes (PHH). The RNA samples (4 replicates of PHH and 4 experimental samples of hESC-derived hepatocytes) were analysed on the Agilent miRNA platform (using Agilent's SurePrint G3 Human v16 microRNA 8x60K microarray slides; miRbase version 16.0).

hsa-miR-221-3p	4.988289183	35.43515551	6.047606994	42.96019866	100	Xp11.3
hsa-miR-224-5p	4.216325184	29.95137874	5.863396753	41.65163006	100	Xq28
hsa-miR-2276	2.831064559	20.1109457	5.567690079	39.55102772	54.54545455	13q12.12
hsa-miR-23a-3p	8.369316464	59.45285437	9.2666837	65.82745424	100	19p13.13
hsa-miR-23b-3p	7.84616685	55.73657265	9.20038125	65.35646358	100	9q22.32
hsa-miR-24-3p	8.311629805	59.04306744	9.166945457	65.11894677	100	9q22.32 /// 19p13.13
hsa-miR-25-3p	6.685005927	47.48806973	8.159537635	57.96265499	100	7q22.1
hsa-miR-26a-5p	7.010850118	49.80275903	8.782112163	62.3852184	100	3p22.2 /// 12q14.1
hsa-miR-26b-5p	7.887656757	56.03130322	9.20038125	65.35646358	100	2q35
hsa-miR-27a-3p	7.070116486	50.22376769	8.24897089	58.59795924	100	19p13.13
hsa-miR-27b-3p	7.760195925	55.12586365	9.34381318	66.37535654	100	9q22.32
hsa-miR-28-5p	4.614680979	32.78116647	6.020154252	42.76518346	90.90909091	3q28
hsa-miR-2861	8.098232261	57.52716191	11.77690063	83.65920458	100	9q34.11
hsa-miR-30a-3p	2.950765003	20.96125804	4.534663185	32.21274654	63.63636364	6q13
hsa-miR-30a-5p	6.145492589	43.65554553	7.458327192	52.98148807	100	6q13
hsa-miR-30b-5p	6.546012759	46.50070827	7.941037626	56.41050324	100	8q24.22
hsa-miR-30c-5p	4.341174699	30.83826837	5.716816843	40.6103749	90.90909091	1p34.2 /// 6q13
hsa-miR-30e-3p	2.959039546	21.02003765	4.481761629	31.8369514	72.72727273	1p34.2
hsa-miR-30e-5p	5.432525493	38.59086323	6.891326276	48.95370121	100	1p34.2
hsa-miR-31-3p	1.917007372	13.61778595	3.803379697	27.01795066	45.45454545	9p21.3
hsa-miR-31-5p	2.482850148	17.63734577	5.235933105	37.19433597	45.45454545	9p21.3
hsa-miR-3124-5p	1.762034727	12.51691157	4.011269468	28.49473079	27.27272727	1q44
hsa-miR-3125	3.744020805	26.59628473	5.090800321	36.1633607	100	2p24.3
hsa-miR-3127-5p	3.293369985	23.39501045	5.834190844	41.44416096	72.72727273	2q11.2
hsa-miR-3137	2.024382356	14.38054229	4.097587661	29.10790666	36.36363636	3q29
hsa-miR-3138	2.135530188	15.17009971	4.393786163	31.2120028	36.36363636	4p16.1
hsa-miR-3141	5.767174081	40.96809605	8.494581071	60.34269268	100	5q33.2
hsa-miR-3148	2.369747636	16.83390295	4.222428371	29.99473375	54.54545455	8p12
hsa-miR-3156-5p	2.410880989	17.12610068	4.964394851	35.26541808	54.54545455	10q11.21 /// 18p11.21 /// 21q11.2
hsa-miR-3162-5p	8.079116607	57.39137063	9.428341899	66.97582058	100	11q12.1
hsa-miR-3189-3p	1.562705153	11.10094023	3.595719016	25.5427979	27.27272727	19p13.11
hsa-miR-3191-5p	1.925673313	13.67934593	4.011269468	28.49473079	36.36363636	19q13.32
hsa-miR-3194-5p	1.967760055	13.97831621	3.966179414	28.17442596	36.36363636	20q13.2
hsa-miR-3195	6.693009447	47.54492409	8.629280443	61.29955244	100	20q13.33
hsa-miR-3196	6.794186938	48.2636555	8.739987987	62.0859822	100	20q13.33
hsa-miR-3198	5.172946014	36.74689652	6.457343715	45.87083272	100	22q11.21 /// 12q13.13
hsa-miR-32-5p	2.221762751	15.7826673	3.814202968	27.09483559	45.45454545	9q31.3
hsa-miR-320a	6.064389577	43.07941657	8.039474417	57.10976563	100	8p21.3
hsa-miR-320b	7.151715081	50.80341711	9.20038125	65.35646358	100	1p13.1 /// 1q42.11
hsa-miR-320c	8.230368171	58.46581168	9.951193434	70.68998485	100	18q11.2 /// 18q11.2
hsa-miR-320d	7.725435848	54.87893956	9.428341899	66.97582058	100	13q14.11 /// Xq27.1
hsa-miR-320e	7.356786278	52.26017503	9.166945457	65.11894677	100	19q13.32
hsa-miR-324-3p	5.300069944	37.64994285	6.488825654	46.09447	100	17p13.1
hsa-miR-324-5p	4.49681939	31.94391675	5.468096887	38.84355064	90.90909091	17p13.1
hsa-miR-331-3p	7.044867749	50.04440902	8.494581071	60.34269268	100	12q22
hsa-miR-338-3p	2.500761434	17.76458161	3.872137461	27.50638306	54.54545455	17q25.3
hsa-miR-33a-5p	2.095408822	14.8850908	3.752587461	26.65713942	45.45454545	22q13.2
hsa-miR-340-5p	4.307660302	30.60019318	5.628631779	39.98393738	90.90909091	5q35.3
hsa-miR-342-3p	5.312297351	37.7368023	6.891326276	48.95370121	100	14q32.2
hsa-miR-345-5p	2.022335691	14.36600346	5.307697101	37.70412365	54.54545455	14q32.2
hsa-miR-3529-3p	3.279464699	23.2962319	4.97754762	35.35885099	90.90909091	15q26.1
hsa-miR-3610	2.916603406	20.71858536	6.233434393	44.280255	45.45454545	8q24.11
hsa-miR-3613-3p	1.833489088	13.0244997	4.481761629	31.8369514	27.27272727	13q14.2
hsa-miR-362-3p	3.732515475	26.51455467	5.333142011	37.88487587	90.90909091	Xp11.23
hsa-miR-362-5p	3.063632943	21.76303453	5.287277176	37.55906726	72.72727273	Xp11.23
hsa-miR-3620	1.916020994	13.61077905	4.268604247	30.32275189	36.36363636	1q42.13
hsa-miR-3646	2.378256536	16.89434736	5.487612049	38.98217989	36.36363636	20q13.12
hsa-miR-3651	5.96417265	42.36750869	9.34381318	66.37535654	100	9q22.31
hsa-miR-3653	4.365243802	31.00924731	6.457343715	45.87083272	81.81818182	22q12.2
hsa-miR-3656	6.79527371	48.27137557	10.20739641	72.50996603	100	11q23.3
hsa-miR-365b-3p	7.351961072	52.22589835	8.449858467	60.0249981	100	17q11.2
hsa-miR-3665	9.552278389	67.85622439	12.88839682	91.55490564	100	13q22.3
hsa-miR-3667-5p	3.284815365	23.33424126	8.004693565	56.86269397	36.36363636	22q13.33
hsa-miR-3676-3p	3.64853392	25.9179775	4.602704884	32.69609225	100	17p13.1
hsa-miR-3679-5p	6.597281304	46.86490304	9.428341899	66.97582058	100	2q21.2
hsa-miR-3692-5p	1.749766601	12.42976285	4.393786163	31.2120028	27.27272727	6q25.3
hsa-miR-3713	1.783968337	12.67272067	3.779902166	26.85117404	36.36363636	15q24.3
hsa-miR-374a-5p	6.637281637	47.14905217	8.307345268	59.0126315	100	Xq13.2
hsa-miR-375	2.79980384	19.8888799	4.314074629	30.64575844	63.63636364	2q35
hsa-miR-3917	1.810940875	12.86432465	3.562103075	25.30400138	36.36363636	1p36.11
hsa-miR-3935	2.140621	15.20626315	4.964394851	35.26541808	36.36363636	16q12.2
hsa-miR-3937	2.033564882	14.44577192	4.109507663	29.19258242	36.36363636	Xp11.4
hsa-miR-3940-3p	1.514500304	10.75850894	3.814202968	27.09483559	18.18181818	19p13.3

Supplementary Table 1.6 (b): The list of 220 microRNAs commonly expressed in stem cell (H9) – derived hepatocytes (day 18) and primary human hepatocytes (PHH). The RNA samples (4 replicates of PHH and 4 experimental samples of hESC-derived hepatocytes) were analysed on the Agilent miRNA platform (using Agilent's SurePrint G3 Human v16 microRNA 8x60K microarray slides; miRbase version 16.0).

hsa-miR-422a	2.052950141	14.58347839	4.314074629	30.64575844	36.36363636	15q22.31
hsa-miR-423-3p	2.172437369	15.43227611	3.652512778	25.94624199	54.54545455	17q11.2
hsa-miR-423-5p	5.293541426	37.60356641	6.81014592	48.37702283	100	17q11.2
hsa-miR-425-3p	3.884924864	27.59722053	5.143929899	36.54077564	100	3p21.31
hsa-miR-425-5p	4.917363749	34.9313247	5.994724118	42.58453621	100	3p21.31
hsa-miR-4259	1.37179534	9.744780104	3.714713499	26.38809533	9.090909091	1q23.2
hsa-miR-4274	1.653315521	11.7446063	4.024114051	28.58597446	27.27272727	4p16.1
hsa-miR-4281	9.817200194	69.73814122	12.26005643	87.09138348	100	5q35.2
hsa-miR-4284	10.63253305	75.52999597	12.88839682	91.55490564	100	7q11.23
hsa-miR-4286	10.13008898	71.96079963	12.26005643	87.09138348	100	8p23.1
hsa-miR-4290	2.298701585	16.32921532	5.032584172	35.74981245	54.54545455	9q22.2
hsa-miR-4291	2.547862817	18.09917425	4.798541198	34.08724862	45.45454545	9q22.32
hsa-miR-4298	5.512091705	39.15607527	8.962374449	63.66574202	100	11p15.5
hsa-miR-4299	6.196038079	44.01460396	7.047227741	50.06117362	100	11p15.3
hsa-miR-4306	4.970258284	35.30706997	5.567690079	39.55102772	100	13q32.3
hsa-miR-4312	1.981447562	14.07554773	4.546875495	32.29949875	36.36363636	15q23
hsa-miR-4313	4.137015132	29.38798637	5.354448634	38.03623107	100	15q24.2
hsa-miR-4327	4.357748635	30.95600413	7.047227741	50.06117362	90.90909091	21q22.11
hsa-miR-449a	2.257026606	16.03317006	4.949522624	35.1597707	45.45454545	5q11.2
hsa-miR-449b-3p	2.841666032	20.18625506	5.164175203	36.68459158	72.72727273	5q11.2
hsa-miR-449c-3p	2.132960588	15.15184612	4.74185466	33.68456621	45.45454545	5q11.2
hsa-miR-450a-5p	1.62227387	11.52409669	4.097587661	29.10790666	18.18181818	Xq26.3 /// Xq26.3
hsa-miR-455-3p	4.859824581	34.52258549	6.72659457	47.78350169	90.90909091	9q32
hsa-miR-455-5p	2.852716444	20.26475353	5.523791743	39.23918846	45.45454545	9q32
hsa-miR-484	3.507815356	24.91835939	4.7701092	33.88527711	90.90909091	16p13.11
hsa-miR-485-3p	1.931620513	13.72159287	4.889324858	34.73214569	36.36363636	14q32.31
hsa-miR-491-3p	2.79097818	19.82618533	5.749949854	40.84574084	72.72727273	9p21.3
hsa-miR-494	8.283241846	58.84140877	9.2666837	65.82745424	100	14q32.31
hsa-miR-498	2.042204194	14.50714273	4.128734764	29.32916537	36.36363636	19q13.42
hsa-miR-500a-3p	2.531922596	17.98594019	4.393786163	31.2120028	63.63636364	Xp11.23
hsa-miR-500a-5p	2.013446043	14.30285435	3.836693986	27.25460434	54.54545455	Xp11.23
hsa-miR-502-3p	1.809240846	12.85224821	3.886555557	27.60880444	36.36363636	Xp11.23
hsa-miR-502-5p	1.490801471	10.59016028	3.625588668	25.75498202	18.18181818	Xp11.23
hsa-miR-505-3p	4.297800682	30.53015371	5.2540446	37.32299404	100	Xq27.1
hsa-miR-505-5p	2.540686049	18.04819286	3.779902166	26.85117404	72.72727273	Xq27.1
hsa-miR-513a-5p	3.157323374	22.42858035	5.994724118	42.58453621	81.81818182	Xq27.3 /// Xq27.3
hsa-miR-514b-3p	1.382131538	9.818205037	3.828411682	27.1957696	9.090909091	Xq27.3
hsa-miR-514b-5p	1.902062062	13.51161941	4.646466678	33.00696156	36.36363636	Xq27.3
hsa-miR-520b	2.658295224	18.88364952	6.317471652	44.87722788	36.36363636	19q13.42
hsa-miR-520e	2.203213737	15.65090125	4.660504415	33.10668099	36.36363636	19q13.42
hsa-miR-542-3p	1.510684728	10.73140435	3.537066614	25.12615065	18.18181818	Xq26.3
hsa-miR-548c-5p	1.908237818	13.55548994	4.993857538	35.47471125	45.45454545	12q14.2
hsa-miR-548d-5p	1.665941498	11.83429706	5.077772801	36.07081751	18.18181818	8q24.13 /// 17q24.2
hsa-miR-548q	1.884876552	13.38953924	4.033989956	28.65612962	36.36363636	10p13
hsa-miR-548y	1.590730845	11.30002548	4.798541198	34.08724862	18.18181818	14q21.3
hsa-miR-572	5.299110117	37.64312455	8.351444508	59.32589791	100	4p15.33
hsa-miR-574-3p	6.738285613	47.86655099	8.307345268	59.0126315	100	4p14
hsa-miR-574-5p	6.309902776	44.82346109	7.529016836	53.48364391	100	4p14
hsa-miR-575	5.508253983	39.12881336	7.360508577	52.286617	100	4q21.22
hsa-miR-576-3p	1.441526988	10.24013065	4.481761629	31.8369514	9.090909091	4q25
hsa-miR-583	2.349409727	16.68942917	5.618428218	39.91145467	36.36363636	5q15
hsa-miR-584-5p	1.953219225	13.87502296	4.204958561	29.87063401	36.36363636	5q32
hsa-miR-590-5p	3.62519098	25.75215698	4.92801709	35.0070025	90.90909091	7q11.23
hsa-miR-595	2.533720676	17.99871316	4.426959826	31.44765752	54.54545455	7q36.3
hsa-miR-601	2.495110907	17.72444214	5.523791743	39.23918846	36.36363636	9q33.3
hsa-miR-622	1.987259396	14.11683307	3.836693986	27.25460434	36.36363636	13q31.3
hsa-miR-623	2.102125464	14.93280361	4.565506063	32.43184414	36.36363636	13q32.3
hsa-miR-629-3p	2.576928339	18.3056461	4.74185466	33.68456621	54.54545455	15q23
hsa-miR-636	2.87515986	20.42418413	5.941433092	42.20597439	54.54545455	17q25.1
hsa-miR-638	7.871257032	55.914805	11.26571402	80.02790407	100	19p13.2
hsa-miR-654-3p	1.577967188	11.20935668	3.919572726	27.84334748	27.27272727	14q32.31
hsa-miR-654-5p	1.988699375	14.12706221	3.828411682	27.1957696	36.36363636	14q32.31
hsa-miR-660-5p	4.883626779	34.69166842	6.457343715	45.87083272	100	Xp11.23
hsa-miR-670	2.181052967	15.49347847	3.652512778	25.94624199	54.54545455	11p11.2
hsa-miR-671-5p	3.572143416	25.37532464	8.389540218	59.59651722	45.45454545	7q36.1
hsa-miR-708-5p	2.188349404	15.54530994	5.052081488	35.88831493	36.36363636	11q14.1
hsa-miR-720	12.96589229	92.10540783	14.07723238	100	100	3q26.1
hsa-miR-744-5p	3.261608841	23.16938979	5.643112092	40.08680074	63.63636364	17p12
hsa-miR-762	6.884747527	48.90696795	9.023659859	64.1010933	100	16p11.2
hsa-miR-764	1.417116093	10.06672374	3.662623558	26.01806562	18.18181818	Xq23
hsa-miR-765	2.803470829	19.91492897	6.256605335	44.4448537	54.54545455	1q23.1
hsa-miR-766-3p	3.844533615	27.31029447	5.889589913	41.83769761	90.90909091	Xq24
hsa-miR-769-5p	1.776484643	12.61955898	4.024114051	28.58597446	27.27272727	19q13.32
hsa-miR-874	5.604346965	39.8114261	7.529016836	53.48364391	100	5q31.2
hsa-miR-892b	1.894749864	13.45967598	3.850146141	27.350164	36.36363636	Xq27.3
hsa-miR-937	2.072552938	14.72273017	4.576235395	32.50806176	54.54545455	8q24.3
hsa-miR-939	5.706233587	40.53519495	7.851199509	55.77232299	100	8q24.3
hsa-miR-940	6.790849694	48.23994883	8.696390017	61.77627664	100	16p13.3
hsa-miR-96-5p	4.977460703	35.35823356	6.773394597	48.11595359	90.90909091	7q32.2

Supplementary Table 1.6 (c): The list of 220 microRNAs commonly expressed in stem cell (H9) – derived hepatocytes (day 18) and primary human hepatocytes (PHH). The RNA samples (4 replicates of PHH and 4 experimental samples of hESC-derived hepatocytes) were analysed on the Agilent miRNA platform (using Agilent's SurePrint G3 Human v16 microRNA 8x60K microarray slides; miRbase version 16.0).

miRNA ID	q-value	Fold-change	FC interpretation	Mean log2 intensity	Relative mean intensity (%	Max. log2 intensity	Relative max. intensity (%	Times detected (%)	Chromosome Band
hsa-miR-367-3p	0.006216967	166.609765	2D is up-regulatec	1.925673	13.679346	4.011269	28.494731	36.363636	19q13.32
hsa-miR-10a-5p	0.001450354	111.6681019	2D is up-regulatec	8.14278	57.843615	10.369825	73.663804	100	Xq26.2
hsa-miR-363-3p	0.001768226	88.74062756	2D is up-regulatec	3.744021	26.596285	5.0908	36.163361	100	2p24.3
hsa-miR-302c-3p	0.00631854	79.20295295	2D is up-regulatec	4.322427	30.705093	6.391693	45.404472	90.909091	17q23.1
hsa-miR-302a-3p	0.005319514	73.38721242	2D is up-regulatec	2.765103	19.64238	4.366871	31.020809	72.727273	13q31.3
hsa-let-7d-5p	0.00392552	-59.53733561	2D is down-regula	3.13543	22.273056	7.684292	54.586664	45.454545	9q22.32
hsa-miR-302d-3p	0.005719979	58.58515953	2D is up-regulatec	12.099637	85.951814	12.888397	91.554906	100	17q23.1
hsa-miR-483-3p	0.007780986	50.94123812	2D is up-regulatec	3.284815	23.334241	8.004694	56.862694	36.363636	22q13.33
hsa-let-7g-5p	0.002644448	-48.81526984	2D is down-regula	1.450601	10.304592	3.752587	26.657139	18.181818	9q22.32
hsa-miR-302a-5p	0.005719979	47.70794123	2D is up-regulatec	8.980866	63.797102	11.265714	80.027904	100	13q31.3
hsa-let-7b-5p	0.003731103	-42.23072965	2D is down-regula	4.89201	34.751218	9.166945	65.118947	100	22q13.31
hsa-miR-124-3p	0.00254598	41.71368478	2D is up-regulatec	3.99777	28.398832	5.235933	37.194336	100	16p13.3
hsa-miR-302b-3p	0.006607641	39.64912998	2D is up-regulatec	7.60986	54.057926	9.54323	67.791951	100	Xq26.2
hsa-miR-9-3p	0.003661016	39.48245758	2D is up-regulatec	2.852716	20.264754	5.523792	39.239188	45.454545	9q32
hsa-miR-205-5p	0.003726865	36.86764498	2D is up-regulatec	4.204837	29.869768	5.120227	36.372396	100	20q13.33
hsa-miR-142-3p	0.001386123	-35.79791775	2D is down-regula	6.649179	47.233568	9.685938	68.805697	100	1p36.13
hsa-let-7f-5p	0.001768226	-32.69364117	2D is down-regula	4.315044	30.652647	5.195763	36.908979	90.909091	19q13.41
hsa-miR-885-5p	0.00982556	-28.13687256	2D is down-regula	4.859825	34.522585	6.726595	47.783502	90.909091	9q32
hsa-miR-130a-3p	0.001768226	27.48975085	2D is up-regulatec	4.4537	31.63761	6.745974	47.921164	72.727273	9q34.3
hsa-miR-195-5p	0.003215809	-26.20303676	2D is down-regula	8.507874	60.437119	9.685938	68.805697	100	13q14.2 /// 3q25.33
hsa-miR-424-5p	0.005719979	26.08790096	2D is up-regulatec	1.93188	13.723436	4.070104	28.912672	36.363636	14q32.2
hsa-let-7a-5p	0.002409861	-24.17825557	2D is down-regula	6.54328	46.481296	10.654474	75.685856	100	9q22.32 /// 11q24.1 ///
hsa-miR-99b-5p	0.00113966	23.57227583	2D is up-regulatec	2.312112	16.424481	5.307697	37.704124	36.363636	17p13.1
hsa-miR-98	0.001768226	-21.10142844	2D is down-regula	2.790978	19.826185	5.74995	40.845741	72.727273	9p21.3
hsa-miR-199a-3p	0.003215809	20.31973615	2D is up-regulatec	4.71761	33.512338	6.609646	46.952734	100	20q11.21
hsa-miR-10b-5p	0.001386123	19.96746988	2D is up-regulatec	7.743955	55.010491	9.200381	65.356464	100	7q22.1
hsa-let-7i-5p	0.00254598	-19.28726264	2D is down-regula	5.995091	42.587139	10.369825	73.663804	90.909091	9q22.32 /// Xp11.22
hsa-miR-204-5p	0.004881779	17.657277	2D is up-regulatec	4.106883	29.173939	4.949523	35.159771	100	3p21.31
hsa-miR-9-5p	0.005319514	17.41420901	2D is up-regulatec	3.196699	22.70829	5.333142	37.884876	72.727273	3p23
hsa-miR-149-5p	0.001768226	17.22573669	2D is up-regulatec	4.568911	32.45603	7.458327	52.981488	72.727273	14q32.31
hsa-miR-223-3p	0.001386123	-16.84805657	2D is down-regula	5.426277	38.546477	7.888192	56.035108	100	1p13.3
hsa-miR-145-5p	0.001450354	16.39274846	2D is up-regulatec	4.957478	35.216281	6.488826	46.09447	100	4q34.3
hsa-miR-141-3p	0.016438066	16.34619258	2D is up-regulatec	2.701053	19.187383	4.082699	29.002145	72.727273	11p11.2
hsa-miR-497-5p	0.001408222	-16.06973507	2D is down-regula	1.783968	12.672721	3.779902	26.851174	36.363636	15q24.3
hsa-miR-200c-3p	0.00392552	15.8667121	2D is up-regulatec	1.881356	13.364527	4.082699	29.002145	36.363636	19p13.3
hsa-miR-219-5p	0.009263772	15.38610417	2D is up-regulatec	5.945512	42.234949	8.962374	63.665742	100	1q41 /// 11q13.1
hsa-miR-301a-3p	0.04514623	15.28567709	2D is up-regulatec	1.968516	13.983688	4.713407	33.482483	36.363636	1q32.2
hsa-miR-135b-5p	0.009676961	14.81423358	2D is up-regulatec	6.451751	45.831106	8.089788	57.46718	100	3q21.3
hsa-let-7c	0.00727818	-14.7793576	2D is down-regula	4.776818	33.932934	8.782112	62.385218	81.818182	21q21.1
hsa-miR-122-3p	0.005812963	-13.18474061	2D is down-regula	3.725254	26.462975	6.35071	45.11334	72.727273	19p13.2
hsa-miR-200a-3p	0.015136803	-12.83049084	2D is down-regula	5.437408	38.625545	7.606615	54.034874	100	13q31.3
hsa-miR-3907	0.001818216	-11.50509526	2D is down-regula	5.30007	37.649943	6.488826	46.09447	100	17p13.1
hsa-miR-663a	0.009553921	11.08632066	2D is up-regulatec	2.547863	18.099174	4.798541	34.087249	45.454545	9q22.32
hsa-miR-29b-3p	0.009176736	-10.87871508	2D is down-regula	3.930191	27.918775	6.317472	44.877228	72.727273	12p13.31
hsa-miR-29a-3p	0.009479841	-10.68985878	2D is down-regula	2.720455	19.325215	5.856481	41.6025	45.454545	1p36.33
hsa-miR-301b	0.00392552	10.30155433	2D is up-regulatec	4.470073	31.753919	7.047228	50.061174	72.727273	1q32.2
hsa-miR-134	0.005319514	10.18260673	2D is up-regulatec	7.082825	50.314048	9.54323	67.791951	100	6p21.31
hsa-miR-34b-5p	0.044943801	-9.763632483	2D is down-regula	6.546013	46.500708	7.941038	56.410503	100	8q24.22
hsa-miR-29c-5p	0.001386123	-9.241603002	2D is down-regula	4.46233	31.698918	8.159538	57.962655	72.727273	9q21.12

Supplementary Table 1.7 (a): The list of 147 microRNAs differentially expressed in stem cell (H9) – derived hepatocytes (day 18) and primary human hepatocytes (PHH). The RNA samples (4 replicates of PHH and 4 experimental samples of hESC-derived hepatocytes) were analysed on the Agilent miRNA platform (using Agilent's SurePrint G3 Human v16 microRNA 8x60K microarray slides; miRbase version 16.0).

hsa-miR-A51:J88142-5p	0.001450354	-8.998030658	2D is down-regula	1.866801	13.261134	3.836694	27.254604	45.454545	10q21.3
hsa-miR-199a-5p	0.006400925	8.860890186	2D is up-regulatec	3.262003	23.172192	5.254045	37.322994	81.818182	7q32.2
hsa-miR-153	0.007743766	8.788499396	2D is up-regulatec	3.995737	28.384391	5.402617	38.378404	90.909091	16q22.1
hsa-miR-130b-3p	0.003215809	8.739756787	2D is up-regulatec	9.74456	69.222131	11.265714	80.027904	100	14q24.3
hsa-miR-200b-3p	0.031426129	-8.52822124	2D is down-regula	4.792322	34.043069	6.726595	47.783502	100	Xq26.2
hsa-miR-192-3p	0.018021085	-8.509942579	2D is down-regula	6.759416	48.016653	7.908332	56.17817	100	8q24.3
hsa-miR-378a-3p	0.026624467	-8.213035783	2D is down-regula	7.356786	52.260175	9.166945	65.118947	100	19q13.32
hsa-miR-551b-3p	0.011499027	8.047258674	2D is up-regulatec	1.5145	10.758509	3.814203	27.094836	18.181818	19p13.3
hsa-miR-335-5p	0.001768226	7.905635181	2D is up-regulatec	5.015419	35.62788	7.047228	50.061174	90.909091	17q22
hsa-miR-29c-3p	0.009166364	-7.882767531	2D is down-regula	3.126896	22.212432	4.798541	34.087249	72.727273	14q32.33
hsa-miR-146a-5p	0.032799954	-7.627917385	2D is down-regula	9.489043	67.40702	12.048653	85.589645	100	11q12.1
hsa-miR-372	0.019688253	7.038613049	2D is up-regulatec	3.073202	21.831009	5.008503	35.578746	72.727273	9q31.3
hsa-miR-630	0.009431134	7.025409159	2D is up-regulatec	1.653316	11.744606	4.024114	28.585974	27.272727	4p16.1
hsa-miR-125a-5p	0.005196602	7.015441931	2D is up-regulatec	2.33652	16.597867	5.533499	39.308142	36.363636	12q13.3
hsa-miR-139-3p	0.005719979	-6.989712073	2D is down-regula	4.906138	34.851578	7.000447	49.728861	100	22q13.2
hsa-miR-625-5p	0.011032117	6.950431943	2D is up-regulatec	6.576286	46.715759	8.38954	59.596517	100	3p25.1
hsa-miR-199b-5p	0.013076595	6.92958479	2D is up-regulatec	3.599704	25.571105	4.964395	35.265418	90.909091	22q11.21
hsa-miR-106a-5p	0.005121252	6.8276196	2D is up-regulatec	5.0368	35.779762	7.483551	53.160672	100	11q24.1
hsa-miR-3149	0.031354786	6.821027395	2D is up-regulatec	2.831065	20.110946	5.56769	39.551028	54.545455	13q12.12
hsa-miR-194-5p	0.003726865	-6.512361894	2D is down-regula	7.290946	51.792467	9.02366	64.101093	100	3q25.33
hsa-miR-20b-5p	0.005178839	6.461721461	2D is up-regulatec	2.516171	17.874045	5.077773	36.070818	45.454545	11q13.1
hsa-miR-429	0.016438066	-6.307624421	2D is down-regula	1.833489	13.0245	4.481762	31.836951	27.272727	13q14.2
hsa-miR-100-5p	0.003661016	-6.286774015	2D is down-regula	4.653924	33.059938	9.428342	66.975821	90.909091	3p21.1
hsa-miR-129-2-3p	0.003661016	6.282994486	2D is up-regulatec	5.160362	36.657504	7.252453	51.519028	100	19q13.41
hsa-miR-421	0.002357157	6.243070154	2D is up-regulatec	2.500761	17.764582	3.872137	27.506383	54.545455	17q25.3
hsa-miR-582-5p	0.007780986	-6.210325247	2D is down-regula	4.139397	29.404906	6.810146	48.377023	72.727273	Xq26.3
hsa-miR-4270	0.002409861	-6.141232007	2D is down-regula	4.56163	32.404307	6.517332	46.296968	90.909091	11q23.1
hsa-miR-34b-3p	0.021930435	6.119539052	2D is up-regulatec	1.807537	12.840147	3.537067	25.126151	36.363636	8q24.22
hsa-miR-101-3p	0.015974143	-6.011038431	2D is down-regula	4.466184	31.726294	8.039474	57.109766	90.909091	12q14.1
hsa-miR-466	0.034312812	5.89750118	2D is up-regulatec	9.552278	67.856224	12.888397	91.554906	100	13q22.3
hsa-miR-557	0.002929101	-5.771547494	2D is down-regula	2.134854	15.165295	4.139335	29.404464	45.454545	Xq13.2
hsa-miR-34a-3p	0.011375284	-5.754378628	2D is down-regula	2.950765	20.961258	4.534663	32.212747	63.636364	6q13
hsa-miR-99a-5p	0.007780986	-5.65376946	2D is down-regula	8.283242	hsa-miR-A51:J88130b-3p	9.266684	65.827454	100	14q32.31
hsa-miR-20a-5p	0.010423834	5.642091349	2D is up-regulatec	8.285328	58.856229	10.654474	75.685856	100	10p12.31
hsa-miR-21-3p	0.028284818	-5.625521383	2D is down-regula	6.912845	49.106563	9.54323	67.791951	100	11q13.1
hsa-miR-125b-2-3p	0.001768226	-5.597849447	2D is down-regula	5.018803	35.651917	6.517332	46.296968	100	8q24.3
hsa-miR-4257	0.007676182	5.53900874	2D is up-regulatec	7.983591	56.712789	8.914241	63.323818	100	1p36.22
hsa-miR-564	0.017105876	-5.50403732	2D is down-regula	2.05295	14.583478	4.314075	30.645758	36.363636	15q22.31
hsa-miR-4324	0.007743766	-5.49057202	2D is down-regula	3.709141	26.348507	7.000447	49.728861	72.727273	21p11.2
hsa-miR-215	0.007741066	-5.368650288	2D is down-regula	5.623869	39.950102	7.606615	54.034874	100	16p13.12
hsa-miR-29b-1-5p	0.003726865	-5.359722598	2D is down-regula	3.126445	22.209228	6.047607	42.960199	54.545455	1p36.33
hsa-miR-192-5p	0.005910313	-5.346244097	2D is down-regula	3.105493	22.060393	4.889325	34.732146	72.727273	17q21.32
hsa-miR-454-3p	0.011105345	5.332023137	2D is up-regulatec	6.795274	48.271376	10.207396	72.509966	100	11q23.3
hsa-miR-487b	0.003374527	-5.325311587	2D is down-regula	1.749767	12.429763	4.393786	31.212003	27.272727	6q25.3
hsa-miR-4261	0.012024164	-5.227009769	2D is down-regula	3.397281	24.133156	5.79116	41.138481	72.727273	11q23.1
hsa-miR-19b-3p	0.026076718	5.04529004	2D is up-regulatec	5.832657	41.433266	9.266684	65.827454	100	Xp11.23
hsa-miR-3188	0.00974634	-4.991595786	2D is down-regula	8.31163	59.043067	9.166945	65.118947	100	9q22.32 /// 19p13.13
hsa-miR-219-2-3p	0.006165807	4.986703634	2D is up-regulatec	1.787583	12.698396	3.51949	25.001294	36.363636	1q41 /// 11q13.1
hsa-miR-193b-3p	0.007741066	-4.954626676	2D is down-regula	2.817584	20.015187	4.174218	29.652261	63.636364	21q21.3
hsa-miR-3911	0.013725602	-4.873055771	2D is down-regula	4.496819	31.943917	5.468097	38.843551	90.909091	17p13.1
hsa-miR-194-3p	0.00113966	-4.799203383	2D is down-regula	6.190455	43.974947	7.529017	53.483644	100	13q14.2

Supplementary Table 1.7 (b): The list of 147 microRNAs differentially expressed in stem cell (H9) –derived hepatocytes (day 18) and primary human hepatocytes (PHH). The RNA samples (4 replicates of PHH and 4 experimental samples of hESC-derived hepatocytes) were analysed on the Agilent miRNA platform (using Agilent's SurePrint G3 Human v16 microRNA 8x60K microarray slides; miRbase version 16.0).

hsa-miR-92a-3p	0.001768226	4.691319596	2D is up-regulatec	6.783817	48.189989	10.654474	75.685856	100	11p15.5
hsa-miR-4254	0.03426676	4.6909326	2D is up-regulatec	2.697647	19.163189	4.268604	30.322752	72.727273	1p36.22
hsa-miR-30b-3p	0.00113966	-4.644014637	2D is down-regula	2.07166	14.716386	3.537067	25.126151	54.545455	1q24.3
hsa-miR-373-3p	0.005196602	4.60652042	2D is up-regulatec	2.221763	15.782667	3.814203	27.094836	45.454545	9q31.3
hsa-miR-342-5p	0.015456022	4.545802816	2D is up-regulatec	5.031944	35.745262	8.739988	62.085982	72.727273	4q25
hsa-miR-374c-5p	0.007743766	4.530162685	2D is up-regulatec	8.230368	58.465812	9.951193	70.689985	100	18q11.2 /// 18q11.2
hsa-miR-1181	0.010406007	4.52740348	2D is up-regulatec	8.445885	59.996769	9.200381	65.356464	100	10q23.31
hsa-miR-32-3p	0.048586465	4.514914782	2D is up-regulatec	7.760196	55.125864	9.343813	66.375357	100	9q22.32
hsa-miR-18b-5p	0.017795105	4.38389616	2D is up-regulatec	5.161869	36.66821	6.317472	44.877228	100	12q13.13
hsa-miR-146b-5p	0.018005132	-4.383521474	2D is down-regula	6.457012	45.868476	8.004694	56.862694	100	22q11.21
hsa-miR-1280	0.007377137	-4.359696228	2D is down-regula	1.366141	9.704612	3.652513	25.946242	9.090909	2q31.3
hsa-miR-214-3p	0.003374527	4.346332512	2D is up-regulatec	4.085079	29.019053	5.605092	39.816719	100	17q11.2
hsa-miR-361-5p	0.001450354	4.281126352	2D is up-regulatec	2.95904	21.020038	4.481762	31.836951	72.727273	1p34.2
hsa-miR-483-5p	0.045987593	4.23656287	2D is up-regulatec	6.156958	43.736991	10.207396	72.509966	72.727273	4q25
hsa-miR-3652	0.009111126	4.128461864	2D is up-regulatec	5.767174	40.968096	8.494581	60.342693	100	5q33.2
hsa-miR-718	0.005196602	-4.077917824	2D is down-regula	4.137015	29.387986	5.354449	38.036231	100	15q24.2
hsa-miR-93-5p	0.001802779	4.053021187	2D is up-regulatec	5.927516	42.107109	7.391498	52.506752	100	11p15.5
hsa-miR-1247-5p	0.031611456	4.051299538	2D is up-regulatec	2.735901	19.434933	6.432835	45.696731	36.363636	3p21.31
hsa-miR-3663-3p	0.001768226	-3.991724194	2D is down-regula	8.079117	57.391371	9.428342	66.975821	100	11q12.1
hsa-miR-877-3p	0.038767617	3.860153875	2D is up-regulatec	2.07344	14.729029	4.109508	29.192582	45.454545	17q22
hsa-miR-18a-5p	0.024434202	3.793670823	2D is up-regulatec	7.715909	54.811261	9.343813	66.375357	100	7p15.2
hsa-miR-196b-5p	0.008582669	3.614466324	2D is up-regulatec	3.717873	26.410539	5.605092	39.816719	90.909091	13q31.3
hsa-miR-371b-3p	0.01680877	3.475143067	2D is up-regulatec	5.172946	36.746897	6.457344	45.870833	100	22q11.21 /// 12q13.13
hsa-miR-328	0.031354786	3.415548063	2D is up-regulatec	7.243368	51.454487	9.166945	65.118947	100	1q32.2
hsa-miR-374c-3p	0.015456022	3.413331292	2D is up-regulatec	7.151715	50.803417	9.200381	65.356464	100	1p13.1 /// 1q42.11
hsa-miR-106b-5p	0.014014879	3.321003311	2D is up-regulatec	5.961815	42.350758	8.159538	57.962655	100	1p31.3 /// 9p24.1
hsa-miR-664-3p	0.013725602	-3.308474718	2D is down-regula	5.512092	39.156075	8.962374	63.665742	100	11p15.5
hsa-miR-3648	0.003978971	3.265961729	2D is up-regulatec	2.024382	14.380542	4.097588	29.107907	36.363636	3q29
hsa-miR-4271	0.00532593	3.206081258	2D is up-regulatec	3.279465	23.296232	4.977548	35.358851	90.909091	15q26.1
hsa-miR-34a-5p	0.031426129	-3.143537876	2D is down-regula	6.145493	43.655546	7.458327	52.981488	100	6q13
hsa-miR-22-3p	0.017105876	-3.109875188	2D is down-regula	2.729919	19.392444	6.391693	45.404472	45.454545	17p13.1
hsa-miR-19a-3p	0.038294357	3.107605968	2D is up-regulatec	3.107642	22.07566	4.576235	32.508062	81.818182	1p31.1
hsa-miR-361-3p	0.016438066	-3.096822314	2D is down-regula	5.82178	41.356001	7.219022	51.281543	100	8q24.22
hsa-miR-15a-5p	0.027919433	-2.911347564	2D is down-regula	4.615061	32.783869	7.814427	55.511103	72.727273	12p13.31
hsa-miR-532-5p	0.029595192	2.600635049	2D is up-regulatec	1.810941	12.864325	3.562103	25.304001	36.363636	1p36.11
hsa-miR-222-3p	0.008544941	-2.538630293	2D is down-regula	1.811606	12.869052	3.575528	25.399367	36.363636	7p15.2
hsa-miR-103b	0.002929101	2.509982363	2D is up-regulatec	1.562494	11.09944	4.03399	28.65613	18.181818	20q13.33 /// 18q11.2
hsa-miR-30d-5p	0.006478808	-2.463169826	2D is down-regula	4.947405	35.144729	7.814427	55.511103	90.909091	4p15.31 /// 5q34
hsa-miR-152	0.020455136	-2.365562993	2D is down-regula	2.082416	14.792794	4.128735	29.329165	45.454545	11q13.4
hsa-miR-15b-5p	0.009263772	2.353383749	2D is up-regulatec	2.545268	18.080743	6.35071	45.11334	27.272727	17q22
hsa-miR-132-3p	0.016438066	-2.313495716	2D is down-regula	8.73956	62.082939	9.951193	70.689985	100	11q21
hsa-miR-193a-3p	0.037839073	-2.255116553	2D is down-regula	2.746676	19.511474	5.14393	36.540776	63.636364	2q35 /// 7q36.3
hsa-miR-1260a	0.014592923	-2.252486973	2D is down-regula	4.341497	30.840561	7.252453	51.519028	72.727273	8p23.1 /// 8q12.3 /// 2
hsa-miR-532-3p	0.015136803	2.199536782	2D is up-regulatec	3.760642	26.714358	6.391693	45.404472	81.818182	9q34.11
hsa-miR-652-3p	0.001768226	2.197033168	2D is up-regulatec	2.127208	15.110979	4.284846	30.43813	36.363636	1p36.33
hsa-miR-140-3p	0.014699923	-2.05231758	2D is down-regula	3.126366	22.208667	4.382662	31.132983	81.818182	17p11.2
hsa-miR-642b-3p	0.011329406	-1.682510959	2D is down-regula	10.130089	71.9608	12.260056	87.091383	100	8p23.1

Supplementary Table 1.7 (c): The list of 147 microRNAs differentially expressed in stem cell (H9) –derived hepatocytes (day 18) and primary human hepatocytes (PHH). The RNA samples (4 replicates of PHH and 4 experimental samples of hESC-derived hepatocytes) were analysed on the Agilent miRNA platform (using Agilent's SurePrint G3 Human v16 microRNA 8x60K microarray slides; miRbase version 16.0).

	DETECTED?/SCORE			
mRNA/miRNA (Human)	**TargetScan**	**miRanda**	**DIANA**	**PicTar**
Examined				
SULT2A1/ miR-324-5p	Yes/ 96% (-0.43)	Yes/ miRSVR: -0.51	No	No
UGT1A1/miR-148a	Yes/ 93% (-0.31)	Yes/ miRSVR: -0.56	No	No
GSTT1/miR-24-3p	Yes/ 84% (-0.19)	No	No	No
Validated				
HNF4a/miR-24 (Takagi *et al*, 2010)	Yes/ (-0.48)	Yes/ miRSVR: -0.22	No	No
HNF4a / miR-34a (Takagi *et al*, 2010)	Yes/ (0.16)	Yes/ miRSVR: -0.31		
PXR/miR-148 (Takagi *et al*, 2008)	Yes/ 86% (- 0.25)	Yes/ miRSVR: -0.15	No	No
CYP3A4/miR-27b (Pan *et al*, 2009)	Yes / 56% (-0.09)	Yes/ miRSVR: -0.13	No	No
ABCC1/ miR-199a-5p (Borel *et al*, 2012)	Yes/ 99% (-0.45)	Yes/ miRSVR: -0.83	Yes/miTG:0.78	No

Supplementary Table 1.8: Computational tools for microRNA target prediction. The level of miR/ mRNA interaction studied in this project (Examined) were examined by different online tools. To validate the efficiency of these algorithms, the binding interactions of already published targets were included (Validated). The table demonstrates that TargetScan Human 6.2 tool was the most successful in predicting miR/mRNA interactions. Abbreviations: SULT2A1, sulfotransferase 2A1; UGT1A1, UDP-glucuronosyltransferase 1A1; GSTT1; glutathione S transferase theta 1; HNF4a, hepatic nuclear factor 4a; PXR, pregnane X receptor; CYP3A4; cytochrome 3A4; ABCC1, ATP-binding cassette C1; miR, microRNAs, miRSVR, miRands microRNA score; miTG; DIANA microRNA score.

REFERENCES

Acharya, A., Das., I., Chandhok, D., and Saha, T (2010) Redox regulation in cancer: a double-edged sword with therapeutic potential. *Oxidative Medicine and Cellular Longevity*. **3** (1): 23-24.

Adams, L., and Angulo, P (2006) Treatment of non-alcoholic liver disease. *Postgraduate Medical Journal*. **82**: 315-322.

Adjei, AA., Gaedigk, A., Simon, SD., Weinshilboum, RM., and Leeder, JS (2008) Interindividual variability in acetaminophen sulfation by human fetal liver: implications for pharmacogenetic investigations of drug-induced birth defects. *Birth Defects Research Part A. Clinical and Molecular Teratology*. **82**: 155-165.

Agarwal, S., Holton, KL., and Lanza, R (2008) Efficient differentiation of functional hepatocytes from human embryonic stem cells. *Stem Cells*. **26**: 1117-27.

Ahokas, JT., Nicholls, FA., Ravenscroft, PJ., and Emmerson, BT (1985) Inhibition of purified rat liver glutathione S-transferase isozymes by diuretic drugs. *Biochemical Pharmacology*. **34** (12): 2157-2161.

Akopian, V., Andrews, PW., Beil, S *et al* (2010) Comparison of defined culture systems for feeder cell free propagation of human embryonic stem cells. *In Vitro Cellular And Developmental Biology –Animal*. **46**: 247-258.

Ala, A., Walker, AP., Ashkan, K., Dooley, JS., and Schilsky, ML (2007) Wilson's disease. *The Lancet*. **9559**: 397-408.

Alcorn, J., and McNamara, PJ (2002) Ontogeny of hepatic and renal systemic clearance pathways in infants. Part 1. *Clinical Pharmacokinetics*. **41**(12): 959-998.

Alexiou, P., Maragkakis, M., Papadopoulos, GL., Reczko, M., Hatzigeorgiu, AG (2009) Lost in translation: an assessment and perspective for computational microRNA target identification. *Bioinformatics*. **25** (23): 3049-3055.

Allain, JE., Dagher, I., Mahieu – Caputo, D., Loux, N., and Androletti, M (2002) Immortalization of primate bipotent epithelial liver cells. *Proc. Natl. Acad. Sci. USA*. **99**:3639-44

Ambros, V., Bartel, B., Bartel, DP., Burge, CB., Carrington, JC., *et al* (2003) A uniform system for microRNA annotation. *RNA*. **9** (3): 277-279.

Amit, M., Margulets, V., Segev, H *et al* (2003) Human feeder layers for human embryonic stem cells. *Biology of Reproduction*. **68** (6): 2150 – 2156.

Amit, M., Shariki, C., Margulets, V., and Itskovitz – Eldor, J (2004) Feeder- layer and serum-free culture of human embryonic stem cells. *Biology of Reproduction*. **70** (3): 837 – 845.

Amit, M., Chebath, J., Margulets, V., Laevsky, I., Miropolsky, Y *et al* (2010) Suspension culture of undifferentiated human embryonic and induced pluripotent stem cells. *Stem Cell Reviews and Reports*. **6** (2): 248-59.

Antoine, DJ., Williams, DP., Kipar, A *et al* (2009) High-mobility group box-1 protein and keratin – 18, circulating serum proteins informative of acetaminophen-induced necrosis and apoptosis *in vivo*. *Toxicological Sciences*. **112**: 521-531.

Antoine, DJ., Jenkins, RE., Dear, JW., Williams, DP *et al* (2012) Molecular forms of HMGB1 and keratin-18 as mechanistic biomarkers for mode of cell death and prognosis during clinical acetaminophen hepatotoxicity. *Journal of Hepatology*. **56** (5): 1070-1079.

Antoine, DJ., Harrill, AH., Watkins, PB., and Park, KB (2014) Safety biomarkers for drug-induced liver injury – current status and future perspectives. *Toxicology Research*. **3**: 75-85.

Anglicheau, D., Pallet, N., Rabant, M., Marquet, P., Cassinat, B., Mèria, P., Beaune, P., Legendre, C., and Thervet, E (2006) Role of P-glycoprotein in cyclosporine cytotoxicity in the cyclosporine- sirolimus interactions. *Kidney International*. **70** (6): 1019-1025.

Aomatsu, E., Takahashi, N., Sawada, S *et al* (2013) Novel SCRG1/BST1 axis regulates self –renewal, and osteogenic differentiation potential in mesenchymal stem cells. *Scientific Reports*. **4** (3652).

Arslan, S., Silig, Y., and Pinarbasi, H. (2009) An investigation of the relationship between SULT1A1 Arg (213) His polymorphism and lung cancer susceptibility in a Turkish population. *Cell Biochemistry and Function*. **27** (4): 211-215.

Asahina, K., Fujimori, H., Shimizu-Saito, K., Kumashiro, Y., Okamura, K *et al* (2004) Expression of the liver – specific gene CYP7A1 reveals hepatic differentiation in embryoid bodies derived from mouse embryonic stem cells. G*enes Cells*. **9**: 1297-308.

Aurich, I., Mueller, LP., Aurich, H *et al* (2007) Functional integration of hepatocytes derived from human mesenchymal stem cells into mouse livers. *Gut*. **56**: 405-415.

Avior, Y., Ley, G., Zimerman, M *et al* (2015) Microbial – derived litocholic acid and vitamin K2 drive the metabolic maturation of pluripotent stem cells-derived and fetal hepatocytes. *Hepatology*. **62** (1): 265- 278.

Azuma, H., Paulk, N., Ranade, A *et al* (2007) Robust expansion of human hepatocytes in Fah(-/-)/Rag(-/-)/Il2rg(-/-) mice. *Nature Biotechnology*. **25**: 903-910.

Bader, AG., Brown, D., and Winkler, M (2010) The promise of microRNA replacement therapy. *Cancer Research*. **70** (18): 7027-7030.

Baek D., Villen, J., Shin, C *et al* (2008) The impact of microRNAs on protein output. *Nature*. **455** (7209): 64-71.

Bai, J., and Cederbaum, AI (2004) Adenovirus mediated overexpression of CYP2E1 increases sensitivity of HepG2 cells to acetaminophen induced cytotoxicity. *Molecular and Cellular Biochemistry*. **262**: 165-176.

Ballatori, N., Krance, SM., Notenboom, S., Shi, S., Tieu, K., and Hammond, CL (2009) Glutathione dysregulation and the ethology and progression of human diseases. *Biological Chemistry*. **390** (3): 191-214.

Banas, A., Teratani, T., Yamamoto, Y *et al* (2007) Adipose tissue – derived mesenchymal stem cells as a source of human hepatocytes. *Hepatology.* **46**: 219-228.

Barad, O., Meiri, E., Avniel, A *et al* (2004) MicroRNA expression detected by oligonucleotide microarrays: system establishment and expression profiling in human tissues. *Genome Research*. **14**: 2486 – 2494.

Barbera-Guillem, E; Arrue, JM., Ballestros, J., and Vidal-Vanaclocha, F (1986) Structural changes in endothelial cells of developing rat liver in transition from fetal to postnatal life. *Journal of Ultrastructure and Molecular Structure Research*. **97**: 197-206.

Bari K., and Fontana, RJ (2014) Acetaminophen overdose: what practitioners need to know. *Clinical Liver Disease*. **4** (1): 17-21.

Bartel, DP. (2004) MicroRNAs: Genomics, biogenesis, mechanism, and function. *Cell*. **116**:281-297.

Basma, H., Soto – Guttierez, A., Yannam, GR., Liu, L., Ito, R *et al* (2009) Differentiation and transplantation of human embryonic stem cell – derived hepatocytes. *Gastroenterology*. **136** (3): 990-99.

Battaler, R., and Brenner, D (2005) Liver fibrosis. *Journal of Clinical Investigations*. **115** (2): 209-218.

Beattie, GM., Lopez, AD., Bucay, N *et al* (2005) Activin A maintains pluripotency of human embryonic stem cells in the absence of feeder layers. *Stem Cells*. **23**: 489 – 495.

Bechmann, LP., Marquitan, G., Jochum, C *et al* (2008) Apoptosis versus necrosis rate as a predictor in acute liver failure following acetaminophen intoxication compared with acute-on-chronic liver failure. *Liver International*. **28**: 713-716.

Bender, W (2008) MicroRNAs in the *Drosophila bithorax* complex. *Genes and Development*. **22** (1): 14-19.

Benjamini, Y., and Hochberg, Y (1995) Controlling the false discovery rate: a practical and powerful approach to multiple testing. *Journal of the Royal Statistical Society: Series B.* **57**: 289-300.

Berg, T., Rountree, CB., Lee, L., Estrada, J., Sala, FG., Choe, A *et al* (2007) Fibroblast growth factor 10 is critical for liver growth during embryogenesis and controls hepatoblast survival via beta-catenin activation. *Hepatology.* **46:** 1187-1197.

Bernardini, S., Hirvonen, A., Järventaus, H., and Norppa, H (2001) Trans-stilbene oxide-induced sister chromatid exchange in cultured human lymphocytes: influence of GSTM1 and GSTT1 genotypes. *Mutagenesis*. **16** (3): 277-281.

Bessems, JG., and Vermeuelen, NP (2001) Paracetamol (acetaminophen)-induced toxicity: molecular and biochemical mechanisms, analogues, and protective approaches. *Critical Reviews in Toxicology*. **31** (1): 55-138.

Bhatia, SN., Yarmush, ML., and Torner, M (1997) Controlling cell interactions by micropatterning in co-cultures: hepatocytes and 3T3 fibroblasts. *Journal of Biomedical Material Research*. **34**: 189-199.

Bhattacharyya, SN., Habermacher, R., Martine, U., Closs, EI., and Filipowicz, W (2006) Relief of microRNA-mediated translational repression in human cells subjected to stress. *Cell*. **126** (6): 1111-1124.

Blanco, MJ., Barallo-Gimeno, A., Acloque, H., Reyes, AE *et al* (2007) Snail1a and Snail1b cooperate in the anterior migration of the axial mesoendoderm in the zebrafish embryo. *Development.* **134**: 4073-4081.

Blouin, A; Bolender, RP, and Weibel, ER (1977) Distribution of organelles and membranes between hepatocytes and nonhepatocytes in the rat liver parenchyma. A sterological study. *Journal of Cell Biology*.**72**: 441-455.

Borel, F., Han, R., Visser, A *et al* (2012) Adenosine triphosphate – binding cassette transported genes up-regulation in untreated hepatocellular carcinoma is mediated by cellular microRNAs. *Hepatology*. **55** (3): 821 – 831.

Borst, P., de Wolf, C., and van de Wetering K (2007) Multidrug resistance – associated proteins 3, 4, and 5. *Pfluger Arch*. **453**: 661-673.

Bort, R., Signore,M., Tremblay, K., Barbera, JP, and Zaret, KS (2006) Hhex homebox gene controls the transition of the endoderm to pseudostratified, cell emergent epithelium for liver bud development. *Developmental Biology*. **290**: 44-56.

Bosma, PJ. (2003) Inherited disorders of bilirubin metabolism. *Journal of Hepatology*. **38** (1):107-117.

Bossard, P., and Zaret, KS (1998) GATA transcription factors as potentiators of gut endoderm differentiation. *Development.* **125:** 4909-4917.

Bośina, N., Bradamante, V., and Lovrić, M (2009) Genetic polymorphism of metabolic enzymes P450 (CYP) as a susceptibility factor for drug response, toxicity, and cancer risk. *Arhiv za higijenu rada i toksikologiju*. **60** (2): 217-242.

Braam, SR., Zeinstra, L., Litjens, S *et al* (2008) Recombinant vitronectin is a functionally defined substrate that supports human embryonic stem cell self-renewal via alphabeta5 integrin. *Stem Cells*. **26** (9): 2257-2265.

Breving K., and Esquela – Kerscher, A. (2010) The complexities of microRNA regulation: mirandering around the rules. *The International Journal of Biochemistry and Cell Biology*. **42:** 1316-1329.

Brinkmann, U., and Eichelbaum, M (2001) Polymorphisms in the ABC drug transporter gene *MDR1*. *The Pharmacogenomics Journal*. **1**: 59-64.

Brok, J., Buckley, N., Gluud, C (2006) Intervensions for paracetamol (acetaminophen) overdose. *Cochrnae Database of Systemic Reviews*. CD003328

Brolen, G., Sivertsson, L., Björquist, P., Eriksson, G *et al* (2010) Hepatocyte-like cells derived from human embryonic stem cells specifically via definitive endoderm and a progenitor stage. *Journal of Biotechnology*. **145**: 284-294.

Burchell, B., Brierley, CH., Rance, D. (1995) Specificity of human UDP-gluruconosyltransferases and xenobiotic glucuronidation. *Life Sciences*. **57** (20). 1819-1831.

Burkhart, KK., Janco, N., Kulig, KW *et al* (1995) Cimetidine as adjunctive treatment for acetaminophen overdose. *Human and Experimental Toxicology*. **14**:299-304

Cai, J., Ito, M., Westerman, KA., Kobayashi,N., Leboulch, P., Fox, IJ (2000) Construction of non- tumorigenic rat hepatocyte cell line for transplantation: reversal of hepatocyte immortalization by site-specific excision of the SV40 T antigens. *Journal of Hepatology*. **33**:701-708.

Cai, J., Chen, J., Liu, Y *et al* (2006) Assesing self-renewal and differentiation in human embryonic stem cell lines. *Stem Cells (Dayton, Ohio)*. **24** (3): 516-530.

Cai, J., Zhao, Y., Liu, Y., Ye,F., Song, Z *et al* (2007) Directed differentiation of human embryonic stem cells into functional hepatic cells. *Hepatology*. **45**: 1229-39.

Calmont, A., Wandzioch, E., Tremblay, KD., Minowada, G *et al* (2006) An FGF response pathway that mediates hepatic gene induction in embryonic endoderm cells. *Developmental Cell*. **11** (3): 339-348.

Caraco, Y., Sheller, J., and Wood, AJ (1997) Pharmacogenetic determinants of codeine induction by rifampin; the impact on codein's respiratory, psychomotor and miotic effects. *Journal of Pharmacology and Experimental Therapeutics*. **281** (1): 330-336.

Carpenter, MK., Rosler, ES., Fisk, GJ (2004) Properties of four human embryonic stem cell lines maintained in a feeder – free culture system. *Developmental Dynamics*. **229**: 243 – 258.

Chalasani, N., and Björnsson, E (2010) Risk factors of idiosyncratic drug-induced liver injury. *Gastroenterology*. **138** (7): 2246-2259.

Chang, J., Nicolas, E., Marks, D *et al* (2004) miR-122, a mammalian liver-specific microRNA, is processed from hcr mRNA and mat downregulate the high affinity cationic amino acid transporter CAT-1. *RNA Biology*. **1**(2): 106-113.

Chang, CY., and Schiano, TD (2007) Review article: drug hepatotoxicity. *Alimentary Pharmacology Therapeutics*. **25**: 1135-1151.

Chang, TC., Wentzel, EA., Kent, OA., Ramachandran, K., Mullendore, M., Lee, KH *et al* (2007) Transactivation of miR-34a by p53 broadly influences gene expression and promotes apoptosis. *Molecular Cell*. **26** (5): 745-752.

Chang, TC., Yu, D., Lee, YS., Wentzel, EA., Arkin, DE., West, KM *et al* (2008) Widespread microRNA repression by Myc contributes to tumorigenesis. *Nature Genetics*. **40** (1): 43-50.

Chao, P., Maguire, T., Novik, E *et al* (2009) Evaluation of microfluidic based cell culture platform with primary human hepatocytes for the prediction of hepatic clearance in human. *Biochemical Pharmacology*. **78**: 625-632.

Chase, LG., and Firpo, M. (2007) Development of serum-free culture systems for human embryonic stem cells. *Current Opinion in Chemical Biology*. **11**: 367 – 372.

Chen, SY., Wang, Y., Telen, MJ., and Chi, JT (2008) The genomic analysis of erythrocyte microRNA expression in sickle cell disease. *PloS ONE*. **3**: e2360.

Chen, Y., Tseng, H., Kuo, W., Yang, S., Chen, DR., and Tsai, HT (2010) Glutathione-S-Transferases P1 (GSTP1) gene polymorphism increases age-related susceptibility to hepatocellular carcinoma. *BMC Medical Genetics*. **11**:46.

Chen, G., Gulbranson, DR., Hou, Z *et al* (2011) Chemically defined conditions for human iPS cell derivation and culture. *Nature Methods*. **8** (5): 424-429.

Chen, CH. (2012) Activation and Detoxification Enzymes. Functions and Implications. Springer. DOI 10.1007/978-1-4614-1049-2_2.

Cheng, Z., Radominska-Pandya, A., and Tephly, TR (1999) Studies on the substrate specificity of human intestinal UDP- glucuronosyltransferases 1A8 and 1A10. *Drug Metabolism and Disposition.* **27**: 1165-1170.

Cheng, L., Hammong, H., Ye, Z *et al* (2003) Human adult marrow cells supported prolonged expansion of human embryonic stem cells in culture. *Stem Cells*. **21** (2): 131-142.

Chendrimada, TP., Gregory, RI., Kumaraswamy, E., Norman, J., Cooch, N., Nishikura, K., and Shiekhattar, R (2005) TRBP recruits the Dicer complex to Ago2 for microRNA processing and gene silencing. *Nature*. **436**: 740-744.

Choi, JS., Choi, I., Choi, DH (2013) Effects of nifedipine on the pharmacokinetics of repaglinide in rats: Possible role of CYP3A4 and P-glycoprotein inhibition by nifedipine. *Pharmacological Reports*. **65**. 1422-1430.

Chong, VH (2007) Acetaminophen overdose and N-acetylcysteine therapy. *Annals Academy of Medicine Singapore*. **36**:704.

Chun, LJ., Tomg, MJ., Busutti, RW., and Hiatt, JR (2009) Acetaminophen hepatotoxicity and acute liver failure. *Journal of Clinical Gastroenterology*. **43** (4): 342-349.

Chung, WS., Shin,CH., and Stainier, DY (2008) BMP2 signalling regulates the hepatic versus pancreatic fate decision. *Developmental Cell*. **15** (5): 738-748.

Coffman, BL., King, CD., Rios, GR., and Tephly TR. (1998) The glucuronidation of opioids, other xenobiotics, and androgens by human UGT2B7Y (268) and UGT2B7H (268). *Drug Metabolism and Disposition.* **26** (1):73-77.

Comer, KA., Falany, JL., and Falany, CN (1993) Cloning and expression of human liver dehydroepiandrosterone sulphotransferase. *Biochemical Journal*. **289** (Pt1):233-240.

Conlon, FL., Lyonos, KM., Takaesu,N., Barth, KS., Kispert, A., Herrmann, B., and Roberston, EJ (1994) A primary requirement for nodal in the formation and maintenance of the primitive streak in the mouse. *Development.* **120:** 1919-1928.

Conrad, S., Kauffmann, HM., Ito, K *et al* (2002) A naturally occurring mutation in MRP1 results in a selective decrease in organic anion transport and in increased doxorubicin resistance. *Pharmacogenetics*. **12**:321-330.

Coughtrie, MW., Burchell, B., Leakey, JE., and Hume R (1988) The inadequacy of perinatal glucuronidation: immunoblot analysis of the development expression expression of individual UDP-glucuronosyltransferase isoenzymes in rat and human liver mocrosomes. *Molecular Pharmacology*. **34** (6): 729-735.

Court, MH., Freytis, M., Wang, X et al (2013) The UDP-glucuronosyltransferase (UGT) 1A polymorphism c.2042C>G (rs8330) is associated with increased human liver acetaminophen glucuronidation, increased UGT1A Exon 5a/5b splice variant mRNA ratio, and decreased risk of unintentional acetaminophen-induced acute liver failure. *Journal of Pharmacology and Experimental Therapeutics*. **345**: 297-307.

Craft, AW., Brochlebank, JT., Hey, EN., and Jackson, RH (1974) The 'gray toddler': chloramphenicol toxicity. *Archives of Disease in Childhood*. **49**: 235-237.

Craig, DG., Lee, P., Pryde, EA; Hayes, PC., and Simpson, KJ (2013) Serum ne *Alimentary Pharmacology and Therapeutics*. **38**: 1395-1404.

Cummings, J., Hodgkinson, C., Odedra, R., Sini, P *et al* (2008) Preclinical evaluation of M30 and M65 ELISAs as biomarkers of drug induced tumour cell death and antitumour activity. *Molecular Cancer Therapy*. **7**(3): 455-463.

Daige, CL., Wiggins, JF., Priddy,L., Nelligan – Davis, T., Zhao, J., and Brown, D (2014) Systemic delivery of a miR-34a mimic as a potential therapeutic for liver cancer. *Molecular Cancer Therapeutics.* **13** (10): 2352-2360.

Dajani, R., Hood, AM., and Coughtrie, MW (1998) A single amino acid, glu146, governs the substrate specificity of a human dopamine sulfotransferase, SULT1A3. *Molecular Pharmacology*. **54** (6): 942-948.

Dalgetty, D., Medine, C., Iredale, JP., and Hay, DC (2009) Progress and future challenges in stem cell – derived future technologies. *American Journal of Physiology. Gastrointestinal and liver physiology*. **297** (2): G241-48.

Dandara, C., Swart, M., Mpeta, B *et al* (2014) Cytochrome P450 pharmacogenetics in African populations: implications for public health. *Expert Opinion in Drug Metabolism and Toxicology*. **10**: 769-785.

D'Amour, KA., Agulnick, AD., Eliazer, S., Kelly OG., Kroon, F., and Baetge, EE (2005) Efficient differentiation of human embryonic stem cells to definitive endoderm. *Nature Biotechnology.* **23**: 1534-1541.

Darlington, GJ (1999) Molecular mechanisms of liver development and differentiation. *Current Opinion in Cell Biology*. **11**: 678-682.

Darnell, DK., Kaur, S., Stanislaw, S., Konieczka, JH., Yatskievych, TA., and Antin, PB (2006) MicroRNA expression during chick embryo development. *Developmental Dynamics*. **235** (11): 3156-3165.

Delgado, JP., Paraouchev, A., Allain, JE., Pennarum, G., Gauthier, LR *et al* (2005) Long-term controlled immortalization of primate hepatic progenitor cell line after Simian virus 40 T – antigen gene transfer. *Oncogene*. **24**: 541-51.

Denli, AM., Tops, BB., Plasterk, RH., Ketting, RF., and Hannon, GJ (2004) Processing of primary microRNAs by the Microprocessor complex. *Nature.* **432**: 231-235.

De Santi, C., Pietrabissa,A., Mosca, F., Rane, A., and Pacifici GM (2002) Inhibition of phenol suloftransferase (SULT1A1) by quercetin in human adult and foetal livers. *Xenobiotica.* **32** (5): 363-368.

Dessimoz, J., Opoka, R., Kordich, JJ., Grapin-Botton, A., and Wells, JM (2006) FGF signalling is necessary for establishing gut tube domains along the anterior – posterior axis *in vivo*. *Mechanism of Development*. **123**: 42-55.

Deutsch, G., Jung, J., Zheng, M., Lora, J., and Zaret, KS (2001) A biopotential precursor population for pancreas and liver within the embryonic endoderm. *Development.* **128**: 871-881.

Djuranovic, S., Nahvi, A., and Green, R (2012) miRNA – mediated gene silencing by translational repression followed by mRNA deadenylation and decay. *Science*. **336** (6078): 237-240.

Dluzen, DF., Dun, D., Salzber, AC *et al* (2014) Regulation of UDP-glucuronosyltransferase 1A1 expression and activity by microRNA 491-3p. *Journal of Pharmacology and Experimental Therapeutics.* **348**: 465-477.

Dongning, HE., Meloche, CA., Dumas, NA., Frost, AR., and Falany, CN (2004) Different subcellular localization of sulphotransferase 2B1b in human placenta and prostate. *Biochemical Journal*. **379** (3): 533-540.

Donovan, PJ., and Gearhart, J (2001) The end of the beginning for pluripotent stem cells. *Nature*. **414**: 92-97.

Dougan, ST., Warga, RM., Kane, DA., Schier, AF.,and Talbot, WS (2003) The role of the zebrafish nodal-related genes squint and cyclops in patterning of mesendoderm. *Development*. **130**: 1837-1851.

Doyle, LA., Ross, DD (2003) Multidrug resistance mediated by the breast cancer resistance protein BCRP (ABCG2). *Oncogene*. **22**: 7340-7358.
Du, Y., Chia, SM., Han, R *et al* (2006) 3D hepatocyte monolayer on hybrid RGD/galactose substratum. *Biomaterials*. **27**: 5669-5680.

Du, Y., Wang, J., Jia, J., Song, N *et al* (2014) Human hepatocytes with drug metabolic function induced from fibroblasts by lineage reprogramming. *Cell Stem Cell*. **14**: 394-403.

Duan, Y., Catan, A., and Meng, Y (2007) Differentiation and enrichment of hepatocyte-like cells from human embryonic stem cells *in vitro* and *in vivo*. *Stem Cells*. **25**: 3058-68.

Duan, Y., Ma, X., Zou, W., Wang, C., Bahbahan, IS., Ahuja, TP., Toistikov, V., and Zern, MA (2010) Differentiation and characterization of metabolically functioning hepatocytes from human embryonic stem cells. *Stem Cells*. **28** (4): 678-86.

Duanmu, Z., Weckle, A., Koukouritaki, SB *et al* (2006) Developmental expression of aryl, estrogen, and hydroxysteroid sulfotransferases in pre- and postnatal human liver. *Journal of Pharmacology and Experimental Therapeutics*. **316** (3): 1310-1317.

Duffield, S., Forbes, SJ., Constandinou, C., Clay, S., Partolina, M (2005) Selective depletion of macrophages reveals distinct, opposing roles during liver injury and repair. *Journal of Clinical Investigation.* **115** (1): 56-65.

Duncan,S., and Watt, J (2001) BMPs on the road to hepatogenesis. *Genes and Development.* **15**: 1879-1881.

Ehmer, U., Lankisch, TO., Erichsen, TJ., Kalthoff, S., Freiberg, N., Wehmeier, M., Manns, MP., Strassburg, CP (2008) Rapid allelic discrimination by TaqMan PCR for the deletion of the Gilbert's syndrome marker UGT1A1*28. *Journal of Molecular Diagnostics*. **10** (6): 549-552.

Ek, M., Soderdahal, T., Kuppers-Munther, B., Edsbagge, J *et al* (2007) Expression of drug metabolizing enzymes in hepatocyte-like cells derived from human embryonic stem cells. *Biochemical Pharmacology*. **74**: 496-503.

El Hassan, H., Anwar, K., Macanas-Pirard, P *et al* (2003) Involvement of mitochondria in acetaminophen-induced apoptosis and hepatic injury: roles of cytochrome c, Bax, Bid, and caspases. *Toxicology and Applied Pharmacology*. **191**: 118-129.

Elmen, J., Lindow, M., Schütz, S., Lawrence, M., Petri, A *et al* (2008) LNA-mediated microRNA silencing in non-human primates. *Nature*. **452**: 896-899.

Enosawa, YTS., Jomura, T., Ozeki, E *et al* (20110 JSSX Annual Meeting; Hiroshima, Japan.

Esau, C., Davis, S., Murray, SF., Yu, XX., Pandey, SK., *et al* (2006) miR-122 regulation of lipid metabolism revealed by *in vivo* antisense targeting. *Cell Metabolism*. **3** (2): 87-98.

Esau, CC (2008) Inhibition of microRNA with antisense oligonucleotides. *Methods*. **44** (1): 55-60.

Evans, MJ., and Kaufman, MH (1981) Establishment in culture of pluripotent cells from mouse embryos. *Nature*. **292** (5819): 154 – 156.

Fabian, MR., Sonenberg, N., and Filipowicz W (2010) Regulation of mRNA translation and stability by microRNAs. *Annual Review of Biochemistry*. **79**: 351-379.

Falany, CN., Krasnykh,V., and Falany, JL (1995) Bacterial expression and characterization of a cDNA for human liver estrogen sulfotransferase. *Journal of Steroid Biochemistry and Molecular Biology*. **52** (6): 529-539.

Faulkner, L., Martinsson, K., Santoyo-Castelazo, A *et al* (2012) The development of *in vitro* culture methods to characterize primary T-cell responses to drugs. *Toxicological Sciences*. **127**: 150-158.

Feretti, E., De Smaele, E., Miele, E., Laneve, P *et al* (2008) Concerted microRNA control of Hedgehog signalling in cerebellar neuronal progenitor and tumour cells. *EMBO Journal*. **27**(19): 2616-2627.

Filipowicz, W., Bhattacharyya, SN., and Sonenberg, N (2008) Mechanisms of post-transcriptional regulation by microRNAs: are the answers in sight? *Nature Reviews Genetics*. **9**: 102-114.

Fletcher, J., Cui, W., Samuel, K *et al* (2008) The inhibitory role of stromal cell mesenchyme on human embryonic stem cell hepatocyte differentiation is overcome by Wnt3a treatment. *Cloning Stem Cells*. **10** (3): 331-339.

Fontana, RJ (2008) Acute liver failure including acetaminophen overdose. *Medical Clinics of North America*. **97** (4):761-794.

Fontana, RJ (2014) Pathogenesis of idiosyncratic drug-induced liver injury and clinical perspectives. *Gastroenterology*. **146**: 914-928.

Friedman, RC., Farh, KK., Burge, CB., and Bartel, DP (2009) Most mammalian mRNAs are conserved targets of microRNAs. *Genome Research*. **19**: 92-105.

Fu, H., Tie,Y., Xu, C *et al* (2005) Identification of human fetal liver miRNAs by a novel method. *FEBS Letters*. **579**: 3849 – 3854.

Fugelseth, D., Lindemann, R., Liestøl, K., Kiserud, T., and Langslet, A (1998) Postnatal closure of ductus venosus in preterm infants ≤ 32 weeks: an ultrasonographic study. *Early Human Development*. **53**(2): 163-169.

Fujita, K., Nagata, K., Ozawa, S., Sasano, H., and Yamazoe, Y. (1997) Molecular cloning and characterisation of rat ST1B1 and human ST1B2 cDNAs, encoding thyroid hormone sulfotransferases. *Journal of Biochemistry*. **122** (5): 1052-1061.

Fukuda, M., Kawahara, Y., Hirota, T., Akizuki, S *et al* (2010) Genetic polymorphism of hepatic ABC – transporter in patients with hepatocellular carcinoma. *Journal of Cancer Therapy.* **1**: 114-123.

Fukui, A., Goto, T., Kitamoto, J., Homma, M., and Asashima, M (2007) SDF-1 alpha regulates mesendodermal cell migration during frog gastrulation. *Biochemical and Biophysical Research Communications.* **354:** 472-477.

Funakoshi, N., Duret, C., Pascussi, JM., Blanc, P *et al* (2011) Comparison of hepatic-like cell production from human embryonic stem cells and adult liver progenitor cells: CAR transduction activates a battery of detoxification genes. *Stem Cell Reviews*. **7** (3): 518-531.

Gamage, N., Barnett, A., Hempel, N., Duggleby, RG., Windmill, KF., Martin, JL., McManus, ME. (2006) Human sulfotransferases and their role in chemical metabolism. *Toxicological Sciences*. **90** (1): 5-22.

Garcia, NP., Lores, OF., Portuonodo Fuentes, D *et al* (2014) Reduction of hepatotoxicity induced by acetaminophen overdoses in a mouse model of inflammation induced by Freunds' adjuvants. *Journal of Allergy and Therapy*. doi: 10.4172/2155-6121.1000183.

Geese, WJ., and Raftogianis, RB (2001) Biochemical characterization and tissue distribution of human SULT2B1. *Biochemical and Biophysical Research Communications*. **288** (1): 280-289.

Gerets, HH., Tilmant, K., Gerin, B *et al* (2012) Characterization of primary human hepatocytes, HepG2 cells, and HepaRG cells and the mRNA level and CYP activity in response to inducers and their predictivity for the detection of human hepatotoxins. *Cell Biology and Toxicology*. **28**: 69-87.

Gibbings, DJ., Ciaudo, C., Erhardt, M., and Voinnet, O (2009) Multivescular bodies associate with components of miRNA effector complexes and modulate miRNA activity. *Nature Cell Biology*. **11**: 1143-1149.

Gieseck III, RL., Hannan, NRF., Bort, R *et al* (2014) Maturation of induced pluripotent stem cell derived hepatocytes by 3D –culture. *PLOS One*. **9** (1): e86372.

Gines, P., Cardenas, A., Arroyo, V., and Rodes, J (2004) Management of cirrhosis and ascites. *The New England Journal of Medicine*. **350**: 1646-54.

Glatt, H., and Meinl, W (2004) Pharmacogenetics of soluble sulfotransferases (SULTs). *Naunyn – Schmiedeberg's Archives of Pharmacology*. **369** (1): 55-68.

Godoy, P., Hewitt, NJ., Albrecht, U *et al* (2013) Recent advances in 2D and 3D *in vitro* systems using primary hepatocytes, alternative hepatocyte sources and non-parenchymal liver cells and their use in investigating mechanisms of hepatotoxicity, cell signalling and ADME. *Archives of Toxicology*. **87**: 1315-1530.

Godoy, P., Schmidt-Heck, W., Natarajan, K *et al* (2015) Gene networks and transcription factor motifs defining the differentiation of stem cell into hepatocyte –like cells. *Journal of Hepatology*. doi: 10.1016/j.hep.2015.05.013.

Gonzalez, F., and Tukey, R. Drug Metabolism, In: Goodman and Gilman's, The Pharmacological Basis of Therapeutics, 11th Edition, 2005, Chapter 3.

Gonzalez, FJ (2008) Regulation of hepatocyte nuclear factor 4 alpha-mediated transcription. *Drug Metabolism and Pharmacokinetics*. **23** (1): 207

Gow, PJ., Ghabrial, H., Smallwood, RA., Morgan, DJ., and Ching, MS (2000) Neonatal hepatic drug elimination. *Pharmacology and Toxicology*. **88**: 3-15.

Gramantieri, L., Fornari, F., Callegari, E., Sabbioni, S., Lanza, G *et al* (2008) MicroRNA involvement in hepatocellular carcinoma. *Journal of Cellular and Molecular Medicine*. **12**: 2189-2204.

Grapin – Botton, A. Endoderm specification (November 30, 2008), StemBook, ed. The Stem Cell Research Community, StemBook, doi/10.3824/stembook.1.30.1. http://www.stembook.org.

Greber, B., Lehrach, H., and Adjaye, J (2007) Fibroblast growth factor 2 modulates transforming growth factor beta signalling in mouse embryonic fibroblasts and human ESCs (hESCs) to support hESC self –renewal. *Stem Cells*. **25**: 455 – 464.

Gregory, PA., Lewinsky, RH., Gardner- Stephen, DA., Mackenzie, PI. (2004) Regulation of UDP glucuronosyltransferases in the gastrointestinal tract. *Toxicology and Applied Pharmacology*. **199**: 354-363.

Grijalva, J., and Vakili, K (2013) Neonatal liver physiology. *Seminars in Pediatric Surgery*. **22**: 185-189.

Grimson, A., Farh, KK., Johnston, WK., Garrett-Engele, P., Lim, LP., and Bartel, DP (2007) MicroRNA targeting specificity in mammals: determinants beyond seed pairing. *Molecular Cell*. **27**: 91-105.

Grubbs, F (1969) Procedures for detecting outlying observations in samples. *Technometrics*. **11** (1): 1-21.

Gualdi, R., Bossard, P., Zheng, M., Hamada, Y., Coleman, JR., and Zaret, KS (1996) Hepatic specification of the gut endoderm *in vitro*: cell signalling and transcriptional control. *Genes and Development*. **10**: 1670-1682.

Guillouzo, A., Corlu, A., Aninant, C., Glaise, D., Morel, F., and Guguen – Guillouzo, C (2007) The human hepatoma HepaRG cells: a highly differentiated model for studies of liver metabolism and toxicity of xenobiotics. *Chemico-Biological Interactions*. **168** (1): 66-73.

Gujral, JS., Knight, TR., Farhood, A *et al* (2002) Mode of cell death after acetaminophen overdose in mice: apoptosis or oncotic necrosis? *Toxicological Sciences*. **67**: 322-328.

Gunness, P., Mueller, D., Shevchenko, V *et al* (2013) 3D organotypic cultures of human HepaRG cells, a tool for *in vitro* toxicity studies. *Toxicological Sciences*. **133**: 67-78.

Gupta, A., Gartner, JJ., Sethupathy, P., Hatzigeorgiou, AG., and Fraser, NW (2009) Anti-apoptotic function of microRNA encoded by the HSV-1 latency –associated transcript. *Nature*. **442**: 82-85.

Halegoua-De Marzio, D., and Navarro, VJ (2008) Drug-induced hepatotoxicity in humans. *Current Opinion in Drug Discovery Development.* **11**:53-59.

Han, L., Witmer, PD., Casey, E., Valle, D., and Sukumar, S (2007) DNA methylation regulates microRNA expression. *Cancer Biology and Therapy*. **6**(8): 1284-1288.

Hannan, NRF., Segeritz, CP., Touboul, T., and Vallier, L (2013) Production of hepatocyte – like cells from human pluripotent stem cells. *Nature Protocols*. **8**: 430 – 437.

Hannoun, Z (2011) The role of SUMO modification in hepatocyte differentiation. PhD dissertation. University of Edinburgh.

Haugen, G., Hanson, M., Kiserud, T., Crozier, S., Inskip, H., Godfrey, KM (2005) Fetal liver-sparing cardiovascular adaptations linked to mother's slimness and diet. *Circulation Research*. **96** (1): 12-14.

Hay, DC., Zhao, D., Ross, A., Mandalam, R., Lebkowski, J., and Cui, W (2007) Direct differentiation of human embryonic stem cells to hepatocyte-like cells exhibiting functional activities. *Cloning Stem Cells*. **9** (1): 61-62.

Hay, DC., Fletcher, J., Payne, C., Terrace, JD., Gallagher, RC *et al* (2008a) Highly efficient differentiation of hESCs to functional hepatic endoderm requires Activin A and Wnt3a signalling. *Proc. Natl. Acad. Sci. USA*. **105**: 12301-6.

Hay, DC. (2010) Cadaveric hepatocytes repopulate diseased livers: after death. *Gastroenterology*. **139** (3): 729-31.

Hay, DC., Perngallo, S., Diaz-Mochon, J., Medine, C., Greenhough, S *et al* (2011) Unbiased screening of polymer libraries to define novel substrates for functional hepatocytes with inducible drug metabolism. *Stem Cell Research*. **6**: 92-102.

Hay, DC., Zhao, D., Fletcher, J., Hewitt, Z., McLean, D *et al* (2008b) Efficient differentiation of hepatocytes from human embryonic stem cells exhibiting markers recapitulating liver development *in vivo*. *Stem Cells*. **26** (4): 894-902.

Hayes, JD., and Strange RC (2000) Glutathione S- transferase polymorphisms and their biological consequences. *Pharmacology*. **61** (3): 154-166.

Hannoun, Z., Fletcher, J., Greenhough, S., Medine, CN., Samuel, K *et al* (2010) The comparison between conditioned media and serum-free media in human embryonic stem cell culture and differentiation. *Cell Reprogramming*. **12** (2): 133-40.

Hariparsad, N., Carr, BA., Evers, R., and Chu, X (2008) Comparison of immortalized Fa2N-4 cells and human hepatocytes as *in vitro* models for cytochrome P450 induction. *Drug Metabolism and Disposition*. **36** (6):1046-55.

He, D., Frost, AR., Falany, CN (2005) Identification and immunohistochemical localization of Sulfotransferase 2B1b (SULT2B1b) in human lung. *Biochimica et Biophysica Acta*. **1724** (1-2): 119-126.

Heidet, L., and Gubler, MC (2009) The renal lesions of Alport Syndrome. *Journal of the American Society of Nephrology*. **20** (6): 1210-1215.

Hempel, N., Wang, H., LeCluyse, EL., McManus, ME., and Negishi, M (2004) The human sulfotransferase SULT1A1 gene is regulated in a synergistic manner by Sp1 and GA binding protein. *Molecular Pharmacology*. **66** (6): 1690-1701.

Henke, JI., Goergen, D., Zheng, J., Song, Y., Schüttler, CG., Fehr,C., Jünneman, C., and Niepmann, M (2008) microRNA-122 stimulates translation of hepatitis C virus RNA. *The EMBO Journal*. **27**: 3300-3310.

Henkel, AS., Gooijert, KE., Havinga, R *et al* (2013) Hepatic overexpression of Abcb11 in mice promotes the conservation of bile acids within the enterohepatic circulation. *American Journal of Physiology. Gastrointestinal and Liver Physiology*. **304** (2): G221-G226.

Hines, RN., and McCarver, DG (2002) The ontogeny of human drug-metabolizing enzymes: phase I oxidative enzymes. *Journal of Pharmacology and Experimental Therapeutics*. **300**: 355-360.

Hinson, JA., and Forkert, PG (1995) Phase II enzymes and bioactivation. *Canadian Journal of Physiology and Pharmacology*. **73** (10): 1407-1413.

Hinson, JA., Roberts, DW., and James, LP (2010) Mechanisms of acetaminophen-induced liver necrosis. *Handbook of Experimental Pharmacology*. **196**: 369-405.

Hirrlinger, J., Konig, J., Keppler, D *et al* (2001) The multidrug resistance protein MRP1 mediates the release of glutathione disulphide from rat astrocytes during oxidative stress. *Journal of Neurochemistry*. **76**: 627-636.

Holmgren, G., Sjögren, AK., Barragan, I., Sabirsh, A *et al* (2014) Long – term chronic toxicity testing using human pluripotent stem cell – derived hepatocytes. *Drug Metabolism and Disposition*. **42**: 1401-1406.

Hoffman, LM., and Carpenter, MK (2005) Characterization and culture of human embryonic stem cells. *Nature Biotechnology*. **23** (6): 699-708.

Hoofnagle, JH., Carithers, RL., Shapiro C., *et al* (1995) Fulminant hepatic failure: summary of a workshop. *Hepatology*. **21**: 240-252.

Hooijberg, JH., Broxterman, HJ., Kool, M., Assaraf, YG., Peters, GJ., Noordhuis, P., Scheper, RJ., Borst, P., Pinedo, HM., and Jansen, G (1999) Antifolate resistance mediated by the multidrug resistance proteins MRP1 and MRP2. *Cancer Research.* **59** (11): 2532-2535.

Hou, W., Tian, Q., Zheng, J., and Bonkovsky, HL (2010) MicroRNA-196 represses Bach1 protein and hepatitis C virus gene expression in human hepatoma cells expressing hepatitis C viral proteins. *Hepatology*. **51**: 1494-1504.

Hu, Y., Oscarson, M., Johansson, I *et al* (1997) Genetic polymorphisms of human CYP2E1, characterization of two variant alleles. *Molecular Pharmacology*. **51**: 370 – 376.

Huang, SK., Chiu, AW., Pu, YS., Huang, YK., Chung, CJ., Tsai, HJ., Yang, MH., Chen, CJ., and Hsueh, YM (2009) Arsenic methylation capability, myeloperoxidase and sulfotransferase genetic polymorphisms, and the stage and grade of urothelial carcinoma. *Urologia Internationalis*. **82** (2):227-234.

Huang, P., He, Z., Ji, S., Sun, H., Wang, X and Hui, L (2011) Induction of functional hepatocyte-like cells from mouse fibroblast by defined factors. *Nature*. **475**: 386-89.

Huang, Q., Deshmukh, RS., Ericksen, SS., and Szklarz, GD (2012) Preferred binding orientation of phenacetin in CYP1A1 and CYP1A2 are associated with isoform-selective metabolism. *Drug Metabolism and Disposition*. **40** (12): 2324-2331.

Huang, P., Zhang, L., Gao, Y., He, Z *et al* (2014) Direct reprogramming of human fibroblasts to functional and expandable hepatocytes. *Cell Stem Cell*. **14**: 370-384.

Huch, M., Dorrell, C., Boj, SF., Van Es, JH., Li, VSW *et al* (2013) *In vitro* expansion of single Lgr5+ liver stem cells induced by Wnt-driven regeneration. *Nature.* **494**: 247-250.

Huch, M., Gehart, H., Van Boxtel, R., Hamer, K *et al* (2015) Long-term culture of genome-stable bipotent stem cells from adult human liver. *Cell*. **160**: 299-312.

Huelsken, J., Vogel, R., Brinkmann, V., Erdmann, B., Birchmeier, C., and Birchmeier, W (2000) Requirements for β-catenin and anterior-posterior axis formation in mice. *Journal of Cell Biology*. **148:**567-578.

Hulot, JS., Villard, E., Maguy, A *et al* (2005) A mutation in the drug transporter gene ABCC2 associated with impaired methotrexate elimination. *Pharmacogenet Genomics*. **15**: 277.

Hustert, E., Zibat, A., Presecan – Siedel, E., Eiselt, R. *et al* (2001) Natural protein variants of pregnane X receptor with altered transactivation activity toward CYP3A4. *Drug Metabolism and Disposition*. **29**: 1454-1459.

Hwang, HW., and Mendell, JT (2006) MicroRNAs in cell proliferation, cell death, and tumorigenesis. *British Journal of Cancer*. 94: 776-780.

Ieiri, I., Tainaka, H., Morita, T et al (2000) Catalytic activity of three variants (Ile, Leu, and Thr) at amino acid residue 359 in human CYP2C9 gene and simultaneous detection using single-strand conformation polymorphism analysis. *Therapeutic Drug Monitoring*. **22**: 237-244.

Ingelman-Sunberg, M., Daly, A.K., and Nebert, D.W (2007) Home Page of the Human Cytochrome P450 (CYP) Allele Nomenclature Committee, http://www.cypalleles.ki.se.

Iredale, JP (2007) Models of liver fibrosis exploring the dynamic nature of inflammation and repair in a solid organ. *Journal of Clinical Investigation*. **117**(3): 539-48.

Ishii, T., Fukumitsu, K., Yasuchika, K., Adachi, K., Kawase, E., Suemori, H., Nakatsuji, N., Ikai,I., and Uemoto, S (2008) Effects of extracellular matrixes and growth factors on the hepatic differentiation of human embryonic stem cells. *American Journal of Physiology. Gastrointestinal and Liver Physiology*. **295**: 313-321.

Ishii, T., Yasuchika, K., Fukumitsu, K., Kawamoto, T., Kawamura-Saitoh, M., Amagai, Y., Iaki, I., Uemoto, S., Kawase, E., Suemori, H., and Nakatsuji, N (2010) *In vitro* hepatic maturation of human embryonic stem cells by using a mesenchymal cell line derived from murine fetal livers. *Cell and Tissue Research*. **339**: 505-512.

Ishii, T., and Mann, GE (2014) Redox status in mammalian and stem cells during culture *in vitro*: critical roles of Nrf2 and cysteine transporter activity in the maintenance of redox balance. *Redox Biology*. **2**: 786-794.

Ishikawa, KS., Masui, T., Ishikawa, K., and Shiojiri (2001) Immunolocalization of hepatocyte growth factor and its receptor (c-Met) during mouse liver development. *Histochemistry and Cell Biology*. **116**: 453-462.

Iwamura, A., Fukami, T., Hosomi, H *et al* (2011) CYP2C9-mediated metabolic activation of losartan detected by a highly sensitive cell-based screening assay. *Drug Metabolism and Disposition*. **39** (5): 838-846.

Jackson, JE (1991) A user's guide to principal component. *New York: John Wiley and Sons.*

Jaeschke, H., and Bajt, ML (2006) Intracellular signalling mechanisms of acetaminophen-induced liver cell death. *Toxicological Sciences*. **89** (1): 31-41.

Jaeschke H, McGill MR, Ramachandran A. (2012) Oxidant stress, mitochondria, and cell death mechanisms in drug-induced liver injury: lessons learned from acetaminophen hepatotoxicity. *Drug Metab Rev.*, **44** (1):88-106.

James, D., Levine, AJ., Besser, D *et al* (2005) TGFbeta/activin/nodal signalling is necessary for the maintenance of pluripotency in human embryonic stem cells. *Development*. **132**: 1273 – 1282.

Jancova, P., Anzenbacher,P., and Anzenbacherova, E. (2010) Phase II Drug Metabolism Enzymes. *Biomedical Papers of the Medical Faculty of the University of Palacky, Olomouck, Czech Republic*. **154** (2): 103-116.

Jedlitschky, G., Leier, I., Buchholz, U., Hummel-Eisenbeiss, J., Burchell, B., and Keppler, D (1997) ATP-dependent transport of bilirubin glucuronides by the multidrug resistance protein MRP1 and its hepatocyte canalicular isoform MRP2. *Biochemical Journal*. **327**: 305-310.

John, B., Enright, AJ., Aravin, A *et al* (2004) Human microRNA targets. *PLoS Biology*. **2** (11): e363.

Johnsrud, EK., Koukouritaki, SB., Divakaran, K *et al* (2003) Human hepatic CYP2E1 expression during development. *Journal of Pharmacology and Experimental Therapeutics*. **307**: 402 – 407.

Jopling, CI., Yi, Y., Lancaster, AM., Lemon, SM., and Sarnow, P (2005) Modulation of hepatitis C virus RNA abundance by a liver-specific microRNA. *Science*. **309**: 1577-1581.

Jozefczuk, J., Prigione, A., Chavez, L., and Adjaye, J (2011) Comparative analysis of human embryonic stem cell and induced pluripotent stem cell- derived hepatocyte-like cells reveals current drawbacks and possible strategies for improved differentiation. *Stem Cells and Development*. **20**: 1259-1275.

Jung, J., Zheng, M., Goldfarb, M., and Zaret, KS (1999) Initiation of mammalian liver development from endoderm by fibroblast growth factors. *Science.* **284** (5422): 1998-2003.

Kadakol, A., Ghosh,SS., Sappal, BS., Sharma, G., Roy Chowdury J., and Roy Chowdury, N (2000) Genetic lesions of bilirubin uridine-diphosphoglucuronate glucuronosyltransferase (UGT1A1) causing Crigler-Najjar syndromes: correlation of genotype to phenotype. *Human Mutation*. **16** (4):297-306.

Kalscheuer, S., Zhang, X., Zeng, Y *et al* (2008) Differential expression of microRNAs in early-stage neoplastic transformation in the lungs of F344 rats chronically treated with the tobacco carcinogen 4-(methylnitrosamino)-1—(3-pyridyl)-1-butanone. *Carcinogenesis.* **29**: 2394-2399.

Kamiya, A., Kinoshita, T., Ito Y., Matsui, T., Morikawa, Y., Senba, E., Nakashima, K., Taga, T., Yoshida, K., Kishimoto, T., and Miyajima, A (1999) Fetal liver development requires a paracrine action of oncostatin M through the gp130 signal transducer. *EMBO Journal*. **18** (8): 2127-2136.

Kamiya, A., Kinoshita, T., and Miyajima, A (2001) Oncostatin M and hepatocyte growth factor induce hepatic maturation via distinct signalling pathways. *FEBS Letters.* **492** (1-2): 90-94.

Kamiyama, Y., Matsubara, T., Yoshinari, K., Nagata, K., Kamimura, H., Yamazoe, Y (2007) Role of human hepatocyte nuclear factor 4alpha in the expression of drug-metabolising enzymes and transporters in human hepatocytes assessed by use of small interfering RNA. *Drug Metabolism and Pharmacokinetics*. **22** (4): 287-298.

Kaplowitz, N (2004) Drug-induced liver injury. *Clinical Infectious Diseases*. **38**. Suppl 2: S44-48.

Kia, R., Sison, RLC., Heslop, J., Kitteringham, NR *et al* (2012) Stem cell-derived hepatocytes as predictive model for drug-induced liver injury: are we there yet? *British Journal of Clinical Pharmacology*. **75** (4): 885-896.

Kinoshita, T., Sekiguchi, T., Ming-jiang, X *et al* (1999) Hepatic differentiation induced by oncostatin M attenuates fetal liver hematopoiesis. *Proc. Natl. Acad Sci USA*. **96** (13): 7265-7270.

Kitada, M., and Kamataki, T (1994) Cytochrome P450 in human fetal liver: significance and fetal specific expression. *Drug Metabolism Reviews*. **26**: 305-323.

Kedde, M., Strasser, MJ., Boldajipour, B., Oude Vrielink, JA., Slanchev, K., le Sage, C *et al* (2007) RNA- binding protein Dnd1 inhibits microRNA access to target mRNA. *Cell*. **131** (7): 1273-1286.

Keng, VW., Yagi, H., Ikawa, M., Nagano, T., Myint, Z., Yamada, K *et al* (2000) Homebox gene Hhex is essential for onset of mouse embryonic liver development and differentiation of the monocyte lineage. *Biochemical and Biophysical Research Communications.* **276**: 1155-1161.

Kertesz, M., Iovino, N., Unnerstall, U., Gaul, U., and Segal, E (2007) The role of the site accessibility in microRNA target recognition. *Nature Genetics*. **39** (10): 1278-1284.

Khetani, SR., and Bhatia, SN (2008) Microscale culture of human liver cells for drug development. *Nature Biotechnology*. **26**: 120 – 126.

Khetani, SR., Kanchagar, C., Ukairo, O *et al* (2013) Use of micropatterned cocultures to detect compounds that cause drug-induced liver injury in humans. *Toxicological Science*s. **132** (1): 107-117.

Khvorova, A., Reynolds, A., Jayasena, SD (2003) Functional siRNAs and miRNAs exhibit strand bias. *Cell*. **115**: 209-216.

Kim, N., Kim, H., Jung, I., Kim,Y., Kim, D., Han, YM (2011) Expression profiles of miRNAs in human embryonic stem cells during hepatocyte differentiation. *Hepatology Research*. **41** (2):170-83.

Kimura, S., Umeno, M., Skoda, RC.,Mejer, UA., and Gonzalez, FJ. (1989) The human debrisoquine 4- hydroxylase (CYP2D6) locus: sequence and identification of the polymorphic CYP2D6 gene, related gene, and a pseudogene. *The American Journal of Human Genetics*. **45**: 889-904.

King, CD., Rios, GR., Green, MD., and Tephly, TR (2000) UDP-glucuronosyltransferases. *Current Drug Metabolism*. **1** (2):143-161.

King, RS., Ghosh, AA, and Wu, J (2006) Inhibition of human phenol and estrogen sulfotransferase by certain non-steroidal anti-inflammatory agents. *Current Drug Metabolism.* **7** (7): 745-753.

Kiriakidou, M., Nelson, PT., Kouranov, A *et al* (2004) A combined computational-experimental approach predicts human microRNA targets. *Genes and Development*. **18** (10): 1165-1178.

Kinoshita, T., Sekiguchi,T., Xu, MJ., Ito, Y., Kamiya, A., Tsuji, K., Nakahata, T., and Miyajima, A (1999) Hepatic differentiation induced by oncostatin M attenuates fetal liver haematopoiesis. *PNAS*. **96** (13):7265-7270.

Kinoshita, T., and Miyajima, A (2002) Cytokine regulation of liver development. *Biochimica et Biophysica Acta*. **1592** (3): 303-312.

Kirchheiner, J., Tsahuridu, M., Jabrane, W., Roots, I., and Brockmöller, J. (2004) The CYP2C9 polymorphism. From enzyme kinetics to clinical dose recommendations. *Future Medicine*. **1** (1): 63-84.
Kitada, M., and Kamataki, T (1994) Cytochrome P450 in human fetal development: significance and fetal specific expression. *Drug Metabolism Reviews*. **26**: 305-323.

Kmiec, Z (2001) Cooperation of liver cells in health and disease. *Advances in Anatomy, Embryology, and Cell Biology.* **161**: (3-13): 1-151.

Kohjitani, A., Fuda, H., Hanyu, O., and Strott, CA (2006) Cloning, characterization and tissue expression of rat SUL2B1a and SULT2B1b steroid/sterol sulfotransferase isoforms: divergence of the rat SULT2B1 gene structure from orthologous human and mouse genes. *Gene*. **367** (1-2): 66-73.

Kola, I., and Landis, J (2004) Can the pharmaceutical industry reduce attrition rates? *Nature Reviews. Drug Discovery*. **3**: 711-716.

Kon, K., Kim, JS., Jaeshke, H., and Lemasters, JJ (2004) Mitochondrial permeability transition in acetaminophen – induced necrosis and apoptosis of cultured mouse hepatocytes. *Hepatology*. **40**: 1170-1179.

Kondo, M., Itoh, S., Kunikata, T *et al* (2001) Time of closure ductuc venosus in term and preterm neonates. *Archives of Disease in Childhood. Fetal and Neonatal Edition*. **85** (1): F57-F59.

Kostrubsky, SE., Sinclair, JF., Strom SC *et al* (2005) Phenobarbital and phenytoin increased acetaminophen hepatotoxicity due to inhibition of UDP-glucuronosyltransferases in cultured human hepatocytes. *Toxicological Sciences*. **87**: 146-155.

Kota, J., Chivukula, RR., O'Donnell, KA., Wentzel, EA *et al* (2009) Therapeutic microRNA delivery suppresses tumorigenesis in a murine liver cancer model. *Cell.* **137**: 1005-1017.

Kovalchuk, O., Filkowski,J., Meservy, J *et al* (2008) Involvement of microRNA – 451 in resistance of the MCF-7 breast cancer cells to chemotherapeutic drug doxorubicin. *Molecular Cancer Therapeutics*. **7**:2152-2159

Kozer, E., and Koren, G. (2001) Management of paracetamol overdose: current controversies. *Drug Safety*. **24** (7): 503-512.

König, J., Nies, AT., Cui, Y., Leier, I., and Keppler, D (1999) Conjugate export pumps of the multidrug resistance protein (MRP) family: localization, substrate specificity, and MRP2-mediated drug resistance. *Biochimica et Biophysica Acta (BBA)-Biomembranes*. **1461** (2): 377-394.

Krasniak, AE., Knipp, GT., Svensson, CK., and Liu, W (2014) Pharmacogenomics of acetaminophen in pediatric populations: a moving target. *Frontiers in Genetics*. **5**: 314.

Krauer, B., and Dayer, P (1991) Fetal drug metabolism and its possible clinical implications. *Clinical Pharmacokinetics*. **21** (1): 70-80.

Krishnamurthy, P., Ross, DD., Nakanishi, T. *et al* (2004) The stem cell marker BCRP/ABCG2 enhances hypoxic cell survival through interactions with heme. *Journal of Biological Chemistry*. **279**: 24218-24225.

Krützfeld, J., Rajewsky, N., Braich, R., Rajeev, KG., *et al* (2005) Silencing of microRNAs *in vivo* with 'antagomirs'. *Nature*. **438** (7068): 685-689.

Kulkarni, KK., Kulkarni, AP. (1995) Retinoids inhibit mammalian glutathione transferases. *Cancer Letters*. **91** (2):185-189.

Kumar, M., Jordan, N., Melton, D., and Grapin-Botton, A (2003) Signals from lateral plate mesoderm instruct endoderm toward pancreatic fate. *Developmental Biology*. **259**: 109-122.

Kung, JWC., Currie, IS., Forbes, SJ., and Ross, JA (2010) Liver development, regeneration, and carcinogenesis. *Journal of Biomedicine and Biotechnology*. DOI: 10.1155/2010/984248.

Kuo, TK., Hung, SP., Chuang, CH *et al* (2008) Stem cell therapy for liver disease: parameters governing the success of using bone marrow mesenchymal stem cells. *Gastroenterology*. **134**: 2111-2121.

Lacroix, D., Sonnier, M., Moncion, G., Cheron, G., and Cresteil, T (1997) Expression of CYP3A in the human liver. Evidence that the shift between CYP3A7 and CYP3A4 occurs immediately after birth. *European Journal of Biochemistry*. **247**: 625-634.

Lagos- Quintana, M., Rauhut, R., Yalcin, A., Meyer, J., Lendeckei, W., and Tuschi, T (2002) Identification of tissue –specific microRNAs from mouse. *Current Biology*. **12** (9): 735-739.

Lamba, J., Lamba, V., and Schuetz, E (2005) Genetic variants of PXR (NR1I2) and CAR (NR1I3) and their implications in drug metabolism and pharmacogenetics. *Current Drug Metabolism*. **6**: 369-383.

Lanford, RE., Hildebrandt-Eriksen, ES., Petri, A., Persson, R *et al* (2010) Therapeutic silencing of microRNA 122 in primates with chronic hepatitis C virus infection. *Science.* **327** (5962): 198-201.

Lang, T., Hitzl, M., Burk, O *et al* (2004) Genetic polymorphism in the multidrug resistance- associated protein 3 (ABCC3, MRP3) gene and relationship to its mRNA and protein expression in human liver. *Pharmacogenetics.* **14**: 155.

Larijani, M., Seifinejad, A., Pournasr, B., Hajihoseini, V., Hassani, SN *et al* (2011) Long-term maintenance of undifferentiated human embryonic and induced pluripotent stem cells in suspension. *Stem Cells and Development*. **20** (11): 1911-23.

Larson, AM, Poison, J., Fontana, RJ *et al* (2005) Acetaminophen-induced acute liver failure: results of a United States multicentre, prospective study. *Hepatology*. **42**: 1364-1372.

Larson, AM (2007) Acetaminophen hepatotoxicity. *Clinics in Liver Disease*. **11** (3): 525-548.

Lavon, N., Yanuka, O., and Benvenisty, N (2004) Differentiation and isolation of hepatic-like cells from human embryonic stem cells. *Differentiation.* **72** (5): 230-238.

Le Douarin, NM (1975) An experimental analysis of liver development. *Medical Biology*. **53**: 427-455.

Lee, Y., Kim, M., Han, J., Yeom,KH., Lee,S., Baek, SH., and Kim, VN (2004) MicroRNA genes are transcribed by RNA polymerase II. *The EMBO Journal*. **23**: 4051-4060.

Lee, WM. (2003) Drug-induced hepatotoxicity. *New England Journal of Medicine.* **349** (5): 474-485.

Lee, WM (2004) Acetaminophen and the U.S Acute Liver Failure Study Group: lowering the risks of hepatic failure. *Hepatology*. **40** (1): 6-9.

Lee, KD., Kwang-Chn Kuo, T., Whang-Peng, J., Chung, YF *et al* (2004) *In vitro* hepatic differentiation of human mesenchymal stem cells. *Hepatology*. **40** (6): 1275-1284.

Lee, H., Shamy, GA., Elkabetz, Y *et al* (2007) Directed differentiation and transplantation of human embryonic stem cell-derived motoneurons. *Stem Cells*. **25** (8): 1931-1939.

Leier, I., Jedlitschky, G., Buchoholz, U., Center, M., Cole, SP., Deelay, RG., and Keppler, D (1996) ATP-dependant glutathione disulphide transport mediated by the MRP gene-encoded conjugate export pump. *Biochemical Journal*. **314** (Pt2):433-437.

Lemaigre, FP (2003) Development of biliary tract. *Mechanism of Development*. **120**: 81-87.

Lemos, C., Giovanetti, E., Zucali, PA., Assaraf, YG *et al* (2011) Impact of ABCG2 polymorphism on the clinical outcome and toxicity of gefitinib in non-small-cell lung cancer patients. *Pharmacogenomics.* **12**(2): 159-170.

Leslie, EM., Deeley, RG and Cole, SP (2005) Multidrug resistance proteins: role of P-glycoprotein, MRP1, MRP2 and BCRP (ABCG2) in tissue defense. *Toxicology and Applied Pharmacology*. **204**: 216-237.

Lewinsky, RH., Smith, PA., and Mackenzie, PI (2005) Glucuronidation of bioflavonoids by human UGT1A10: structure –function relationships. *Xenobiotica*. **35** (2): 117-129.

Lewis, DF (2003) P450 structures and oxidative metabolism of xenobiotics. *Pharmacogenomics*. **4:** 387-395.

Lewis, DF (2003b) Human cytochromes P450 associated with the phase 1 metabolism of drugs and other xenobiotics: a compilation of substrates and inhibitors of CYP1, CYP2, and CYP3 families. *Current Medicinal Chemistry*. **10** (19): 1955-1972.

Lewis, BP., Burge, CB., and Bartel, DP (2005) Conserved seed pairing, often flanked by adenosines, indicates that thousands of human genes are microRNA targets. *Cell*. **120**: 15-20

Levy, G., Khanna, NN., Soda, DM., Tsuzuki, O., and Stern, L (1975) Pharmacokinetics of acetaminophen in the human neonate: formation of acetaminophen glucuronide and sulfate in relation to plasma bilirubin concentration and D-glucaric acid excretion. *Pediatrics*. **55**: 818-825.

Li, X., Clemens, DL., and Anderson, RJ (2000) Sulfation of iodothyronines by human sulfotransferase 1C1 (SULT1C1)*. *Biochemical Pharmacology*. **60** (11):1713-1716.

Li, M., Yang, Y., Zhi-Xu,H *et al* (2013) MicroRNA – 561 promotes acetaminophen-induced hepatotoxicity in HepG2 cells and primary human hepatocytes through down-regulation of the nuclear receptor co-repressor dosage –sensitive sex reversal adrenal hypoplasia congenital critical region on X chromosome, Gene 1 (DAX-1). *Drug Metabolism and Disposition*. doi: 10.1124/dmd.113.052670.

Liao, R., Sun, J., Zhang, L *et al* (2008) MicroRNAs play a role in the development of human hematopoietic stem cells. *Journal of Cellular Biochemistry*. **104**: 805-817.

Lindena, J., Sommerfeld, U, Hopfel, C *et al* (1986) Catalytic enzyme activity concentration in tissue of man, dog, rabbit, guinea pig, rat, and mouse. Approach to quantitative diagnostic enzymology, III. Communication. *Journal of Clinical Chemistry and Clinical Biochemistry*. **24**: 35-47.

Lindsay, J., Wang, LL., Li,Y., and Zhou, SF (2008) Structure, function and polymorphism of human cytosolic sulfotransferases. *Current Drug Metabolism.* **9** (2): 99-105.

Liow, JS., Lu, S., McCarron, JA., Hong, J., Musachio, JL., Pike,VM., Innis,RB., and Zoghbi, SS (2007) Effect of P-glycoprotein inhibitor, Cyclosporin A, on the disposition in rodent brain and blood of the 5-HT1A receptor radioligand, [11C](R)-(-)-RWAY. *Synapse.* **61** (2): 96-105.

Liu, P., Wakamiya, M., Shea, MJ., Albrecht, U., Behringer, RR., and Bradley, A (1999) Requirement for Wnt3 in vertebrate axis formation. *Nature Genetics*. **22**: 361-365.

Liu, N., and Olson, EN (2010) MicroRNA regulatory networks in cardiovascular development. *Developmental Cell*. **18** (4): 510-525.

Liu, Z., Li, L., Wu, H., Hu, J *et al* (2015) Characterization of CYP2B6 in a CYP2B6-humanized mouse model: inducibility in the liver by phenobarbital and dexamethasone and role in nicotine metabolism *in vivo*. *Drug Metabolism and Disposition*. **43** (2): 208-216.

Liyou, NE., Buller, KM., Tresillian, MJ *et al* (2003) Localization of a brain sulfotransferase, SULT4A1, in the human and rat brain: an immunohistochemical study. *Journal of Histochemistry and Cytochemistry*. **51** (12): 1655-1664.

Loberant, N., Herskovitos, M., Barak, M *et al* (1999) Closure of ductus venosus in premature infants. Finding on real-time gray-scale, color-flow doppler, and duplex doppler sonography. *American Journal of Roentgenology*. **172** (1): 227-229.

Loe, DW., Stewart, RK., Massey, TE., Deeley, RG., and Cole, SPC (1997) ATP – dependent transport of aflatoxin B_1 and its glutathione conjugates by the product of the multidrug resistance protein (MRP) gene. *Molecular Pharmacology*. **51** (6): 1034-1041.

Lucendo – Villarin, B., Khan, F., Pernagallo, S., Bradley, M., Iredale, JP., and Hay, DC (2012) Maintaining hepatic stem cell gene expression on biological and synthetic substrata. *BioResearch Open Access*. **1**:50-53.

Lucendo –Villarin, B., Cameron, K., Szkolnicka, D., Travers, P., Khan, F., Walton, J., Iredale, J., Bradley,M., and Hay, DC. (2014) Stabilizing Hepatocellular Phenotype Using Optimized Synthetic Surfaces. *Journal of Visualized Experiments*. **91**; e51723

Lucendo - Villarin, B., Cameron, K., Szkolnicka, D *et al* (2015) Polymer supported directed differentiation reveals unique gene signature predicting stable hepatocyte performance. *Advance Healthcare Materials*. doi: 10.1002/adhm.201500391.

Lynch, T (2011) Management of drug-drug interactions: considerations for special populations – focus on opioid use in elderly and long term care. *The American Journal of Managed Care*.**17**: S293-S298.

Lysy, PA., Campard, D., Smets, F *et al* (2008) Persistence of a chimerical phenotype after hepatocyte differentiation of human bone marrow mesenchymal stem cells. *Cell Proliferation.* **41**: 36-58.

Mackenzie, PI., Owens, PI., Burchell, K *et al* (1997) The UDP-glucuronosyltransferase gene superfamily: recommended nomenclature update based on evolutionary divergence. *Pharmacogenetics*. **7**: 255-269.

Mackenzie, PI., Rogers, A., Treloar,J., Jorgensen, BR., Miners, JO., and Meech, R. (2008) Identification of UDP glucuronosyltransferase 3A1 as a UDP N-acetylglucosaminyltransferase. *The Journal of Biological Chemistry*. **283** (52):36205-36210.

Macsween, RNM; and Scothorne, RJ Developmental anatomy and normal structure. In: *Pathology of the liver*. Eds.: RNM Macsween. Churchill Livingstone. 1994. 1-50.

Makin, AJ., Wendon, J., and Williams, R (1995) A 7-year experience of severe acetaminophen-induced hepatotoxicity (1987-1993). *Gastroenterology*. **109**: 1907-1916.

Maiti, S., Chen,X., and Chen, G. (2005) All-trans retinoic acid induction of sulfotransferases. *Basic and Clinical Pharmacology and Toxicology*. **96** (1): 44-53.

Malhi, H., Gores, GJ., and Lemasters, JJ (2006) Apoptosis and necrosis in the liver: a tale of two deaths? *Hepatology.* **43** (2): 31-39.

Margagliotti, S., Clotman, F., Pierreux, CE., Beaundry, JB., Jacquemin, P., Rousseau, GG., and Lemaigre, FP (2007) The Onecut transcription factors HNF6/OC-1 and OC-2 regulate early liver expansion by controlling hepatoblast migration. *Developmental Biology*. **311**: 579-589.

Margagliotti, S., Clotman, F., Pierreux, CE., Lemoine, P., Rousseau, GG., Henriet, P., and Lemaigre, FP (2008) Role of metalloproteinases at the onset of the liver development. *Development Growth and Differentiation*. **50**: 331-338.

Marongiu, F., Gramignoli, R., Dorko, K., Miki, T *et al* (2011) Hepatic differentiation of amniotic epithelial cells. *Hepatology*. **53**(5): 1719-1729.

Martignoni, M., Groothuis, G., de Kanter, R (2006) Species differences between mouse, rat, dog, monkey, and human CYP-mediated drug metabolism, inhibition and induction. *Expert Opinion on Drug Metabolism and Toxicology*. **2** (6): 875-894.

Marzolini, C., Paus, E., Buclin, T., and Kim, RB (2004) Polymorphisms in human MDR1 (P-glycoprotein): recent advances and clinical relevance. *Clinical Pharmacology and Therapeutics*. **75** (1): 13-33.

Matimba, A., Del-Favero, J., Van Broeckhoven, C (2009) Novel variants of major drug – metabolising enzyme genes in diverse African populations and their predicted functional effects. *Human Genomics*. **3**: 169 – 190.

Matsumoto, K., Yoshitomi, H., Rossant, J., and Zaret, KS (2001) Liver organogenesis promoted by endothelial cells prior to vascular function. *Science*. **294**: 559-563.

McGill, MR., Yan, HM., Ramachandran, A *et al* (2011) HepaRG cells: a human model to study mechanisms of acetaminophen hepatotoxicity. *Hepatology*. **53**: 974-982.

McLin, VA., Rankin, SA., and Zorn, AM (2007) Repression of Wnt/β – catenin signalling in the anterior endoderm is essential for liver and pancreas development. *Development*. **134**: 2207-2217.

Medine. C., Greenhough, S., and Hay, DC (2010) Role of stem-cell-derived hepatic endoderm in human drug discovery. *Biochemical Society Transactions*. **38** (4): 1033-06.

Medine, C., Lucendo –Villarin, B., Storck, C., Wangm F., Szkolnicka, D., Khan,F., Pernagallo, S., Black, JR., Marriage, HM., Ross, JA., Bradley, M., Iredale, JP, Flint, O., and Hay, DC (2013) Developing high- fidelity hepatotoxicity models from pluripotent stem cells. *Stem Cells Translational Medicine*. **2**: 505-509.

Meijerman, I., Beijnen, JH., and Schellens, JHM (2006) Herb-drug interactions in oncology: focus on mechanisms of induction. *Oncologist*. **11** (7): 742-752.

Melkoumian, Z., Weber, JL., Weber, DM et al (2010) Synthetic pepetide-acrylate surfaces for long – term self-renewal and cardiomyocyte differentiation of human embryonic stem cells. *Natrue Biotechnology*. **28** (6): 606-610.

Meinl, W., Meerman, JH., and Glatt, H.(2002) Differential activation of promutagenes by alloenzymes of human sulfotransferase 1A2 expressed in *Salmonella typhimurium*. *Pharmacogenetics.* **12**(9):677-689.

Meyer, U.A (1996) Overview of enzymes of drug metabolism. *Journal of Pharmacokinetics and Biopharmaceutics*. **24**: 449-459.

Michlewski, G., Guil, S., Semple, CA., and Canceres, JF (2008) Posttranscriptional regulation of miRNAs harbouring conserved terminal loops. *Molecular Cell*. **32** (3): 383-93.

Miki, T., Ring, A., and Gerlach, J (2011a) Hepatic differentiation of human embryonic stem cells is promoted by three- dimensional dynamic perfusion culture conditions. *Tissue Eng. Part C Methods*. **17**: 557-68.

Miki, T (2011b) Hepatic differentiation of human embryonic and induced pluripotent stem cells for regenerative medicine. In *Embryonic Stem Cells: Differentiation and Pluripotent Alternatives*, ed. MS Kallos, pp. 303-20. Rijeka, Croatia. In Tech.

Mikkelsen, S., Feilberg, VL., Christensen, CB., Lundstrom, KE (1994) Morphine pharmacokinetics in premature and mature newborn infants. *Acta Paediatrica*. **83** (10): 1025-1028.

Mills, JB., Rose, KA., Sadagopan, N., Sahi, J., and de Morais, SM (2004) Induction of drug metabolism enzymes and MDR1 using a novel human hepatocyte cell line. *Journal of Pharmacology and Experimental Therapeutics*. **309** (1): 303-309.

Miners., JO., Knights, KM., Houston, JB., Mackenzie, PI (2006) *In vitro-in vivo* correlation for drugs and other compounds eliminated by glucuronidation in humans. pitfalls and promises. *Biochemical Pharmacology*. **71** (11): 1531-1539.

Miranda, KC., Huynh, T., Tay, Y *et al* (2006) A pattern-based method for identification of microRNA binding sites and their corresponding heteroduplexes. *Cell*. **126** (6): 1203-1217.

Mitchell, PS., Parkin, RK., Kroh, EM *et al* (2008) Circulating microRNAs as stable blood-based markers for cancer detection. *PNAS*. **105**: 10513-10518.

Mizoguchi, T., Verkade, H., Heath, JK., Kuroiwa, A, and Kikuchi, Y (2008) Sdf1/Cxcr4 signalling controls the dorsal migration of endodermal cells during zebrafish gastrulation. *Development.* **135** (15):2521-9.

Mooij, MG., Schwarz, UI., de Koning, BA., Leeder, JS., *et al* (2014) Ontogeny of huma hepatic and intestinal transporter gene expression during childhood: age matters. *Drug Metabolism and Disposition*. **42** (8): 1268-1274.

Monga, SP., Mars, WM., Pediaditakis, P., Bell, A., Mule, K *et al* (2002) Hepatocyte growth factor induces Wnt-independent nuclear translocation of beta-catenin after Met-beta-catenin dissociation in hepatocytes. *Cancer Research*. **62**: 2064-2071.

Moore –Scott, BA., Opoka, R., Lin, SC., Kordich,JJ., and Wells, JM (2007) Identification of molecular markers that are expressed in discrete anterior-posterior domains of the endoderm from the gastrula stage to mid-gestation. *Developmental Dynamics.* **236:** 1997-2003.

Morel, F., Rauch, C., Petit, E., Piton, A *et al* (2004) Gene and protein characterization of the human glutathione S-transferase kappa and evidence for a peroxisomal localization. *Journal of Biological Chemistry*. **279** (16): 16246-16253.

Morrisey, EE., Tang, Z., Sigrist, K., Lu, MM., Jiang, F., Ip., HS., and Parmacek, MS (1998) GATA6 regulates HNF4a and is required for differentiation of visceral endoderm in the mouse embryo. *Genes and Development*. **12:** 3579-3590.

Moss, EG., Lee, RC., and Ambros, V (1997) The Cold shock domain protein LIN-28 controls developmental timing in C.elegans and is regulated by the lin-4 RNA. *Cell*. **88**: 637-646.

Mueller, CF., Widder, JD., McNally, JS *et al* (2005) The role of the multidrug resistance protein -1 in modulation of endothelial cell oxidative stress. *Circulation Research.* **97**: 637-644.

Muraglia, A., Cancedda, R., and Quarto, R (2000) Clonal mesenchymal progenitors from human bone marrow differentiate *in vitro* according to a hierarchical model. *Journal of Cell Science*. **113**: 1161-1166.

Musana, K., Yale, S., and Abdulkarim, A. (2004) Test of liver injury. *Clinical Medicine and Research*. **2** (2):129-131.

Müller, FJ., Brändl, B., Lorinfg, JF (2012) Assessment of human pluripotent stem cells with PluriTest. StemBook, ed. The Stem Cell Research Community, StemBook, doi/10.3824/stembook.1.84.1.

Nagano, K., Hoshino, H., Nishimura, D., Katada, N., Sano, H., and Kato, K (1999) Patent *ductus venosus*. *Journal of Gastroenterology and Hepatology*. **14** (3): 285-288.

Nair, RR., Khanna, A., Singh, K (2013) Association of GSTT1 and GSTM1 polymorphisms with early pregnancy in Indian population and meta-analysis. *Reproductive Biomedicine Online*. **26** (4): 313-322.

Nakajima, M., and Yokoi, T (2011) MicroRNAs from biology to future pharmacotherapy: regulation of cytochrome P450s and nuclear receptors. *Pharmacology and Therapeutics*. **131** (3): 330-337.

Nakatomi, K., Yoshikawa, M., Oka, M *et al* (2001) Transport of 7-ethyl-10-hydroxycamptothecin (SN-38) by breast cancer resistance protein ABCG2 in human lung cancer cells. *Biochemical and Biophysical Research Communications*. **288**:827-832.

Nakaya, Y., Sukowati, EW., Wu,Y., and Sheng, G (2008) RhoA and microtubule dynamics control cell-basement membrane interaction in EMT during gastrulation. *Nature Cell Biology*. **10** (7):765-75.

Negishi, T., Nagai, Y., Asaoka, Y., Ohno,M., Namae, M., Mitani,H., Sasaki,T *et al* (2010) Retinoic acid signalling positively regulates liver specification by inducing wnt2bb gene expression in medaka. *Hepatology*. **51** (3): 1037-1045.

Nejak-Bowen, K., and Monga, SPS (2008) Wnt/β – catenin signalling in hepatic organogenesis. *Organogenesis.* **4** (2): 92-99.

Nelson, SD (1990) Molecular mechanisms of the hepatotoxicity caused by acetaminophen. *Seminars in Liver Disease*. **10** (4): 267-278.

Nemoto, N., and Sakurai, J (1992) Activation of CYP1A1 and CYP1A2 genes in adult mouse hepatocytes in primary cultures. *Japanese Journal of Cancer Research*. **84**: 272 – 278.

Nemoto, N., Sakurai, J., Funae, Y (1995) Maintenance of phenobarbital – inducible CYP2B gene expression in C57BL/6 mouse hepatocytes in primary culture as spheroids. *Archives of Biochemistry and Biophysics*. **316**: 363 – 369.

Newman, MA., Thomson, JM., and Hammond, SM (2008) Lin-28 interaction with the Let-7 precursor loop mediates regulated microRNA processing. *RNA.* **14** (8): 1539-1549.

Nies, AT., and Keppler, D. (2007) The apical conjugate efflux pump ABCC2 (MRP2). *Pfluger Arch*. **453**: 643-659.

Noguchi, K., Katayama, K., and Sugimoto, Y (2014) Human ABC transporter ABCG2/BCRP expression in chemoresistance: basic and clinical perspectives for molecular cancer therapeutics. *Pharmacogenomics and Personalized Medicine*. **7**: 53-64.

Nourjah, P., Ahmad, SR., Karwoski, C., and Willy, M (2006) Estimates of acetaminophen (paracetamol) – associated overdoses in the United States. *Pharmacoepidemiology and Drug Safety*. **15** (6): 398-405.

O'Brien, PJ.; Slaughter, MR., Polley, SR., and Kramer, K (2002) Advantages of glutamate dehydrogenase as a blood biomarker of acute hepatic injury in rats. *Laboratory Animals*. **36** (3): 313-321.

O'Connell, RM (2012) MicroRNAs function on a new level. *Blood*. **119** (17): 3875-3876.

Oglesby, IK., Bray, IM., Chotirmall, SH., Stallings, RL (2010) MiR-126 is downregulated in cystic fibrosis airway epithelial cells and regulates TOM1 expression. *Journal of Immunology.* **184**: 1702-1709.

Ohlsson Teague, EM., Van der Hoek, KH., Van der Hoek, MB., Perry, N., Wagaarachchi, P *et al* (2009) MicroRNA-regulated pathways associated with endometriosis. *Molecular Endocrinology*. **23** (2): 265-275.

Olena, AF., and Patton, JG (2010) Genomic organization of microRNAs. *Journal of Cellular Physiology.* **222**:540-545.

Orloff, J., Douglas, F., Pinheiro, J., Levinson, S *et al* (2009) The future of drug development: advancing clinical trial design. *Nature Reviews. Drug Discovery*. **8** (12): 949-957.

Ostapowicz, G., Fontana, RJ., Schiodt, FV *et al* (2002) Results of prospective study of acute liver failure at 17 tertiary care centers in the United States. *Annals of Internal Medicine*. **137** (12): 947-954.

Oyagi, S., Hirose, M., Kojima, M *et al* (2006) Therapeutic effect of transplanting HGF-treated bone marrow mesenchymal cells into CCl4-injured rats. *Journal of Hepatology*. **44**: 742-748.

Pan, YZ., Gao, W., and Yu, AM (2009a) MicroRNAs regulate CYP3A4 expression via direct and indirect targeting. *Drug Metabolism and Disposition*. **37**: 2112-2117.

Pan, YZ., Morris, ME., and Yu, AM (2009b) MicroRNA-328 negatively regulates the expression of breast cancer resistance protein (BCRP/ABCG2) in human cancer cells. *Molecular Pharmacology*. **75**: 1374-1379.

Pascussi, JM., Gerbal-Chaloin, S., Drocourt, L., Manuel, P and Vilarem, MJ. (2003) The expression of CYP2B6, CYP2C9, and CYP3A4 genes: a tangle of networks of nuclear and steroid receptors. *Biochimica et Biophysica Acta*. **1619:** 243-253.

Pastori, C., Magistri, M., Napoli, S., Carbone, GM., and Catapano, CV (2010) Small RNA-directed transcriptional control. *Cell Cycle*. **9** (12): 2353-2362.

Payne, C., Samuel, K., Pryde, A., King, J., Brownstein, D *et al* (2010) Persistence of functional hepatocyte-like cells in immune-compromised mice. *Liver International*. **31**: 254-62.

Payushina, OV (2012) Hematopoietic microenvironment in the fetal livers: roles of different cell populations. *ISRN Cell Biology*. DOI: 10.5402/2012/979480.

Phillips, KA., Veenstra, DL., Oren, E., Lee, JK., and Sadee, W (2001) Potential role of pharmacogenomics in reducing adverse drug reactions: a systematic review. *JAMA*. **286**: 2270-2279.

Piirilä, P., Wikman, H., Luukkonen, R., Käärlä, K., Rosenberg, C., Nordman, H., Norppa, H., Vainio, H., and Hirvonen, A (2001) Glutathione –S- transferase genotypes and allergic responses to diisocyanate exposure. *Pharmacogenetics.* **11** (5): 437-445.

Place, RF., Li, LC., Pookot, D., Noonan, EJ., and Dahiya, R (2007) MicroRNA-373 induces expression of genes with complementary promoter sequences. *Proceedings of the National Academy of Sciences of the United States of America*. **105** (5): 1608-1613.

Polson, JP., Lee,WM., (2005) AASLD position paper: The management of acute liver failure. *Hepatology*. **41**: 1179-97.

Radomiska-Pandya,A., Czernik, PJ., Little, JM., Battaglia, E., and Mackenzie, PI (1999) Structural and functional studies of UDP-glucuronosyltransferases. *Drug Metabolism Reviews*. **31**: 817-899.

Raijimakers, MT., Steegers, EA., and Peters, WH (2001) Glutathione S-transferases and thiol concentrations in embryonic and early fetal tissues. *Human Reproduction*. **16** (11): 2445-2450.

Rashid, S., Corbineau, S., Hannan, N., Marciniak, S., and Miranda E (2010) Modelling inherited metabolic disorders of the liver using human induced pluripotent stem cells. *Journal of Clinical Investigation*. **120** (9): 3127- 36.

Ray, SD., Mumaw, VR., Raje, RR., Fariss, MW (1996) Protection of acetaminophen-induced hepatocellular apoptosis and necrosis by cholesteryl hemisuccinate pretreatment. *Journal of Pharmacology and Experimental Therapeutics*. **279**: 1470-1483.

Rayner, KJ., Suárez, Y., Dávalos, A., Parathath, S., Fitzgerald, ML *et al* (2010) MiR-33 contributes to the regulation of cholesterol homeostasis. *Science.* **328** (5985): 1570-1573.

Rayner, KJ., Sheedy, FJ., Esau, CC., Hussain, FN., Temel, RE. *et al* (2011) Antagonism of miR-33 in mice promotes reverse cholesterol transport and regression of atherosclerosis. *Journal of Clinical Investigation*. **121** (7): 2921-2931

Redman, AR., Zheng, J., Shamsi, SA., *et al* (2008) Variant CYP2C9 alleles and warfarin concentrations in patients receiving low-dose versus average-dose warfarin therapy. *Clinical and Applied Thrombosis/Hemostasis*. **14**: 29-37.

Reubinoff, BE., Pera, MF., Fong, CY., Trounson, A., and Bongso, A (2000) Embryonic stem cell lines from human blastocysts: somatic differentiation *in vitro*. *Nature Biotechnology.* **18**: 399-404.

Ring, JA., Ghabrial, H., Ching MS., Smallwood, RA., and Morgan DJ. (1999) Fetal hepatic drug elimination. *Pharmacology and Therapeutics.* **84** (3):429-445.

Ritchie, KJ., Walsh, S., Sansom,O., Henderson, C., and Wolf, R (2009) Markedly enhanced colon tumorigenesis in Apc^{Min} mice lacking glutathione S-transferase Pi. *PNAS*. **106** (49): 20859-20864.

Rius, M., Nies, AT., Hummel-Eisenbeiss, J., Jedlitschky G., and Keppler D (2003) Cotransport of reduced glutathione with bile salts by MRP4 (ABCC4) localized to the basolateral hepatocyte membrane. *Hepatology*. **38**: 374-384.

Roberts, DJ., Johnson, RL., Burke, AC., Nelson, CE., Morgan, BA., and Tabin, C (1995) Sonic hedgehog is an endodermal signal inducing Bmp-4 and Hox genes during induction and regionalization of the chick hindgut. *Development.* **121**: 3163-3174.

Robinton, DA., and Daley, GQ (2012) The promise of induced pluripotent stem cells in research and therapy. *Nature.* **481**: 295-305.

Rogler, CE., LeVoci, L., Ader, T., Massimi, A. *et al* (2009) MicroRNA-23b cluster microRNAs regulate transforming growth factor-beta/bone morphogenetic protein signalling and liver stem cell differentiation by targeting Smads. *Hepatology*. **50** (2): 575-583.

Rodin, S., Domogatskaya, A., Ström, S *et al* (2010) Long –term self –renewal of human pluripotent stem cells on human recombinant laminin – 511. *Nature Biotechnology*. **28**: 611 – 515.

Rodin, S., Antonsson, L., Niaudet, C *et al* (2013) Clonal culturing of human embryonic stem cells on laminin – 521 / E – cadherin matrix in defined and xeno – free environment. *Nature Communications*. **5** (3195).

Rossi, JM., Dunn, NR., Hogan, BL, and Zaret, KS (2001) Distinct mesodermal signals, including BMPs from the septum transversum mesenchyme, are required in combination for hepatogenesis from the endoderm. *Genes and Development*. **15:** 1998-2009.

Rottiers, V., and Näär, AM (2012) MicroRNAs in metabolism and metabolic disorders. *Nature Reviews Molecular Cell Biology*. **13**: 239-250.

Rudolph, AM (1983) Hepatic and *ductus venosus* blood flows during fetal life. *Hepatology*. **3**: 254.

Rumack, BH (2002) Acetaminophen hepatotoxicity: the first 35 years. *Journal of Toxicology. Clinical Toxicology.* **40** (1): 3-20.

Russel, FGM (2010) Enzyme-and Transporter-Based Drug-Drug Interactions, Progress and Future Challenges. Transporters: Importance in Drug Absorption, Distribution, and Removal. Springer. DOI: 10.1007/978-1-4419-0840-7_2

Russmann, S., Kullak-Ublick, GA., and Grattagliano, I (2009) Current concepts of mechanisms in drug-induced liver injury. *Current Medicinal Chemistry*. **16**: 3041-3053.

Sarkadi, B., Homolya, L., Szakacs, G., and Varadi, A (2006) Human multidrug resistance ABCB and ABCG transporters: participation in chemoimmunity defense system. *Physiological Reviews*. **86**: 1179-1236.

Sekiya, S., and Suzuki, A (2011) Direct conversion of mouse fibroblasts to hepatocyte-like cells by defined factors. *Nature*. **475**: 390-93.

Schinkel, AH., Mol, CAAM., Wagenaar, E., van Deemter, L., Smit, JJM., and Borst, P (1995) Multidrug resistance and the role of P-glycoprotein knockout mice. *European Journal of Cancer*. **31** (7-8): 1295-1298.

Schmelzer, E., Mitig, K., Shrade, P *et al* (2009) Effect of human patient plasma e*x vivo* treatment on gene expression and progenitor cell activation of primary human liver cells in multi-compartment 3D perfusion bioreactors for extra-corporeal liver support. *Biotechnology and Bioengineering*. **103**: 817-827.

Schmidt, LE., and Dalhoff, K. (2001) Risk factors in the development of adverse reactions to N-acetylcysteine in patients with paracetamol poisoning. *British Journal of Clinical Pharmacology.* **51** (1): 87-91.

Schrader, J., Gordon-Walker, T., Aucott, R., van Deemter, M., Quaas A., *et al* (2011) Matrix stiffness modulates proliferation, chemotherapeutic response, and dormancy in hepatocellular carcinoma cells. *Hepatology.* **53** (4):1192-205.

Schutte, B; Henfling, M., Kölgen W., Bouman, M. *et al* (2004) Keratin 8/18 breakdown and reorganization during apoptosis. *Exerimental Cell Research*. **297** (1): 11-26.

Sengupta, S., Johnson, BP., Swanson, SA., Stewart, R *et al* (2014) Aggregate culture of human embryonic stem cell-derived hepatocytes in suspension are an improved *in vitro* model for drug metabolism and toxicity testing. *Toxicological Sciences*. Doi: 10.1093/toxsci/kfu069.

Sharom, FJ (2011) The P-glycoprotein multidrug transporter. *Essays in Biochemistry.* **50** (1):161-78.

Sheehan, D., Maede, G., Foley, VM., and Dowd, CA (2001) Structure, function and evolution of glutathione transferases: implications for classification of non-mammalian members of an ancient enzyme superfamily. *Biochemical Journal*. **360** (Pt 1):1-16.

Shen, C., Zhang, G., Qiu, H., Meng, Q (2006) Acetaminophen-induced hepatotoxicity of gel entrapped rat hepatocytes in hollow fibers. *Chemico – Biological Interactions*. **162**: 53-61.

Shen, MM (2007) Nodal signalling: development roles and regulation. *Development.* **134:** 1023-1034.

Sheps, JA and Ling, V (2007) Preface: the concept and consequences of multidrug resistance. *Pfluger Archiv*. **453**: 545-553.

Shifley, ET., Kenny, AP., Rankin, SA., and Zorn, AM (2012) Prolonged FGF signalling is necessary for lung and liver induction in *Xenopus. BMC Developmental Biology*. **12**:27.

Shimizu, C., Fuda, H., Yanai, H., and Strott, CA (2003) Conservation of the hydroxysteroid sulfotransferase SULT2B1 gene structure in the mouse: pre-and postnatal expression, kinetic analysis of isoforms, and comparison with prototypical SULT2A1. *Endocrinology*. **144** (4): 1186-1193.

Shin, D., Shin, CH., Tucker,J., Ober, EA., Rentzsch, F., Poss, KD *et al* (2007) BMP and FGF signalling are essential for liver specification in zebrafish. *Development*. **134** (11):2041-2050.

Shiojiri, N (1997) Development and differentiation of bile ducts in the mammalian liver. *Microscopy Research and Technique*. **39**: 328-335.

Shmelzer, E., Wauthier, L., and Reid, M (2006) The phenotypes of pluripotent human hepatic progenitors. *Stem Cells*. **24**:1852-1858.

Sies, H (1999) Glutathione and its role in cellular function. *Free Radical Biology and Medicine.* **27**: 916-921.

Sindrup, SH., and Brøsen, K (1995) The pharmacogenetics of codeine hypoalgesia. *Pharmacogenetics.* **5**(6): 335-46.

Sinner, D., Rankin, S., and Zorn, AM (2004) Sox17 and beta-catenin cooperate to regulate the transcription of endodermal genes. *Development.* **131**(13): 3069-3080.

Sinz, M., Wallace, G., Sahi, J (2008) Current industrial practices in assessing CYP450 enzyme induction: preclinical and clinical. *AAPS Journal*. **10**:391-400.

Si-Tayeb, K., Lemaigre,FP., and Duncan, SA (2010a) Organogenesis and Development of the Liver. *Developmental Cell*. **18**(2):175-189.

Si-Tayeb, K., Noto, FK., Nagaoka, M *et al* (2010b) Highly efficient generation of human hepatocyte-like cells from induced pluripotent stem cells. *Hepatology*. **51**: 297-305

Sivaraman, A., Leach, JK., Townsend, S *et al* (2005) A microscale *in vitro* physiological model of the liver: predictive screens for drug metabolism and enzyme induction. *Current Drug Metabolism*. **6**: 569-591.

Skardal, A., Smith, L., Bharadwaj, S *et al* (2012) Tissue specific synthetic ECM hydrogels for 3D *in vitro* maintenance of hepatocyte function. *Biomaterials*. **33** (18):4565 – 4575.

Sneitz, N., Court, MH., Zhang, X., Laajanen, K., Yee, KK., Dalton, P., Ding, X., Finel, M., (2009) Human UDP- glucuronosyltransferase UGT2A2: cDNA construction, expression, and functional characterisation in comparison with UGT2A1 and UGT2A3. *Pharmacogenetics and Genomics.* **19** (12): 923-934.

Soboll, S., Grundel, S., Harris, J., Kolb-Bachofen, V., Ketterer, B., and Sies, H (1995) The content of glutathione and glutathione S-transferases and glutathione peroxidase activity in rat liver nuclei determined by a non-aqueous technique of cell fractionation. *Biochemical Journal*. **311** (Pt3): 889-894.

Stafford, D., Hornbruch, A., Mueller, PR., and Prince, VE (2004) A conserved role for retinoid signalling in vertebrate pancreas development. *Development Genes and Evolution*. **214**: 432-441.

Starkey Lewis, PJ., Dear, J., Platt, V *et al* (2011) Circulating microRNAs as potential markers of human drug-induced liver injury. *Hepatology*. **54** (5): 1767-1776.

Stock, P., Brückner, S., Winkler, S *et al* (2014) Human bone marrow mesenchymal stem cell –derived hepatocytes improve the mouse liver after acute acetaminophen intoxication by preventing progress of injury. *International Journal of Molecular Sciences*. **15**: 7004-7028.

Stoller, JK., and Aboussouan, LS (2005) α1-antitrypsin deficiency. *The Lancet*. **9478**: 2225-2236.

Strassburg, CP., Strassburg, A., Kneip, S., Barut, S., Tukey, RH., Rodeck, B., and Manns MP. (2002) Developmental aspects of human hepatic drug glucuronidation in young children and adults. *Gut*. **50** (2): 259-265.

Stubbins, MJ., Harries, LW., Smith, G., Tarbit, MH., and Wolf, CR (1996) Genetic analysis of the human cytochrome P450 CYPC9 locus. *Pharmacogenetics.* **6**: 429-439.

Suh, MR., Lee, Y., Kim, JY., Kim, SK., Moon, SH., Lee, JY., Cha, KY., Chung, HM., Yoon, HS., Moon, SY., Kim, VN., and Kim, KS (2004) Human embryonic stem cell express a unique set of microRNAs. *Developmental Biology*. **270** (2): 488-498.

Sullivan-Klose, TH., Ghanayem, BI., Bell, DA *et al* (1996) The role of the CYP2C9-Leu359 allelic variant in the tolbutamide polymorphism. *Pharmacogenetics*. **6**: 341-349.

Sullivan, GJ., Hay, DC., Park, IH *et al* (2010) Generation of functional human hepatic endoderm from human induced pluripotent stem cells. *Hepatology*. **51**: 329 – 335.

Swart, M., and Dandara, C (2014) Genetic variation in the 3' UTR of CYP1A2, CYP2B6, CYP2D6, CYP3A4, NR1I2, and UGT2B7: potential effects on regulation by microRNA and pharmacogenomics relevance. *Frontiers in Genetics.* **5**: 1-11.

Szakacs, G., Varadi, A., Ozvegy-Laczka, C., and Sarkadi, B (2008) The role of ABC transporters in drug absorption, distribution, metabolism, excretion and toxicity (ADME-Tox). *Drug Discovery Today*. **13**: 379-393.

Szkolnicka, D., Zhou,W., Lucendo – Villarin, B., and Hay, DC (2013) Pluripotent stem cell –derived hepatocytes: Potential and challenges in pharmacology. *Annual Review of Pharmacology and Toxicology*. **53**: 147-59.

Szkolnicka, D., Farnworth, SL., Lucendo-Villarin, S., and Hay, DC (2014a) Deriving functional hepatocytes from pluripotent stem cells. *Current Protocols in Stem Cell Biology*. **30**: 1G.5.1.

Szkolnicka, D., Farnworth, SL., Lucendo-Villarin, B., Storck, C., Zhou, W., Iredale, JP., Flint, Flint, O., and Hay, DC (2014b) Accurate prediction of drug-induced liver injury using stem cell- derived populations. *Stem Cells Translational Medicine*. **3**:141-148.

Takagi, S., Nakajima, M., Mohri, T., Yokoi, T (2008) Post-transcriptional regulation of human pregnane X receptor by microRNA affects the expression of cytochrome P450 3A4. *Journal of Biological Chemistry*. **283**: 9674-9680.

Takagi, S., Nakajima, M., Kida, K., Yamura, Y., Fukami, T., and Yokoi, T (2010) MicroRNAs regulate human hepatocyte nuclear factor 4a, modulating the expression of metabolic enzymes and cell cycle. *Journal of Biological Chemistry*. **285**: 4415-4422.

Takahashi, K., and Yamanaka, S (2006) Induction of pluripotent stem cells from mouse embryonic and adult fibroblast cultures by defined factors. *Cell.* **124** (6): 663-76.

Takahashi, K., Tanabe, K., Ohnuki, M., Narita, M., Ichisaka, T *et al* (2007) Induction of pluripotent stem cells from adult human fibroblasts by defined factors. *Cell*. **131**: 1-12.

Takayama, K., Inamura, M., Kawabata, K., Katayama, K., Higuchi, M., Tashiro, K., Nonaka, A., Fuminori, S., Hayakawa, T., Furue, MK., and Mizoguchi, H (2012) Efficient genereation of functional hepatocytes from human embryonic stem cells and induced pluripotent stem cell by HNF4a transduction. *Molecular Therapy*. **20**: 127-137.

Takayama, K., Nagamoto, Y., Mimura, N., Tashiro, K., Sakurai, F., Tachibana, M., Hayakawa, T., Kawabata, K., and Mizuguchi, H (2013) Long-term self –renewal of human ES/iPS-derived hepatoblast-like cells on human laminin 111-coated dishes. *Stem Cell Reports*. **1**:322-335.

Takebe, T., Sekine, K., Enomura, M *et al* (2013) Vascularized and functional human liver and iPSC-derived organ bud transplant. *Nature*. **499**: 481 – 484.

Tanaka, C., Sakuma, R., Nakaruma, T., Hamada, H., and Saijoh, Y (2007) Long-range action of Nodal requires interaction with GDF1. *Genes and Development*. **21**: 3272-3282.

Tang, Y., Forsyth, CB., Farhadi, A., Rangan, J., Jakate, S *et al* (2009) Nitric oxide-mediated intestinal injury is required for alcohol-induced gut leakiness and liver damage. *Alcoholism: Clinical and Experimental Research*. **33**: 1220-1230.

Tanimizu, N., and Miyajima,A (2004) Notch signalling controls hepatoblast differentiation by altering the expression of liver-enriched transcription factors. *Journal of Cell Science.* **117**: 3165-3174.

Tatsumi, N., Miki, R., Katsu, K., and Yokuochi, Y (2007) Neurturin-GFRalpha2 signalling controls liver bud migration along the ductus venosus in the chick embryo. *Developmental Biology.* **307**: 14-28.

Teo, AKK., Arnold, SJ., Trotter MWB *et al* (2011) Pluripotency factors regulate definitive endoderm specification through eomesodermin. *Genes and Development*. **25** (3): 238-250.

Thier, R., Wiebel, FA., Hinkel, A., Burger, A., Brüning, T., Morgenroth, K., Senge, T., Wilhelm, M., and Schulz, TG (1998) Species differences in the glutathione transferase GSTT1-1 acitvity towards the model substrates methyl chloride and dichloromethane in liver and kidney. *Archives of Toxicology*. **72** (10): 622-629.

Thomson, Ja., Itskovitz-Eldor, J., Shapiro, SS., Waknitz, MA., Swiergiel, JJ *et al* (1998) Embryonic stem cell lines derived from human blastocysts. *Science.* **282**: 1145-47.

Thong, VD., Akkarathamrongsin, S., Poovorawan, K., Tangkijvanich, and Poovorawan, Y (2014) Hepatitis C virus genotype 6: virology, epidemiology, genetic variation and clinical implication. *World Journal of Gastroenterology*. **20** (11):2927-2940.

To KK., Zhan,Z., Litman, T *et al* (2008) Regulation of ABCG2 expression at the 3' untranslated region of its mRNA through modulation of transcript stability and protein translation by a putative microRNA in the S1 colon cancer cell line. *Molecular Cell Biology*. **28**: 5147-5167.

Tomankova, T., Petrek, M., and Kriegova, E (2010) Involvement of microRNAs in physiological and pathological process in the lung. *Respiratory Research*. **11**: 159-169.

Tong, AW., Fulgham, P., Jay, C., Chen, P., Khalil, I *et al* (2008) MicroRNA profile analysis of human prostate cancers. *Cancer Gene Therapy*. **16** (3): 206-216.

Touboul, T., Hannan, NR., Corbineau, S *et al* (2010) Generation of functional hepatocytes from human embryonic stem cells under chemically defined conditions that recapitulate liver development. *Hepatology*. **51**: 1754-1765.

Trabucchi, M., Briata, P., Garcia-Mayoral, M., Haase, AD., Filipowicz, W., Ramos, A. *et al* (2009) The RNA-binding protein KSRP promotes the biogenesis of a subset of microRNAs. *Nature*. **459** (7249): 1010-1014.

Tremblay, KD and Zaret, KS (2005) Distinct populations of endoderm cells converge to generate the embryonic liver bud and ventral foregut tissues. *Developmental Biology*. **280**: 87-99.

Tsuchiya, Y., Nakajima, M., Takagi, S *et al* (2006) MicroRNA regulates the expression of human cytochrome P450 1B1. *Cancer Research.* **66**: 9090-8.

Tsuruga, Y., Kiyono, T., Matsushita, M *et al* (2008) Establishment of immortalized human hepatocytes by introduction of HPV16 E6/E7 and hTERT as cell sources for liver cell-based therapy. *Cell Transplantation*. **17** (9): 1083-1094.

Tujios, S., and Fontana, RJ (2011) Mechanisms of drug-induced liver injury: form bedside to bench. *Nature Reviews*. **8**: 202-211.

Tukey, R.H., and Strassburg, C.P (2000) Human UDP-glucuronosyltransferases: metabolism, expression and disease. *Annual Reviews in Toxicology and Pharmacology*. **40**: 581-616.

Tuleuova, N., Lee, JY., Lee, J., Ramanculov, E., Zern, MA., and Revzin, A (2010) Using growth factor arrays and micropatterned co –cultures to induce hepatic differentiation of embryonic stem cells. *Biomaterials*. **31**: 9221-9231.

Tzur, G., Israel, A., Ley, A., Benjamin, A., Meiri, E. *et al* (2009) Comprehensive gene and microRNA expression profiling reveals a role for microRNAs in human liver development. *PlosOne*. **4** (10): d7511.

Uchaipichat, V., Mackenzie, PI., Elliot, DJ., Miners, JO. (2006a) Selectivity of substrate (trifluoperazine) and inhibitor (amitriptyline, androsterone, canrenoic acid, hecogenin, phenylbutazone, quinidine, quinine, and sulfinpyrazone) 'probes' for human UDP-glucuronosyltransferases. *Drug Metabolism and Disposition*. **34** (3): 449-456.

Uchaipichat, V., Winner, LK., Mackenzie, PI., Elliot, DJ., Williams, JA., and Miners, JO (2006b) Quantitative prediction of *in vitro* data: the effect of fluconazole on zidovudine glucuronidation. *British Journal of Clinical Pharmacology*. **61**(4): 427-439.

Ulvestadt, M., Nordell, P., Asplund, A (2013) Drug metabolizing enzyme and transporter protein profiles oh hepatocytes derived from human embryonic and induced pluripotent stem cells. *Biochemical Pharmacology*. **86**: 691-702.

Underhill, TJ., Greene, MK., and Dove, AF (1990) A comparison of the efficacy of gastric lavage, ipecacuanha and activated charcoal in the emergency management of paracetamol overdose. *Archives of Emergency Medicine*. **7**:148-154.

Unger, C., Skottman, H., Blomberg, P *et al* (2008) Good manufacturing practice and clinical - grade human embryonic stem cell lines. *Human Molecular Genetics*. **17**: R48 – R53.

Urquhart, BL., Tirona, RG., and Kim, RB (2007) Nuclear receptors and the regulation of drug metabolizing enzymes and drug transporters: implications for interindividual variability in response to drugs. *Journal of Clinical Pharmacology*. **47**: 566-578.

Wang, K., Shindoh, H., Inoue, T., and Horii, I (2002) Advantages of *in vitro* cytotoxicity testing by using primary rat hepatocytes in comparison with established cell lines. *Journal of Toxicological Sciences*. **27**: 229-237.

Wang, L., and Boyer, JL (2004) The maintenance and generation of membrane polarity in hepatocytes. *Hepatology*. **39** (4): 892-899.

Wang, G., Zhang, H., Zhao, Y *et al* (2005) Noggin and bFGF cooperate to maintain the pluripotency of human embryonic stem cells in the absence of feeder layers. *Biochemical and Biophysical Research Communications*. **330** (3): 934 – 942.

Wang, X., Chowdhury, JR., and Chowndhury, NR. (2006) Bilirubin metabolism: Applied Physiology. *Current Opinion in Pediatrics*. **16** (1): 70-74.

Wang, L., Schulz, TC., Sherrer, ES *et al* (2007) Self – renewal of human embryonic stem cell requires insulin-like growth factor -1 receptor and ERBB2 receptor signalling. *Stem Cells In Hematology*. **110** (12): 4111 – 4119.

Wang, DD., Kreigstein, AR., and Ben- Ari, Y (2008) GABA regulates stem cell proliferation before nervous system formation. *Epilepsy Currents*. **8** (5): 137 – 139.

Wang, K, Zhang, S., Marzolf, B *et al* (2009) Circulating microRNAs, potential biomarkers for drug-induced liver injury. *Proc. Natl. Acad. Sci.U.S.A.* **106** (11): 4402-4407.

Wang, Y., Chen, T., and Tong, W (2014) MiRNAs and their application in drug-induced liver injury. *Biomarkers in Medicine*. **8** (2): 161-172.

Ware, BR., Berger, DR., and Khetani, SR (2015) Prediction of drug-induced liver injury in micropatterned co-cultures containing iPSC-derived human hepatocytes. *Toxicological Sciences*. doi: 10.1093/toxsci/kfv048.

Warnich, L., Drogemoller, BI., Pepper, MS *et al* (2011) Pharmacogenomic research in South Africa: lessons learned and future opportunities in the rainbow nation. *Current Pharmacogenomics and Personalized Medicine*. **9**: 191- 207.

Watt, AJ; Zhao, R., Li, J., and Duncan, SA (2007) Development of the mammalian liver and ventral pancreas is dependent on GATA4. BMC Developmental Biology. **7**. 37.

Wedlund, PJ (2000) The CYP 2C19 enzyme polymorphism. *Pharmacology*. **61**: 174-83.

Wei, R., Yang, F., Urban, T *et al* (2012) Impact of interaction between 3' – UTR SNPs and microRNA on the expression of human xenobiotic metabolism enzyme and transporter genes. *Frontiers in Genetics*. **3**: 248.

Wege, H., Chui, MS., Le, HT., Strom, SC., and Zern, MA (2003) *In vitro* expansion of human hepatocytes is restricted by telomere – dependent replicative aging. *Cell Transplantation.* **12**: 897-906.

Weinshilbourn, RM., Otterness, DM., Aksoy, IA., Wood, TC., Her, C., and Raftogianis, RB (1997) Sulfation and sulfotransferases 1: Sulfotransferase molecular biology. cDNAs and genes. *FASEB Journal*. **11** (1): 3-14.

Wells, JM., and Melton, DA (2000) Early mouse endoderm is patterned by soluble factors from adjacent germ layers. *Development*. **127**: 1563-1572.

Wells, PG., Mackenzie, PI., Chowdhury, JR., Guillemette, C., Gregory, PA., Ishii, Y., Hansen, AJ., Kessler, FK., Kim, PM., Chowdhury, NR., Ritter, JK. (2004) Glucuronidation and the UDP-glucuronosyltransferases in health and disease. *Drug Metabolism and Disposition.* **32** (3): 281-290.

Weinmann, L., Hock, J., Ivacevic, T., Ohrt, T., Mutze, J., Schwille, P *et al* (2009) Importin 8 is a gene silencing factor that targets argonaute proteins to distinct mRNAs. *Cell.* **136** (3): 496-507.

Weinshilbourn, RM., Otterness, DM., Aksoy, IA., Wood, TC., Her, C., and Raftogianis, RB (1997) Sulfation and sulfotransferases 1: Sulfotransferase molecular biology. cDNAs and genes. *FASEB Journal*. **11** (1): 3-14.

Weiss, CF., Glazko, AJ., and Weston, JK (1960) Chloramphenicol in the newborn infant. A physiological explanation of its toxicity when given in excessive doses. *New England Journal of Medicine*. **262**: 787-794.

Wen, Z., Tallman, MN., Ali, SY., and Smith, PC (2007) UDP-glucuronosyltransferase 1A1 is the principal enzyme responsible for etoposide glucuronidation in human liver and intestinal microsomes: structural characterization of phenolic and alcoholic glucuronides of etoposide and estimation of enzyme kinetics. *Drug Metabolism and Disposition.* **35**: 371-380.

Wieckowska, A., Zein, NN., Yerian, LM., Lopez, AR *et al* (2006) *In vivo* assessment of liver cell apoptosis as a novel biomarker of disease severity in non-alcoholic fatty liver disease. *Hepatology*. **44** (1): 27-33.

Williams, DP., Shipley, R., Ellis, MJ., Webb, S., Ward, J., Gardner, I., and Creton, S (2013) Novel *in vitro* and mathematical models for the prediction of chemical toxicity. *Toxicology Research*. **2**: 40-59.

Williamson, G., DuPont, MS., Wanigatunga, S., Heaney, RK., Musk, SRR., Fenwick, GR., and Rhodes, MJC. (1997) Induction of glutathione S' – transferase activity in hepG2 cells by extracts from fruits and vegetables. *Food Chemistry.* **60** (2):157-160.

Wilkinson, GR. (2005) Drug metabolism and variability among patients in drug response. *The New England Journal of Medicine*. **352**: 2211-21.

Wilson, E., Leszczynska, K., Poulter, N *et al* (2014) RhoJ interacts with the GIT-PIX complex and regulates focal adhesion assembly. Journal of Cell Science. 127: 3039 – 3051.

Witkos, TM., Koscianska, E., and Krzyzosiak, WJ (2011) Practical aspects of microRNA target prediction. *Current Molecular Medicine*. **11**:93-109.

Wobus, AM., and Loser, P (2011) Present state and future perspectives of using pluripotent stem cells in toxicology research. *Archives of Toxicology*. **85**: 79-117.

Wu, H., Kong, L., Zhou, S., Cui, W., Xu, F et al (2014) The role of microRNAs in diabetic nephropathy. *Journal of Diabetes Research*. **2014**. Article ID: 920134.

Vallier, L., Alexander, M., and Pedersen, R (2005) Activin/Nodal and FGF pathways cooperate to maintain pluripotency of human embryonic stem cells. *Journal of Cell Science*. **118**: 4495 – 4509.

Van Bladeren, PJ (2000) Glutathione conjugation as a bioactivation reaction. *Chemico – Biological Interactions*. **129** (1-2): 61-76.

Van Iersel, MLPS; Van Lipzig, MMH., Rietjens, IMC., Vervoort, J., and Van Balderen, PJ (1998) GSTP1-1 stereospecifically catalyzes glutathione conjugation of ethacrynic acid. *FEBS Letters*. **441** (1): 153-157.

Vara, D., Salazar, M., Olea – Herrero, N., Guzmńan, M., Velasco, G., and Diaz-Laviada, I (2011) Anti-tumoral action of cannabinoids on hepatocellular carcinoma: role of AMPK- dependent activation of autophagy. *Cell Death and Differentiation.* **8** (7): 1099-111.

Vazin, T., and Freed, WJ (2010) Human embryonic stem cells: derivation, culture, and differentiation: a Review. *Restorative Neurology and Neuroscience*. **28**(4): 589-603.

Vasudevan, S., Tong, Y., and Steitz, JA (2007) Switching from repression to activation: microRNAs can up-regulate translation. *Science*. **318** (5858): 1931-1934.

Vasudevan, S., and Steitz, JA (2007b) AU-rich-element-mediated upregulation of translation by FXR1 and Argonaute 2. *Cell*. **128** (6): 1105-1118.

Vieira, I., Sonnier, M., and Cresteil, T (1996) Developmental expression of CYP2E1 in the human liver. *European Journal of Biochemistry*. **238**: 476-438.

Vietri, M., Pietrabissa, A., Mosca, F., Rane, A., and Pacifici GM. (2003) Curcumin is a potent inhibitor of phenol sulfotransferase (SULT1A1) in human liver and extrahepatic tissue. *Xenobiotica*. **33** (4): 357-363.

Vignati, L., Turlizzi, E., Monaci, S *et al* (2005) An *in vitro* approach to detect metabolite toxicity due to CYP3A4-dependent bioactivation of xenobiotics. *Toxciology*. **216**: 154-167.

Viollon, C., Nicod, L., Benay, C *et al* (1991) Toxicity of erythromycin, paracetamol and isoniazide in human hepatocytes in primary culture and in the human hepatoma cell line HepG2. Comparison with rat and mouse hepatocytes in primary culture. *Cell Biology and Toxicology*. **11** (3-4): 195-227.

Visk, D (2015) Will advances in preclinical *in vitro* models lower the costs of drug development? *Applied In Vitro Toxicology*. doi; 10.1089/aivt.2015.1503.

Vosough, M., Omidinia, E., Kadivar, M., Shokrgozar, MA., Pournasr,B., Aghdami, N., and Baharvand, H (2013) Generation of functional hepatocyte-like cells from human pluripotent stem cells in a scalable suspension culture. *Stem Cells and Development.* **22**: 2693-2705.

Vuoristo, S., Toivonen, S., Weltner, J., Mikkola, M., Ustinov, J., Trokovic, R., Palgi, J., Lund, R., Tuuri, T., and Otonkoski, T (2013) A novel feeder-free culture system for human pluripotent stem cell culture and induced pluripotent stem cell derivation. *Plos One*. **8**: e76205.

Xiao, L., Yuan, X., and Sharkis, SJ (2006) Activin A maintains self – renewal and regulates fibroblast growth factor, Wnt, and bone morphogenetic protein pathways in human embryonic stem cells. *Stem Cells*. **24**: 1476 – 1486.

Xiao, Q., Luo, Z., Pepe, AE et al (2008) Embryonic stem cell differentiation into smooth muscle cells is mediated by Nox-4-produced H_2O_2. *American Journal of Physiology*. **294** (4): C711-C23.

Xie, HG., Kim, RB., Wood, AJJ., and Stein, CM (2001) Molecular basis of ethnic differences in drug disposition and response. *Annual Reviews in Pharmacology and Toxicology.* **41:** 815-50.

Xu, C., Inokuma, MS., Denham, J *et al* (2001) Feeder – free of undifferentiated human embryonic stem cells. *Nature Biotechnology*. **19**: 971 – 974.

Xu, C., Yong-Tao Li, C., and Tony Kong, AN (2005) Induction of Phase I, II and III Drug Metabolism/Transport by Xenobiotics. *Archives of Pharmacal Research*. **28** (3): 249-268.

Xu, C., Li, CY., Kong, AN (2005) Induction phase I, II, and III drug metabolism/transport by xenobiotics. *Archives of Pharmacal Research.* **28** (3): 249-268.

Xu, RH., Sampsell-Barron, TL., Gu, F *et al* (2008) NANOG is a direct target of TGB/Activin mediated SMAD signalling in human ESCs. *Cell Stem Cell*. **3**: 196-206.

Xu, HS., Zong, HL., Shang, M., Ming, X *et al* (2014) MiR-324-5p inhibits proliferation of glioma by target regulation of GLI1. *European Review for Medical and Pharmacological Sciences*. **18**: 828-832.

Yang, W., Chendrimada, TP; Wang, Q., Higuchi, M., Seeburg, PH., Shiekhattar, R *et al* (2006) Modulation of microRNA processing and expression through RNA editing by ADAR deaminases. *Nature Structural and Molecular Biology.* **13** (1):13-21.

Yasanuga, M., Tada, S., Torikai-Nichikawa, S., Nakano, Y et al (2005) Induction and monitoring of definitive and visceral endoderm differentiation of mouse ES cells. *Nature Biotechnology*. **23**: 1542-1550.

Yi, R., Qin, Y., Macara, IG., and Cullen, BR (2003) Exportin-5 mediates the nuclear export of pre-microRNA and short hairpin RNAs. *Genes and Development*. **17**: 3011-3016.

Yildirimman, R., Brolen, G., Vilardell, M., Eriksson, G *et al* (2011) Human embryonic stem cell derived hepatocyte-like cells as a tool for *in vitro* hazard assessment of chemical carcinogenicity. *Toxicological Sciences*. **124**: 278-290.

Yokoi, AM., and Pan, YZ (2012) Noncoding microRNAs: small RNAs play a big role in regulation of ADME? *Acta Pharmacetutica Sinica B.* **2**: 93-101.

Yokoi, T., and Nakajima, T (2013) microRNA as mediators of drug toxicity. *Annual Review in Pharmacology and Toxicology*. **53**: 19.1 – 19.24

Youdim, KA., Tyman, CA., Jones, BC *et al* (2007) Induction of cytochrome P450: assessment in immortalized human hepatocyte cell line (Fa2N4) using a novel higher throughput cocktail assay. *Drug Metabolism and Disposition*. **35**: 275-282.

Yu, L., Li-Hawkins, J., Hammer, RE *et al* (2002) Overexpression of ABCG5 and ABCG8 promotes biliary cholesterol secretion and reduced fractional absorption of dietary cholesterol. *Journal of Clinical Investigation*. **110** (5): 671-680.

Yu, AM (2009) Role of microRNAs in the regulation of drug metabolism and disposition. *Expert Opinion in Drug Metabolism and Toxicology*. **5** (12): 1514-1528.
Yu, AM., and Pan, YZ (2012) Noncoding microRNAs: small RNAs play a big role in regulation of ADME? *Acta Pharmaceutica Sinica B.* **2** (2): 93-101.

Yu, X., Dhakal, IB., Beggs, M., *et al* (2010) Functional genetic variants in the 3' untranslated region of sulfotransferase isoform 1A1 (SULT1A1) and their effect on enzymatic activity. *Toxicological Sciences*. **118**: 391-403.

Yusa, K., Rashid, S., Strick- Marhand, H., Varela, I., Liu, PQ *et al* (2011) Targeted gene correction of α1- antitrypsin deficiency in induced pluripotent stem cells. *Nature.* **478**: 391-94.

Zampetaki, A., and Mayr, M (2012) MicroRNAs in vascular and metabolic disease. *Circulation Research*. **110** (3): 508-522.

Zardo, G., Ciolfi, A., Vian, L *et al* (2012) Polycombs and microRNA-223 regulate human granulopoiesis by transcriptional control of target gene expression. *Blood*. **119** (17): 4034-4046.

Zaret, KS (2008) Genetic programming of liver and pancreas progenitors: lessons for stem-cell differentiation. *Nature Reviews Genetics.* **9** (5):329-40.

Zern, MA (2009) Cell transplantation to replace whole liver transplantation. *Gastroenterology*. **136**: 767-769.

Zimmerman, LB., De Jesus-Escobar, JM, and Harland, RM (1996) The Spemann organizer signal noggin binds and inactivates bone morphogenetic protein 4. *Cell*. **84** (4): 599-606.

Zhao, R., Watt, AJ., Li, J., Luebke- Wheeler, J., Morrisey, EE., and Duncan, SA (2005) GATA6 is essential for embryonic development of the liver but dispensable for early heart formation. *Molecular Cell Biology*. **25**: 2622-2631.

Zhao, R., Watt, AJ., Battle, MA., Li,J., Bondow, BJ., and Duncan, SA (2008) Loss of both GATA4 and GATA6 blocks cardiac myocyte differentiation and results in acardia in mice. *Developmental Biology*. **317**: 614-619.

Zheng, L., Lv., GC., Sheng, J., and Yang, YD (2010) Effect of miRNA-10b in regulating cellular steatosis level by targeting PPAR-alpha expression, a novel mechanism for the pathogenesis of NAFLD. *Journal of Gastroenterology and Hepatology*. **25**: 156-163.

Zhou, W., Hannoun, Z., Jaffray, E., Medine, CN., Black, JR. *et al* (2012) SUMOylation of HNF4a regulates protein stability and hepatocyte function. *Journal of Cell Science.* **125**: 3630-35.

Zhou,X., Sun, P., Lucendo-Villarin,B., Angus, AGN., Szkolnicka, D., Cameron, K., Farnworth, SL., Patel, AH., and Hay, DC (2014) Modulating innate immunity improves hepatitis C virus infection and replication in stem cell – derived hepatocytes. *Stem Cell Reports*. **3** (1): 204-214

Zhu, H., Wu,H., Liu,X *et al* (2008) Role of microRNA miR-27a and miR-451 in the regulation of MDR1/P-glycoprotein expression in cancer cells. *Biochemical Pharmacology*. **76**: 582-588.

Zorn, AM., Liver development (October 31, 2008) StemBook, ed. The Stem Cell Research Community, StemBook, doi/10.3824/stembook.1.25.1, http://www.stembook.org

Zorn, AM, and Wells, JM (2007) Molecular basis of vertebrate endoderm development. *International Review of Cytology*. **259:** 49-111.

Zuppa, AF., Hammer, GB., and Barrett, JS (2011) Safety and population pharmacokinetic analysis of intravenous acetaminophen in neonates, infants, children, and adolescents. with pain or fever. *Journal of Pediatric Pharmacology*. **16**: 246-261